Monday Morning, October 19, 2015

2D Materials Focus Topic
Room: 212C - Session 2D+EM+NS+PS+SP+SS+TF-MoM

2D Materials: Growth and Fabrication
Moderator: Cory Dean, Columbia University, Peide Ye, Purdue University

8:20am 2D+EM+NS+PS+SP+SS+TF-MoM1 Growth and FTIR Characterization of 2D Hexagonal Boron Nitride on Metal Substrates, *Boris Feigelson*, *V.M. Bermudez, J.K. Hite, Z.R. Robinson, V.D. Wheeler, K. Sridhara, S.C. Hernández*, US Naval Research Laboratory

Atomically thin two dimensional hexagonal boron nitride (2D h-BN) is one of the key materials in the development of new van der Waals heterostructures due to its outstanding properties including an atomically smooth surface, high thermal conductivity, high mechanical strength, chemical inertness and high electrical resistance. The development of 2D h-BN growth is still in the early stages and largely depends on rapid and accurate characterization of the grown monolayer or few layers h-BN films.

In this work, the IR-active out-of-plane vibrational mode of 2D h-BN films grown in vertical reactor by atmospheric-pressure CVD on metal substrates (mainly Cu but also Ni) is exploited to identify 2D h-BN directly on substrates and studied both computationally and experimentally.

Fourier transform grazing-incidence infrared reflection absorption spectroscopy (FT-IRRAS) data have been used to characterize monolayer and few-layer h-BN films directly on metal substrates. Two sub-bands of the A_{2u}(LO) vibrational mode were, for the first time, found for thin 2D h-BN films in contact with Cu and Ni [1]. To unveil the nature of the discovered sub-bands, ab-initio calculations were performed and verified using 2D h-BN films grown on various Cu substrates with varying coverage and with individual crystallites of different shapes and size up to 4 mm. It was shown that the lower-energy A_{2u}(LO)1 sub-band around 819 cm^{-1} is related to 2D h-BN coupled with Cu substrate, while the higher energy A_{2u}(LO)2 sub-band around 824 cm^{-1} is related to decoupled (essentially free standing) 2D h-BN. These findings demonstrate not only a new and facile method for immediate 2D h-BN identification and characterization, but also a method that provides a simple means to characterize the degree of coupling between 2D h-BN and the substrate. This approach also provides an opportunity to determine which growth conditions lead to the absorption of foreign species on the substrate prior to the h-BN deposition and which conditions can prevent the formation of the interfacial layer between h-BN and the substrate. Such interfacial layers, like oxidized Cu, were shown to result in easily-recognizable shifts in the A_{2u}(LO) peak. The degree to which the interaction of the h BN layer with the substrate is uniform and homogenous can also be assessed easily by examining the width and fine structure of the A_{2u}(LO) band. The developed approach can also be used to study growth and formation of h-BN/graphene and other 2D heterostructures.

References

1. B. N. Feigelson, V. M. Bermudez, J. K. Hite, Z. R. Robinson, V. D. Wheeler, K. Sridhara, and S. C. Hernandez, Nanoscale **7**, 3694 (2015)

8:40am 2D+EM+NS+PS+SP+SS+TF-MoM2 Effect of Surface Termination on the Growth of Graphene on Cu Single Crystal Substrates, *Tyler Mowll*, *E.W. Ong,* University at Albany-SUNY, *P. Tyagi,* GLOBALFOUNDRIES, *Z.R. Robinson,* College at Brockport-SUNY, *C.A. Ventrice, Jr.*, SUNY Polytechnic Institute

The most common technique for synthesizing single-layer graphene films with large lateral dimensions is chemical vapor deposition (CVD) on Cu foil substrates. The primary reasons for choosing Cu substrates are the extremely low solubility of carbon in Cu, which allows a self-limited growth of graphene, and the relatively low cost of the Cu foil substrates. However, the transport properties of the CVD grown graphene films are typically a couple of orders of magnitude lower than for graphene flakes mechanically exfoliated from graphite. One of the reasons for the reduction in transport properties is the presence of crystalline defects in the CVD grown films. These structural defects arise in part from the multidomain structure of the Cu films. In order to achieve a better understanding of the influence of the surface termination of the Cu substrate on the crystallization of graphene during the CVD growth process, a systematic study of graphene growth on Cu(100), Cu(110), and Cu(111) crystals has been performed. The growth process is performed in an ultra-high vacuum (UHV) chamber that has been modified to perform CVD growth at pressures as high as 100 mTorr. The precursor gas used is ethylene. This growth procedure allows for the preparation of the clean surfaces in UHV, growth under typical CVD conditions, and characterization of the surface structure in UHV, without exposing the sample to atmospheric contaminants. Our results indicate that the Cu(111) surface has the lowest catalytic activity of the three surfaces for the decomposition of ethylene. In fact, the decomposition rate is so low that graphene growth is suppressed because of the sublimation of Cu at the elevated temperatures used to grow the graphene. By using an Ar overpressure, it was found that graphene could be grown on that surface. The surface symmetry of the Cu substrate has a strong influence on the rotational alignment of the graphene grains as they nucleate on each surface. For Cu(111), single-domain graphene growth can be achieved for ethylene pressures of 5 mTorr or less. For both Cu(100) and Cu(110), a minimum of two graphene domains is always observed.

9:00am 2D+EM+NS+PS+SP+SS+TF-MoM3 Thermally Annealed and Electropolished Cu Substrates for CVD Growth of 2D Materials: Graphene, h-BN and MoS$_2$, *Karthik Sridhara*, Texas A&M University, *B.N. Feigelson, J.K. Hite,* US Naval Research Laboratory, *A. Nath,* George Mason University, *M. Fuhrer,* Monash University, Australia, *D.K. Gaskill,* US Naval Research Laboratory, *H. Castaneda, L.O. Nyakiti*, Texas A&M University

The growth of two dimensional (2D) materials such as graphene, hexagonal boron nitride (h-BN) and molybdenum disulphide (MoS$_2$) have been demonstrated by chemical vapor deposition (CVD) on polycrystalline catalytic copper substrates. These Cu foil substrates (25 μm thick) are produced by metallurgical rolling leading to the formation of irregular ridges on the foil surface along with a film of native oxide on the surface. These processing artifacts are a limiting factor for controlled and reproducible large area (several cm^2) growth of 2D materials. Greater control of growth can be achieved by controlling the density of nucleation sites and improving the catalytic activity of Cu by removing the Cu native oxide on the surface. Previous attempts to pre-treat the Cu substrate by using wet chemistry or thermal annealing to control growth has been weakly addressed.

In this work, electropolishing combined with prior thermal annealing at 1030°C for 5 hrs under H$_2$ is used to control the degree of roughness of cold rolled polycrystalline Cu foils, and subsequently, to explore the influence of electropolishing on the growth of 2D materials: graphene, h-BN and MoS$_2$. Electropolishing dissolves a thin surface layer of Cu, which contains surface defects and contaminants. This helps in decreasing the density of spontaneous nucleation sites by producing a morphologically uniform and contaminant-free surface. Secondary effects, etch pits which are ascribed to O$_2$ bubbling at random nucleation sites on Cu surface, are mitigated by using additives, such as acetic acid and ethylene glycol, in the H$_3$PO$_4$ electrolyte. Thermal annealing and electropolishing results in this work reveal that a roughness of ~1.2 nm (R$_q$) can be achieved as measured by Atomic Force Microscope (AFM) along with a greatly planarized Cu foil. AFM will also be used to establish the Cu substrate morphology and its relationship to the growth of 2D materials. Fourier Transform Infrared, and Raman spectroscopy will be used to confirm the existence of the 2D material. Preliminary growth studies of h-BN on these high quality Cu substrates demonstrate improved growth, as assessed by the metrics of size and count of h-BN crystals from Scanning Electron Microscopy (SEM) micrographs [1]. This work will demonstrate that thermal annealing followed by electropolishing leads to optimization of Cu foil surface resulting in the larger crystal size and a reduction in nucleation sites that induce 2D material crystal growth [1].

[1] K. Sridhara. "Growth of hexagonal boron nitride on electrochemically prepared polycrystalline Cu substrates." M.S. Thesis, University of Maryland, College Park, MD, 2014.

9:20am 2D+EM+NS+PS+SP+SS+TF-MoM4 *In Situ* Optical Diagnostics During Molybdenum Disulfide Chemical Vapor Deposition, *Berc Kalanyan*, *J.E. Maslar, W.A. Kimes, B.A. Sperling,* National Institute of Standards and Technology (NIST), *R. Tieckelmann, T. Orzali,* SEMATECH, *R. Beams, S.J. Stranick, A.V. Davydov*, National Institute of Standards and Technology (NIST)

Two dimensional (2D), layered transition-metal dichalcogenides (TMDs), e.g., MoS$_2$, are of increasing interest for next-generation nanoelectronic and optoelectronic devices. These materials have thickness dependent optical and electrical properties that make them suitable for a variety of applications including integrated circuits. For many applications, high volume manufacturing (HVM) of devices based on TMDs will require deposition techniques that are capable of reproducibly growing wafer-scale, 2D TMD films with monolayer control. To date, such a capability has not been widely demonstrated with typical TMD deposition processes.

This work aims to identify promising chemistries for HVM TMD chemical vapor deposition (CVD) processes. We focus on MoS_2 CVD using a variety of precursors (including organometallics, elemental sulfur, and organosulfur compounds) in a research grade single-wafer deposition system equipped with *in situ* optical diagnostics. The precursor flux is measured using optical mass flow meters installed on the delivery lines while deposition chemistry is characterized in the reactor volume above the deposition surface using *in situ* Fourier transform infrared (FR-IR) spectroscopy. As-deposited and annealed films are characterized with *ex situ* techniques, including Raman and photoluminescence spectroscopy, scanning and transmission electron microscopy, and X-ray photoelectron spectroscopy.

Stoichiometric MoS_2 films have been prepared from (η^5-ethylcyclopentadienyl)-dicarbonylnitrosyl molybdenum and elemental sulfur. As-grown films are smooth and continuous with major MoS_2 Raman modes present. Film thickness scales approximately with Mo precursor exposure time and few-layer films can be produced using pulsed injection mode. Furthermore, optical *in situ* diagnostics allow us to relate metal precursor flux to film crystallinity and facilitate the study of precursor decomposition in the thermal boundary layer.

9:40am 2D+EM+NS+PS+SP+SS+TF-MoM5 Controlled Interfaces in 2D Materials, *Arend van der Zande*, University of Illinois at Urbana Champaign **INVITED**
Interfaces are ubiquitous in material science and technologies. For example, grain boundaries often dominate the mechanical and electrical properties in crystalline materials, while interfaces between dissimilar materials form the fundamental building blocks to diverse technologies, such as building electrical contacts in transistors and PN diodes in solar cells. Interfaces become even more important in 2D materials such as graphene and transition metal dichalcogenides, where the lack of dangling bonds enables material stability down to a single monolayer. In this entirely surface-dominated limit, the usual rules governing 3D interface devices, such as depletion regions, break down.

In this talk, we will discuss our work on engineering in- and out-of-plane 2D materials interfaces. We will first examine the structure of atomically-thin membranes and the impact of defects such as grain boundaries on the mechanical, optical, and electronic properties. We fabricate out-of-plane interfaces by stacking 2D materials to form heterostructures, which we utilize to tailor the bandgap in 2D materials and build new optoelectronic devices such as tunable photodiodes. Looking to the future, the rapidly expanding family of 2D materials with a diverse set of electronic properties provide a promising palette for discovering emergent phenomena and a motivation for developing overarching design principles for understanding and controlling interfaces in 2D.

10:40am 2D+EM+NS+PS+SP+SS+TF-MoM8 Obtaining Clean Suspended CVD Graphene: Comparative Examination of Few Transfer and Cleaning Protocols, *Alexander Yulaev*, National Institute of Standards and Technology (NIST), University of Maryland (UMD), *G. Cheng, A. Hight Walker,* National Institute of Standards and Technology (NIST), *M. Leite,* University of Maryland (UMD), *A. Kolmakov*, NIST
Clean suspended graphene is used as supporting media in TEM, filtering membranes, and as electron transparent windows in ambient pressure electron spectroscopy and microscopy. CVD grown graphene is the most popular material for these applications due to its large-scale and high yield production. Multiple approaches such as sacrificial layer based methods [1] and direct transfer method on perforated carbon mesh by IPA droplet [2] have been implemented to transport graphene from copper or nickel foil onto a target substrate. However, the cleanness of the suspended graphene remains to be an issue, and controversial results on lateral size of atomically clean graphene domains have been reported [2-5]. We conduct the comparative analysis of the most widely-used CVD graphene transfer and cleaning protocols. In particular, using extreme surface sensitivity of low energy SEM, we compare the standard PMMA based approach with direct graphene transfer method. We also propose alternative graphene transfer protocol which is based on employment of polycyclic aromatic hydrocarbon (PAH) as a sacrificial layer. The advantage of PAH method over others consists in facile sublimation of sacrificial layer upon heating PAH material within moderate temperature range of 100-150 ºC. All three methods of graphene transfer were compared under the same conditions followed by similar graphene cleaning procedures by platinum catalysis [4] and activated carbon adsorption [5]. Both SEM and TEM study revealed the superiority of PAH method to achieve cleaner suspended CVD graphene. We envision that novel approach of graphene transfer can be employed under conditions when exposure of the sample to moisture is prohibited such as in battery research.

[1] "Transfer of CVD-Grown Monolayer Graphene onto Arbitrary Substrates", Ji Won Suk *et al*., ACS Nano, 2011, 5 (9), pp. 6916.

[2] "A direct transfer of layer-area graphene", William Regan *et al*., Appl. Phys. Lett., 2010, 96, 113102.

[3] "Low-energy electron holographic imaging of gold nanorods supported by ultraclean graphene", Jean-Nicolas Longchamp *et al*., Ultramicroscopy 145 (2014) 80.

[4] "Ultraclean freestanding graphene by platinum-metal catalysis", Jean-Nicolas Longchamp *et al*., J. Vac. Sci. Technol. B 31, 020605 (2013).

[5] "Dry-cleaning of graphene", Gerardo Algara-Siller *et al*., Applied Physics Letters 104, 153115 (2014).

11:00am 2D+EM+NS+PS+SP+SS+TF-MoM9 Low-Energy Electron Microscopy of Transition Metal Dichalcogenides Prepared by Various Methods, *Sergio de la Barrera*, *S. Satpathy, R. Feenstra*, Carnegie Mellon University, *S. Wu, X.D. Xu,* University of Washington, *S. Vishwanath, X. Liu, J. Furdyna, D. Jena, H. Xing,* University of Notre Dame, *Y.-C. Lin, S.M. Eichfeld, J.A. Robinson,* Pennsylvania State University, *P. Mende*, Carnegie Mellon University
Recent work on two-dimensional materials has focused on transition metal dichalcogenides (TMDs), owing to their semiconducting behavior. Characterizing as-grown TMDs is crucial in improving the understanding of the effects of growth conditions, and ultimately improving material quality. Low-energy electron microscopy (LEEM) is a powerful tool for this purpose, providing real-space images with ~10 nm spatial resolution as well as selected-area low-energy electron diffraction (μLEED) of local crystal orientation at length scales down to ~ 1 μm. Additionally, by varying the incident electron beam energy, low-energy electron reflectivity (LEER) spectra are extracted.

In this work, comparative LEEM results are presented from three TMD materials: MoS_2 prepared by exfoliation (onto Si), $MoSe_2$ grown by molecular beam epitaxy (MBE) (on epitaxial graphene), and WSe_2 grown by chemical vapor deposition (CVD) (also on epitaxial graphene). It is found that for TMDs generally, the LEER spectra do not exhibit the oscillatory behavior (in the $0 – 6$ eV range) that is seen for both graphene and hexagonal boron nitride (h-BN) for various numbers of monolayers (MLs). This lack of oscillatory behavior is interpreted as being due to the weak coupling of the interlayer states localized in between the MLs, which is itself a result of the relatively large out-of-plane lattice parameter. Nevertheless, additional "band structure" features in the LEER spectra permit clear identification of the TMD materials relative to the substrates. The exfoliated flakes are seen to extend over many 10's of mm, the MBE-grown $MoSe_2$ forms a nearly continuous film, and the CVD-grown WSe_2 forms triangular islands several mm in extent. μLEED studies of the MBE-grown $MoSe_2$ and CVD-grown WSe_2 reveal preferential orientation with the underlying graphene substrates.

The reduced work functions of the TMD materials relative to the underlying substrate are clearly evident in the onset voltages for the LEER spectra (i.e. the onset shifts in accordance with the local work function of the surface). Most significantly, for the WSe_2 islands, a predominant "tail" is observed in this onset, extending about 5V below the usual onset location. This tail is tentatively interpreted as arising from charging of the islands, perhaps due to polar termination at the edges of the TMD islands. Comparison of the data with simulated LEER spectra will be presented, as a test of this model for edge charge of the islands.

11:20am 2D+EM+NS+PS+SP+SS+TF-MoM10 Atomically-Thin 2D Layers of Group IV Semiconductors, *Joshua Goldberger*, The Ohio State University **INVITED**
Similar to how carbon networks can be sculpted into low-dimensional allotropes such as fullerenes, nanotubes, and graphene with fundamentally different properties, it is possible to create similar "allotropes" of Ge or Sn with unique optoelectronic properties as well. Here, we will describe our recent success in the creation of hydrogen and organic-terminated group 14 graphane analogues, from the topochemical deintercalation of precursor Zintl phases, such as $CaGe_2$. We will discuss how the optical, electronic, and thermal properties of these materials can be systematically controlled by substituting either the surface ligand or via alloying with other Group 14 elements. Additionally, we have also developed an epitopotaxial approach for integrating precise thicknesses of Germanane layers onto Ge wafers that combines the epitaxial deposition of $CaGe_2$ precursor phases with the topotactic interconversion into the 2D material. Finally, we will describe

our recent efforts on the synthesis and crystal structures of Sn-containing graphane alloys in order to access novel topological phenomena predicted to occur in these graphanes.

Electronic Materials and Processing
Room: 211A - Session EM+AS+SS-MoM

Rectenna Solar Cells, MIM Diodes, and Oxide Interfaces
Moderator: John Conley, Oregon State University, Dale Kotter, RedWave Energy, Inc.

8:20am **EM+AS+SS-MoM1 Harvesting Energy with Optical Rectennas: Challenges and Innovations**, *Garret Moddel*, University of Colorado and RedWave Energy, Inc., *S. Joshi, B. Pelz, A. Belkadi, S. Yuan,* University of Colorado at Boulder, *P. Brady, D. Kotter,* RedWave Energy, Inc. **INVITED**
Optical rectennas are of interest for radiant heat and light energy harvesting, and ultra-fast detectors that work for terahertz waves up through visible-light wavelengths. The devices work under constraints that are different from those of either microwave rectennas or conventional solar cells. These antenna-coupled diodes incorporate micron-scale antennas and diodes that must operate at frequencies in the tens to hundreds of terahertz, but the antenna size and diode speed are not the most daunting challenges. The current produced by the antenna – particularly for rectennas operating at close to visible-light frequencies – samples the diode at discrete voltages described by a quantum approach instead of at continuously varying voltages described by classical electromagnetic theory – which makes for a fascinating theory of operation. The consequence is a quantum limit to the power conversion efficiency, similar to the Shockley-Queisser limit for conventional solar cells. The optical frequency and intensity determine whether the rectenna operation can be described classically or must involve a quantum analysis. Because rectennas gather current from the entire antenna, if the light is not spatially coherent cancellation occurs, resulting in reduced efficiency. This limits the amount of power received by each diode, which further limits the diode rectification efficiency. Over the last decade the number of groups investigating various parts of rectenna technology has grown from almost none to at least 50. This growing community of researchers, with innovative solutions, is needed to meet optical rectenna challenges and enable a practical technology. Some emerging solutions will be presented.

9:00am **EM+AS+SS-MoM3 Demonstration of Traveling-Wave Metal-Insulator-Metal Diodes for 28 THz (10.6 µ m) Rectennas**, *Bradley Pelz,* University of Colorado at Boulder, *G. Moddel,* University of Colorado at Boulder and Redwave Energy
Lumped element rectennas encounter an efficiency limitation above several terahertz due to the RC time constant of an MIM diode. A traveling-wave diode (TWD) takes advantage of nanoscale geometries to achieve a lower capacitance than that of a lumped element diode. The TWD behaves as a MIM transmission line for surface plasmons in which the rectification occurs as the wave travels down its length. Due to the distributed nature of the rectifier, the impedance seen by the antenna is the characteristic impedance of the transmission line. COMSOL simulations have shown this gives a reactive component of diode impedance that is substantially smaller than either the real component of the characteristic impedance for the TWD or the reactance from the parallel plate capacitance of an equivalently sized lumped element MIM diode. This allows for a much higher coupling efficiency from the antenna than in the case of a lumped element diode, and a substantially reduced RC time constant.

To obtain a resistance that matches that of the antenna simulations show that the TWD requires a width of 100 nm or less, which is too small for conventional lithography techniques. This small critical dimension was achieved using a germanium shadow mask technique. After fabrication, the DC junction characteristics were measured using a four-point technique. The open circuit voltage of these unbiased devices was measured under 28 THz illumination using a CO_2 laser and a lock-in amplifier. The TWD coupled to a bow tie antenna showed both polarization and power dependence. Since these measurements were completed at zero bias, the response could not have been bolometric, and the device must have been operating in energy harvesting mode.

9:20am **EM+AS+SS-MoM4 Basic Efficiency Limits for Rectenna Solar Power Conversion**, *Heylal Mashaal, J.M. Gordon,* Ben-Gurion University of the Negev, Israel
The prospect of employing aperture rectennas for solar power conversion will be explored in this presentation. Sunlight is commonly viewed as

incoherent – hence seemingly unsuitable for antenna harvesting – but all electromagnetic radiation exhibits spatial coherence on a sufficiently small scale. The first direct measurement of the spatial coherence of sunlight will be presented, and the ramifications for using optical concentrators that can effectively replace orders of magnitude of antenna and rectifier elements will be discussed.

Rooted in the partial spatial coherence of sunlight, a derivation of the thermodynamic limit for coherence-limited solar power conversion will be presented – an expansion of Landsberg's elegant basic bound, originally limited to incoherent converters at maximum flux concentration. The results do not depend on a particular conversion strategy. As such, they pertain to systems that span geometric to physical optics.

Last, a basic upper bound will be presented for the ability to rectify the broadband signals using a full wave rectification scheme.

Our findings indicate promising potential for rectenna power conversion.

9:40am **EM+AS+SS-MoM5 Coherence Effects in Periodic Arrays of Nano-Antennas used for Energy Harvesting and Self-Imaging**, *Peter Lerner,* SciTech Associates, LLC, *P.H. Culter, N.M. Miskovsky,* Penn State University
Coherence effects in periodic arrays of nano-antennas used for energy harvesting and self-imaging

P. B. Lerner [1] , N. M. Miskovsky[1,2] , P. H. Cutler[1,2]

Modern technology allows the fabrication of antennas with a characteristic size comparable to the electromagnetic wavelength in the optical region. [1] This has led to the development of new technologies using nanoscale rectifying antennas (rectennas) for solar energy conversion and sensing of terahertz, IR and visible radiation. For example, a rectenna array can collect incident radiation from an emitting source and the resulting conversion efficiency and operating characteristics of the device will depend on the spatial and temporal coherence properties of the absorbed radiation. For solar radiation, the intercepted radiation by a micro- or nano-scale array of devices has a relatively narrow spatial and angular distribution. Using the Van Cittert-Zernicke Theorem, we show that the coherence length (or radius) of solar radiation on an antenna array is, or can be, tens of times larger than the characteristic wavelength of the solar spectrum, i.e., the thermal wavelength, $\lambda_T = 2\pi\hbar c/(k_B T)$, which for T=5000K is about 2 microns. Such an effect is advantageous, making possible the rectification of solar radiation with nanoscale rectenna arrays, whose size is commensurate with the coherence length. Furthermore, using the van Cittert-Zernicke Theorem, we also examine the blackbody radiation emitted from an array of antennas at temperature T, which can be quasi-coherent and lead to a modified self-image, analogous to the Talbot-Lau self-imaging process [2] but with thermal rather than monochromatic radiation. This coherence of the antennas' blackbody radiation can also introduce an angular spectrum, which may be concentrated (enhanced) along certain spatial directions, giving rise to additional features not present in the original array. The self-emitted thermal radiation may be important as a non-destructive means for quality control of the array.

[1] Miskovsky, N. M., P. H. Cutler, A. Mayer, B. L. Weiss, B. Willis, T. E. Sullivan, and P. B. Lerner (2012) Nanoscale Devices for Rectification of High Frequency Radiation from the Infrared through the Visible: A New Approach, *Journal of Nanotechnology*, Article ID 512379, 19 pages, http://dx.doi.org/10.1155/2012/512379 .

[2] Gori, F. (1979) Lau Effect and Coherence Theory, *Optics Communications*, 31(1), 4.

1 SciTech Associates, Woodland Drive, State College, 16803.

2 Physics Department (emeritus), Penn State University, University Park, 16802.

10:00am **EM+AS+SS-MoM6 Metamaterial Enhanced Rectenna for Efficient Energy Harvesting**, *D. Lu, Won Park,* University of Colorado Boulder, *P. Brady,* Redwave Energy Inc.
Rectenna solar cell offers an important alternative to the conventional semiconductor solar cell technology. Direct rectification of electromagnetic radiation faces many challenges one of which is the high frequency of operation. Thermal emission from hot bodies peaks at 10 ~ 100 THz while solar radiation has its maximum at around 600 THz. One may circumvent this difficulty if sufficiently strong thermal radiation is available at lower frequencies. In general, thermal emission is described well by the theory of blackbody radiation while the property of the non-black surface is characterized by its emissivity. When the surface supports surface waves, however, the properties of thermal emission can deviate substantially from the blackbody radiation, offering a new avenue for engineering thermal emission. For example, spatially coherent and spectrally selective thermal emission may be achieved. The presence of surface waves also means

enhanced local density of states near the surface, which consequently leads to strongly modified thermal emission intensity and spectrum in the near field. In this paper, we report a metamaterial design to achieve enhanced thermal emission at 1 THz.

Two types of metamaterial designs were investigated: a 1D array of parallel trenches and a 2D array of holes etched on copper. The metamaterial surface was designed to support surface waves resembling the surface plasmon on metal surface. Numerical simulations by the finite element method confirmed the presence of surface waves and strong electric field near the surface at 1 THz. The strongly enhanced electric field is the direct consequence of enhanced local density of states. To further confirm the surface modes can be excited by thermal emission, we also conducted finite-difference time-domain simulations in which thermal emission was calculated by using the fluctuation dissipation theorem. Once the enhanced thermal emission is confirmed, a bowtie antenna was placed close to the metamaterial surface to capture the enhanced thermal emission in the near field. The antenna was optimized to maximize the electromagnetic energy delivered to the antenna gap. Since the antenna should couple efficiently with the surface modes, the optimal antenna design became quite different from the free space bowtie antenna operating at the same frequency. The optimized metamaterial and antenna design resulted in an antenna voltage of 10 mV at 1 THz, three orders of magnitude larger than the free space antenna. Such a large enhancement makes the metamaterial approach a highly promising route to efficient energy harvesting with rectenna.

11:00am EM+AS+SS-MoM9 Modeling of and Power from Nb-NbOx-based Nanorectenna Arrays, *Richard M. Osgood*, US Army NSRDEC, *J. Xu, G.E. Fernandes,* Brown University, *M. Rothschild, K. Diest,* MIT Lincoln Laboratory, *M. Kang, K.B. Kim,* Seoul National University, Republic of Korea, *L. Parameswaran,* MIT Lincoln Laboratory, *P. Periasamy,* IBM, *M. Chin,* Army Research Laboratory, *S. Kooi,* MIT Institute for Soldier Nanotechnologies, *S. Giardini,* US Army NSRDEC, *R. O'Hayre, P. Joghee,* Colorado School of Mines

We investigate arrays of "microrectennas" (with sub-micron features tuned for the near-and short-wave infrared) consisting of "stripe-teeth" metamaterial antennasconducting vertically through the coupled, underlying metal-insulator-metal (MIM) diode into a metallic substrate. Stripes, with cross-stripe resonances, conduct current out of the array, while antenna-like teeth break left-right symmetry and concentrate a high vertical electric field (E_z) at the end of the teeth at their antenna resonance. If plasmonic field enhancement and concentration reduce the capacitance and/or increase the effective voltage across the MIM diode, new research and development of large-area ultrafast optical rectennas will be enabled, requiring patterning and alignment of only the top metal layer.

Stripe-teeth arrays were designed, fabricated, and analyzed both experimentally and theoretically. Substrates were layers ("ground planes") of Nb and Al, and a Au nanowire array patterned using novel high-throughput e-beam technology.[1] Substrates were oxidized/anodized, or had oxides deposited, to form microantenna-coupled MIM diodes consisting of Al-Al$_2$O$_3$-Al, Au/Ti-NbO$_x$-Nb, Al-Al$_2$O$_3$-Au, Ag/Ti-NbO$_x$-Nb, Ag/Ti-NiO-Ni, Pt-NbO$_x$-Nb, after deposition of top metal layers of Ag/Ti, Au/Ti, Pt, and Al (only a few nm of Ti). Conduction through 10-25 nm thick oxide layers in the MIM diodes occurred via quantum mechanical tunneling and thermionic emission, with asymmetric barrier heights all less than 1 V except for the Al-Al$_2$O$_3$-Al diodes. The Au-Al$_2$O$_3$-Al system required modeling the "hot spot" from top metal protrusions into the Al$_2$O$_3$barrier layers and in close (tunneling) proximity to the ground plane, probably because of the surface roughness and variation in Al$_2$O$_3$ thickness; the planar-planar MIM diode model was inapplicable in this case.

The top metal was patterned into the stripe-teeth arrays. Reflective Al substrates provided sharp optical antenna resonances while Nb layers produced broader, weaker antenna resonances due to Nb absorption, similar to stripe-only arrays reported in Ref. 2. We also report the result of visible light (514 nm – 630 nm) laser illumination of Nb/NbO$_x$/Ag(Ti) stripe-teeth arrays, including the observation of a short-circuit current and open-circuit voltage, in response to power densities in the range 80 W/cm^2.

1. H. S. Lee, *et. al.*, "Electron beam projection nanopatterning using crystal lattice images obtained from high resolution transmission electron microscopy", Adv. Mats. **19** 4189 (2007).

2. Wu, C., *et.al.*" Large-area wide-angle spectrally selective plasmonic absorber," *Phys. Rev. B*, Vol. 84, 075102-7, 2011.

11:20am EM+AS+SS-MoM10 Metal-Insulator-Insulator-Metal Diodes for Rectenna Applications, *Shijia Lin*, N. Murari, J.F. Conley, Jr., Oregon State University

A metal-insulator-metal (MIM) tunnel diode has a capacitor-like structure with a thin insulating layer sandwiched by two metals. Because of their potential for femtosecond-fast transport when dominated by tunnel transport, MIMs are of interest for rectenna based solar cells, hot electron

transistors, and IR detectors. The common strategy to achieving rectification in MIM devices relies on the use of dissimilar work function metal electrodes to produce an asymmetric electron tunneling barrier with polarity dependent tunneling probability. The performance of single layer MIM devices is limited by the workfuction difference that can be achieved between the electrodes and the metal-insulator band offsets. Small electron affinity oxides are limited by high V_{ON}. Large electron affinity dielectrics have small V_{ON}, but tend to have limited asymmetry due to thermal emission dominated conduction. An alternative approach to controlling asymmetry is to use nanolaminate pairs of insulators with different bandgaps and band offsets to produce asymmetric tunnel barrier metal-insulator-insulator-metal (MIIM) diodes. Asymmetry in MIIM devices may be enhanced by step tunneling[1] or defect enhanced direct tunneling.[2]

In this work, we investigate asymmetry in HfO$_2$/ Nb$_2$O$_5$ bilayer insulator MIIM diodes. HfO$_2$ and Nb$_2$O$_5$ were deposited via atomic layer deposition (ALD) using tetrakis (ethylmethylamino) hafnium (TDMAHf) and niobium ethoxide metal precursors, respectively with H$_2$O as the oxidant. Nanolaminate films were deposited at a chamber temperature of 250°C in one continuous run without breaking vacuum. Sputtered TaN or amorphous metals were used as the bottom electrode and evaporated Al dots were used as a top electrode. MIIM I-V asymmetry and non-linearity are shown to be a function of stack thickness, relative layer thickness, and insulator layer position with respect to the electrodes. Overall, bilayer insulators are shown to be an effective method of enhancing the performance of MIIM tunnel diodes.

1. N. Alimardani and J.F. Conley Jr, Appl. Phys. Lett. 102, 143501 (2013).

2. N. Alimardani and J.F. Conley, Jr., Appl. Phys. Lett. 105, 082902 (2014).

11:40am EM+AS+SS-MoM11 Built-in Potential in Fe$_2$O$_3$-Cr$_2$O$_3$ Superlattices for Improved Photoexcited Carrier Separation, *Tiffany Kaspar*, D.K. Schreiber, S.R. Spurgeon, S.A. Chambers, Pacific Northwest National Laboratory

Hematite, α-Fe$_2$O$_3$, is an ideal photocatalyst to split water as a source of H$_2$ fuel because it is non-toxic, Earth-abundant, stable in aqueous environments, and possesses a bandgap in the visible wavelength range (~2.1 eV). However, fast photogenerated electron-hole recombination, facilitated in part by slow carrier transport kinetics, has long been identified as a major obstacle in the utilization of hematite photocatalysts. A direct method to reduce photogenerated carrier recombination is to employ heterojunctions to spatially separate excited electrons and holes. Our approach is to engineer built-in electric fields by exploiting the band alignment characteristics of epitaxial Fe$_2$O$_3$/Cr$_2$O$_3$ heterojunctions. The Fe$_2$O$_3$-Cr$_2$O$_3$ system exhibits non-commutative band offsets which differ by approximately 0.4 eV depending on the order of deposition. The non-commutative band offset properties of Fe$_2$O$_3$-Cr$_2$O$_3$ interfaces can be utilized in a superlattice structure, deposited by oxide molecular beam epitaxy, to build up an intrinsic electric field; this potential may be sufficient to spatially separate photogenerated electrons and holes. We demonstrate precise control over the Fe$_2$O$_3$-Cr$_2$O$_3$ interface structure with atomic-resolution atom probe tomography and scanning transmission electron microscopy. Direct evidence that Fe$_2$O$_3$-Cr$_2$O$_3$ superlattice layers generate an intrinsic built-in potential is observed with x-ray photoelectron spectroscopy. The individual interfacial band offset values, and thus the overall potential, can be tailored by altering the cation stoichiometry at the interfaces. Doping the component layers to improve transport characteristics requires a deep understanding of the dopant-induced electronic structure changes. To illustrate how the built-in potential in optimized Fe$_2$O$_3$-Cr$_2$O$_3$ superlattice structures can be harnessed to drive holes to the surface and electrons into the bulk, photoconductivity and photochemical degradation results will be presented.

Energy Frontiers Focus Topic
Room: 211B - Session EN+AS+EM+NS+SE+SS+TF-MoM

Solar Cells I
Moderator: Jason Baxter, Drexel University, Chintalapalle Ramana, University of Texas at El Paso

8:20am EN+AS+EM+NS+SE+SS+TF-MoM1 Elevated Temperature Phase Stability of CZTS-Se Thin Films for Solar Cells, *E. Chagarov, K. Sardashti,* University of California at San Diego, *D.B. Mitzi,* Duke University, *R.A. Haight,* IBM T.J. Watson Research Center, *Andrew C. Kummel*, University of California at San Diego

Density-functional theory simulations of CZTS, CZTSe and CZTS$_{0.25}$Se$_{0.75}$ photovoltaic compounds have been performed to investigate stability of

CZTS$_{0.25}$Se$_{0.75}$ alloy vs. decomposition to CZTS, CZTSe and other secondary compounds. The Gibbs energy for vibration contribution was estimated by calculating phonon spectra and thermodynamic properties at finite temperatures. It was demonstrated that CZTS$_{0.25}$Se$_{0.75}$ alloy is stabilized not by enthalpy of formation but by vibration and mixing contributions to the Gibbs energy. A set of phase diagrams was built in multidimensional space of chemical potentials at 300K and 900K temperatures to demonstrate alloy stability and boundary compounds at various chemical conditions. The Gibbs energy gain/loss for several decomposition reactions was calculated as a function of temperature with/without Cu/Zn intermixing and vibration contributions to the Gibbs energy demonstrating CZTS$_{0.25}$Se$_{0.75}$ that even defect-free (no Cu/Zn intermixing) CZTS$_{0.25}$Se$_{0.75}$ can be stable at typical processing temperatures.

8:40am EN+AS+EM+NS+SE+SS+TF-MoM2 Chemical and Electrical Characterization of Polycrystalline CZTS,Se and CIGS,Se Grain Boundaries by NanoAuger and Kelvin Probe Force Microscopy (KPFM), *Kasra Sardashti*, UC San Diego, *P.D. Antunez, R.A. Haight*, IBM T.J. Watson Research Center, *A.C. Kummel*, UC San Diego

Polycrystalline Copper-zinc-tin-sulfide/selenide (CZTS,Se) compounds have received wide research interest due to their potential as inexpensive absorber materials composed of earth-abundant elements. Photovoltaic devices fabricated on CZTS,Se have reached conversion efficiencies of 12.6 %. One of the key parameters to further boost the conversion efficiency is to control the concentration of recombination sites at the surface, secondary phase interfaces and in the grain boundaries. To determine the presence of secondary phases on the surface and composition of grain boundaries, this work has employed Auger nanoprobe electron spectroscopy (NanoAuger) with 8nm lateral resolution combined with high resolution ambient Kelvin Probe Force Microscopy (KPFM) with dual-lock-in setup. NanoAuger was performed in planar and cross-sectional modes on CZTS,Se surfaces before and after top surface oxide removal by NH$_4$OH clean. Elemental maps before and after NH$_4$OH clean show Sn-/O-rich and Cu-poor grain boundaries suggesting that grain boundaries are terminated by tin-oxide (SnOx). Secondary phases such as SnSe and ZnSe were observed in the cross-sectional maps. Kelvin probe force microscopy (KPFM) on the cleaned surfaces showed that SnOx-terminated grain boundaries have 80-200 mV larger work function than grains, resulting in upward band bending between grains and grain boundaries. The upward band bending accompanied by the large valence band offset between the SnOx and CZTS,Se lead to relatively large energy barriers for both electrons and holes to travel into the grain boundaries and recombine. Comparison with the elemental maps for CIGSe (with device efficiencies as high as 18%) revealed the absence of the grain boundary oxide passivation.

9:40am EN+AS+EM+NS+SE+SS+TF-MoM5 Spin Coating Thin Film CZTS for Efficient, Low-Cost Solar Cells on Flexible Glass Substrates, *D. Kava, J. Galindo, C.O. Sana, S. Shahriar, Deidra Hodges*, University of Texas at El Paso

Photovoltaic's contribution to energy production continues to grow as costs continue to decrease. As silicon cells approach their limits, other materials are emerging. The development of Cu$_2$ZnSnS$_4$ (CZTS) thin film solar cells using non-vacuum liquid-based spin coating techniques have been previously investigated. The focus of this paper is the optimization of p-type CZTS thin film solar cells onto flexible substrates. Flexible solar panel costs are higher than their traditional counterparts. CZTS currently reports only a 3.2% efficiency on flexible glass, while the record for CZTS on non-flexible substrates is 12.6%. The cells are created using a single solution ink sol–gel method. All metals are dissolved in a single step prior to deposition onto substrates (nickel foil and corning willow glass) as a thin film. Corning Willow glass is a new material introduced recently to the market, while nickel is a inexpensive flexible reflective foil. The Corning Willow glass is coated with a molybdenum layer as a reflective back contact layer. By using a single step and a solution deposition method, lower production cost are achievable. For thin film deposition, we used a non-vacuum spin coater (WS650 spin processor, Laurell Technologies) with an optimized spin coat programming. Annealing took place under vacuum in a RTP furnace while time, temperature and ramp functions were varied. The other layers of the device consists of cadmium sulfide n-type window layer and a zinc oxide doped with aluminum transparent top contact layer. Characterization and analysis of the thin films were performed using Raman spectroscopy, scanning election microscope (Zeiss NEON 40), X-ray diffraction (Philipps X'Pert), proflimeter (Veeco Dektak 150), UV-Vis-NIR Spectrophotometer (Carry 5000), Hall Effect measurement system (HMS3000) and 4 point probe (Lucas Labs) measurements. Results show CZTS thin film solar cells on flexible glass is obtainable.

10:00am EN+AS+EM+NS+SE+SS+TF-MoM6 Band Gap Profile of Cu(In,Ga)(Se,S) 2 Thin Films via High-Resolution Reflection Electron Energy Loss Spectroscopy, *Sung Heo, H.I. Lee, J.B. Park, G.S. Park*, Samsung Advanced Institute of Technology, Republic of Korea, *D.H. Lee, J.G. Nam*, Samsung, Republic of Korea, *H.J. Kang*, Chungbuk National University, Republic of Korea, *B.D. Choi*, Sungkyunkwan University, Republic of Korea

Cu(In,Ga)Se$_2$ (CIGS)-based solar cells was investigated with an aim of enhancing cell performance because these cells provided high conversion efficiency at relatively low cost. The efficiency of CIGS cells has recently approached 19.7% at small sizes. In general, Cu(In$_{1-x}$,Ga$_x$)(Se$_{1-y}$S$_y$)$_2$(CIGSS) composition profiles are double-graded, and they can improve the open-circuit voltage (V$_{OC}$) and the efficiency of solar cells because band gaps increase toward both the surface (i.e., with the increase of sulfur) and the bottom (i.e., with the increase of gallium). It is important to accurately measure the band gap at the top and the bottom of the CIGSS cell. Nevertheless, the band gap profile measurement of the CIGSS as a function of depth is challenging.

In this study, we obtained the depth profile of the CIGSS cell using the quantitative Auger Electron Spectroscopy method, for which the relative sensitivity factor was corrected using the inductively coupled plasma-atomic emission spectrometry (ICP-AES) method. We also measured the band gap directly using high-resolution reflection electron energy loss spectroscopy (HR-REELS) with a monochromatic electron gun, which has low electron energy at 300 eV.

For the direct measurement of a band gap profile, HR-REELS spectra were obtained as a function of depth during Ar ion sputtering at 3.0 kV. The band gap profile shows a double-graded band gap as a function of depth. The band gap values are 1.32 eV at the surface (E$_{g1}$), 1.08 eV at the depth between 0.3 and 0.7μm (E$_{g\ min.position}$), and 1.50 eV at the depth of about 2.2 μm (E$_{g2}$), respectively. Our findings suggest a new analytical method which directly determines the band gap profile as function of depth.

10:40am EN+AS+EM+NS+SE+SS+TF-MoM8 Spatial Atmospheric ALD of Zinc Oxysulfide Buffer Layers for CIGS Solar Cells, *C. Frijters, P.J. Bolt, P. Poodt, Andrea Illiberi*, Solliance/TNO, Netherlands

Copper Indium Gallium di-Selenide (CIGS) solar cells are a promising approach in photovoltaic technology, having low production costs, high conversion efficiencies (> 20 %), as well as the possibility to manufacture them on flexible substrates. State-of-the-art in CIGS solar cells manufacturing is to use a stack of CdS, intrinsic ZnO (*i*-ZnO) and an Al-doped ZnO TCO on top of the CIGS film. Replacement of CdS by a non-toxic Cd-free layer with wider band gap (> 2.4 eV) would *a)* decrease the production cost by avoiding the expensive treatment of toxic wastes and *b)* increase the overall cell efficiency by enhancing the quantum efficiency in the blue range. Moreover, the use of a "soft" and highly conformal deposition technique is preferred to improve the electrical properties of the buffer layer/CIGS interface.

In this paper we present spatial atmospheric atomic layer deposition of a Zn(O,S) buffer layer as CdS replacement for CIGS solar cells. Spatial ALD is emerging as an industrially scalable deposition technique at atmospheric pressure which combines the advantages of temporal ALD, i.e. excellent control of film composition and uniformity on large area substrates, with high growth rates (up to nm/s). Films are grown by sequentially exposing the substrate to oxygen and sulfur precursors (H$_2$O, H$_2$S) and the zinc metal precursor (i.e., DEZn). By controlling the kinetics of surface reactions between evaporated precursors and reactive sites at the film surface, the composition of Zn(O,S) can be precisely tuned. The incorporation of S into ZnO results in a bowing of the band gap in the range from 3.3 eV (ZnO) to 2.7 (S/O+S ~ 0.5) and 3.4 eV (ZnS), as measured by spectrophotometry. The morphology of the Zn(O$_{x-1}$,S$_x$) films varies from polycrystalline (for 0<x<30 and 70<x<100) to amorphous (30<x<70), as measured by X-ray diffraction. CIGS solar cells with a Spatial ALD Zn(O,S) buffer layer show an increased spectral response around 400 nm compared to solar cells with a CdS buffer layer. The solar cells with the Zn(O,S) buffer layer had an efficiency of 15.9 %, compared to 15.5 % for the reference solar cells with a CdS buffer layer.

11:00am EN+AS+EM+NS+SE+SS+TF-MoM9 Deep Level Electron Traps in Epitaxial CuInSe$_2$ Probed using Photo-Modulated X-ray Photoelectron Spectroscopy, *Nicole Johnson*, University of Illinois at Urbana-Champaign, *P. Aydogan*, Bilkent University, Turkey, *A. Rockett*, University of Illinois at Urbana-Champaign, *S. Suzer*, Bilkent University, Turkey

Performance in a variety of electronic devices is largely controlled by minority carrier charge capture on point defects. To date there is no experimental method to directly identify these point defects in a chemically specific fashion. Photo-modulated X-ray Photoelectron Spectroscopy (XPS)

utilizes the chemical and charge sensitivity of XPS to identify changes in peak shape due to changing atomic charge state from capture of light-generated minority carriers. Epitaxial thin films of CuInSe$_2$ (CIS) were chosen as a case study for this technique because their defect chemistry is still relatively unknown as compared to traditional solar cell materials. The 500-1000nm thick films were grown by a hybrid sputtering and evaporation technique on GaAs(001) substrates at600-700°C. Aligned surface morphology features matching the substrate geometry in scanning electron microscopy (SEM) images indicate epitaxial growth, which was confirmed by x-ray diffraction (XRD).A layer of CdS was deposited on the CIS via chemical bath deposition to protect the CIS surface from oxidation in storage and to duplicate the heterojunction used in solar cells. Prior to loading in the XPS, the CdS was etched off to expose a Cd doped CIS surface for analysis. The photo-modulated XPS used monochromatic AlKα x-rays with a 532 nm laser as the illumination source. Under illumination, each film constituent was observed to exhibit unique binding energy shifts. Based on their peak shifts relative to the surface photovoltage profile, Cd and In were found to be right at the surface while Cu and Se were deeper into the film, consistent with a Cd-doped, In-rich surface. The technique is therefore shown to provide a chemically-sensitive depth profile non-destructively that can be obtained even on a relatively rough sample. Additionally, shape changes in the Se 3d doublet spectra indicate electron capture in a deep trap state that is likely due to cation vacancies. Measurements at varying temperatures indicate air-induced surface recombination states are passivated by annealing at 80C, allowing the surface photovoltage to persist. At 230C, an irreversible change happens in the surface properties such that the surface photovoltage gets much smaller and reverses sign. This work was supported by a joint NSF-TUBITAK collaborative research project (NSF Grant No: 1312539 TUBITAK Grant No: 212M051).

11:20am EN+AS+EM+NS+SE+SS+TF-MoM10 The Role of ZnTe Buffer Layers on the Performance and Stability of CdTe Solar Cells, *Jiaojiao Li*, Colorado School of Mines, *A. Abbas,* Loughborough University, UK, *D.M. Meysing, J.D. Beach, D.R. Diercks,* Colorado School of Mines, *M.O. Reese, T.M. Barnes,* National Renewable Energy Laboratory, *C.A. Wolden,* Colorado School of Mines, *J.M. Walls*, Loughborough University, UK

The use of ZnTe buffer layers at the back contact of CdTe solar cells has been credited with contributing to recent improvements in both record cell efficiency and module stability. To better understand the underlying reasons high resolution transmission microscopy (HR-TEM) and atom probe tomography (APT) were used to study the evolution of the back contact region before and after rapid thermal activation of this layer. During activation the 150 nm ZnTe layer, initially nanocrystalline and homogenous, transforms into a bilayer structure consisting of an amorphous region in contact with CdTe characterized by significant Cd-Zn interdiffusion, and a crystalline layer that shows evidence of grain growth and twin formation. This graded layer may passivate interface defects and account fo the improved open circuit voltage and fill factor that accompanies the RTP activation step. Copper, co-evaporated uniformly within ZnTe, is found to segregate dramatically after rapid thermal activation, either collecting near the ZnTe|Au interface or forming Cu$_x$Te clusters in CdTe at defects or grain boundaries near the interface. Further examination of the Cu$_x$Te clusters revealed that they are encased in a thin layer of Zn, and it is postulated that this structure may limit the extent of diffusion into CdTe and play an important role in device stability.

11:40am EN+AS+EM+NS+SE+SS+TF-MoM11 The Performance and Durability of Broadband Anti-Reflection Coatings for Thin Film CdTe Solar Cells, *G. Womack, P.M. Kaminski, John Walls*, Loughborough University, UK

Light reflection from the glass surface of a photovoltaic (PV) module is a significant source of energy loss for crystalline silicon and all types of thin film PV devices. The reflection at the glass and air interface accounts for ~4% of the total energy. Single layer anti-reflection coatings using magnesium fluoride or porous silica with sufficiently low refractive index have been reported but these are only effective over a narrow range of wavelengths. In this paper we report on the design, deposition and testing of multilayer broadband anti-reflection coatings that reduce the weighted average reflection over the wavelength range used by thin film CdTe devices to ~1.22% resulting in a useful 3.6% increase in photocurrent. In this study we have used multilayer stacks consisting of silica and zirconia layers deposited using a reactive magnetron sputtering process. Details of the stack design, sputtering process parameters and the optical and micro-structural properties of the layers are provided.

Thin film CdTe devices pose a special problem because the anti-reflection coating is applied to one side of the glass while device layers are deposited directly on to the opposite glass surface in the superstrate configuration In thin film CdTe production, the glass is exposed to high temperature processes during the absorber deposition and during the cadmium chloride activation treatment. If glass pre-coated with a broadband anti-reflection coating is to be used then the coating must withstand temperatures of up to ~550°C. Surprisingly, our studies have shown that multilayer silica/zirconia anti-reflection coatings on soda lime glass remain unaffected by temperatures up to 600 °C at which point mild crazing is observed. This is an important observation since it means that low cost glass which is pre-processed with a broadband anti-reflection coating by glass manufacturers is potentially useable in thin film CdTe module production

In-Situ Spectroscopy and Microscopy Focus Topic
Room: 211C - Session IS+AS+SS-MoM

Fundamental Studies of Surface Chemistry of Single Crystal and Nanomaterials under Reaction Conditions
Moderator: Franklin (Feng) Tao, University of Kansas, Zili Wu, Oak Ridge National Laboratory

8:20am **IS+AS+SS-MoM1 Hot Electron In-Situ Surface Chemistry at Oxide-Metal Interfaces. Foundations of Acid-Base Catalysis**, *Gabor Somorjai*, University of California, Berkeley **INVITED**
The development of Catalytic Metal-Semiconductor Nanodiodes (CMSN) to measure the flow of electrons excited during exothermic catalytic reactions at the metal interface proved that oxidation on platinum generates a steady flux of hot electrons [1] Evidence is presented that the steady state of chemicurrent is correlated to the turnover frequency and that the exothermic hot electron production during reactions on transition metal particles may be widespread. The CO/O2 and H2/O2 reactions were studied most frequently by this method and semiconductors included TiO2, GaN, CoOx, NbOx and TaOx Charge transport between the metal and oxide interfaces also influences the product distribution of multipath reactions. These were shown in the hydrogenation of furfural and croton aldehyde at platinum/TiO2 interfaces as compared to the platinum/silica interfaces [2]. The oxide-metal interfaces appear to produce ions, which carry out reactions that have long been called by the organic chemistry community as acid base catalysis. The typical catalytic structure is mesoporous oxide that is produced to hold the metal nanoparticles. The structures produce high surface area oxide metal interfaces and this is a catalytic architecture for acid base catalysis. Studies in changing the transition metal oxide using a single metal of platinum as nanoparticles, shows the tremendous amplification effect of the oxide metal interfaces in the reactions such as the carbon monoxide oxidation. Platinum alone produces on silica three orders of magnitude less CO2 by the CO oxidation process than on cobalt oxide, that is the most active of these acid base oxide metal interface catalytic systems [3]. Nevertheless, not just cobalt oxide, but nickel oxide, manganese oxide, and iron oxide, produces much higher activity for this reaction than platinum alone. In other reactions, when n-hexane isomerization or cyclisation reactions studied, the pure oxides niobium or tantalum do not produce any reaction other than cracking two smaller molecular fragments. However, at the platinum-oxide interfaces with niobium oxide or tantalum oxide, almost 100% selectivity for isomerization could be achieved [4]. Thus it appears that charge catalysis plays a very important role, which is equal in importance to the role of pure metal covalent catalysis that produces molecules without any apparent charge flow. Generation of hot electron flows and the catalytic activity of two-dimensional arrays of colloidal Pt nanoparticles with different sizes are investigated using catalytic nanodiodes. Pt nanoparticles of smaller size lead to higher chemicurrent yield, which is associated with the shorter travel length for the hot electrons, compared with their inelastic mean free path [5]. In many oxide supports microporous sites are used, which are less than 1 nm in size and do not allow the larger platinum nanoparticles inside these pores. In that case, the metal that is used to create the catalysts are deposited on the outside surface of the microporous support. This sort of system, where the metal is outside, but the acidic microporous oxides are inside, can be active only by a spill over of the reaction intermediates from the metal to the oxide - and this is quite well known. However if the micropores are substituted by mesopores in the oxide phase the metal nanoparticles can go inside and then single site oxide-metal interface catalysis commences. These two different catalytic processes, where both the oxide and the metal are catalytically active, deserve attention and distinction.

9:00am IS+AS+SS-MoM3 In-situ GISAXS/GIXAS Characterization of $Co_{1-x}Pt_x$ Bimetallic Clusters under H_2 and $CO + H_2$ Mixture, *Bing Yang*, Material Science Division, Argonne National Laboratory, *G. Khadra, J. Tuaillon-Combes*, Institut Lumière Matière, University Lyon & CNRS, France, *E. Tyo*, Material Science Division, Argonne National Laboratory, *S. Seifert*, X-ray Science Division, Argonne National Laboratory, *X. Chen*, Department of Mechanical Engineering, Northwestern University, *V. Dupuis*, Institut Lumière Matière, University Lyon & CNRS, France, *S. Vajda*, Material Science Division, Argonne National Laboratory

CoPt alloy particles have recently attracted great interests for their excellent catalytic and magneticproperties. The alloy phase of cobalt and platinum may create dual-functional sites at the mixed interface which enables novel catalytic properties and synergic effect at nanometer scale. In-situ characterization is thus essential to probe the structure and composition of bimetallic clusters under reaction conditions in a catalytic process of interest.

$Co_{1-x}Pt_x$ bimetallic clusters with atomic-precise Pt/Co atomic ratio (x=0, 0.25, 0.5, 0.75, 1) were synthesized using mass-selected low energy clusters beam deposition (LECBD) technique and soft-landed onto the amorphous alumina thin film prepared by atomic layer deposition (ALD). The median diameter of size-selected $Co_{1-x}Pt_x$ alloy clusters is 3nm with size dispersion lower than 10 % according to transmission electron microscopy (TEM). Utilizing X-ray photoemission spectroscopy (XPS), the oxidation state of as-made clusters as well as the aged particles after extended exposure to air was characterized. After exposure to air, both cobalt and platinum species in the bimetallic clusters are found to be oxidized, while the shift of their covalent state exhibits a non-linear correlation with their atomic composition (Pt/Co).

Utilizing *in-situ* grazing incidence small-angle X-ray scattering and X-ray absorption spectroscopy (GISAXS/GIXAS), the evolution of particle size/shape and the oxidation state of the individual metals are monitored under atmosphere reaction conditions. The as-made $Co_{1-x}Pt_x$ clusters were first pretreated with hydrogen and further exposed to CO and H_2 mixture up to 225°C. The change in the oxidation state of Co and Pt of the supported bimetallic clusters exhibited a non-linear dependency on the Pt/Co atomic ratio. For example, low Pt/Co ratio (x≤0.5) facilitates the formation of $Co(OH)_2$, whereas, high Pt/Co ratio (x=0.75) stabilizes Co_3O_4 composition instead, due to the formation of Co@Pt core-shell structure where the platinum shell inhibits the reduction of cobalt in the core of the $Co_{1-x}Pt_x$ alloy clusters.

In this work, we have demonstrated *in-situ* measurement of particle size/shape and the oxidation state of supported $Co_{1-x}Pt_x$ bimetallic clusters under operating conditions, and elucidated the different surface structure and chemical state with respect to their atomic ratio. The obtained results indicate ways for optimizing the composition of binary alloy clusters for catalysis.

9:20am IS+AS+SS-MoM4 Novel Surface Oxide on Pt(111) as the Active Phase for NO and CO Oxidation Studied with the ReactorSTM, *Matthijs van Spronsen*, J.W.M. Frenken, I.M.N. Groot*, Leiden University, Netherlands

Platinum finds its main application as a car catalyst to control the emission of exhaust gases. Although automotive catalysis has been extensively investigated, challenges still exist. One of the challenges arises when increasing the oxygen/fuel ratio. Under oxygen-rich reaction conditions, much uncertainty exist about the structure of the active surface phase. This is even true for the Pt(111) surface, which is the facet lowest in energy and the simplest model catalysts available.

An early *operando* Scanning Tunneling Microscopy (STM) study [1] showed a stepwise increase in CO oxidation activity at oxygen-rich conditions. This increase concurred with a dramatic and instantaneous morphology change. From the STM images, the atomic structure could not be resolved, but roughening on a long length scale was observed. Under similar conditions, Surface X-ray Diffraction found the formation of thin, bulk-like α-PtO_2 [2]. Surprisingly, a theoretical study concluded that this oxide is inert to CO oxidation [3].

With the high-pressure, high-temperature ReactorSTM [4], we studied the oxidation of Pt(111) both by exposing to O_2 and to NO oxidation conditions.

Upon oxidation with O_2 (1.0 bar, 423-523 K), we found a stable surface oxide consisting of triangles assembled in a 'spoked-wheel' superstructure. In addition, we found a second structure consisting of a lifted-row pattern. The two structures were coexisting on different regions on the surface. The lifted-row structure was becoming more predominant at higher O_2 pressure. We propose that both oxides share the same building block, which are expanded Pt oxide rows.

After evacuation of the reactor, the ordered structures disappeared, although some remnants remained. The surface oxidation is a clear example of the pressure-gap effect. Furthermore, lower-temperature (291-323 K) experiments did not yield any ordered structure showing the dependence on atomic mobility.

Exposure of Pt(111) to NO and O_2 or exposure to NO_2 resulted in the formation of a mixture of small domains of both the spoked-wheel and the lifted-row structures.

The surface oxidation was accompanied with roughening of terraces. This is attributed to relaxation of adsorbate-induced stress on the surface. Identical roughness development was previously found under CO oxidation conditions [1]. Therefore, we argue that a surface oxide was also the relevant structure under CO oxidation conditions.

[1] Bobaru, PhD thesis, Leiden University, 2006

[2] Ackermann, PhD thesis, Leiden University, 2007

[3] Li & Hammer, Chem. Phys. Lettt., 409, 1, 2005

[4] Herbschleb, *et al*., Rev. Sci. Instrum., 85, 083703, 2014

9:40am IS+AS+SS-MoM5 *In Operando* Study of Dimethyl Methylphosphonate Degradation Over Metallic and Oxidized Cu(111) Surfaces via Ambient-Pressure X-ray Photoelectron Spectroscopy, *Lena Trotochaud, A.R. Head*, Lawrence Berkeley National Laboratory (LBNL), *Y. Yu*, University of Maryland, *O. Karslioglu, M. Hartl*, LBNL, *B. Eichhorn*, University of Maryland, *H. Bluhm*, LBNL

Filtration systems for absorption and decomposition of chemical warfare agents (CWAs) are the first line of defense against exposure to these toxic compounds. Composite materials (such as ASZM-TEDA) commonly used in filtration systems consist of high-surface-area carbon supports impregnated with various metals and metal oxides. Despite decades of work to develop highly effective and versatile filtration materials with long-term usability, little is known about the mechanisms of CWA degradation by material surfaces and catalyst deactivation and poisoning, in part due to the challenges involved with spectroscopic characterization of catalyst surfaces under operating conditions. Enabling the rational design of more advanced filtration and decomposition materials for broad-spectrum protection against CWAs and other toxic industrial compounds requires a sophisticated understanding of the chemical mechanisms behind CWA sorption and degradation on the molecular scale.

We will present the surface spectroscopic study of metallic and oxidized Cu(111) single crystal surfaces for catalytic decomposition of dimethyl methylphosphonate (DMMP), a CWA simulant. Ambient-pressure X-ray photoelectron spectroscopy (APXPS) enables examination of these surfaces during DMMP adsorption and decomposition. Initial experiments indicate that adsorption of DMMP on Cu(111) is observed at pressures as low as 1×10^{-7} Torr, and degradation of DMMP is observed at this pressure and higher (60 mTorr) at room temperature. Possible mechanisms of DMMP degradation and deactivation of the surface will also be discussed.

10:00am IS+AS+SS-MoM6 Bridging the Pressure and Materials Gap between Surface Science and Catalysis: Probing the Surface of Metal Oxide Nanoparticles under Reaction Conditions, *Maria Kipreos, M. Foster*, University of Massachusetts, Boston

Traditionally, surface science employs ultra-high vacuum, cryogenic conditions and well defined crystal planes; however, heterogeneous catalysis and photocatalysis occur in ambient conditions with complex substrates composed of several crystal planes. Consequently, materials and pressure gaps exist that need to be bridged in order to better understand the surface chemistry of catalysts under reaction conditions. Metal oxide particles employed in catalysis contain a complex matrix of crystal planes, metal/oxygen bonds, metal/hydroxyl bonds, and oxide/water interactions. We utilize *in situ* Diffuse Reflectance Infrared Fourier Transform Spectroscopy (DRIFTS) to monitor reactions from ambient to high pressures between gaseous adsorbates (water, formic acid, and methanol) and metal oxide particles (TiO_2 and ZnO, semiconductors and ZrO_2, an insulator) commonly used as components of catalysts. The internal and external scattering of light that occurs in DRIFTS is well suited for analysis of reactions on the surface of metal oxide nanoparticles. Spectral shifts in frequency, peak area and width values, and absorbance values are used to interpret the structure and reactivity of the surface. Additionally, the use of Confocal Raman Spectroscopy aids in determining the structural variability in these substrates. The use of gaseous probes and these instrumental techniques provides a better understanding of the structure and reactivity of solid nanoparticles surfaces.

---

* Morton S. Traum Award Finalist

10:40am IS+AS+SS-MoM8 The Use of Integrated *Operando, In Situ* and DFT Techniques to Unravel the Steps of Heterogeneous Catalytic Reactions, *Fabio Ribeiro, W.N. Delgass, J. Greeeley, R. Gounder, J. Miller,* Purdue University, *W.F. Schneider,* University of Notre Dame **INVITED**

Our quest to understand catalysis is limited by our ability to observe the active site while it is turning over. To facilitate this task we developed model catalysts where the active sites are deposited on the external surface area of an appropriate support. Effective characterization, however, happens only with the simultaneous measurement of the rate of reaction while the catalyst is in operation, called operando measurements. The application of operando techniques is becoming a more common tool to help unravel catalytic functions. Our group has custom-built an operando reactor for the measurement of X-ray absorption spectroscopy. While operando measurements are a major improvement, they provide a static picture of a system that is actually dynamic. Dynamic techniques where the catalyst kinetic and structural properties can be followed simultaneously with a time resolution of a fraction of a turnover are the techniques of choice. We will show examples using a transmission FTIR cell we developed. The great advantage and sometimes necessity of performing experiments in the dynamic and operando modes will be discussed. The help from theory will also be illustrated.

11:20am IS+AS+SS-MoM10 In Situ XPS Of Graphene-Catalyst Interactions During Chemical Vapor Deposition, *Robert Weatherup*, Lawrence Berkeley National Laboratory

Critical to controlling the growth of graphene and carbon nanotubes during chemical vapor deposition (CVD) is a detailed understanding of the role of the catalyst, however this remains incomplete due the wide parameter space. Here we investigate the dynamics of graphene-catalyst interactions during CVD using time- and depth-resolved X-ray photoelectron spectroscopy[1-2], in situ scanning tunneling microscopy,[3] and grand canonical Monte Carlo simulations coupled to a tight-binding model[1]. We focus on Ni(111) as a model catalyst surface and probe in-operando a wide range of hydrocarbon exposure pressures (10^{-6}-10^{-1} mbar). The key atomistic mechanisms of graphene formation on Ni are thereby revealed and our data highlights an interdependency between the distribution of carbon close to the catalyst surface and the strength of the graphene-catalyst interaction.

The strong interaction of epitaxial graphene with Ni(111) causes a depletion of dissolved carbon close to the catalyst surface, which prevents additional layer formation leading to a self-limiting graphene growth behavior for low exposure pressures (10^{-6}-10^{-3} mbar). Increasing the hydrocarbon pressure further (to ~10^{-1} mbar) leads to weakening of the graphene-Ni(111) interaction accompanied by additional graphene layer formation, mediated by an increased concentration of near-surface dissolved carbon. We also reveal that the growth of more weakly adhered, rotated graphene on Ni(111) is linked to an initially higher level of near-surface carbon compared to the case of epitaxial graphene growth. We relate these results to the simple kinetic growth model that we have previously established,[6] and use them to consistently explain previous graphene CVD results in the literature. The key implications for graphene growth control and their relevance to carbon nanotube growth are thereby highlighted.

References

(1) Weatherup et al. J. Am. Chem. Soc. 2014, 136, 13698-13708

(2) Weatherup et al. Nano Lett. 2011, 11, 4154-4160

(3) Patera et al. ACS Nano 2013, 7, 7901-7912

(4) Weatherup et al. ACS Nano 2012, 6, 9996-10003

11:40am IS+AS+SS-MoM11 Mechanism Study for Salen Ligand Homogeneous Catalyst in a Heterogeneous Catalysis System, *Niclas Johansson, S. Chaudhary, A.R. Head, O. Snezhkova, J.N. Andersen, J. Knudsen, J. Schnadt,* Lund University, Sweden

Surface-immobilization of transition metal complexes otherwise used as homogeneous catalysts, i.e. in the same (solution) phase as the reactants and products, and their use as heterogeneous catalysts has been an active field of research for many years. The attractiveness of the idea of surface-immobilization lies in the potential to significantly increase the efficiency and selectivity of heterogeneous catalysts [1], the ease of catalyst and product separation [1], and the fact that the need for solvents and highly oxidizing agents might be eliminated in the heterogeneous system.

Here we direct our attention towards the transition metal Mn(III)-salen complex[R,R(-)N,N'Bis(3,5-di-t-butylsalicylidene, 1,2-cyclohexane diaminomanganese(III)chloride) which have been shown to be very effective homogeneous catalysts for enatioselective epoxidation of unfunctionalised olefins. Yet, while much research has been done to investigate the salen complexes' catalytic properties in the homogeneous phase, very few surface science studies have been performed [2,3].

Here we report a study starting from standard UHV conditions and bridging the pressure gap into more realistic conditions. Here, we will show UHV spectra coupled to Torr-range Ambient Pressure X-ray Photoelectron Spectroscopy (APXPS).

We investigated propylene(C_2H_6) epoxidation reaction using surface-deposited Mn(III)-Salen on Au(111) as catalyst. With APXPS we were able to follow the electronic structure changes during reaction conditions in a gas mixture of propylene and oxygen. The spectra acquired show gas phase interactions and changes was found that were specific to the gas mixture. Surprisingly, O 1s spectra acquired at room temperature shows CO_2 which indicates complete oxidation of propylene. This result was further confirmed with a mass spectrometer in direct connection with the reaction chamber. Indeed, the complexes are active even in a heterogeneous system supporting the possibility of transferring homogeneous catalysts into heterogeneous catalytical systems.

References

[1] C. Copéret and J.-M. Basset, Adv. Synth. Catal. 349 , 78 (2007)

[2] K. Lämel et al, Nano Lett. 10, 2965 (2010)

[3] A. Schwartz et al., J. Phys. Chem. C 117, 1105 (2013)

Surface Science
Room: 113 - Session SS+AS+EN-MoM

Synthesis, Structure and Characterization of Oxides
Moderator: Sylvie Rangan, Rutgers, the State University of New Jersey

8:20am SS+AS+EN-MoM1 Oxygen Uptake on Rh(111), *Daniel Killelea, J. Derouin, R.G. Farber,* Loyola University Chicago

Rhodium surfaces are of high utility for the partial oxidation of small molecules. We present results from a study of the uptake of gas-phase oxygen atoms on the Rh(111) surface. A combination of temperature programmed desorption (TPD), Auger electron spectroscopy (AES), and scanning tunneling microscopy (STM) were used to determine the total amount of oxygen, the oxygen surface coverages, and the surface structures, respectively. Our findings suggest that oxygen atoms are readily incorporated in to the near-surface region on Rh(111) while retaining low oxygen surface coverages and structures. We further studied how the surface changes when the subsurface oxygen atoms emerge to the surface. These finding provide insight to the formation of bulk oxides, and show that high-coverages of oxygen are not necessary for absorption of oxygen into the selvedge.

8:40am SS+AS+EN-MoM2 Formation of Subsurface Oxygen and Surface Oxides on Ag(111) by Atomic Oxygen, *Jonathan Derouin*, R.G. Farber, D.R. Killelea,* Loyola University Chicago

Understanding the interaction of oxygen with transition metal surfaces is important in many areas including corrosion and catalysis. The oxygen/silver system in particular has been studied extensively both experimentally and theoretically. Interest is driven largely by the role of silver in two widely used industrial reactions: the epoxidation of ethylene to produce ethylene oxide and the partial oxidation of methanol to produce formaldehyde. In addition, the oxygen/silver system can serve as a model for the dissociative chemisorption of diatomic molecules on close packed metal surfaces. Despite extensive research, the oxygen/silver system is still not well understood. To better understand this system, we use UHV-STM, AES and TPD to study the adsorption of atomic O on an Ag(111) crystal. Atomic O is generated by thermally cracking molecular O. By varying the power of the thermal cracker we are able to change the flux of atomic O reaching the Ag surface. Higher atomic O fluxes produce O structures which desorb at significantly higher temperatures than structures produced with lower O fluxes. We then use UHV-STM to further characterize the various oxide structures produced.

9:00am SS+AS+EN-MoM3 Surface and Bulk Properties of Pure and Mixed Titania, *Matthias Batzill,* University of South Florida **INVITED**

Titanium oxide in its different polymorphs remains a model system for structure property relationships in simple oxides. In this talk we address issues related to both the bulk and the surface properties of TiO2. Measuring the photocatalytic activity of anatase- and rutile- epitaxial films we conclude that charge carriers excited deeper in the bulk contribute to the surface photocatalytic activity for anatase compared to rutile [1]. This

* Morton S. Traum Award Finalist

difference may be an important factor for explaining the generally higher photocatalytic activity of anatase-TiO_2. In the second part of the talk, surface properties are presented on the example of rutile $TiO_2(011)$. The (011) surface orientation is less frequently studied compared to the (110) surface. Under UHV-conditions the (011) surface reconstructs into a complex 2x1 structure. We investigate the stability of this reconstruction under chemical adsorption. We find that for strongly adsorbing molecules the surface restructures to enable stronger adsorption. We show that this restructuring is strongly anisotropic resulting in quasi-1D adsorbate structures [2]. The instability of the rutile $TiO_2(011)$-2x1 surface may also be exploited for the formation of unique mixed oxide surfaces. This we demonstrate with iron oxide, which forms an ordered mixed TiFeOx surface oxide layer. Such mixed oxide surface may also form by impurity segregation from the bulk and thus may be a common surface structure in Fe-doped TiO_2.

[1] "Why is anatase a better photocatalyst than rutile? - Model studies on epitaxial TiO_2 films" T. Luttrell, S. Halpegamage, J.G. Tao, A. Kramer, E. Sutter, M. Batzill Sci. Rep. 4, 4043 (2014).

[2] "Adsorbate Induced Restructuring of $TiO_2(011)$-(2×1) Leads to One-Dimensional Nanocluster Formation" Q. Cuan, J. Tao, X.Q. Gong, M. Batzill Phys. Rev. Lett. 108, 106105 (2012).

9:40am SS+AS+EN-MoM5 Characterizations of Non-polar Polar Interfaces: Cr_2O_3 on ZnO (0001) and (000-1), *Xiaodong Zhu, M.D. Morales-Acosta, J. Shen, F.J. Walker, J. Cha, E.I. Altman,* Yale University
The growth of non-polar Cr_2O_3 on oppositely poled ZnO surfaces was characterized to determine how the polar substrate influences the properties of the non-polar film. Photoelectron spectroscopy (XPS and UPS), electron diffraction (RHEED and LEED), High-resolution transmission electron microscopy (HRTEM), X-ray diffraction (XRD) and X-ray reflectivity (XRR) have been performed to determine the growth mode, film quality and interfacial electronic properties are influenced by the substrate polarization. The growth is 2D; however, the films appear initially disordered on both substrates. With increasing film thickness, the films ordered with a well-defined epitaxial relationship. The HRTEM and XRD/XRR results for thicker films confirm a clear interface and well-defined lattice structure near the interface and throughout the film, indicating that above a critical thickness the entire film reorganizes into an ordered structure. The polar interfaces show a small but noticeable band offset that decayed with increasing film thickness. Statistical analysis of UPS valence band spectra revealed an enhanced density of states near the Fermi level for Cr_2O_3 on the positive surface consistent with stabilization of the positive interface by charge transfer; in contrast, no significant valence band differences were observed between bulk Cr_2O_3 and thin Cr_2O_3 thin layers on the negative surface. The results will be compared with those obtained for $ZnO/Cr_2O_3/$ ZnO (0001) and (000-1) to determine if the interfacial properties are sensitive to how the interface is formed.

10:40am SS+AS+EN-MoM8 Exploring Iron Oxide Clusters and Films Supported on HOPG with HREELS and AES, *Joel Langford,* University of California, Irvine, *F. Rosner,* Technical University of Munich, Germany, *J. Kwon, J.C. Hemminger,* University of California, Irvine
We are using High Resolution Electron Energy Loss Spectroscopy (HREELS) and Auger Electron Spectroscopy (AES) to investigate nanoclusters and films of iron oxide supported on highly oriented pyrolytic graphite (HOPG). For the films, two AES oxidation profiles were generated by annealing in oxygen. One profile was at a constant sample temperature of 500 K with varying exposure, the other by varying sample temperature while keeping exposure at a constant 1000 L. Both oxidation profiles saturate at an AES O/Fe ratio of 1.2. This ratio is below the O/Fe ratio of magnetite (Fe_3O_4), and hematite (Fe_2O_3) indicating incomplete oxidation of the film. Additional evidence for incomplete film oxidation comes from the absence of Fuchs-Kliewer phonons in the HREEL spectra. For the nanoclusters we are investigating two systems; polydispersed iron oxide nanoclusters on HOPG, and platinum nanoclusters supported on iron oxide nanoclusters. The polydispersed nanoclusters are more susceptible to oxidation than the film as evident by the higher AES O/Fe ratio and the presence of Fuchs-Kliewer phonons in the HREEL spectra. The platinum nanoclusters are synthesized on the iron oxide nanoparticles by an ex-situ photodeposition technique and therefore adventitious carbon is adsorbed prior to transfer into the UHV chamber. To remove the adventitious carbon we annealed in oxygen at a sample temperature of 1000 K. HREEL spectra show that the annealing procedure removes adventitious carbon because of the absence and appearance of a CO resonance before and after cleaning, respectively. HREEL spectra after low temperature CO adsorption and as a function of subsequent anneal temperature will be presented.

11:00am SS+AS+EN-MoM9 Computational Materials Design®: Ionic Conduction in Rare-Earth-Metal Oxides from the First Principles-based Studies, *Susan Aspera, M. Sakaue, M. Alaydrus, T.P.T. Linh, N.H. Linh, H. Nakanishi,* Osaka University, Japan, *H. Kasai,* Akashi College, Japan
Solid oxide fuel cells (SOFC) have been one of the most promising technologies to tap alternative sources of energy. This technology utilizes abundant fuel materials such as H_2, CH_4 and other hydrocarbon materials to lessen our dependence on non-renewable fossil fuels that are nearly depleting. It takes into advantage the efficiency brought about by high kinetics of reaction at the electrolyte sides occurring at high working temperature. With this, ceramic based materials are often used as electrolyte and electrode materials. However, the working temperature of SOFCs is often too high (700˚C to 1000˚C). This limits the application of SOFCs and consequently high cost of producing durable materials for high working temperature. Recently, research related to this technology focuses on materials that work at intermediate temperature (IT-SOFC). This entails finding/designing materials that have high ionic conductivity at IT-SOFC working temperature.

Recent developments in computational simulation techniques, coupled with the rapid progress in computer efficiency, make first principles-based COMPUTATIONAL MATERIALS DESIGN (CMD®) a relevant field in the world of surface science and condensed matter physics. In this scheme, quantum mechanical calculations are performed to design promising materials, and understand the necessary mechanisms for the realization of an efficient technological device. Here, we employed the CMD® process and density functional theory-based analysis to study the atomic and electronic properties of several rare-earth-metal oxides (Pr_2NiO_2, La_2GeO_5, $LaGaO_3$ and CeO_2) which has potential application in IT-SOFC. These materials are known to have different structures according to symmetry, and the mechanism by which O ion conducts, i.e. via oxygen vacancies (O_{vac}) migration or O interstitial migration. The O ion migration path is dependent on the structure of the material, and the corresponding activation energy barrier for oxygen ion migration (E_{ac}) is affected by the concentration of O_{vac} and the presence of dopants, for O ion conduction via vacancies. In most of these systems, dopants with the same ionic radius as the host materials create high probability for O_{vac}, which then affects ionic conductivity, and the E_{ac} is found to be least for dopants with ionic radius near to that of the host material. Furthermore, as ionic migration is sensitive to the atomic structure, E_{ac} is party due to the structural alteration brought about by the presence of impurities such as dopants and creation of heterostructure interfaces. With these understanding, we can comment on the methods by which ionic conductivity can be enhanced in these materials.

11:20am SS+AS+EN-MoM10 Modeling and Characterization of Exemplar Sealing Glasses to Develop Chemistry-Structure-Property Relationships, *Michael Brumbach, T. Zeitler, T. Alam, M. Rodriguez, L. Criscenti, M. Kalan, A. Mirabal, D. Bencoe, K. Ewsuk,* Sandia National Laboratories
The performance of joining materials in many applications, such as glass-to-metal seals in solid oxide fuel cells and medical devices, require improvements in glass properties for greater reliability. In this work, simple sealing glass compositions have been used to develop experimentally-validated molecular models. The goal is to understand glass chemistry and structure such that modeling can be used to guide glass design, for manufacturability, and optimized performance. The coupled modeling and experimental work will be discussed.

Technological glasses are used in many applications where inorganic joining is required. Applications of joining glasses include glass in glass-to-metal seals (in solid oxide fuel cells or medical components), glass-bonded ceramics (such as debased aluminas), and low temperature co-fired ceramic (LTCC) packaging for microelectronics. For these applications, well-controlled processing conditions and high reliability in the end-product are of paramount importance. To better understand materials performance and reliability our objective is to develop experimentally-validated simulation tools to predict and control glass chemistry-structure property relationships. These tools will be used to predict structure-function relationships in bulk glasses and at joining interfaces.

Results from experimental characterization of several barium aluminosilicate glasses will be discussed. Solid-state NMR, lab-based and synchrotron X-ray scattering, and EXAFS have been used to determine structural characteristics of the exemplar glasses. Comparison of experimental results to molecular dynamics modeling of the three-component glass will be presented. Additional simulations of glass properties and comparisons to measurements will also be discussed.

Sandia National Laboratories is a multi-program laboratory managed and operated by Sandia Corporation, a wholly owned subsidiary of Lockheed

Thin Film
Room: 111 - Session TF+AS+SS-MoM

Self-Assembled Monolayers, Layer-by-Layer, etc.
Moderator: Han Zuilhof, Wageningen University, Netherlands

8:20am TF+AS+SS-MoM1 The Effects of Embedded Dipoles in Aromatic Self-Assembled Monolayers, *Swen Schuster*, Universität Heidelberg, Germany, *T. Abu-Husein,* Universität Frankfurt, Germany, *D.A. Egger, I. Hehn,* Graz University of Technology, Austria, *M. Kind,* Universität Frankfurt, Germany, *E. Zojer,* Graz University of Technology, Austria, *A. Terfort,* Universität Frankfurt, Germany, *M. Zharnikov,* Universität Heidelberg, Germany

Self-assembled monolayers (SAMs) are frequently used as intermediate films to modify charge-carrier injection from metal-electrodes into an organic semiconductor. This is usually achieved by use of the terminal dipolar groups comprising the SAM-ambience interface and affecting, at the same time, the growth chemistry of the semiconductor. Here we suggest an alternative approach, viz. embedding dipolar element into the molecular backbone, which allows decoupling the dipole control and the interfacial chemistry. As molecular backbone we use oligophenyl moiety which provides a suitable structural match to most organic semiconductors. As polar unit we use pyrimidine, varying its orientation in the molecular backbone and, consequently, the direction of the embedded dipole moment. The electronic and structural properties of these embedded-dipole SAMs are thoroughly analyzed using a number of complementary characterization techniques combined with quantum-mechanical modeling. We show that such mid-chain substituted monolayers are highly interesting from both fundamental and application viewpoints, as the dipolar groups are found to induce a potential discontinuity inside the monolayer, electrostatically shifting the energy levels in the regions above and below the dipoles relative to one another. These SAMs also allow for tuning the substrate work function in a controlled manner independent of the docking and interfacial chemistry. In addition, a mixture of the embedded-dipole molecules with opposite orientations of dipoles makes possible a fine tuning of the work function between the ultimate values, associated with a particular dipole orientation. Quantum-mechanical modeling in conjunction with x-ray photoelectron spectroscopy experiments provides insight into the molecular organization of such mixed monolayers.

8:40am TF+AS+SS-MoM2 IR Spectroscopic studies of Molecular Thin Films exhibiting Spontaneous Dipole Alignment, *Alexander Rosu-Finsen*, Heriot-Watt University, UK, *J. Lasne,* Heriot-Watt University, France, *A. Cassidy, D. Field,* Aarhus University, Denmark, *M.R.S. McCoustra*, Heriot-Watt University, UK

In recent years, observations of the presence of a spontaneous and powerful static electric field within thin films of molecular solids have been reported by Field and co-workers [1]. These electric fields, which can approach 10^8 V m^{-1} or more, are believed to arise from alignment of the molecular dipoles in the thin films. Seeking to provide an independent means of observing this phenomenon of the "spontelectric phase", the first new electrically-unique, structural phase to have emerged in decades, we have used reflection-absorption infrared spectroscopy (RAIRS) to investigate thin films of nitrous oxide (N_2O). The presence of a static electric field within the thin film, the defining characteristic of spontelectrics, is demonstrated through the observed temperature dependence of longitudinal-transverse optical (LO-TO) splitting in RAIR spectra, using an analysis based on the vibrational Stark effect [2]. Tentative evidence for the surface-templating of the growth of the spontelectric phase will be presented from RAIRS studies of solid carbon monoxide (CO) on a range of water substrates (porous amorphous solid water, compact amorphous solid water and crystalline water) [3].

[1] Spontaneous electric fields in solid films: spontelectrics. D. Field, O. Plekan, A. Cassidy, R. Balog, N.C. Jones and J. Dunger, *Int. Rev. Phys. Chem.*, 2013, **32**, 345-392.

[2] Spontaneously electrical solids in a new light. J. Lasne, A. Rosu-Finsen, A. Cassidy, M. R. S. McCoustra and D. Field, *Phys. Rev. Lett.*, submitted.

[3] Templating dipole alignment in solid carbon monoxide on water ice surfaces. A. Rosu-Finsen, J. Lasne, A. Cassidy, D. Field and M. R. S. McCoustra, *Phys. Rev. Lett.*, in preparation.

9:00am TF+AS+SS-MoM3 Coordination-Based Molecular Assemblies as Electrochromic Materials: Ultra-High Switching Stability and Coloration Efficiencies[1], *Michal Lahav*, Weizmann Institute of Science, Israel

Layer-by-Layer (LbL) deposition, combined with metal-ligand coordination, has served as a powerful tool for generating functional architectures.[2] Such systems might find interesting applications in molecular electronics, sensor, solar cells and data storage. More significantly, owing to their interesting electrochromic (EC) behavior, they are promising candidates for use in smart windows and display devices. In this study we used a dip-coating process to generate molecular assemblies (**MA**) from metal polypyridyl complexes cross-linked with PdCl₂. These polypyridyl complexes are considered ideal chromophores for fabricating electrochromic materials, due to their excellent stability and light absorption that greatly depends on their oxidation state.[3],[4] The number of pyridine moieties of the chromophores is varied to control (i) the materials' stability, (ii) color, (iii) redox-chemistry, and (iv) the film growth (i.e., linear *vs.* exponential). We also observed that minor structural differences (i.e., the pyridine-bipyridine bond order) at the molecular level become apparent when the stability and electrochromic properties are examined (Figure 1). The **MA**s exhibit high coloration efficiencies and are extremely stable: they are thermally robust and have exceptionally high (spectro)electrochemical activity. Furthermore, we demonstrated the formation of a first-generation solid-state set-up.[1],[5]

1) S. Shankar, M. Lahav, M. E. van der Boom, *J. Am. Chem. Soc.* **2015**, *137, Just Accepted Manuscript.*

2) R. J. Mortimer, *Annu. Rev. Mater. Res.*, **2011**, 41, 241.

3) G. de Ruiter, M. Lahav, M. E. van der Boom, *Acc. Chem. Res.*, **2014**, 47, 3407-3416.

4) G. de Ruiter, M. Lahav, H. Keisar, M. E. van der Boom, *Angew. Chem., Int. Ed.* **2013**, 52, 704-709.

5) M. E. van der Boom, M. Lahav, S. Shankar, US Patent 61/906,565, **2013**.

9:20am TF+AS+SS-MoM4 New Approaches to the Preparation of Well-defined Metal Films on Top of Self-assembled Monolayers, *Michael Zharnikov*, Universität Heidelberg, Germany

Self-assembled monolayers (SAMs) can be potentially used as ultrathin insulating dielectric layers or intermediate films in different electronic and spintronic devices. Whereas the bottom electrode in such assemblies is represented by the metal substrate, the top electrode should be prepared at the SAM-ambience interface. Regretfully, the formation of a well-defined metal film on top of the SAMs is a non-trivial task, since the metal atoms deposited onto the SAM-ambient interface do not stay there, but penetrate into the monolayer and diffuse to the metal substrate following a strong thermodynamical drive. Here I discuss three new approaches to suppress the above penetration and diffusion, taken a representative ferromagnetic metal, nickel, as a test adsorbate. The first approach relies on irradiation-induced cross-linking of a thiol-substituted aromatic SAM. Whereas 2D-polymerization of such a SAM prevents penetration of the metal atoms into the monolayer, the thiol groups at the SAM-ambient interface serve as nucleation centers for the growing "top" film. The second approach, relying on SAMs of perfluoroterphenyl-substituted alkanethiols, utilizes a chemical reaction between the SAM constituents and adsorbate atoms. The primary process is the Ni mediated loss of fluorine atoms followed by extensive cross-linking between the partly defluorinated molecular backbones. The stability of these backbones and the rapid development of the cross-linking are the key components to hinder the metal penetration. Finally, the penetration of deposited metal atoms into a SAM can be nearly completely inhibited by the preliminary formation of palladium-chloride seeding layer at the SAM-ambience interface. The palladium atoms in the seeding layer serve as nucleation centers for the growing metal film, staying at its bottom during the growth. In contrast, the chlorine atoms are transferred from palladium to the deposited metal, staying on the top of the growing metal film and serving as surfactants.

9:40am TF+AS+SS-MoM5 N-Heterocyclic Carbenes as Novel Ligands for Self Assembled Monolayers on Gold, *Cathleen Crudden*, Queen's University, Canada **INVITED**

The use of N-heterocyclic carbenes (NHCs) to modify homogeneous metal catalysts is widespread, however despite the versatility of these complexes, the high metal–NHC bond strength and oxidative stability of NHC–ligated metals, and the ease of synthesis of NHCs, there have been only a handful of reports of mostly ill-defined surfaces functionalized by NHCs.

We will describe the use of NHCs to form self-assembled monolayers on gold surfaces. In particular, films prepared by the deposition of 1,3-dihydro- 1,3-bisisopropylbenzimidazol-2-ylidene, show molecular ordering on the surface and remarkable stability. They show no decomposition upon heating for 24 hrs in THF, in boiling in water for 24hrs or upon treatment

with acid (pH 2) or base (pH 12). Incredibly, they even survive largely after 24 hr exposure to hydrogen peroxide. This remarkable increase in stability relative to thiol-based SAMs will greatly increase the number of reagents and conditions to which the SAMs can be exposed.

The use of these films in SPR-based biosensing will be described, as will novel methods for the preparation of such films that can be carried out in air on the bench top.

10:40am TF+AS+SS-MoM8 Improved Stability of Ag Thin Films due to Several Organic Surface Monolayers, *Midori Kawamura*, Kitami Institute of Technology, Japan, *C. Kudo, T. Sasaki, Y. Abe, K.H. Kim, T. Kiba*, Kitami Institute of Technology

Due to excellent physical properties, Ag thin films have been used as low-e coating, optical mirror, and so on. It is necessary to prevent degradation of the Ag films in air or humid atmosphere. For the purposes, it has been reported that several metal oxide nanolayers and organic monolayers are effective to make Ag thin films stable. Previously, we reported that modification of Ag films with 3-mercaptopropyltrimethoxysilane (MPTMS) monolayer can improve durability of the Ag films after environmental tests because strong bonds were formed between thiol moiety and Ag films, and also between silanol moiety and glass substrate. In the present study, we attempted to use other type of organic molecules, namely straight chain alkylthiols, such as 1-octadecanthiol (1-ODT), 1-dodecanthiol (1-DT) for protection of Ag film surface and compared with MPTMS.

Ag thin films (10nm) were deposited on clean glass substrates by vacuum evaporation. Then monolayer of 1-ODT and 1-DT were formed over the Ag thin films by solution method. The samples were kept in a constant temperature and humidity chamber (40 degree Celsius and 90 RH%) for a week. The electrical resistance, surface morphology, optical transmittance were measured before and after the test. Ag film without the monolayer, and that with MPTMS were also examined for comparison.

The surface roughness of the Ag film without the monolayer drastically increased from 2.7 nm to 27 nm after the test. However, the increase was within 1nm on Ag films with 1-DT and 1-ODT surface layers. These changes were smaller than that on Ag film with MPTMS surface layer. By the measurement of electrical resistivity, it was found that increase in the resistivity after the test was very much suppressed in the Ag film with these monolayers. In addition, optical transmittance measurement showed that transmittance spectrum of Ag films with these monolayers did not change after the test. These results accord with the Ag film morphology change. Consequently, excellent passivation effect of 1-DT and I-ODT surface monolayers on Ag films was confirmed.

11:00am TF+AS+SS-MoM9 Electronic Structures of the Biaxially-strained GaSb(111) Films, *Takuya Hatayama*, The University of Electro-Communications (UEC-Tokyo), Japan, *A. Akaishi*, The University of Electro-Communications (UEC-Tokyo), *J. Nakamura*, The University of Electro-Communications (UEC-Tokyo), Japan

III–V compound semiconductors have been extensively researched as alternative channel materials of complementary metal-oxide-semiconductor devices because of their superior carrier mobility[1]. In particular, GaSb is one of the promising p-channel materials, because its hole transport properties are significantly improved compared to Si. Recently, Ohtake *et al*. Have reported that high-quality GaSb films can be epitaxially grown on the Si(111) substrate using the InAs buffer layer[2]. The lattice constant in the plane of growth for the thin GaSb epilayer inherits the lattice constant of InAs, causing an inherent strain in the GaSb film. As a result, the electronic structure of the GaSb film can be modified. In this study, we evaluate the electronic properties of the strained GaSb bulk and the (111) films, especially the band gap formation, the effective mass, and the electronic conductivity, using first-principles calculations within the density functional theory. In general, the local density approximation (LDA) is commonly applied to the exchange correlation term. However, it has been well-known that the band gap of semiconductors is significantly underestimated with LDA. In order to rectify the underestimation of the band gap and to correctly evaluate electronic dispersions at band edges, we use the hybrid functional proposed by Heyd-Scuseria-Ernzerhof (HSE06) for the exchange-correlation term[3]. The spin-orbit interaction is also included.

We assume the biaxial strain parallel to the GaSb (111) plane. For the bulk with a direct band gap at ambient pressure, GaSb becomes an indirect band gap material under the compressive biaxial strain. The biaxial strain makes the twofold-degenerate heavy-hole and light-hole bands split into two bands at the Gamma point of the valence band. Interestingly, under the biaxial tensile strain, the effective mass of holes becomes anisotropic. We will also report on changes in electronic properties of the GaSb (111) ultrathin films under the biaxial strain.

[1] J. A. del Alamo, Nature **479**, 317 (2011)

[2] A. Ohtake, T. Mano, N. Miyata, T. Mori, and T. Yasuda, Appl. Phys. Lett. **104**, 032101 (2014)

[3] J. Heyd, G. E. Scuseria, and M. Ernzerhof, J. Chem. Phys. **118**, 8207 (2003); *ibid* **124**, 219906€ (2006)

11:20am TF+AS+SS-MoM10 How to Repel Polymer Adsorption on Flat Surfaces?, *Zhanhua Wang*, *S.P. Pujari, M.M.J. Smulders, H. Zuilhof*, Wageningen University, Netherlands

Organic monolayers or polymer brushes, often in combination with surface structuring, are widely used to prevent nonspecific adsorption of polymeric or biological material on sensor and microfluidic surfaces. Here we show for the first time how robust, covalently attached alkyne– derived monolayers or ATRP-produced polymer brushes, with a varying numbers of fluorine atoms, on atomically flat Si(111), effectively repel a wide range of apolar polymers without the need for micro– or nanostructuring of the surface. We have studied the antifouling property of fluoro-hydro monolayers and of fluorine-containing polymer brushes towards a range of commonly used polymers/plastics with comparable molecular weight in non– aqueous solvent, and have investigated the effect of polymer molecular weight on the fouling behavior. These studies relied on a range of characterization methods: wettability studies, ellipsometry, X– ray photoelectron spectroscopy (XPS) and atomic force microscopy (AFM). We developed a novel surface morphology survey by AFM characterization that can accurately quantify the degree of fouling.

These studies consistently displayed that especially the mono–fluorinated (F1) monolayer shows excellent anti– fouling behavior, even more so than e.g. corresponding monolayers with perfluorinated alkyl tails. In this presentation the causes of this unprecedented and surprising finding are discussed. Second, we will focus on polymer brush properties that further reduce the adsorption of polymers. These findings and analysis offer significant potential for antifouling applications of ultrathin and covalently bound fluorine– containing coatings for a range of micro– and nanotechnological applications.

11:40am TF+AS+SS-MoM11 Symmetric Attachment of Annulated Aromatic Hydrocarbons in Self-assembled Monolayers by Use of Oxazoles, *C. Partes*, University of Frankfurt, Germany, *S. Schuster, T. Wächter*, University of Heidelberg, Germany, *Martin Kind*, University of Frankfurt, Germany, *M. Zharnikov*, University of Heidelberg, Germany, *A. Terfort*, University of Frankfurt, Germany

Self-assembled monolayers (SAMs) have proven to be powerful tools for tuning surface properties because of the uncomplicated method of their preparation and the high variability of their organic moieties. The suitability of SAMs in applications like, e.g., organic electronics is frequently investigated. An aim for the use of SAMs is the reduction of injection barriers that occur at the interfaces between organic semiconductors and technologically relevant substrates like gold or silicon.

A SAM ideal for this purpose should exhibit a high vertical conductivity. In view of this, we investigated several aromatic and araliphatic SAMs, e.g. terphenyl-terminated monolayers on gold [1]. In a more recent ansatz, we have examined SAMs bearing annulated moieties such as anthracene, which in contrast to oligophenyls are entirely planar [2]. However, as a consequence of the asymmetric substitution of anthracene to the thiol anchor group it is hardly possible to alter the tilt angle of these thiolate molecules within the SAMs [2].

To overcome this drawback, we extended the annulated system of the SAM-forming thiols with an oxazole unit, which allows for a quasi-symmetric attachment to the ancor group. This restores the possibility to influence the tilt angle of the aromatic units using the so-called odd-even effect in SAMs.

Here, we like to present preliminary results on preparation and structural properties of SAMs made from aromatic oxazole thiols on gold surfaces.

REFERENCES

[1] Shaporenko, A.; Brunnbauer, M.; Terfort, A.; Grunze, M.; Zharnikov, M./J. Phys. Chem. B/108, 14462-14469 (2004).

[2] Dauselt, J.; Zhao, J.; Kind, M.; Binder, R.; Bashir, A.; Terfort, A.; Zharnikov, M./ J. Phys. Chem. C/115, 2841-2854 (2011).

Monday Afternoon, October 19, 2015

Electronic Materials and Processing
Room: 211A - Session EM+AS+SS-MoA

MIM Diodes, Functional Oxides, and TFTs
Moderator: Pat Brady, RedWave Energy, Inc., John Conley, Oregon State University

2:20pm **EM+AS+SS-MoA1 Engineered Tunnel-Barrier Terahertz Rectifiers for Optical Nantennas**, *Ivona Mitrovic, N. Sedghi, A.D. Weerakkody, J.F. Ralph, S. Hall, J.S. Wrench, P.R. Chalker,* University of Liverpool, UK*, Z. Luo, S. Beeby*, University of Southampton, UK
Thin film metal-insulator-metal rectifying devices using double, triple or quadruple insulator layers are currently the focus of attention for the development of next-generation optical nantennas for infrared energy harvesting. The interest is driven by their distinctive attributes, such as nanoscale footprint, room temperature operation, zero bias voltage requirement, and ease of integration with Complementary Metal Oxide Semiconductor technology. Highly asymmetric and nonlinear current-voltage (IV) behaviour at low applied voltages is critical for this application. In this paper, we present comprehensive experimental and theoretical work on tunnel-barrier rectifiers comprising double (Ta_2O_5/Al_2O_3 and Nb_2O_5/Al_2O_3) and triple ($Ta_2O_5/Nb_2O_5/Al_2O_3$) insulator configurations engineered to enhance low voltage nonlinearity. There are two mechanisms that allow metal-insulator-insulator-metal (MIIM) rectifiers to have a high nonlinearity while keeping the resistance low: (i) resonant tunnelling, and (ii) step tunnelling. This paper focuses on the former approach. A modified multi-layer Tsu-Esaki method has been used for IV calculations from the transmission coefficient by the transmission matrix method. The theoretical work indicates that the onset of resonant tunneling in MIIM and MIIIM rectifiers can be adjusted to be close to zero volts by appropriate choice of work function difference of the metal contacts, the thickness of insulator layers, and the depth of the quantum well. The double and triple insulator rectifiers were fabricated using atomic layer deposition (ALD) and rf magnetron sputtering, while different metal contacts including Al, Ta, W, Nb, Cr and Ag were defined by photolithography or shadow mask and deposited by e-beam and thermal evaporation. The thickness, band gap, surface roughness, band offsets and work functions have been extracted from variable angle spectroscopic ellipsometry, atomic force microscopy, x-ray and inverse photoelectron spectroscopy on fabricated devices to ascertain the quality of the interfaces and to measure barriers. The key rectifier properties, asymmetry, nonlinearity and responsivity have been assessed from current voltage measurements performed in the range 293-370 K. A superior low voltage asymmetry (18 at 0.35 V) and responsivity (9 A/W at 0.2 V) has been observed for fabricated bilayer Ta_2O_5/Al_2O_3 and Nb_2O_5/Al_2O_3 MIIM devices respectively, in advance of state-of-the-art experimental values. The results demonstrate ALD and rf sputtered tunnel-barrier rectifiers which enhance low voltage nonlinearity and have the potential to be employed in optical nantennas for infrared energy harvesting.

2:40pm **EM+AS+SS-MoA2 MIM Diodes for RF Energy Harvesting**, *A.A. Khan, A. Syed, F. Ghaffar, Atif Shamim*, King Abdullah University of Science and Technology
Metal Insulator Metal (MIM) diodes that work on fast mechanism of tunneling have been used in a number of very high frequency applications such as (Infra Red) IR detectors and optical Rectennas for energy harvesting. Their ability to operate under zero bias condition as well as the possibility of realizing them through additive techniques makes them attractive for (Radio Frequency) RF applications. However, two major issues namely, high surface roughness at the metal-insulator junction which effects the reliability of the diode, and very high resistance (typically in Mega Ohms) which complicates its matching with RF antenna have prevented its wide spread use in RF rectennas.

In this work, various metal deposition methods such as sputtering and electron beam evaporation are compared in pursuit of achieving low surface roughness. Amorphous metal alloy has also been investigated in terms of its low surface roughness. Zinc oxide has been studied for its suitability as a thin dielectric layer for MIM diodes. Finally, comprehensive RF characterization of MIM diodes has been performed in two ways: 1) by standard S-parameter methods, and 2) by investigating their rectification ability under zero bias operation.

It is concluded from the Atomic Force Microscopy (AFM) imaging that surface roughness as low as sub 1 nm can be achieved reliably from crystalline metals such as copper and platinum. This value is comparable to surface roughness achieved from amorphous alloys, which are non-crystalline structures and have orders of magnitude lower conductivities. Relatively lower resistances of the order of 1 Kilo Ohm with a sensitivity of 1.5 V^{-1} have been obtained through DC testing of devices with MIM diode structure of platinum/zinc oxide/ titanium. Finally, RF characterization reveals that input impedances in the range of 300 Ω to 25 Ω can be achieved in the low GHz frequencies (from 0.5-10 GHz). From the rectification measurements at zero bias, a DC voltage of 4.7 mV has been obtained from an incoming RF signal of 0.4 W at 2.45 GHz, which indicates the suitability of these diodes for RF rectenna devices without providing any bias. These preliminary results indicate that with further optimization, MIM diodes are attractive candidates for RF energy harvesting applications.

3:00pm **EM+AS+SS-MoA3 Diode Structure Based on Carbon Materials for Ultra high Frequency Driving**, *JaeEun Jang*, Daegu Gyeongbuk Institute of Science and Technology (DGIST), Republic of Korea
If the antenna can be designed to absorb wavelengths in the range of a few hundred THz with multi-antenna array design, it results in high conversion efficiency due to power production from various light sources between ultraviolet (UV) and infrared (IR) radiation that is often thought of as heat and exists beyond the visible range for humans. One of the problems in this idea, however, is the nature of visible or IR light to oscillate at ultra-high frequencies. Therefore, a rectifier working at such an ultra-high frequency should be developed with a highly efficient coupling between antenna and light. Because Schottky diode is limited to frequencies less than ~ THz level, nanometer size MIM diode structure has been suggested as alternative design. Two different metals have used normally to make an asymmetric characteristic of current-voltage. However the work function difference between the metals cannot produce a high asymmetry, which causes a poor rectifier performance, even though the structure can be driven in THz range. To solve this issue, we used a structural asymmetric MIM design. The planar asymmetric design using various metals or grapheme showed better asymmetric I-V characteristics than that of simple MIM structure. In addition, for the vertical aligned design, single multi-wall carbon nanotube was formed as one electrode to get high tunneling current caused by the structural effect of sharp tip. The structural asymmetry can make a different field density states to the metals, which induces a high rectify characteristics. The contrast ratio between the forward and the reverse bias is ~10^4 level. The estimated cut-off frequency is about 4.74THz. The electrical characteristics are stable up to 423K.

3:20pm **EM+AS+SS-MoA4 Optical Rectenna Arrays using Vertically Aligned Carbon Nanotubes**, *Baratunde Cola*, Georgia Institute of Technology
The response of a multiwall carbon nanotube to visible light has been reported to be consistent with conventional radio antenna theory. Researchers have proposed that this result might be exploited to realize an optical rectification device – that is, a device that converts free-propagating electromagnetic waves at optical frequencies to localized d.c. electricity. However, an experimental demonstration of this concept requires that the multiwall carbon nanotube antenna be coupled to a diode that operates on the order of 1 petahertz (switching speed on the order of a femtosecond). Ultralow capacitance, on the order of a few attofarads, could allow a diode to operate at these frequencies; and the development of metal-insulator-metal tunnel junctions with nanoscale dimensions has emerged as a potential path to diodes with ultralow capacitance, but these structures remain extremely difficult to fabricate and couple to a nanoscale antenna reliably. Here we demonstrate optical rectification by engineering metal-insulator-metal tunnel diodes at the tips of multiwall carbon nanotubes, which act as the antenna and metallic electron emitter in the diode. This performance is achieved using diode areas based on the diameter of a single carbon nanotube (about 10 nanometers), geometric field enhancement at the carbon nanotube tips, and a low work function semi-transparent top metal contact. Using vertically-aligned arrays of the diodes, we measure d.c. open-circuit voltage and short-circuit current at visible and infrared electromagnetic frequencies that is due to a rectification process, and quantify minor contributions from thermal effects. Our devices show evidence of photon-assisted tunneling, and exhibit zero-bias diode responsivity on the order of 0.1 amps per Watt and zero-bias differential resistance as low as 100 ohms-centimeter squared under illumination. Additionally, power rectification is observed under simulated solar illumination. Numerous current-voltage scans on different devices, and between 5-77 degrees

Celsius, show no detectable change in diode performance, indicating a potential for robust operation.

3:40pm **EM+AS+SS-MoA5 World Record Tunable Microwave Dielectrics**, *C.H. Lee,* Cornell University, *N.D. Orloff,* National Institute of Standards and Technology (NIST), *T. Birol, Y. Zhu, Y. Nie,* Cornell University, *V. Goian,* Institute of Physics ASCR, *R. Haislmaier,* Pennsylvania State University, *J.A. Mundy,* Cornell University, *J. Junquera,* Universidad de Cantabria, *P. Ghosez,* Université de Liège, *R. Uecker,* Leibniz Institute for Crystal Growth, *V. Gopalan,* Pennsylvania State University, *S. Kamba,* Institute of Physics ASCR, *L.F. Kourkoutis, K.M. Shen, D.A. Muller,* Cornell University, *I. Takeuchi,* University of Maryland, College Park, *J.C. Booth,* National Institute of Standards and Technology (NIST), *C.J. Fennie,* **Darrell Schlom**, Cornell University **INVITED**
The miniaturization and integration of frequency-agile microwave circuits—relevant to electronically tunable filters, antennas, resonators, phase shifters and more—with microelectronics offers tantalizing device possibilities, yet requires thin films whose dielectric constant at GHz frequencies can be tuned by applying a quasi-static electric field. Appropriate systems, e.g., $Ba_xSr_{1-x}TiO_3$, have a paraelectric-to-ferroelectric transition just below ambient temperature, providing high tunability. Unfortunately such films suffer significant losses arising from defects. Recognizing that progress is stymied by dielectric loss, we start with a system with exceptionally low loss—$Sr_{n+1}Ti_nO_{3n+1}$ phases—where $(SrO)_2$ crystallographic shear planes provide an alternative to point defect formation for accommodating non-stoichiometry. Guided by theoretical predictions, we biaxially strain a $Sr_{n+1}Ti_nO_{3n+1}$ phase with $n = 6$ to introduce a ferroelectric instability and create a new type of tunable microwave dielectric. This tunable dielectric exhibits a world record figure of merit at room temperature and frequencies up to 125 GHz. Our studies also reveal details about the microscopic growth mechanism of these phases, which are relevant to preparing atomically precise oxide interfaces to these and other Ruddlesden-Popper phases.

4:20pm **EM+AS+SS-MoA7 Bandgap Engineering and Application of SiZnSnO Amorphous Oxide Semiconductor**, *Sang-Yeol Lee*, Cheongju University, Republic of Korea **INVITED**
The band gap of the amorphous SiZnSnO (SZTO) semiconductor has been controlled by bandgap engineering using Si ratio. The addition of small amount of Si in SZTO channel layer can change the position of Fermi level in band gap. By investigating the ultraviolet photoelectron spectroscopy (UPS) characteristics, it is verified that Si atoms can modify the Fermi energy level of SZTO thin films. Carrier generation originated from the oxygen vacancy could modify the Fermi level in the band gap of oxide thin films since Si could be an oxygen vacancy suppressor. This is also related with the origin of defect state which was observed to be involved with the creation of oxygen vacancies. Since it is not so easy to derive directly the change of the Fermi energy level in the energy band gap of amorphous oxide semiconductor, no report of the relation between the Fermi energy level in the energy band gap of oxide semiconductor and the device stability of oxide thin film transistors has been reported. We derive directly band gap and Fermi energy level by using the ultraviolet photoelectron spectroscopy (UPS) characteristics, Kelvin probe (KP) and electron energy loss spectroscopy (EELS). The instability mechanism of amorphous oxide thin film transistors based on the band parameter of oxide semiconductor will be discussed and applied to display applications.

5:00pm **EM+AS+SS-MoA9 Self-aligned Vertical ZnO-based Circuits by Spatial ALD**, **Shelby Nelson**, *C.R. Ellinger, L.W. Tutt,* Eastman Kodak Company
Metal oxide thin-film transistors (TFTs) are becoming the mainstream for display backplanes. These TFTs are fabricated with traditional photolithographic techniques, typically on rigid substrates. In our lab, we explore approaches that are more "print-compatible", with broad alignment tolerance and no small-gap mask features. We deposit zinc oxide (ZnO) semiconductors, aluminum oxide (Al_2O_3) dielectrics, and aluminum-doped zinc oxide conductors by the fast, atmospheric pressure, large-area-compatible, spatial atomic layer deposition (SALD) process. In addition to depositing good-quality thin-film transistor layers at temperatures at and below 200 °C, this process can work with a wide variety of rough and deformable substrates.

Here we describe vertical TFT and circuit architectures that unite process simplicity with high performance. The liberal design rules result from vertical transistors with self-aligned source and drain contacts that define the sub-micron channel length. Using 10-micron design rules for both the minimum line/space dimensions and for alignment tolerances, we have fabricated 9-stage ring oscillators with greater than 1 MHz oscillation frequency, at supply voltage below 6 V. Starting with a gate layer with a re-entrant profile on the edge, these devices use spatial ALD to conformally

coat the Al_2O_3 gate dielectric and ZnO semiconductor, and a line-of-sight deposition process such as evaporation for the aluminum electrodes. Individual device characteristics as well as circuit performance will be discussed.

5:20pm **EM+AS+SS-MoA10 Geometrically Asymmetric Tunneling Nanostructures by Atomic Layer Deposition**, *Jie Qi, X. Jiang, B.G. Willis*, University of Connecticut
Geometrically asymmetric tunneling nanostructures are of interest to make ultra-high frequency diodes for applications in detection and solar energy harvesting. Atomic layer deposition (ALD) is one of the most promising techniques for fabrication of tunneling nanostructures. In previous work, it has been demonstrated that individual metal-vacuum-metal (MVM) tunnel junctions with a gap distance of 1-2 nm can be fabricated by selective-area ALD of Cu onto Pd templates. However, optimizing nonlinearity and scaling up to large arrays of tunneling devices both introduce new challenges that include achieving precise control of nucleation and good quality conformal growth on sharply defined asymmetric nanostructures.

In this study, the fabrication of large arrays of MVM tunnel junctions is investigated using selective-area ALD. Nano-patterned Pd nanostructures with sharp asymmetric features are prepared as seed layers for planar, geometrically-asymmetric junctions on SiO_2 / silicon substrates by high-resolution electron beam lithography. Selective-area ALD applied to patterned Pd nanostructures allows tuning the size of junctions to nanometer dimensions. Microscopy and chemical analysis are used to evaluate nanostructure morphology, tunnel junction uniformity, and selective area growth characteristics. In-situ electrical measurements are used to measure DC current-voltage curves and nonlinearity. It was found that film nucleation and growth selectivity can be greatly affected by different pre-deposition sample treatments. UV/Ozone (UVO) cleaning and hydrogen annealing before ALD both enhance the nucleation of Cu thin films on Pd seed layers. In addition, UVO treatment promotes selective growth on Pd vs. SiO_2 areas while boiling samples in water to hydroxylate SiO_2 surface area contributes to a loss of selectivity. In-situ measured electrical data during ALD growth demonstrate a gradual convergence to tunneling with sub-nm control provided by the ALD method. However, control of tunneling non-linearity and geometric asymmetry is complicated by an incomplete understanding of the growth mechanism and the morphology evolution of nanostructures. There is a compromise between conditions that promote good ALD growth and those that maintain geometric asymmetry. We conclude with suggestions to promote growth, maintain sharp asymmetric features, and achieve non-linear tunneling characteristics.

Energy Frontiers Focus Topic
Room: 211B - Session EN+AS+EM+NS+SE+SS+TF-MoA

Solar Cells II
Moderator: Adrie Mackus, Stanford University

2:20pm **EN+AS+EM+NS+SE+SS+TF-MoA1 Influence of Annealing Temperature in the Bulk Defect Formation in Perovskite Thin Films**, *Weina Peng, B.X. Anand, L.-H. Liu, S.C. Sampat, B.E. Bearden, A.V. Malko, Y.J. Chabal*, University of Texas at Dallas
Perovskites are emerging as front-runners for solar cell applications because of their superior optoelectronic properties. Over the past few years the grain size of perovskites has been continuously improved from several hundred of nanometers to a few millimeters which resulted in better solar conversion efficiencies. In addition to surface and grain boundary related defects, perovskites are prone to the formation of bulk defects as well. However the role of bulk defects in the determination of photovoltaic performance of perovskites is rarely explored. To this end we investigate the impact of annealing temperature on the defect density in polycrystalline $CH_3NH_3PbI_3$ thin films of ~1 micron average grain size prepared using vapor assisted solution process (VASP). The photoluminescence (PL) intensity and lifetime show systematic reduction when the annealing temperature is increased from 150°C to 200°C. A rough estimate of the defect state density obtained using fluence dependent PL measurements reveal a 5 fold increase in defect density for a 25°C increase in annealing temperature although the average grains size stays unchanged. Furthermore, surface passivation of perovskite films using Al_2O_3 via atomic layer deposition leads to an improvement in PL intensity and lifetime. But the PL quantum efficiency, as well as the lifetime, of the surface passivated 200°C annealed sample remains significantly lower than that of the un-passivated 150°C annealed sample indicating that the majority of the defects states we observe in the high temperature annealed samples originate from bulk defects. Thus the present study shows that minimizing the number of bulk defects, in addition

to surface defects, is very important in the realization of highly efficient perovskite solar cells.

3:00pm EN+AS+EM+NS+SE+SS+TF-MoA3 Tandem Solar Cells Using Perovskites, Silicon and CIGS, *M.D. McGehee, Tomas Leijtens*, Stanford University **INVITED**

The efficiency of perovskite solar cells has soared from a few percent to over 20% in the last 3 years. They are very attractive for multijunction solar cell applications because the bandgap of perovskite semiconductors can be easily tuned in the range of 1.55 to 2.2 eV and the open circuit voltage of the cells is large. We have made highly efficient semitransparent perovskite solar cells using silver nanowire meshes as the top electrode. These cells can be used in combination with either silicon or copper indium gallium diselenide solar cells to make four-terminal and two-terminal tandems. We will also present detailed characterization of perovskite semiconductors made with different processing conditions to show what needs to be done to minimize recombination and make the solar cells stable.

3:40pm EN+AS+EM+NS+SE+SS+TF-MoA5 Lifetime, Mobility, and Diffusion of Photoexcited Carriers in Ligand-Exchanged Lead Selenide Nanocrystal Films Measured by Time-Resolved Terahertz Spectroscopy, *G.W. Guglietta*, Drexel University, *B.T. Diroll, E.A. Gaulding, J.L. Fordham,* University of Pennsylvania, *S. Li,* Drexel University, *C.B. Murray,* University of Pennsylvania, *Jason Baxter*, Drexel University

Colloidal semiconductor nanocrystals have been used as building blocks for electronic and optoelectronic devices ranging from field effect transistors to solar cells. Properties of the nanocrystal films depend sensitively on the choice of capping ligand to replace the insulating synthesis ligands. Thus far, ligands leading to the best performance in transistors result in poor solar cell performance, and vice versa. To gain insight into the nature of this dichotomy, we used time-resolved terahertz spectroscopy measurements to study the mobility and lifetime of PbSe nanocrystal films prepared with five common ligand-exchange reagents. Non-contact terahertz spectroscopy measurements of conductivity were corroborated by contacted van der Pauw measurements of the same samples. The films treated with different displacing ligands show more than an order of magnitude difference in the peak conductivities and a bifurcation of time-dynamics. Inorganic chalcogenide ligand-exchanges with sodium sulfide (Na_2S) or ammonium thiocyanate (NH_4SCN) show high THz mobilities above 25 $cm^2V^{-1}s^{-1}$, which is desirable for transistors, but nearly complete decay of transient photocurrent within 1.4 ns. The high mobility with NH_4SCN and Na_2S exchanges is more than offset by their short lifetimes and results in diffusion lengths of only ~200 nm. In contrast, ligand exchanges with 1,2-ethylenediamine (EDA), 1,2-ethanedithiol (EDT), and tetrabutylammonium iodide (TBAI) show ~5x lower mobilities but much longer carrier lifetimes, with ~30% of photoexcited carriers remaining for >10 ns. The long lifetimes with EDA, EDT, and TBAI yield diffusion lengths of at least 500 nm, which is approaching the film thickness desired for strong light absorption in solar cells. This bifurcated behavior may explain the divergent performance of field-effect transistors and photovoltaics constructed from nanocrystal building blocks with different ligand exchanges.

4:00pm EN+AS+EM+NS+SE+SS+TF-MoA6 iCVD Synthesis and Integration of Poly(vinylpyrrolidone) and Poly(4-vinylpyridine) as Polymer Electrolytes in Dye Sensitized Solar Cells, *Yuriy Y. Smolin*, S. *Janakiraman, A.J. Sauter, M. Soroush, K.K.S. Lau,* Drexel University

Initiated chemical vapor deposition (iCVD) is used to synthesize and integrate poly(4-vinylpyridine) (P4VP) and polyvinylpyrrolidone (PVP) as polymer electrolytes within the mesoporous TiO_2 photoanode of dye sensitized solar cells (DSSCs). DSSCs with conventional liquid electrolytes are prone to leakage and evaporation, which hinders DSSC durability and field implementation. In addition, liquid electrolytes lead to significant electron recombination within the cells that limit DSSC performance. In contrast, polymer electrolytes do not suffer from the practical disadvantages and could potentially enhance the cell's I-V behavior.

However, in order to enable good contact between the TiO_2 electrode and the polymer electrolyte, a major obstacle is the difficulty in achieving good pore filling of the polymer into the mesoporous TiO_2 layer. Mesoscale pore diameter, high aspect ratio, and tortuous pore structure of the photoanode along with liquid surface tension, poor wettability, and solute steric hindrance make pore filling extremely limited when using liquid techniques. This leads to poor electrical contact and lower efficiency. To overcome the challenges of pore filling, we directly synthesized polymer electrolytes inside the pore volume of the photoanode using the solvent-free technique of iCVD. iCVD relies on the vapor delivery of monomer and initiator, which facilitates infiltration into the porous TiO_2 substrate, and by controlling the relative rates of diffusion and surface polymerization through iCVD process parameters, uniform and conformal growth of

polymer is achieved. The pore filling of the polymer electrolyte into 5–10 μm photoanodes using iCVD is typically 90–100% which is significantly better than that achievable with liquid techniques like spin coating.[1]

In this work, we will show that iCVD P4VP and PVP polymer electrolytes can be effectively integrated within TiO_2 mesoporous photoanodes to produce enhanced DSSCs. By varying the polymer electrolyte chemistry including the use of a crosslinking agent during iCVD to stabilize the resulting polymer structure, DSSC I-V characteristics, such as open-circuit voltage, short-circuit current density and fill factor, are tuned.[2] To gain a better understanding on the effect of the polymer electrolyte, experimental techniques such as linear sweep voltammetry, intensity modulated spectroscopy, and impedance spectroscopy are used. Mathematical modeling of DSSC behavior is also performed to relate these experimental observations with the dynamics of the operation of the cell.

1. S. Nejati and K. K. S. Lau, *Nano Lett.*, 2010, 11, 419-423.

2. Y. Y. Smolin et al., *J. Power Sources*, 2015, 274, 156-164.

4:20pm EN+AS+EM+NS+SE+SS+TF-MoA7 Interfacial Effects on Device Performance in Organic Solar Cells, *Huanxin Ju*, J.F. Zhu, University of Science and Technology of China, *D.S. Ginger*, University of Washington

The better understanding of the underlying mechanisms is essential for the further development of highly efficient organic photovoltaics (OPVs) devices. In this paper, the transient photovoltage (TPV) and charge extraction (CE) measurements in combination with the synchrotron radiation photoemission spectroscopy (SRPES) were used to gain insights intothe correlation between the microscopic interfacial properties and macroscopic device performance. The OPV devices based on PCDTBT: $PC_{70}BM$ with Ca interlayer were studied as a reference system to investigate the interfacial effects on device performance. The charge carrier decay dynamics demonstrated that the device with the Ca interlayer exhibited a lower recombination constant (k_{rec}) than that only with the Al cathode at a given charge carrier density (n). In addition, the interfacial energy band structures indicated that the strong dipole moment produced by the Ca interlayer can facilitate electron extraction as well as drive hole away at the cathode/polymer interface, resulting in retarding interfacial recombination losses. Finally, we examined the device performance with the Ca interlayer to find that the efficiency is improved by 28% as compared to that without the Ca interlayer, which shows good correlation with the observed interfacial properties.

4:40pm EN+AS+EM+NS+SE+SS+TF-MoA8 Tungsten-Titanium Mixed Oxide Thin Films for Improved Structural and Optical Properties for Solar Driven Applications, *Mirella Vargas*, The University of Texas at El Paso, *N.R. Murphy,* Air Force Research Laboratory, *R.V. Chintalapalle*, The University of Texas at El Paso

Tungsten oxide (WO_3) is a well-established n-type semiconductor possessing unique optical and electronic properties. WO_3 has become the most interesting inorganic material for electrochromic applications due to the reversible spectral absorption properties associated with WO_3. WO_3 thin films and nanostructures exhibit an optical band gap that permits efficient use of the solar spectrum including absorption in the blue part of the visible region and the ultraviolet region, as well as a high transmission region that extends from the near-infrared (IR) to the visible spectrum. Coupled with good electronic transport properties, photosensitivity, and chemical integrity, WO_3-based materials are attractive for applications related to sustainable energy production including energy efficient windows and architecture, photoelectrochemical (PEC) water-splitting, photocatalysis and solar cells. Anion or cation doping into WO_3 has been extensively studied as this offers the opportunity to tailor the transport properties that may influence the efficiency of solar driven devices. Titanium doping into WO_3 has proven to enhance the electrochromic response and the cyclic lifetime by a factor of five in PEC devices. In the present case a systematic investigation of progressively increasing the Ti content in the W-Ti target for reactive sputtering has been employed to tune the structure, chemistry, and properties of the films. Tungsten-titanium (W-Ti) mixed oxide thin films were fabricated using reactive sputtering of W-Ti alloy targets with Ti content ranging from 0 to 30 wt.%. X-ray photoelectron spectroscopy confirms the existence of W and Ti in their highest oxidation states of +6 and +4, respectively. Quantification of binding energy shifts for W and Ti core-level transitions confirms the formation of WO_3-TiO_2 composite oxide films. Optical analyses made from spectrophotometry measurements indicate a decrease in band gap with a discrete amount of Ti incorporation. The band gap decreases with increasing Ti from 3.0 eV to 2.5 eV. Such films are expected to have the possibility for tuning the electrical conductivity while retaining the optical transparency to make them efficient for photoelectrochemical cells and photovoltaics.

5:00pm EN+AS+EM+NS+SE+SS+TF-MoA9 Potential Resolution to the "Doping Puzzle" in Pyrite FeS$_2$, *X. Zhang, M. Li, L. O'Brien, J. Walter, M. Manno, F. Mork, J. Kakalios,* **Eray Aydil**, *C. Leighton*, University of Minnesota

In principle, pyrite FeS$_2$ is one of the most suitable photovoltaic materials for sustainable low-cost, large-scale solar cell manufacturing because it has high absorbance in the visible and comprises earth-abundant inexpensive elements. However, current efficiencies of solar cells based on pyrite FeS$_2$ have not exceeded 2.8%. Early research on this material concluded that unintentionally doped FeS$_2$ thin films are *p*-type and subsequent solar cell work evolved based on this presumption. In fact, it is now widely accepted that FeS$_2$ thin films almost always exhibit *p*-type conduction even though single crystals are typically found to be *n*-type. This discrepancy between single crystals and thin films is perplexing and to date this puzzle remains unexplained. In this talk we reexamine the conclusion that undoped FeS$_2$ films are predominantly *p*-type and provide an explanation for this "doping puzzle" in pyrite. Using a combination of Hall effect, thermopower, and temperature-dependent resistivity measurements on a large set of well characterized single crystals and thin films, we show that the widely accepted predominant *p*-type behavior in pyrite films may, in fact, be an artifact of hopping conduction and should be revisited. Specifically, both Hall effect and thermopower measurements establish that all of our high-mobility (>1 cm^{2}V^{-1}s^{-1}) films and single crystals are *n*-type. Temperature-dependent resistivity measurements on these high mobility films and crystals establish diffusive electronic transport. We find that films with lower mobility (4x10^{-3}-1 cm^{2}V^{-1}s^{-1}) also show *n*-type Hall effect but exhibit a *p*-type Seebeck coefficient, leading to a discrepancy in the measured carrier type. Temperature-dependent resistivity measurements on these intermediate mobility films show a transition from diffusive to hopping transport. Finally, both Hall and Seebeck coefficients are strongly suppressed and invert in the lowest mobility thin films (<4x10^{-3} cm^{2}V^{-1}s^{-1}) indicating apparent *p*-type conduction. Temperature-dependent resistivity measurements establish unambiguous hopping behavior in these lowest mobility films. Based on this evolution of Hall and Seebeck coefficients with carrier mobility, and the well-known suppression of the Hall and Seebeck effects in conductors with hopping electronic transport, we conclude that the apparent crossover from *n*-type to *p*-type with decreasing mobility is, in fact, an artifact of hopping conduction.

5:20pm EN+AS+EM+NS+SE+SS+TF-MoA10 Interparticle Contact Radius and Electron Transport in Thin Films Comprised of Nanocrystals, *Elijah Thimsen*, *D. Lanigan*, Washington University, St. Louis

Thin films comprised of nanocrystals are being explored for a variety of applications that involve electron transport. For traditional applications such as photovoltaic solar cells, the goal is often to utilize solution processing to make an inexpensive thin film that essentially behaves as a bulk material with diffusive transport. For other applications, such as neuromorphic computing, variable range hopping (VRH) transport is more desirable because it enables a given nanocrystal to have orders of magnitude more nearest neighbors than it physically touches. It is of paramount importance that the structure-property relationships that control electron transport mechanism be elucidated. Previous work has demonstrated that interparticle separation distance affects charge carrier mobility. However, for films comprised of nanocrystals that are physically touching, what is the effect of contact radius? In this work, we present a systematic experimental study of the effect of interparticle contact radius on the electron transport mechanism in thin films comprised of heavily-doped ZnO nanocrystals embedded in Al$_2$O$_3$. As the contact radius increased, the electron transport mechanism crossed over from VRH to diffusive conduction. For large contact radius between nanocrystals, the room-temperature electron mobility in the film approached the local mobility within a nanocrystal, approximately 10 cm^{2}V^{-1} s^{-1}. The conclusion is that for nanocrystals that are physically touching, the interparticle contact radius determines the transport mechanism. With the ability to control the electron transport mechanism in films comprised of ZnO nanocrystals, we performed an exploratory study of the Hall effect in these materials. Hall effect measurements are of great utility and are routine for determining charge carrier mobility and type, but the interpretation of data for materials that exhibit VRH has been difficult in the past. For well-connected ZnO nanocrystals that exhibit diffusive conduction, the Hall coefficient was independent of temperature, as expected for the high doping level. Alternatively, for films with small contact radius between nanocrystals, which exhibited a VRH transport mechanism, we observed an anomalous behavior of the Hall coefficient at low temperature (100 to 200 K). Surprisingly, for films that exhibited VRH, the magnitude of the Hall coefficient increased exponentially with decreasing temperature, in stark contrast to the conventional wisdom that the Hall effect is suppressed for VRH.

In-Situ Spectroscopy and Microscopy Focus Topic
Room: 211C - Session IS+AS+SA+SS-MoA

Ambient Pressure X-ray Photoelectron Spectroscopy Studies for Catalytic and Energy Materials in Gas Phase
Moderator: Peter Crozier, Arizona State University, Franklin (Feng) Tao, University of Kansas

2:20pm IS+AS+SA+SS-MoA1 In situ Electron Spectroscopy for Energy Science, *Robert Schlögl*, Fritz-Haber-Institut der Max-Planck-Gesellschaft, Germany **INVITED**

The use of volatile renewable electricity in lager amounts in our energy systems requires grid-scale technologies for integration electricity in material energy carrier streams. Several systemic options always suffer from our conceptual weakness to convert free electrons in chemical bonds. This can be achieved with accumulators for limited applications and should be done through water splitting and synthesis of solar fuels in almost unlimited applications. Complex interfacial chemistry is the underlying scientific challenge. To tackle this old challenge with new concepts it is essential to improve our ability to study chemical, electronic and geometric structures of nanoscopic objects in-situ meaning under operation conditions. A whole train of dedicated instrumentation from specimen formation, data acquisition and auxiliary analyses plus sample manipulation is necessary for this task. The presentation gives some aspects of priority challenges and uses examples of operation studies of water splitting catalysts and of CO2 reduction systems to illustrate the present status of insight. In the outlook the possibilities of the novel experiment EMIL at BESSY will be discussed.

3:00pm IS+AS+SA+SS-MoA3 Catalysis on Singly Dispersed Bimetallic Sites on Oxide Support, *Luan Nguyen*, University of Kansas, *A. Frenkel*, Yeshiva University, *J. Li*, Tsinghua University, China, *F. Tao*, University of Kansas

Reaction events of heterogeneous catalysis occur on specific catalytic sites. Atoms of a catalytic site arrange in a specific geometric/electronic configuration for adsorbing/dissociating reactant molecules and subsequent coupling to form product molecules. Bimetallic catalysts play significant roles in chemical and energy transformations due to their tunable catalytic properties through ligand, geometric, bi-functional, or lattice strain effect.

When a bimetallic site (M_1A_n, M and A: metal elements, n ≥ 1) is one of the continuous sites on the surface of a bimetallic NP, this site is in a metallic state. However, when M_1A_n sites are *separately* anchored on a surface of a transition metal oxide support, these isolated bimetallic sites are in cationic state. Such change in electronic structure could cause these bimetallic sites to have stronger chemisorption to reactant or/and intermediate molecules, thus facilitating its dissociation and subsequent coupling. In addition, singly dispersion of metal M in M_1A_n minimizes the potential binding configurations of reactant molecules hence may enhance catalytic selectivity toward a specific reaction pathway. Here we present singly dispersed bimetallic catalyst Rh_1Co_3 prepared on Co oxide support, which exhibits 100% selectivity for the production of N_2 in NO reduction with CO.

Preparation of isolated bimetallic sites Rh_1Co_3 on Co_3O_4 nanorods begins with the formation of hydroxide species $Rh(OH)_n$ on the surface of Co_3O_4, followed by calcination at 150ºC in O_2 to form Rh-O-Co bonds between singly dispersed $Rh(OH)_n$ species and the surface of Co_3O_4, and concluded with a carefully controlled reduction to remove oxygen atoms between Rh and Co and thus a simultaneous formation of Rh-Co bonds. In-situ ambient pressure X-ray photoelectron spectroscopy (AP-XPS) was used to monitor the oxidation and reduction steps and to avoid over or under-reduction.

Formation of singly dispersed Rh atoms was visualized using HAADF-STEM. The bonding environment of Rh to three Co atoms was confirmed using in-situ EXAFS. For reduction of NO with CO, Rh_1Co_3/CoO exhibits high activity at 110 ºC with 100% selectivity toward N_2 production. In contrast, Rh-Co alloy NP/CoO has much lower activity and selectivity (10%) under the same condition. In-situ AP-XPS investigation shows that Rh atoms are at cationic state instead of metallic state. Along with this, DFT calculations suggest that a strong adsorption of intermediate N_2O molecules on Rh_1Co_3 site prevents its desorption as a byproduct and provides a dissociation pathway of N_2O to N_2 with a low activation barrier (~0.21 eV), thus leading to a 100% selectivity to N_2 production.

3:20pm IS+AS+SA+SS-MoA4 Oxidation and Recovery of WC Thin Film Surfaces, *E. Monazami,* University of Virginia*, J.B. McClimon,* University of Pennsylvania*, N. Johansson, P. Shayesteh, S. Urpelainen, J. Schnadt,* Lund University, Sweden*, **Petra Reinke***, University of Virginia

Transition metal carbide (TMC) surfaces are coveted as catalytic materials, electrodes and hard protective coatings. A bottleneck in their use is surface oxidation, which leads to a decay in performance. Our work establishes the feasibility of surface recovery by using a carbon-rich WC layer where recarburization of the surface is initiated by an annealing step. Thin carbon-rich tungsten carbide layers are grown by co-deposition of W and C_{60} on a MgO(001) surface at 1100 K. The MgO substrate serves as a diffusion barrier for carbon, and the films have a well-defined carbon inventory controlled by the deposition rates of the reactants. The film surfaces were studied by in-situ Scanning Tunneling Microscopy and Spectroscopy. Raman spectroscopy confirmed the presence of highly defective graphitic carbon. The oxidation-recarburization (O-R) cycles were studied in the ambient pressure endstation SPECIES at MAX-Lab (J. Synchr. Rad. 701, 19 (2012)) in a pressure of 0.3 mbar of O_2. Oxidation with $p(O_2)$ of 10^{-5} mbar were performed at SPECIES for direct comparison to low $p(O_2)$ STM experiments.

The carbon-rich WC films exhibit a relatively rough surface, which allows only in a few instances true atomic resolution, but graphite as well as graphene layers can be identified. Oxidation at T>550 K leads to etching of surface carbon and the growth of a W-oxide layer and STS maps show the oxide evolution. The oxidation in the low $p(O_2)$ pressure regime progresses slowly and the surface carbide is recovered by annealing.

The use of the SPECIES endstation enabled a quantiative study of the O-R cycles including a detailed analysis of the respective bonding environments which are modified at different times in the O-R cycle. The oxidation in the ambient pressure environment was monitored using the ratio of W-carbide to W-oxide in the W4f core level during the reaction. The steady state thickness of oxide is a function of sample temperature and order of annealing cycles. The surface carbide concentration can be fully recovered in a subsequent annealing step, and repeated O-R cycles were performed. The O-R process is controlled by the interplay between surface oxidation, oxygen and carbon diffusion and our results will be modeled with a simple set of transport equations. We will discuss the role of different bonding environments as we move through the O-R cycle and compare UHV and ambient pressure results up to 800 K. These results clearly illustrate that carbon-rich tungsten carbide materials can be used to achieve a long term use of carbide surfaces in catalysis and fuel cell applications.

3:40pm IS+AS+SA+SS-MoA5 Microscopy, Spectroscopy, and Reactivity of Surfaces in Vacuum and under Ambient Reaction Pressures, *Miquel Salmeron, B. Eren,* Lawrence Berkeley National Laboratory **INVITED**

The goal of surface science research is to provide atomic level understanding of the structural and dynamic properties of surfaces, a goal particularly relevant for chemical applications, including catalysis, photochemistry, batteries and fuel cells. With X-ray Photoemision Spectroscopy (XPS) and X-ray absorption Spectroscopy (XAS) we determine composition and electronic structure. With Scanning Tunneling Microscopy (STM) we image atoms and molecules as they adsorb, diffuse and react on single crystal surfaces. To study surfaces in the presence of gases, in the Torr to Atmospheres range, which is relevant to practical catalysis, new instrumentation is needed. Over the last years we developed high pressure STM, XPS and XAS, to study surfaces under high coverage of adsorbates in equilibrium with gases near ambient pressures and temperature. Using a combination of these techniques I will show how under these conditions the structure of surfaces and the adsorbed layers can be very different from that at low coverage, or even at high coverage but at low temperature. Adsorbates can induce dramatic restructuring of the surface, as I will show in the case of CO induced restructuring of Cu surfaces and the reactions with Oxygen.

4:20pm IS+AS+SA+SS-MoA7 Novel Solutions for Ambient Pressure and *In Situ* Photoelectron Spectro-Microscopy, *Hikmet Sezen, M. Amati, L. Gregoratti,* Elettra-Sincrotrone Trieste, Italy

A technique based on photoelectron spectroscopy (PES) providing simultaneously spectroscopy and microscopy capabilities and being compatible with ambient pressure conditions is still missing. Ambient pressure PES (APPES), based on differential pumping of the electron energy analyzer, offers an optimal spectroscopic solution to overcome pressure barrier for surface related studies[1]. Unfortunately, APPES has very limited spatial resolution. On the other hand, a better than 100 nm spatial resolution scanning photoelectron microscope (SPEM), where the X-ray beam is demagnified down to a 130 nm spot by Zone Plate Fresnel

optics and the sample scanned under the focused beam, is accessible from a few synchrotrons. A direct adaptation of the APPES approach to SPEM technique is not possible because of geometric constrains, stabilities and sustainability of the x-ray optics under near ambient pressures, and mechanical stability of the photoelectron detection system under such severe pumping conditions. In this presentation we will introduce two novel solutions for near-ambient pressure SPEM with ~100 nm spatial resolution and compatible with in-situ/operando conditions operated at ESCAmicroscopy beamline at Elettra synchrotron facility.

Dynamic high pressure (DHP) is the one of our near-ambient pressure SPEM solution. The technique is based on generating high pressure pulsed gas packets directed to the sample. Under influence of gas pulses the sample fells a few mbar pressure in a burst instant, then gas packets dilute into the SPEM chamber to yield a 1×10^{-5} mbar background pressure. From the test results a 10^{-3}-10^{-2} mbar equivalent static pressure was felt by Si and Rh samples during in-situ oxidation reaction.[2] It is available for users.

Effusive cell is another solution for near-ambient pressure SPEM. The sample is encapsulated with a vacuum sealed cell and located just 30-50 μm behind of a 200 μm diameter size pinhole. The focused x-ray beam are scanning the sample trough the pinhole. The generated photoelectrons come out from the same pinhole and are able to reach the electron energy analyzer. Due to the geometric orientation of energy analyzer and the pinhole we can achieve ca. a 200x100 μm^2 aerial point of view on the sample. The pressure inside the cell can be raised up to mbar range while the pressure in the main chamber kept around 1×10^{-5} mbar which is the safety limit for SPEM system. An encapsulated filament is behind the sample for heating, and other electrical connections are ready for biasing of sample, and thermocouple connections.

[1] D. F. Ogletree, et al. Rev. Sci. Instrum. 73, 3872 (2002)

[2] M. Amati, et al. J. Instrum. 8, 05001 (2013)

4:40pm IS+AS+SA+SS-MoA8 *In Situ* Studies of Partial Oxidation of Methanol to Hydrogen on Isolated Bimetallic Site Pt_1Zn_n, *Shiran Zhang, L. Nguyen,* University of Kansas*, A. Frenkel,* Yeshiva University*, J. Liu,* Arizona State University*, F. Tao,* University of Kansas

Partial oxidation of methanol to hydrogen and carbon dioxide offers a novel route in converting liquid fuel to hydrogen for fuel-cell systems and thus has been widely investigated in the past decade. One important category of heterogeneous catalysts for catalyzing this reaction is bimetallic nanoparticles which consist of continuous bimetallic sites in a metallic state. Isolation of such bimetallic sites through anchoring them on oxide could offer distinctly different catalytic performance in contrast to continuous sites on bimetallic nanoparticles.

Here we reported an isolated bimetallic site Pt_1Zn_n supported on ZnO which offers an extremely high catalytic activity with high selectivity for transformation of methanol to hydrogen with oxygen. It was prepared through a restructuring of singly dispersed Pt atoms on ZnO with reducing treatment. The formed isolated Pt atoms on ZnO was characterized with high-angle annular dark-field scanning transmission electron microscopy (HAADF-STEM) along the projected [10-10] of ZnO as well as the corresponding structural model (Figure 1). The bright spots show single dispersion of Pt atoms. The offset of Pt atoms to the Zn atom row suggests Pt atoms are on the column of oxygen atoms, which indicates the bonding of Pt atom to Zn atoms. Photoemission feaures of Pt4f of the catalyst during catalysis were tracked with ambient pressure X-ray photoelectron spectroscopy (AP-XPS) using monochromated Al Kα (Figures 2). The resultant partial reduced state of Pt atoms under reaction conditions is consistent with the electronic state of Pt in Pt_1Zn_n bimetallic site.

Catalytic performance of the formed isolated Pt_1Zn_n bimetallic site in partial oxidation of methanol was evaluated and compared with Pt-Zn bimetallic nanoparticle catalyst (Figure 3). Isolated Pt_1Zn_n bimetallic site catalyst exhibits much higher activity per active site and selectivity to H_2 than Pt-Zn nanoparticle catalyst in transformation of methanol to hydrogen through partial oxidation. The cationic nature of these isolated bimetallic site in contrast to the metallic nature of active sites on a nanoparticle could be responsible for the differences in catalytic performance. This study illustrates that isoaltion of continuous bimetallic sites on a nonmetallic support is a new opportunity to tune catalytic performance of bimetallic catalysts.

5:00pm IS+AS+SA+SS-MoA9 New Developments in Small Spot and Imaging Near Ambient Pressure XPS, *Andreas Thissen*, SPECS Surface Nano Analysis GmbH

Over the last 15 years, Near Ambient Pressure (NAP-) XPS has demonstrated its promising potential in a wide variety of applications. Starting from the Catalysis and Ice paradigm, the focus has shifted towards solid-liquid interfaces, liquid jets and in-situ electrochemistry. Initially, the experiments had to be carried out using advanced synchrotron sources to

reach reasonable count rates. But now, the SPECS PHOIBOS 150 NAP offers optimized transmission for electrons, even at pressures up to and above 100mbar, so researchers can now use it with conventional X-ray and UV sources in their own laboratories. Because of the widened application fields, standard XPS is now also attainable when combined with easily adjustable monochromated X-ray sources that offer stable operation, small excitations spots, and high photon flux densities, even in Near Ambient Pressure conditions. The latest designs and results are presented showing small spot performance for spot sizes < 30 μm, while also showcasing the latest implementations of imaging NAP-XPS that uses a new concept allowing for lateral resolved measurements without a compromise in count rate and usability. Highlighting on how sample environments (in situ cells for gases and liquids, electrochemical cells, gas inlets) and integration are both absolutely essential to obtain relevant results from well-defined samples, the presentation will demonstrate the use of NAP-XPS systems for high throughput-XPS measurements, as well as a variety of applications.

5:20pm IS+AS+SA+SS-MoA10 In Situ Measurement of the Abundances and Temperatures of the Constituents of Semiconductor Manufacturing Plasmas via Terahertz Absorption Spectroscopy: Comparison with Theoretical Models, *Yaser Helal*, C.F. Neese, F.C. De Lucia, The Ohio State University, *A. Agarwal, B. Craver, P.R. Ewing, P.J. Stout, M.D. Armacost*, Applied Materials, Inc.
Plasmas used by the semiconductor manufacturing industry are similar in pressure, temperature, and electron density to those used for the laboratory study of astrophysical neutrals, ions, and radicals. Thus, methods developed over several decades in the submillimeter/terahertz spectral region are directly applicable. Important attributes of terahertz absorption spectroscopy are that it can provide from first principles, without need for calibration, absolute concentrations and temperatures. Furthermore, since there are no intrusive probes, terahertz observations do not impact or change the plasma under study. Such measurements provide details and insight into the interactions and reactions occurring within the plasma and their implications for semiconductor manufacturing processes. In this work, a continuous wave, 0.5 – 0.75 THz absorption spectrometer was developed and used to study the processes in a commercial inductively coupled plasma (ICP) etch chamber. Because of the relatively long wavelength of the terahertz radiation, diffraction is more serious than in the optical regime. As a result, an important part of this work was the development of optical strategies to couple this spectrometer to the plasma reactor using its existing viewports. Comparisons of the experimental results with predictions from equipment models for ICPs will also be presented for $Ar/CF_4/CHF_3$ with varying pressures, powers, and gas mixture ratios. Comparisons such as this provide a basis for validating and improving models, whose development is a complex and difficult science in itself. The results presented in this talk show that terahertz rotational spectroscopy can provide unique and easy to interpret information about manufacturing plasmas and is a useful development tool for process, theoretical and physical models, and the improvement of etch methods.

Surface Science
Room: 113 - Session SS-MoA

Organics and Ionic Liquids: Surfaces, Layers, Interfaces and Chirality
Moderator: Janice Reutt-Robey, University of Maryland, College Park, John Russell, Jr., Naval Research Laboratory

2:20pm SS-MoA1 ZnTPP, PTCDA, TCNQ, and TTF on TiO2(110): Molecule-Oxide Interaction and Electronic Energy Level Alignment, *Charles Ruggieri*, S. Rangan, R.A. Bartynski, Rutgers, the State University of New Jersey, *J.I. Martinez*, Institute of Materials Science of Madrid, Spain, *F. Flores, J. Ortega*, Autonomous University of Madrid, Spain
The injection of charge between transition metal oxides and organic materials depends crucially on the interface barrier that is determined by the organic electronegativity, the possible space charge layer formed in the oxide, and the chemical interaction between the oxide and the organic. We investigate the interfaces of TiO2(110) and four organic molecules, ZnTPP, PTCDA, TCNQ, and TTF, representing a broad range of electronegativities, and the electronic energy level alignment for each interface, using a combination of direct and inverse photoemission spectroscopies and theoretical modelling. In particular, we analyze contributions to the electronic energy level alignment from oxide-molecule chemical hybridization, induced electrostatic dipoles due to molecular distortion, and charge transfer, and the relative importance of these phenomena to each case. In this way, we provide a detailed description of the wide range of

interactions influencing the final electronic energy level alignment for weakly and strongly interacting organic on TiO2 (110).

2:40pm SS-MoA2 Characterizing the Influence of Water on Charging and Layering at Electrified Ionic-Liquid/Solid Interfaces, *Hsiu-Wei Cheng*, Max-Planck-Institut für Eisenforschung GmbH, Germany, *P. Stock*, Max-Planck Institut für Eisenforschung GmbH, Germany, *B. Moeremans*, Universiteit Hasselt, Belgium, *T. Bamipos*, Max Planck Institut fur Eisenforschung GmbH, Germany, *X. Banquy*, University of Montreal, Canada, *F.U. Renner*, Universiteit Hasselt, Belgium, *M. Valtiner*, Max-Planck Institut für Eisenforschung GmbH, Germany
The importance of water on molecular ion structuring and charging mechanism of solid interfaces in room temperature ionic liquid (RTIL) is unclear and has been largely ignored. Water may alter structures, charging characteristics and hence performance at electrified solid/RTIL interfaces utilized in various fields including energy storage and conversion or catalysis. Here, we utilize Atomic Force Microscopy to directly measure how water alters the interfacial structuring and charging characteristics of [C_2mim][Tf_2N] on mica and electrified gold surfaces. On hydrophilic and ionophobic mica surfaces, water-saturated RTILs induce strong ion layering by dissolution of surface-bound cations and a resulting high surface charging. In contrast, layering of dry RTIL at uncharged mica surfaces is weakly structured. At electrified, hydrophobic and ionophilic gold electrodes, significant water effects were found only at positive applied electrochemical potentials. Here, the influence of water is limited to interactions within the RTIL layers, and is not related to a direct electrosorption of water on the polarized electrode. More generally, our results suggest that effects of water on interfacial structuring of RTIL strongly depend on both (1) surface charging mechanism, and (2) interfacial wetting properties. This may greatly impact utilization and design of RTILs and surfaces for interface dominated processes.

3:00pm SS-MoA3 Interfaces of Ionic Liquids, *Hans-Peter Steinrück*, Universität Erlangen-Nürnberg, Germany **INVITED**
Ionic liquids (ILs), salts with melting points below 100 °C, represent a fascinating class of liquid materials, typically characterized by an extremely low vapour pressure. Besides their application as new solvents or as electrolytes for electrochemical purposes, ILs are also used in catalysis. Two important concepts in this context are Supported Ionic Liquid Phase (SILP) and Solid Catalyst with Ionic Liquid Layer (SCILL). In both, a high surface area solid substrate is covered with a thin IL film, which contains either a homogeneously dissolved transition metal complex for SILP, or which modifies catalytically active surface sites at the support for SCILL. Thereby, the interfaces of the IL with the gas phase and with catalytic nanoparticles and/or support materials are of critical importance. It has recently been demonstrated that these interfaces and also the bulk of ILs can be investigated in great detail using surface science studies in an ultrahigh vacuum environment. From angle-resolved X-ray photoelectron spectroscopy, detailed information on the surface and bulk composition of non-functionalized and functionalized ILs, on segregation and enrichment effects, on the dissolution and reactivity of catalytically active metal complexes in ILs, on the growth of ultrathin IL-layers, and even on liquid phase reactions studied in situ in the IL, can be derived. Various examples will be discussed.

H.-P. Steinrück and P. Wasserscheid, *Ionic Liquids in Catalysis*, Catal. Lett. **2015**, 145, 380.

H.-P. Steinrück, *Recent developments in the study of ionic liquid interfaces using X-ray photoelectron spectroscopy and potential future directions*, Phys. Chem. Chem. Phys. **2012**, 14, 2510.

H.-P. Steinrück, *Surface Science goes liquid !*, Surf. Sci. **2010**, 604, 481.

F. Maier, J. M. Gottfried, J. Rossa, D. Gerhard, P. S. Schulz, W. Schwieger, P. Wasserscheid, H.-P. Steinrück, *Surface enrichment and depletion effects of ions dissolved in an ionic liquid. An X-ray photoelectron spectroscopy study*, Angew. Chem. Int. Ed. **2006**, 45, 7778.

3:40pm SS-MoA5 Free-Standing Gold Nanoparticles on Ultrathin Ionic Liquid Films Studies by Low Energy Ion Scattering (LEIS) Analysis, *Thomas Grehl*, P. Bruener, ION-TOF GmbH, Germany, *L. Calabria, P. Migrowski, D.L. Baptista, F. Bernardi*, Laboratory of Molecular Catalysis, UFRGS, Brazil, *H. Brongersma*, ION-TOF GmbH, Germany, *J. Dupont*, Laboratory of Molecular Catalysis, UFRGS, Brazil
Metal nanoparticles (NPs) in ultrathin films have a variety of applications nano-optical and nano-electronic devices. Several methods have been developed in order to synthesize such films. However, those methods result in "capped" NPs, instead of free-standing NPs which would be a more versatile alternative precursor for ultrathin film growth.

Ionic liquids are known to facilitate well-defined formation of Au NPs from sputter deposition and self-organization of the particles close to the surface

[1]. The size and potential shape of the NPs can be tailored by the properties of the ionic liquids. Applying this principle of NP formation to ultrathin films of ionic liquids is a promising route by which to easily form free-standing NPs in a well controlled manner.

In this study we analyze silicon wafer supported ultrathin films of both hydrophilic and hydrophobic imidazolium based ionic liquids forming an "ionic carpet like" structure. This structure is decorated with gold NPs having a size of 5 - 10 nm from the application of sputter deposition of gold onto the ionic liquid. A range of analytical techniques is applied to the samples, including XPS, XRD, AFM and electron microscopy. Here we present primarily the results from high resolution and high sensitivity Low Energy Ion Scattering (LEIS).

LEIS is the most surface sensitive technique for the elemental characterization of the outermost atomic layer. Noble gas ions having a kinetic energy of a few keV are scattered from the individual surface atoms. By measuring the energy loss in the scattering event, the mass of the respective surface atom can be determined, while the intensity of the scattering signal is proportional to the surface coverage. LEIS has been successfully applied to ionic liquids by several groups to elucidate the termination of the liquid. In addition the LEIS data contain information on the composition of the first few nm of the sample. The latter is used to determine the thickness of the self-organized layer of NPs and allows the thickness measurement of any film covering the gold.

The gold nanoparticles are deposited by sputtering into the hydrophobic (AMI.NTf2) and hydrophilic (AMI.BF4) ionic liquids on Si(111) for 5 and 10 s. The LEIS spectra show gold signal for the hydrophobic ionic liquid. Apparently the gold NPs are out of the probed range of the LEIS technique (10 nm). In contrast to that, the LEIS spectra of the hydrophilic ionic liquid after gold deposition show the presence of gold below the surface. The mean thickness of the organic layers covering the NPs is 6 nm (5 s deposition) and 4.3 nm (10 s deposition).

[1] Kauling et al., Langmuir 2013, 29 (46) 14301

4:00pm SS-MoA6 Early-Stage Solid-Electrolyte Interphase (SEI) Formation: Probing Molecular Carbonate Decomposition Pathways and Artificial Lithium Ethylene Dicarbonate Monolayers, *Wentao Song*, *J.E. Reutt-Robey*, University of Maryland, College Park
The Solid Electrolyte Interphase (SEI) formed at the Li-ion battery (LIB) anode plays a major role in battery cycle life and safety. The ethylene carbonate (EC) electrolyte is known to undergo reduction to a mixture of lithium salts at the onset of SEI formation, but the product branching and sensitivity to electrode structure have not been determined. We report the use of temperature programmed desorption (TPD) and reaction spectroscopy (TPRS) to quantify interactions between the molecular carbonates, ethylene carbonate (EC) and dimethyl carbonate (DMC), and model Li- C(0001) anode surfaces prepared in situ. Both EC and DMC interact weakly with the clean C(0001) surface with adsorption energies of 0.60 ± 0.06 and 0.64 ± 0.05 eV, respectively. Submetallic lithiation of C(0001) significantly increases the binding energies of molecular carbonates, and the range of measured values indicates EC solvation of lithium ions. In the presence of metallic lithium, 1.5 monolayers of EC undergoes complete decomposition, resulting in 70.% organolithium products and 30% inorganic lithium product. Further structural analysis of the early stage organolithium salt, lithium ethylene dicarbonate (LEDC), was performed with UHV-STM. A pulsed microaerosol molecular beam source permitted controlled deposition of LEDC (from dimethyl formamide solvent) on Ag(111). Elongated LEDC monolayer islands spontaneously form in three distinct 120 degree rotational domains, all aligned with the close-packed silver direction. Further deposition increases island size and density, with little change in island shape. Molecularly resolved STM images reveal a LEDC monolayer structure with a 1.1874 ± 0.0079 nm x 0.5793 ±0.0055 nm unit cell containing one LEDC. A structural model is presented that accounts for the anisotropy of the LEDC islands. The O-Li-O linkages in the structural model define the long-axis (fast growth direction) of the islands. The LEDC islands are thermally stable up to at least 80°C, and can be imaged over days under UHV. Preliminary STS measurements (performed in Z-V mode) are consistent with significant differences in the local density of electronic states for LEDC islands relative to the Ag(111) substrate.

4:20pm SS-MoA7 Racemization and Enantioselectivity on Metal Surfaces, *Georg Held*, University of Reading, UK **INVITED**
The last decade has seen a dramatic increase in research into chiral surface systems, driven by the growing demand for optically pure chemicals in drug manufacturing and, hence, a desire for enantioselective heterogeneous catalysts. These avoid the problem of phase separation inherent in homogeneous enantioselective processes which are predominantly used today. So far, significant success has been achieved by modifying achiral surfaces with chiral molecules thus creating stereo-selective reaction

environments [1,2]. Alternatively, intrinsically chiral metal and mineral surfaces show enantioselective behavior without such modifiers [3,4], although these mechanisms are much less well understood. In our work we use synchrotron-based spectrocopies, such as XPS and NEXAFS, alongside LEED and temperature-programmed desorption to characterize the thermal stability, bond coordination and orientation of chiral probe molecules on achiral and intrinsically chiral model catalyst surfaces. The talk will present examples of adsorption systems on both types of surfaces. Particular emphasis is on small chiral amino acids (e.g. alanine, serine), which show razemization as well as enantioselectivity at several levels depending on the substrate and the length of the side-chain of the molecule [5-8].

[1] A. Baiker, J. Mol. Catal. A 115 (1997) 473.

[2] C. J. Baddeley, Top. Catal. 25 (2003) 17.

[3] C.F. McFadden, P.S. Cremer, A.J. Gellman, Langmuir 12 (1996) 2483.

[4] G. A. Attard, J. Phys. Chem. B 105 (2001)

[5] G. Held, M. Gladys, Topics in Catalysis, 48 (2008) 128;

[6] T. Eralp, A. Cornish, A. Shavorskiy, G. Held, Topics in Catalysis 54 (2011) 1414

[7] T. Eralp, A. Ievins, A. Shavorskiy, S. J. Jenkins, G. Held, JACS 134 (2012) 9615.

[8] S. Baldanza, A. Cornish, R. E. J. Nicklin, Z. V. Zheleva, G. Held, Surf. Sci. 629 (2014) 114.

5:00pm SS-MoA9 Mapping of Enantioselective Reaction Kinetics across Surface Structure Space: Tartaric and Aspartic Acid on Cu(111) Structure Spread Single Crystals, *Andrew Gellman*, *A. Reinicker*, Carnegie Mellon University
On single crystal metal surfaces, enantioselectivity is, perhaps, the most subtle form of structure sensitive surface chemistry. Enantioselectivity can be observed on naturally chiral metal surfaces with structures that are traditionally described as having flat low Miller index terraces separated by kinked step edges, thereby lacking mirror symmetry. This work has mapped the enantiospecific decomposition kinetics of tartaric acid (TA) and aspartic acid (Asp) on 225 different single crystal planes exposed by the surface of a Cu(111) Surface Structure Spread Single Crystal (S^{4}C). The Cu(111) S^{4}C is a single crystal polished into a spherical dome shape that exposes a continuous distribution of surface orientations vicinal to the Cu(111) plane. During isothermal decomposition, XPS has been used to map the temporal evolution of the coverages of TA and Asp at points across the Cu(111) S^{4}C. On Cu surfaces, both TA and Asp decompose by an explosive, vacancy-mediated decomposition mechanism consisting of an initiation step and a vacancy-mediated explosion step. The rate law for this process is parameterized by an initiation rate constant, k_i, and an explosion rate constant, k_e. Under isothermal conditions, the measured extent of reaction versus time at each point on the S^{4}C has been used to fit the decomposition rate law and estimate the values of k_i, and k_e as functions of local surface structure across the Cu(111) S^{4}C. These maps reveal that k_i is maximum on surfaces with high densities of the close packed (100) steps and minimum on surfaces with high densities of the close packed (110) steps. As the angle between the surface and the (111) plane increases, k_i increases linearly with step density. Along the direction containing the surfaces with (100) steps, the initiation step dominates and the kinetics look first-order. Along the directions exposing (110) steps the kinetics are dominated by the explosion step. In the case of Asp decomposition on the Cu(111) S^{4}C, the decomposition kinetics are also sensitive to the chirality of the local surface orientation. Collectively, these data provide the deepest insight yet obtained in to the structure sensitivity of surface explosion reactions and the structural origins of enantioselectivity on naturally chiral surfaces.

5:20pm SS-MoA10 Enantioselective Adsorption on Platinum Surfaces, *S. Karakalos*, *Francisco Zaera*, University of California
Enantioselectivity in the adsorption of chiral compounds on solid surfaces may lead to preferential crystallization, a possible route to chiral separation of racemic mixtures, and also to a way to design enantioselective catalytic chemical reactions. Tests on the uptake of simple molecules on metal single-crystal surfaces as a function of the enantiocomposition of the adsorbate has revealed several interesting kinetic and thermodynamics. Specifically, we have been exploring possible enantiospecific behavior during the uptake of propylene oxide (PO) on Pt(111) surfaces. Three related observations will be reported here. In the first set of experiments, the amplification of enantioselectivity during adsorption was demonstrated for the case of a surface seeded with a small amount of enantiopure PO and then dosed with propylene, a non-chiral molecule, as the amplifier. Chiral chemical titration and isothermal kinetic adsorption experiments using collimated effusive molecular beams indicated the possibility of reaching enantioselectivity excesses of over 60% this way. Monte Carlo simulations provided a kinetic explanation for this effect in terms of both an adsorbate-assisted adsorption process and a bias in the chiral configuration the

propylene molecules are driven to upon adsorption on the surface. The second example refers to the uptake of PO itself, where lower saturation coverages are seen with the racemic mixtures versus enantiopure samples by approximately 20%. This behavior could be explained in terms of adsorbate-assisted adsorption with different probabilities for homo- versus hetero-enantiomeric pairs. Finally, it was determined that the enantiomeric composition of PO monolayers eventually reverses the direction of the enantiospecfic enrichment seen in the kinetic uptake.

2D Materials Focus Topic
Room: 212C - Session 2D+EM+NS+SS+TF-TuM

Optical and Optoelectronic Properties of 2D Materials
Moderator: Andrea Young, University of California at Santa Barbara

8:00am 2D+EM+NS+SS+TF-TuM1 The Tri-Angular Lattice Exciton (3ALE) Model: Exciton Physics at the Atomic Scale, *F. Tseng*, NRC Research Associate, *E. Simsek*, George Washington University, *Daniel Gunlycke*, Naval Research Laboratory
Descriptions of excitons in pristine semiconducting crystals usually rely on the hydrogen model adopted for excitons. Owing to the weak screening in monolayer transition-metal dichalcogenides, however, the electron and hole separation in the strongest bound excitons is on the atomic scale, necessitating atomistic treatment. In this presentation, we present a minimalistic exciton model that accounts for the lattice and the spin-orbit and exchange interactions, thus making this model appropriate across the spectrum from Wannier to Frenkel excitons. Using this model, we show that the exciton lifetimes could be extended by transitioning the excitons into excitonic dark states. Longer exciton lifetimes could make these materials candidates for applications in energy management and quantum information processing.

This work has been funded by the Office of Naval Research (ONR), directly and through the Naval Research Laboratory (NRL). E.S. and F.T. acknowledge support from NRL through the ONR Summer Faculty Program and the NRC Research Associateship Program, respectively.

8:20am 2D+EM+NS+SS+TF-TuM2 Opposite Dependence of Microwave-Induced vs. Field-Induced Imaging Contrast in NV$^-$ based Fluorescence Microscopy as Function of Optical Excitation, *Etienne Goovaerts*, *S.K.R. Singam*, University of Antwerp, Belgium, *M. Nesladek*, Hasselt University, Belgium, *M. Giugliano*, University of Antwerp, Belgium
The charged nitrogen-vacancy (NV$^-$) center is a remarkable defect in diamond which allows interrogation of spin state through its fluorescence. Among the proposed applications, background-free imaging based on fluorescent nanodiamond (FND) was demonstrated [1-3]. The FNDs emission can be discriminated from spurious fluorescence by switching on resonant microwaves (MW) and/or a static magnetic field [1-3], as demonstrated in cells [1] and potentially in small animals [2]. It is now important to understand the origin of the contrast in either of these approaches, and the optimal experimental parameters.

NV$^-$ defects in single-crystal diamond as well as in FNDs were excited by a 532nm laser through the microscope objective. A compact spectrometer combined with appropriate filters allowed to measure the NV$^-$ and NV^0 emission. MW-induced contrast is achieved using a broadband circular antenna (i.d. 1mm) on a printed plate, and for field-induced contrast we use a small-sized permanent magnet (~300mT). They are placed closely behind the sample with in each case the magnetic field component along the optical axis of the objective.

For shallow implanted NV in (100) diamond as well as for FNDs the fluorescence is quenched by application of either resonant MWs or static field, with contrast levels systematically higher in the single crystal case than for deposited nanoparticles. The contrast values were measured for laser powers covering 6 orders of magnitude. After an initial rise at very low excitation (max. 13% in crystal, 7% in FND), the MW-induced contrast significantly decreases at higher laser powers. In parallel, field-induced contrast increases from about 12% to values of 38% and 20% for the single crystal and FNDs. This is described under steady state conditions using a 5-level model that includes radiative and nonradiative decay and ground state spin relaxation. The MW-contrast results from induced spin transitions in the triplet ground state while the field effect relies on state mixing within the ground and the excited triplets which change the decay rates. The analysis also shows that the applied excitation rates runs through 3 regimes from below the spontaneous relaxation rate, via an intermediate regime, to above the decay rate of the intermediate singlet.

This work demonstrates the advantages of field-induced contrast microscopy over the MW-induced approach. These become particularly important at high excitation rates which are more often applied in confocal microscopy.

[1] R. Igarashi, et al, Nano Lett. 2012, **12**, 5726

[2] A. Hegyi, E. Yablonovitch, Nano Lett. 2013,**13**, 1173

[3] R. Chapman, T. Plakkhoitnik, Opt. Lett. 2013, **38**, 1847

8:40am 2D+EM+NS+SS+TF-TuM3 2D Materials and Heterostructures for Applications in Optoelectronics, *Thomas Mueller*, Vienna University of Technology, Austria **INVITED**
Two-dimensional (2D) atomic crystals are currently receiving a lot of attention for applications in (opto-)electronics. In this talk I will review our research activities on photovoltaic energy conversion and photodetection in 2D semiconductors. In particular, I will present monolayer p-n junctions, formed by electrostatic doping using a pair of split gate electrodes, and MoS2/WSe2 van der Waals type-II heterojunctions. Upon optical illumination, conversion of light into electrical energy occurs in both types of devices. I will present measurements of the electrical characteristics, the photovoltaic properties, and the gate voltage dependence of the photoresponse. In the second part of my talk, I will discuss photoconductivity studies of MoS2 field-effect transistors. We identify photovoltaic and photoconductive effects, which both show strong photoconductive gain. We envision that the efficient photon conversion, combined with the advantages of 2D semiconductors, such as flexibility, high mechanical stability and low costs of production, could lead to new optoelectronic technologies.

9:20am 2D+EM+NS+SS+TF-TuM5 Excitations and Ultrafast Charge Response in Bilayer Transition-Metal Dichalcogenides, *Volodymyr Turkowski*, *T.S. Rahman*, University of Central Florida
We analyze the absorption spectrum and ultrafast charge dynamics in bilayer 2L-MoS2 , 2L- MoSe2 and MoS2-WS2 systems by using time-dependent density functional theory in the density-matrix representation. In particular, we calculate the values of the binding energies of excitons in these structures for both intra- and inter-layer electron-hole excitations and demonstrate that, similar to the case of a single layer, these energies can be as large as hundred(s) of meVs. We also analyze the ultrafast dynamics of the electrons, holes and excitons in the photoexcited bilayers. We pay special attention to the ultrafast hole transfer in these systems and find transfer times of the order 100fs, in agreement with the experimental finding for the MoS2-WS2 system. We perform a detailed *ab initio* study of the spatially- and time-resolved charge density in the systems during the hole transfer and conclude that sulfur and selenium orbitals play an important role in the process. Finally, we discuss possible applications of the results in light harvesting technologies.

Work supported in part by DOE Grant No. DOE-DE-FG02-07ER46354

9:40am 2D+EM+NS+SS+TF-TuM6 Automatic Localization and Identification of 2D-Material Flakes by Spectroscopic Imaging Ellipsometry, *Sebastian Funke*, *P.H. Thiesen*, Accurion GmbH, Germany, *G. Greg Hearn*, Accurion Inc.
With the rising of 2D materials in surface sciences, the localization of mono- to few-layers of 2D materials, such as graphene, Molybdenum disulfide, hexagonal boron nitride is a time consumptive task. With the help of imaging spectroscopic ellipsometry flakes of 2D materials can be found and its layer numbers can be differentiated.

Therefore a spectroscopical mapping of the sample is done. At selected wavelengths nulling ellipsometry for each pixel in the field of view is done to measure Δ/Ψ. The measurement of all pixels is done simultaneously. To cover larger areas than the field of view a XY-patterning is done automatically. For each XY-position spectroscopic Δ/Ψ maps are obtained. Every pixel of a Δ/Ψ map represents the spectroscopic angle Δ/Ψ respectively. By comparing the spectral Δ/Ψ values for each pixel with the ellipsometric model of e.g. graphene monolayer, flakes of graphene monolayers on the sample can be found. To ensure, that only flakes are found, a grid with a threshold is used. The threshold indicates the number of pixels in the grid that need to fit to the model.

In the talk we present the capability of imaging ellipsometry to localize and identify monolayer to few-layers of 2D Materials. Flakes of MoS$_2$ with a size smaller than 10 μm can be localized. Monolayer of graphene can be distinguished from bilayers of graphene. To improve the time factor, the use of a Scheimpflug corrected objective is presented. Further investigations on different 2D materials, e.g. h-BN and the implementation of a Raman System is in progress.

11:00am 2D+EM+NS+SS+TF-TuM10 Systematic Hydrogen Intercalation of Epitaxial Graphene for THz Plasmonics, *Kevin Daniels*, National Research Council postdoc working at NRL, *A. Boyd,* American Society for Engineering Education postdoc working at NRL, *R.L. Myers-Ward, D.K. Gaskill*, Naval Research Laboratory

Epitaxial growth of graphene via sublimation of silicon and graphitization of carbon atoms from silicon carbide (SiC) is ideal for large scale manufacturing of plasmonic devices but due to partially covalent bonding between the SiC (0001) substrate and the first carbon layer ($6\sqrt{3}$ buffer layer), the high room temperature mobility necessary for THz plasmonics is reduced significantly compared to exfoliated graphene. The objective of this work is to improve THz response of EG by increasing the mobility and carrier concentration of graphene through hydrogen intercalation where the Si atoms covalently bound to the buffer layer are satisfied by hydrogen atoms and create quasi free standing graphene.

Epitaxial graphene was grown from 6H-SiC (0001) in an Aixtron/Epigress VP508 horizontal hot-wall reactor, etching in H_2 during temperature ramp to 1570°C and growing graphene in Ar ambient at 1580°C. H-intercalation of EG was carried out in the same reactor at 1050°C with a flow of 80slm of H_2 and chamber pressure of 900mbar for 15-75 minutes. Morphology of the quasi-free standing graphene was observed by AFM and SEM. Raman spectroscopy using a 532nm laser (9.6mW) and spot size of 0.3μm were used to take 80x10μm maps of each sample where release of the buffer layer is observed, with broadening of the 2D peak full-width-half-max (FWHM) before and after H-intercalation is observed on the graphene terraces and step edges. Number of monolayers before and after H-intercalation was determined by XPS.

From SEM, AFM, Raman and Hall we observe changes in degree of hydrogen intercalation with respect to time. Large areas of partially intercalated EG is observed at 15 minutes which confirmed by a mix of charge carriers and reduced carrier mobility at ~250cm^2/Vs. At 30 minutes some graphene terraces remain coupled to the SiC substrate with carrier mobility ~2250cm^2/Vs. From 45, 60 and 75 minutes the buffer layer becomes mostly quasi free standing with small spots possibly coupled to the substrate as observed in the SEM with mobilities of ~3900, ~4000 and ~3700cm^2/Vs respectively. Measurements of the resulting THz transmission spectra are currently underway to determine if the increase in mobility and carrier concentration results in narrower THz response.

11:20am 2D+EM+NS+SS+TF-TuM11 Determining the Optical Properties of Exfoliated 2D Molybdenum Disulfide on Various Substrates with Imaging Spectroscopic Ellipsometry, *Peter H. Thiesen*, Accurion GmbH, Germany, *S. Funke,* HAWK, Germany, *B. Miller, E. Parzinger,* TU München, Germany, *G. Hearn,* Accurion Inc., *A.W. Holleitner, U. Wurstbauer*, TU München, Germany

Ellipsometry is a non-destructive optical method for determining film thickness and optical properties. It measures the change in the state of polarization of the light reflected from the film interfaces. Imaging ellipsometry, which combines the power of ellipsometry with microscopy, has overcome the limitation of poor sample lateral resolution found in conventional non-imaging ellipsometers. The enhanced spatial resolution of imaging ellipsometers potentially expands ellipsometry into new areas of microanalysis, microelectronics, and bio analytics.

Molybdenum disulfide is a layered transition metal dichalcogenide. From the point of current research, 2D-nano materials based on MoS_2 are very promising because of the special semiconducting properties. The bulk material has an indirect 1.2 eV electronic bandgap, but single layer MoS_2 has a direct 1.8 eV bandgap. The monolayer can be used in prospective electronic devices like transistors (MOSFETs) or photo detectors.

Wavelength spectra of ellipsometric parameters Delta and Psi of the MoS_2 monolayers and multilayers were recorded as well as microscopic maps. In case of Sapphire, The psi maps at wavelength of higher energies than the bandgap show a clear contrast between the monolayer and the substrate and at lower energies there is no contrast between the monolayer and the substrate, but the multilayer areas still show a clear contrast-making the unique properties of MoS_2 monolayers directly visible. The advantage of imaging ellipsometry is the visualisation of the shape of the monolayer and the opportunity to classify the homogenity of the optical properties of the microcrystallite. To quantify the optical properties, different approaches of optical modelling will be discussed.

11:40am 2D+EM+NS+SS+TF-TuM12 Nonlinear Optical Spectroscopy of 2D Semiconductor Monolayers, *Xiaobo Yin*, University of Colorado Boulder **INVITED**

Transition metal dichalcogenide (TMDC) monolayers have recently emerged as an important class of two-dimensional semiconductors with

potential for electronic and optoelectronic devices. Unlike semi-metallic graphene, layered TMDCs have a sizeable bandgap. More interestingly, when thinned down to a monolayer, TMDCs transform from indirect-bandgap to direct-bandgap semiconductors, exhibiting a number of intriguing optical phenomena such as valley-selective circular dichroism, doping-dependent charged excitons and strong photocurrent responses. Using nonlinear optical spectroscopy, we probe experimentally the evidence of a series of excitonic dark states as well as structural symmetry in single-layer WS2 and MoS2.

Energy Frontiers Focus Topic
Room: 211B - Session EN+AS+EM+SE+SS-TuM

Photocatalysis
Moderator: Jason Baxter, Drexel University, Manjula Nandasiri, Pacific Northwest National Laboratory

8:00am EN+AS+EM+SE+SS-TuM1 Ultra-dense Hydrogen and Low Energy Nuclear Reactions, *Sveinn Olafsson*, Science Institute, Physics department University of Iceland, *L. Holmlid*, University of Gothenburg, Sweden

For over the last 25 years the science of cold fusion/LENR has been researched around the world with slow pace of progress. Modest quantity of excess heat and signatures of nuclear transmutation and helium production have been confirmed in experiments and theoretical work has resulted in a flora of possible theoretical scenarios. [1-2]

Here we present energy production in several stages of surface processes that result first in the formation of Rydberg matter of Hydrogen [3] that can later condense in a new ultra-dense Hydrogen phase with 2.3 pm short bond distances. This phase is nuclear active showing break-even fusion reaction [7] under 100mW laser pulsing and slow spontaneous fusion occurring without laser pulsing[4,5,6]. The experimental work in around 30 publications is briefly reviewed and latest experimental results presented and discussed.

In that work high-energy particles are detected from the spontaneous processes using scintillation and other similar detectors. Both spontaneous line-spectra and a spontaneous broad energy distribution similar to a beta-decay distribution are observed indicating detection of particles such as muons. The broad distribution is concluded to be due to nuclear particles, giving straight-line Kurie-like plots. They are observed even at a distance of 3 m in air and have a total rate of 10^7-10^{10} s^{-1}. In the talk the link of these observation to Low energy nuclear reactions (LENR) or so called cold fusion will be discussed experimentally and theoretically.

1. The science of low energy nuclear reaction.

Storms E. World Scientific Publishing Company; **2007**.

2. The explanation of low energy nuclear reaction.

Storms E. Ienergy Press; **2014**.

3. Review paper: Experimental Studies and Observations of Clusters of Rydberg Matter and Its Extreme Forms Leif Holmlid. J Clust Sci (**2012**) 23:5–34

4. Spontaneous ejection of high-energy particles from ultra-dense deuterium D(0)

Leif Holmlid and Sveinn Ólafsson

Volume 40, Issue 33, 7 September **2015**, Pages 10559–10567)

5. Charged particle energy spectra from laser-induced processes: nuclear fusion in ultra-dense deuterium D(0) Leif Holmlid and Sveinn Ólafsson submitted **2015**.

6. Muon detection studied by pulse-height energy analysis: Novel converter arrangements

Leif Holmlid and Sveinn Ólafsson. Rev. Sci. Instrum. 86, 083306 (**2015**);

7. Heat generation above break-even from laser-induced fusion in ultra-dense deuterium

Leif Holmlid. AIP Advances 5, 087129 (**2015**);

8:20am EN+AS+EM+SE+SS-TuM2 Optical and Surface Properties of Semiconductor Nanowires for Solar Fuels, *Eleonora Frau, J. Vukajlovic, A. Dalmau-Mallorqui, A. Fontcuberta i Morral, E. Alarcon Llado*, Ecole Polytechnique Fédérale de Lausanne (EPFL), Switzerland

Semiconductor nanowires (NWs) are filamentary crystals with new properties from their bulk counterparts. Their large versatility makes them excellent candidates as building blocks for contributing to solving the energy problem in the near future. In this work, we will assess two main

properties of semiconductor NWs that have an impact to solar energy conversion.

First, it is known that light is strongly absorbed by NW arrays since light resonances give rise to effective absorption cross-sections that are much larger than the geometrical ones. Optical resonances depend on NW geometry and dielectric environment, and can result into absorption effective diameters up to 25 times larger than the geometrical for certain wavelengths. We have used finite-difference time-domain (FDTD) electromagnetic simulations to understand and design NW-based sunlight scavengers. For instance, a GaAs NW array that is only covering 3% of the surface can generate more photocurrent than a planar film, considering a 30% reflectivity (see figure1). Also that thanks to optical resonances, an indirect-bandgap material such as Si is capable of absorbing most of the light within a 2um long NW array that only covers 7% of the device surface.

On the other hand, it is also known that surface states and traps detriment device performances. However, in case where solar energy is directly converted into fuel (such as hydrogen) in a photoelectrochemical (PEC) cell, the large surface-to-volume ratio of NW forests is an important asset. Since the electrochemical reactions happen at the semiconductor surface, NWs enable the use of low-cost catalysts (e.g. MoSx) even though they exhibit lower performances than noble metals (e.g. Pt). In order to assess the effects of nanostructuring photo-electrodes for solar fuel generation, we have studied photo-cathodes based on Silicon nanopillar structures. The photo-cathodes are fabricated by using a top-down approach and their diameters range from ~200 to 900nm and lengths ~2um. We observe that reducing the size of the nanostructure, increases the overpotential, and thus the overall efficiency (see figure 2). By coating the surface with thin TiO_2 layers, the performance is improved in terms of overpotential and fill factor. We explain these findings by using an electrico-kinetic model of the semiconductor-water junction. We find that the TiO_2 layers actually act as a hole blocking layer, preventing recombination.

8:40am EN+AS+EM+SE+SS-TuM3 Engineering Surfaces and Interfaces for Photoelectrochemical (PEC) Water-Splitting, *Thomas Jaramillo*, J.D. Benck, Stanford University, J. Kibsgaard, SLAC National Accelerator Laboratory, T.R. Hellstern, C.J. Hahn, P. Chakthranont, R. Britto, K.D. Fong, Stanford University **INVITED**
The talk will focus on engineering surfaces and interfaces for solar photoelectrochemical (PEC) water-splitting for the direct, renewable production of H_2. In particular, this talk begin by describing research efforts to develop H_2 evolution catalysts that are active, stable, and comprised of only earth-abundant elements, including transition metal sulphides, phosphides, and phosphosulfides.[1-3] Next, we will describe recent efforts to integrate these catalysts onto semiconductor surfaces to provide corrosion protection as well as enhanced interfacial catalysis for PEC water-splitting.[4] This talk will focus on the need for high turnover frequency (TOF) catalysts, which ultimately enable the greatest flexibility in designing optimum interfaces for high performance devices.

[1] J. Kibsgaard, T.F. Jaramillo, F. Besenbacher, "Building an appropriate active site motif into a hydrogen evolution catalyst with thiomolybdate $[Mo_3S_{13}]^{2-}$ clusters," *Nature Chemistry*, **6** (2014) 248.

[2] J.D. Benck, T.R. Hellstern, J. Kibsgaard, P. Chakthranont, T.F. Jaramillo, "Catalyzing the Hydrogen Evolution Reaction (HER) with Molybdenum Sulfide Nanomaterials," *ACS Catalysis*, **4** (2014) 3957.

[3] J. Kibsgaard and T.F. Jaramillo, "Molybdenum Phosphosulfide: An Active, Acid-Stable Earth-Abundant Catalyst for the Hydrogen Evolution Reaction," *Angewandte Chemie*, **53** (2014) 14433.

[4] J.D. Benck, S.C. Lee, K.D. Fong, J. Kibsgaard, R. Sinclair, T.F. Jaramillo, "Designing active and stable silicon photocathodes for solar hydrogen production using molybdenum sulfide nanomaterials," *Advanced Energy Materials*, **4** (2014) 1400739.

9:20am EN+AS+EM+SE+SS-TuM5 Bulk and Surface Effects of Incorporating Titanium Into Hematite Thin Films to Improve Photoelectrochemical Water Splitting, *Anthony Abel*, A.M. Patel, Drexel University, I.G. Torregrosa, Utrecht University, Netherlands, B. Opasanont, J.B. Baxter, Drexel University
Hematite (α-Fe_2O_3) has emerged as a promising photoanode material for photoelectrochemical (PEC) water splitting due to its chemical stability, earth-abundance, low cost, and suitable band gap for both water splitting and visible light absorption. However, poor charge separation due to low hole mobility and high recombination rate, and sluggish oxygen evolution reaction kinetics have limited its potential as an economical water-splitting catalyst. Here, we investigate titanium incorporation into hematite photoanodes and provide insight into the role of Ti^{4+} in improving PEC performance. Planar hematite thin films (~45 nm thick) were deposited by successive ionic layer adsorption and reaction (SILAR) of FeOOH on an

FTO/glass substrate and subsequent annealing to induce phase transition to α-Fe_2O_3, and titanium was incorporated up to 10% Ti/(Ti+Fe) by either modification of the SILAR solution (SM:α-Fe_2O_3) or solid-state diffusion (SSD:α-Fe_2O_3) during the annealing process. PEC measurements revealed substantial improvements in both charge separation efficiency and hole injection into the electrolyte, increasing photocurrent from nearly zero to ~0.6 $mAcm^{-2}$ under 1-sun irradiation at 1.23 V_{RHE}. Mott-Schottky analysis indicated a 100 mV cathodic shift in the flat band potential upon doping with Ti^{4+} regardless of fabrication method, but a 100-fold increase in carrier density only in SM:α-Fe_2O_3 films, resulting in a high 20 % separation efficiency at 1.23 V_{RHE} with optimized 5 % Ti/(Ti+Fe) in the modified SILAR solution. Electrochemical impedance spectroscopy showed a 4x increase in the surface state capacitance peak near the water oxidation onset potential, possibly due to reduced Fermi level pinning as a result of more efficient hole injection into the electrolyte . More importantly, doping with titanium resulted in a 100-fold decrease in the charge transfer resistance from surface states to the electrolyte, revealing the strong influence of Ti^{4+} on interfacial kinetics . Further surface modification with an ultrathin FeOOH surface passivation layer raised the plateau photocurrent to ~0.8 $mAcm^{-2}$ at 1.23 V_{RHE}, representing a 3x improvement over previous reports of SILAR-deposited hematite films and comparable with record performance for planar hematite deposited using high vacuum synthesis techniques.

9:40am EN+AS+EM+SE+SS-TuM6 Iron Oxide Nanoparticle Growth on Highly Oriented Pyrolytic Graphite (HOPG) and Photocatalytic Properties of Pt on Iron Oxide, *Jayde Kwon*, J.C. Hemminger, University of California, Irvine
Highly oriented pyrolytic graphite (HOPG) is an ideal substrate to study the fundamental growth mechanism of iron oxide independent from substrate effects. Platinum on iron oxide is a model heterogeneous catalyst with importance to biotechnology and solar cell applications. Selective growth of iron oxide nanoparticle (NP) either on step edges of HOPG or oxygen plasma treated HOPG by physical vapor deposition (PVD) will be presented. The successful selective iron oxide NP growth was validated by scanning electron microscopy (SEM), transmission electron microscopy (TEM), and X-ray photoelectron spectroscopy (XPS). The development of the NP array system is highly significant in that it can provide an ideal template for theoretical calculations for fundamental metal growth studies. Pt nanoparticles was subsequently deposited on the iron oxide nanoparticles using a selective photodeposition technique. The application of these nano-systems (Pt nanoparticles on iron oxide nanoparticles) towards photocatalysis of methylene blue will be presented. Although iron oxide is a promising semiconductor photocatalyst, it suffers from a short hole diffusion length, low electrical conductivity and a high rate of electron hole recombination. However, this bimetallic system using platinum deposited on iron oxide overcomes these barriers. A novel method was developed using small quantities of Pt on iron oxide to significantly enhance methylene blue decomposition. This system is also being explored as a catalytic model for water-gas shift reactions.

11:00am EN+AS+EM+SE+SS-TuM10 Interface Design for Efficient and Stable Photoelectrochemical Water Splitting, *Joel Ager*, Lawrence Berkeley National Laboratory **INVITED**
Solar photoelectrochemical (PEC) water splitting is potential future carbon-neutral energy source which could dramatically change the landscape of global energy generation and storage. The half reactions for water splitting are as follows:

$2H^+ + 2 e^- <-> H_2$ (1)

$H_2O <-> 2e^- + 2H^+ + 1/2O_2$. (2)
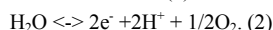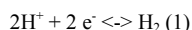
The free energy change for the overall reaction, $H_2O <-> H_2 + 1/2O_2$ corresponds to 1.23 eV per electron transferred; however, typically >1.5 V is required to overcome kinetic limitations, particularly for the O_2 evolution reaction. The most commonly used approach for integrated solar water splitting employs photocathodes (H_2 or hydrocarbon producing) and photoanodes (O_2 producing) linked in a tandem geometry [1].

The interface challenges required to demonstrate a practical system which is both efficient and stable under operation are substantial and severe. In addition to constructing interfaces, either solid-solid or solid liquid, which achieve the desired photovoltaic charge separation, the surfaces of these photoelectrodes can be a failure point under sustained operation due to corrosion. We have found that the use of nanoscale conformal oxide layers can greatly reduce corrosion rates. Moreover, it is possible to achieve both high performance and lifetime by the use of protection layers which are also tuned for selective carrier contact.

Examples of such a strategy will be shown for photocathodes [2-5] and for photoanodes [5]. Recent work on p-type transparent oxides (p-TCOs) used as selective hole contacts for photoanodes will be emphasized. For example, it will be shown that using $NiCo_2O_4$ as the p-TCO and n-type Si as a

prototypical light absorber, a rectifying heterojunction capable of light driven water oxidation can be created. By placing the charge separating junction in the Si using a np$^+$ structure and by incorporating a highly active Ni-Fe oxygen evolution catalyst, efficient light-driven water oxidation can be achieved. The generality of the p-TCO protection approach is demonstrated by multi-hour, stable, water oxidation with n-InP/p-NiCo$_2$O$_4$ heterojunction photoanodes.

References.

1. J. W. Ager *et al.*, Energy Environ. Sci. (2015). DOI:10.1039/C5EE00457H

2. M. H. Lee *et al.*, *Ang. Chemie Int. Edition* **51** 10760 (2012).

2. Y. Lin *et al.*, *Nano Letters* **13** 5615 11 (2013)

3. Y. Lin *et al.*, *J. Phys. Chem.* C **119**, 2308 (2015).

4. J. Yang *et al.*, *J. Amer. Chem. Soc.* **136** 6191 (2014).

11:40am EN+AS+EM+SE+SS-TuM12 Buried, Hetero, and p-i-electrolyte III-V Photoelectrochemical Junctions with Significantly Enhanced Photocurrent Onset Potentials, *James Young*, H. Doscher, J. Turner, T. Deutsch, National Renewable Energy Laboratory
To approach the maximum achievable solar-to-hydrogen (STH) conversion efficiencies with photoelectrochemical (PEC) devices, it is necessary to employ the lowest possible band gap (E$_g$) absorbers that can still provide sufficient voltage to drive water splitting at high rates (1.7-1.8 V for 25% STH). The record 12.4% STH was achieved by a GaInP$_2$/GaAs PEC/photovoltaic (PV) tandem device while an all solid state GaInP$_2$/GaAs PV/PV tandem produces an open-circuit voltage that approaches 2.4 V. Since GaAs (E$_g$ = 1.4 eV) is the current-limiting junction in these devices, it can be substituted by InGaAs with E$_g$ = 1.0 eV to reach 25% STH. The current-for-voltage tradeoff of using lower-E$_g$ absorbers moves toward the constraint of insufficient voltage for spontaneous water splitting. To address this approaching constraint, we investigate several alternative device structures at the III-V/electrolyte interface that show photocurrent onset potential enhancements of a few hundred mV. We will present band diagram calculations and electrochemical measurements to discuss the voltage performance of these structures.

12:00pm EN+AS+EM+SE+SS-TuM13 X-ray Absorption Studies on the Li-S Battery Cathode Side, *Yifan Ye*, University of Science and Technology of China, A. Kawase, Lawrence Berkeley National Laboratory, H.X. Ju, University of Science and Technology of China, E. Cairns, Lawrence Berkeley National Laboratory, J.-H. Guo, Lawrence Berkeley Lab, University of California, Berkeley, J.F. Zhu, University of Science and Technology of China
As increasing global energy consumption in the coming days, sustainable, clean energy technologies are highly desirable. The high theoretical specific capacity of 1675 mA·h/g for elemental S has prompted intense effort to study the Lithium-Sulfur batteries. With the application of cetyltrimethyl ammonium bromide (CTAB), modified sulfur-graphene oxide (S-GO) nano-composite based Li/S batteries exhibited a very high initial discharge capacity of 1440 mA·h/g of sulfur at 0.2C with excellent rate capability of up to 6C for discharge and 3C for charge while still maintaining high specific capacity. And the batteries demonstrated cycling performance up to 1500 cycles with extremely low decay rate of 0.039% per cycle. With the introduction of CTAB, the performance of the GO-S based Li-S battery has been improved significantly, thus it is important to figure out the role of CTAB played in the system. During the synthesis process of the cathode materials, S and Na$_2$S were used as the precursors, the ratio of S/Na$_2$S is crucial to the components of the precursors. Moreover, the sequence of mixing GO/CTAB solution with precursor solution is a key point to effective cathode synthesis procedure. Understanding these information helps to optimize the methodology for the controllable synthesis of desired cathode material that can be used to fabricate an efficiency and well-performed Li/S battery. S K-edge X-ray absorption spectroscopy (XAS) is applied to study the chemical species evolution during the GO-S-CTAB cathode material synthesis. The influences on the cathode materials related to the battery performance are monitored by S K-edge XAS. The research revealed the interaction between CTAB and GO, S, Na$_2$S and Na$_2$S$_x$. It indicated that CTAB can physical absorbed on Na$_2$S$_x$ molecules by bonding with the terminal S atoms of Na$_2$S$_x$ chains, and this kind of bonding can convert to chemical C-S bonding with heating treatment. Thus the interaction of CTAB with GO, formed C-S between CTAB and S and interaction of GO and S provided a tight tri-layer structure which can immobilize the S particles on GO sheet and finally enhanced the battery performance. The information from this work proved the importance of

Na$_2$S:S ratio, CTAB/GO adding procedure in the fabrication process, and we can easily apply XAS to optimize these recipe. And moreover, this work proved strong evidence that XAS tools can be used to do the initial characterization on the battery performance before real cycling procedure.

In-Situ Spectroscopy and Microscopy Focus Topic
Room: 211C - Session IS+AS+SA+SS-TuM

In-situ Studies of Solid-liquid Interfaces
Moderator: Anatoly Frenkel, Yeshiva University, Franklin (Feng) Tao, University of Kansas

8:20am IS+AS+SA+SS-TuM2 Water at Ionic Liquid Interfaces Probed by APXPS, *John Newberg*, Y. Khalifa, A. Broderick, University of Delaware
Ionic liquids (ILs) have a wide array of applications in biotechnology, coatings, synthesis, separations, and energy sciences. Many of these processes involve either IL-solid or IL-vapor interactions. It is therefore critical we understand the fundamental interfacial properties of ILs on a molecular level. Due to the ubiquity of water, its influence on the properties of ILs has been the focus of many bulk studies and, more recently, surface science studies. Here we will highlight the use of a recently commissioned ambient pressure X-ray photoelectron spectroscopy setup in our laboratory and its application in characterizing the interfacial region of hydrophilic and hydrophobic ILs upon interaction with water vapor as a function of increasing pressure.

8:40am IS+AS+SA+SS-TuM3 Probig the Liquid-Solid Interface of polycrystalline Pt in 1.0 M KOH using Ambient Pressure Photoemission Spectroscopy and "Tender" X-rays, *Marco Favaro*, B. Jeon, P.N. Ross, Z. Hussain, J. Yano, Z. Liu, E.J. Crumlin, Lawrence Berkeley National Laboratory (LBNL)
With the previous success in soft X-ray AP-XPS gas-solid interface[1a-e] probing, researchers have started to gain insights into the liquid-solid boundaries[1d]. Taking the cue from these new research frontiers, we have developed on BL 9.3.1 at the Advanced Light Source (LBNL) a new liquid phase AP-XPS system (based on a Scienta R4000 HiPP-2 analyzer) that will shed new light on the understanding of the chemical changes at the electrode surfaces during normal working conditions, leading to a great enhancement of our knowledge on the most important processes in energy conversion and storage[2a,b]. The combination of this new system with synchrotron radiation in the "tender" X-ray region (between 2 and 7 keV), allows us to probe the interface between thin liquid and solid phases using high kinetic energy photons and then, thanks to the in operando approach, directly track the phenomena occurring at the electrode liquid-solid interface during the electrochemical reactions of interest. The technique developed at BL 9.3.1 allows the study of both gas-liquid and liquid-solid interfaces, for pressures up to a hundred of Torr[2a].

In order to deeply investigate the possibilities offered by this new technique and, at the same time, to establish a benchmark, a reference material such as polycrystalline Pt has been studied in 1.0 M KOH electrolyte. In this talk we will demonstrate that it is possible to have fine control of the applied potential[2a,b], measuring the core level binding energy shift of the of the oxygen *1s* and potassium *2p* photoemission lines, according to the applied external potential. Moreover we will discuss the observation, under *in operando* conditions, of the changes of the surface oxidation state[2b] of Pt triggered by the applied potential. Thanks to the innovative experimental approach, we have observed the *in situ* formation of Pt(II) and Pt(IV) species during the oxygen evolution reaction (OER), as well as the reversibility of the surface chemistry passing from anodic to cathodic potentials (up to the hydrogen evolution reaction, HER).

[1] a. Lu et al., *Sci. Rep.* **2**, 715 (2012); b. Zhang et al., *Nat. Mat.* **9**, 944 (2010); c. Axnanda et al., *Nano Lett.* **13**, 6176 (2013); d. Starr et al., *Chem. Soc. Rev.* **42**, 5833 (2013); e. Mudiyanselage et al., *Angew. Chem. Int.Ed.* **52**, 5101 (2013).

[2] a. S. Axnanda, E. Crumlin et al., *Sci. Rep.*, accepted; b. E. Crumlin et al., *in preparation*.

9:00am IS+AS+SA+SS-TuM4 Toward Ambient Pressure Electron Spectroscopy with Conventional XPS Instrumentation, *Andrei Kolmakov*, National Institute of Standards and Technology (NIST)
The current state of the art instrumentation for ambient pressure electron spectroscopy requires highly specialized sophisticated laboratory equipment or dedicated synchrotron radiation facilities. The limited access to these

equipment impedes in situ (in vivo) studies under realistic conditions in catalysis, energy, environmental and bio-(medical) fields. We propose a new sample platform which enables ambient pressure XPS to be conducted using conventional XPS instrumentation. The core of the sample platform is microchannel environmental cells sealed with electron transparent, molecularly impermeable, mechanically and chemically stable graphene layer. The channels can be impregnated with liquids or gases and yet be vacuum compatible. Two major wafer scale fabrication strategies: (i) transferred graphene and (ii) as grown graphene layer were described. The coverage yield, membrane cleanness and leaking rates were comparatively studied. The feasibility tests of the platform included in situ XPS and electron microscopy studies of the water radiolysis and electrochemical processes taking place at liquid electrolyte-solid interface.

9:20am **IS+AS+SA+SS-TuM5 Solvation and Chemistry at the Interface: Near Ambient Pressure Electron Spectroscopy Studies of Aqueous Solution Interfaces**, *John Hemminger*, University of California, Irvine **INVITED**
We have combined liquid-jet photoelectron spectroscopy coupled with classical molecular dynamics simulations to study the composition and chemistry of the liquid/vapor interface of aqueous solutions. Our experiments take advantage of the variable x-ray energy capability of synchrotron radiation and the kinetic energy dependence of the electron inelastic mean free path to carry out experiments with different probe depths. At low x-ray energy the low energy photoelectrons are detected primarily from the surface region of the solution. At higher x-ray energy our experiments probe more deeply into the solution. This allows us to directly compare the liquid/vapor interface with the bulk of the aqueous solution. We will present recent results on aqueous solutions of organonitrile compounds (acetonitrile and propionitrile). Our experiments and MD simulations show that both acetonitrile and propionitrile accumulate at the liquid/vapor interface—even though both nitriles are fully miscible with water. We have also studied the salting in and salting out effects for nitriles in water. We also have studied the effect of ion size on the surface propensity of cations in alkali halide aqueous solutions.

11:00am **IS+AS+SA+SS-TuM10 In situ Single-molecule Microscopy of Photoelectrocatalysis for Solar Water Oxidation**, *Peng Chen*, Cornell University **INVITED**
This talk will present our recent results in using single-molecule super-resolution fluorescence microscopy to image photoelectrochemical reactions on single semiconductor nanostructures in situ under photoelectrochemical water oxidation conditions. We separately image hole and electron induced reactions, driven by light and electrochemical potential, and map the reactions at single reaction temporal resolution and nanometer spatial resolution. We also correlate the surface hole and electron reactivity with the local water oxidation efficiency using sub-particle level photocurrent measurements. By depositing oxygen evolution catalysts in a spatially controlled manner, we further identify the optimal sites for catalyst deposition for photocurrent enhancement and onset potential reduction.

11:40am **IS+AS+SA+SS-TuM12 *In Situ* and *Operando* AP-XPS for the Oxidation State of Pd at Solid/Liquid Interface**, *Beomgyun Jeong*, M. *Favaro, P.N. Ross, Z. Hussain,* Lawrence Berkeley National Laboratory (LBNL), *Z. Liu,* Shanghai Institute of Microsystem and Information Technology, China, *B.S. Mun, J. Lee,* Gwangju Institute of Science and Technology, Republic of Korea, *E.J. Crumlin*, Lawrence Berkeley National Laboratory (LBNL)
A catalyst is defined as a substance that enhances a reaction rate without changing its chemical state. However, often the chemical state of a catalyst surface undergoes changes during the reaction, leading to the degradation of catalyst performance. These phenomena are particularly significant in electrocatalysis in which reaction occurs at solid/liquid interface with electrical potential as an activation energy to drive the reaction. In order to understand the mechanism of catalyst degradation, it is important to have a capability to observe the chemical states of electrode and various chemical species in electrolyte during the reaction taking place at the solid/liquid interface. In order to explore this region, we have developed a new experimental approach [1], using ambient pressure XPS (AP-XPS) coupled with "tender" X-rays (in the range between 2.5 and 7.0 keV) at the Advanced Light Source BL 9.3.1, Lawrence Berkeley National Laboratory. Because of the relatively high kinetic energy of the incoming photons, 'tender' X-rays allow probing solid/liquid interfaces through thin electrolyte films characterized by a thickness of 10-30 nm. This unique functionality allows the ability to simultaneously correlate the electrocatalytic activity of electrodes to both the chemical modifications of the electrode surface, and the electrolyte.
This talk will provide details on *in-situ* and *operando* AP-XPS measurements on the chemical modifications of polycrystalline Pd surface

studied at different electrochemical potentials. Pd is a cost-effective materials alternative to Pt showing similar electrocatalytic property of Pt in various reactions, such as oxygen reduction and electrooxidation of hydrogen and formic acid. On the other hand, it is well known that the Pd activity decreases faster than that of Pt especially in formic acid oxidation [2]. This phenomenology could be understood by the direct observation of the Pd surface chemistry evolution at electrified solid/liquid interface. We will discuss the performance of the Pd electrode in two different aqueous electrolytes, in particular in an alkaline medium and in a formic acid solution, an electroactive liquid organic molecule. We believe that our findings represent a step forward in the rationalization of the electrocatalytic behavior of Pd.

[1] S. Axnanda, E.J. Crumlin *et al.*, *Sci. Rep.* 5 (2015) 9788.; b. E.J. Crumlin *et al.*, in preparation.

[2] H. Jeon, S. Uhm, B. Jeong, J. Lee, *Phys. Chem. Chem. Phys.* 13 (2011) 6192.

12:00pm **IS+AS+SA+SS-TuM13 In situ Characterization of Switchable Ionic Liquids by Liquid ToF-SIMS and SALVi**, *Juan Yao*, *X. Sui, D. Lao, Y. Zhou, S. Nune, D. Heldebrant, Z. Zhu, X.-Y. Yu*, Pacific Northwest National Laboratory
A vacuum compatible microfluidic reactor, SALVI (System for Analysis at the Liquid Vacuum Interface) was employed for *in situ* chemical imaging of switchable ionic liquids (SWILs) using time-of-flight secondary ion mass spectrometry (ToF-SIMS). A model SWIL system consisting of 1,8-diazabicycloundec-7-ene (DBU) and 1-hexanol with CO_2 gas to change solvent polarity was selected. A series of ionic liquids with different CO_2 loading was analyzed. Spatial chemical differences were observed within the same ionic liquid, indicating inhomogeneity of the ionic liquid. Spectral principal component analysis (PCA) was conducted using both positive and negative ToF-SIMS data. Clear distinctions were observed among SWILs of different CO_2 loadings. The loading plots strongly indicate that fully loaded SWILs share similar spectral components as those of the non-loaded Ils. This finding confirms the hypothesis of the biphasic structure in the fully loaded IL predicated by molecular dynamic simulation and presents the first physical evidence of the liquid microenvironment of IL determined by liquid ToF-SIMS. Various ion pairs were also observed in addition to the known SWIL chemistry of the DBU and 1-hexanol system, indicating the complexity of the ionic liquid previously unknown. The vacuum compatible microchannel in SALVI provides a new way to study ionic liquids in vacuum by sensitive surface techniques. Our approach directly visualized spatial and chemical heterogeneity within the SWILs by dynamic liquid ToF-SIMS for the first time.

Surface Science
Room: 112 - Session SS+AS+EN+NS-TuM

Nanostructures, Nanoplasmonics and Surface Reactions
Moderator: Bruce Koel, Princeton University

8:20am **SS+AS+EN+NS-TuM2 ENDOM: A Simple Method to Deposit Nanostructures from Nanowires to Nanopores**, *Ashley Ellsworth*, *A.V. Walker*, University of Texas at Dallas
A key challenge in the practical application of nanostructures is their effective integration through assembly, patterning and alignment on technologically relevant substrates. We have recently demonstrated a new technique, electroless nanowire deposition on micropatterned substrates (ENDOM), by which to simultaneously synthesize and place nanowires on chemically patterned substrates. The nanowires can be precisely oriented on the surface in arbitrary shapes, such as an arch and around a right angle bend. In ENDOM, the shape of the deposit is controlled by the substrate pattern while its width is controlled by the reaction conditions. By employing longer deposition times and the appropriate substrate patterns, nanopores and nanochannels can be produced. However for sensing and nanoelectronic applications, free standing nanopores and nanochannels are generally employed. We have observed that the nanostructure adhesion to the surface is dependent upon the reagent concentrations. For example in Cu ENDOM, upon reduction of triethanolamine (complexing agent and buffer) concentration, nanowires no longer adhere strongly to the substrate and can be transferred to another substrate. In this presentation, we shall discuss the mechanisms of adhesion, transfer of these nanostructures to other substrates and proof-of-concept studies to synthesize free-standing nanostructures.

8:40am SS+AS+EN+NS-TuM3 Chemical Reaction on Photo-excited Plasmonic Nanostructures, *Suljo Linic*, University of Michigan **INVITED**
We will also show that plasmonic silver nanoparticles, optically excited with low intensity visible light, exhibit direct photo-catalytic activity in a number of oxidation reactions.1 We will discuss underlying mechanisms associated with these phenomena and predictive models that can capture the outcome of chemical transformations on these materials.[2,3,4] We propose that this new family of plasmonic metal photo-catalysts could prove useful for many heterogeneous catalytic processes that cannot be activated using conventional thermal processes on metals or photo-catalytic processes on semiconductors. I will show an example of such a process.[5]

1. D. B. Ingram, S. Linic, JACS, 133, 5202, 2011

2. Suljo Linic, Phillip Christopher and David B., Nature Materials, 10, 911, 2011.

3. Ingram P. Christopher, H. Xin, S. Linic, Nature Chemistry, 3, 467, 2011.

4. P. Christopher, H. Xin, M. Andiappan, S. Linic, Nature Materials, 11, 1044, 2012.

5. M. Andiappan, J. Zhang, S. Linic, Science, 339, 1590, 2013

9:20am SS+AS+EN+NS-TuM5 Structured Noble Metal Nanosurfaces for Biosensing and Bioanalysis (4): TLC-SERS and *In Situ* Monitoring of Surface-Adsorbed Target Molecules, *Hiroyuki Takei*, J. Saito, K. Watanabe, Toyo University, Japan, *T. Okamoto*, Riken, Japan, *H. Vieker, A. Beyer, A. Gölzhäuser*, Bielefeld University, Germany
Surface-enhanced Raman spectroscopy, SERS, is a powerful technique for in-situ characterization of chemical species. Requisite noble metal nanosurfaces can be prepared with a variety of techniques, ranging from simple vacuum deposition of a metal followed by annealing to intricate processing by electron beam lithography. Some commercial SERS plates are now available, and it is sometimes possible to detect signals from even single molecules if pure. However, in real-world applications, target molecules are often found in mixtures, either containing other Raman-active chemical species or a background material that can overwhelm the target molecule. It can also happen that one might be interested in directly obtaining SERS spectra of chemical species adsorbed on a solid surface.

When faced with a mixture sample, we can carry out separation before SERS measurement. To do so, we incorporated a SERS layer into a thin layer chromatographic plate. While a number of workers have reported applying noble metal nanoparticles after separation with a conventional TLC plate, we feel that such an additional step is cumbersome and does not guarantee uniformity in SERS signals. Our TLC-SERS is prepared with the following procedure; (1) adsorption of 100 nm diameter SiO_2 nanospheres as a dense monolayer on a glass slide, (2) evaporation of gold or silver with thicknesses up to 100 nm, and (3) spreading of chromatography silica gels. Steps (1) and (2) give rise to surface-adsorbed cap-shaped noble metal nanoparticles. We demonstrate that the TLC-SERS can actually separate mixture samples and provide in-situ SERS spectra. Two examples will be used to demonstrate the utility of our TLC-SERS plates. One deals with a mixture of roughly equal portions of Raman-active chemical species, rhodamine 6 G, crystal violet and BPE. The other is skim milk to which a trace amount of melamine has been added. We show that the three-component mixture could be separated and SERS spectra of all three components could be obtained separately and that melamine added to skim milk could be detected after separation but not before.

For detection of surface-adsorbed chemical species, we prepared silver nanoparticles on a PDMS sheet, using the same protocol as above. The PDMS sheet can be made less than 1 mm thick so that with an appropriate pressurization system, pressure can be applied to the PDMS sheet in order to press the silver nanoparticles against a near-by solid surface to which target molecules are adsorbed. Such a system can be utilized to detect, for example, residual pesticides on agricultural produces. We will demonstrate direct detection of ferbam on a grapefruit.

9:40am SS+AS+EN+NS-TuM6 Growth and Intercalation of Cu and Dy on the Basal Plane of Graphite, *Patricia A. Thiel*, D. Appy, E.J. Kwolek, D. Shao, M. Wallingford, M.C. Tringides, J.W. Evans, Y. Han, Iowa State University, *H. Lei*, Institute of Solid State Physics, CAS, China, *C.-Z. Wang*, Iowa State University
Graphite, and surface processes on graphite, serves as a valuable benchmark for carbon-based materials such as graphene. We have studied copper and dysprosium on graphite, deposited by an e-beam evaporator in UHV and imaged with STM, to determine the characteristic features of nucleation and growth of metal islands. One of the fundamental questions that arises naturally is whether metal nucleates homogeneously on the terraces or whether it nucleates heterogeneously at defect sites. To answer this question we employ several tools, especially a comparison between high-level van der Waals theory for single atom diffusion, and measured island density.

We also present evidence for unexpected metal intercalation at the surface of graphite, after treatment at elevated temperature.

11:00am SS+AS+EN+NS-TuM10 Surface-Mediated Self-assembly of a Flexible Nucleoside Analogue into Micron-sized Hydrogen-bonded Polymers, *Jun Wang*, P. Bonnesen, Oak Ridge National Laboratory, *E. Rangel, E. Vallejo, A. Sanchez-Castillo*, Universidad Autónoma del Estado de Hidalgo, Mexico, *H.J. Cleaves*, Tokyo Institute of Technology, Japan, *A.P. Baddorf, B. Sumpter, M. Pan, P. Maksymovych, M. Fuentes-Cabrera*, Oak Ridge National Laboratory
We report on an extraordinary large-scale surface-mediated molecular self-assembly of a flexible nucleoside analogue into a well-organized hydrogen-bonded polymer on Au(111). The nucleoside analogue is (RS)-N^9-(2,3-Dihydroxypropyl)Adenine $(R,S$-DHPA), and it consists of the Adenine nucleobase and a tethered glycol group. Employing scanning tunneling microscopy and density functional theory calculations we show that the polymer primarily self-assembles along the Au(111) herringbone reconstruction pattern and extends to the micrometer scale and beyond. The profound propensity toward self-assembly in this case arises from the properties of the glycol moiety of the R,S-DHPA molecule: it is linear and flexible, and these features, together with the specific ways in which the glycol and the Adenine moieties can hydrogen bond, confer R,S-DHPA with a superior self-assembly ability. Our results suggest that nucleoside analogues with flexible acyclic groups could provide the means for synthesizing substrate-supported mesoscale hydrogen-bonded polymers.

ACKNOWLEDGEMENTS

11:20am SS+AS+EN+NS-TuM11 Nanowire Kinking during Vapor-liquid-solid Growth: Experiments and Simulations, *Yanming Wang*, Y. Li, Stanford University, *S. Ryu*, Korea Advanced Institute of Science and Technology, *P.C. McIntyre, W. Cai*, Stanford University
Nanowires (NWs) are promising components for next-generation electronic and optical devices, and the vapor-liquid-solid (VLS) growth is a widely studied method for NW fabrication. However, many fundamental questions regarding the VLS mechanism are still not understood, such as NW kinking during growth. Kinking, a sudden change in axial orientation of nanowires during growth, is a common defect that complicates the directed synthesis of these nanocrystals. Understanding such defects is important for better control of the NW orientation, yield and quality required for applications.

Experimental studies of coherent kinking of germanium nanowires detect two different kinking structures. One structure, which is most pronounced for Ge NW's of diameter close to 20 nm, involves kinking from a vertical <111> to <110> growth axis on Ge (111) single crystal substrates. The other involves kinking from the vertical [111] axis to an inclined <111> growth direction for NWs of > 30 nm diameter.

The balance of capillary forces driving these two modes of kinking are analyzed quantitatively. We developed a 3D multi-phase field model for VLS NW growth. The model captures the NW tapering and sidewall facets in good agreement with experimental observations. The model predicts the steady-state NW growth velocity is a linear function of the vapor chemical potential and the inverse of catalyst diameter, providing a confirmation of the Gibbs-Thomson effect in nanowire growth. With anisotropic interfacial energies, the model shows the NW growth orientation dependence on catalyst diameter and hence it provides an explanation of the NW kinking in the steady-state growth regime. In this model, we introduce a perturbation force to induce the NW structural transition and the free energies are evaluated at different stages during the droplet movement. It enables us to discuss the instability of the catalyst droplet for different pedestal structures, which is important for understanding the onset of the kinking at the NW base.

11:40am SS+AS+EN+NS-TuM12 Adsorption of Water and Bromine on Gold Nanoclusters Investigated by Neutralization in Low Energy Alkali Ion Scattering, *Christopher Salvo*, J. Keagy, J.A. Yarmoff, UC Riverside
Small gold (Au) nanoclusters have been heavily studied because of their intriguingly high catalytic activity, especially when compared to bulk gold. We employ a specialized method of Low Energy Ion Scattering (LEIS) to probe the electronic properties of nanoclusters prepared with a variety of methods. The experiments measure the neutralization probability of singly scattered alkali ions, which is acutely sensitive to the local electrostatic potential a few Å's above the surface. Because the Au atoms are much more massive than the substrate atoms, this method allows the signal from the nanoclusters to be separated from that of the substrate so that the neutralization reflects the local properties of the cluster surfaces. Earlier work had demonstrated that the neutralization is a function of cluster size,

and that it is enhanced for the smallest clusters presumably because they are negatively charged [1]. The work presented here investigates the adsorption of water and Br on Au nanoclusters grown on TiO_2 or SiO_2. There are multiple factors that can contribute to a change in the neutralization of the scattered ions, such as the cluster size, shape, or charge state. When Br attaches to a nanocluster, the neutralization decreases presumably due to charge transfer from the cluster to the electronegative Br atom. Surprisingly, it is found that the neutralization of scattered K^+ ions increases in the presence of adsorbed water at liquid nitrogen temperatures. Furthermore, the increase of neutralization for adsorbed water is independent of whether the water or the Au is deposited first. Possible explanations for these observations will be discussed.

[1] G.F. Liu, Z. Sroubek and J.A. Yarmoff, Phys. Rev. Lett., **92**, 216801 (2004).

12:00pm SS+AS+EN+NS-TuM13 Optical Constants Measured for Fe, Ni and Pd by Reflection Electron Energy-Loss Spectroscopy Spectra, *H. Xu, B. Da, S.F. Mao,* University of Science and Technology of China*, J. Toth, K. Tokesi,* Institute for Nuclear Research, Hungarian Academy of Sciences (ATOMKI)*, **Zejun Ding**,* University of Science and Technology of China

The energy loss function (ELF), which is directly related to optical constants of a solid, dominates the energy loss process of an electron moving inside or flying nearby a solid. It is therefore able to obtain optical constants by surface electron spectroscopy technique. Accurate measurement of optical data by optical methods in a photon energy range up to 10^2 eV is still insufficient; delicate experimental conditions are required when measuring data in vacuum ultraviolet region (20-50 eV). Fortunately, such information is essentially contained in and, therefore, can be extracted from a reflection electron energy loss spectroscopy (REELS) spectrum due to the shorter information depth of signal electrons compared with that of photons.

In the present work, reflection electron energy loss spectra of transition metals, Fe, Ni and Pd, were measured at several primary energies ranging from 0.5 keV up to 5 keV and in a wide energy-loss range. Prior to the measurements in situ cleaning of the sample surface was performed using Ar+ ion sputtering with proper current density and time. Vacuum was kept as 1.5×10^{-9} mbar in the measurement chamber during the REELS measurements. Surface cleanness was checked by XPS in several cases after the REELS measurements. An improved reverse Monte Carlo simulation for determination of optical constants via accurate description of electron inelastic transport process was performed. ELF of those metals were extracted from experimental REELS spectra. The accuracy of the obtained optical data has been confirmed by f-sum and ps-sum rules. Comparisions of our data with other sources from either experimental measurements or density functional theory calculation are given.

Surface Science
Room: 113 - Session SS+AS+EN-TuM

Mechanistic Insight of Surface Reactions: Catalysis, ALD, etc. - I
Moderator: Ludwig Bartels, University of California - Riverside

8:00am SS+AS+EN-TuM1 Active Sites of Nitrogen-Doped Carbon Materials for Oxygen Reduction Reaction, *Takahiro Kondo, D. Guo, R. Shibuya, C. Akiba, S. Saji, J. Nakamura,* University of Tsukuba, Japan

Nitrogen-doped carbon materials have been found to demonstrate high electrocatalytic activity for oxygen reduction reaction (ORR) as the non-metal catalysts but the active site is still under debate. This is due to the complexity of the real catalysts, such as mixing of different type of N and inhomogeneity in both structure and conductance. Here we designed the nitrogen doped graphite (HOPG) model catalysts with different type of N dominance and its concentration to directly clarify the ORR active site. ORR measurements showed that active site was created by pyridinic N (N bonded to two carbon atoms). The ORR active site was ascribed to the carbon atom with Lewis base property created by neighbour pyridinic N based on the investigations of intermediate state of ORR, localized electronic states at carbon next to pyridinic N and CO_2 adsorption property by X-ray photoelectron spectroscopy (XPS), scanning tunneling spectroscopy (STS) and temperature programmed desorption (TPD), respectively. The ORR activity of model catalyst per pyridinic N concentration was then found to be in good agreement with that for real nitrogen-doped graphene catalyst.

8:20am SS+AS+EN-TuM2 Cerium Oxide-Induced Intercalation of Oxygen on Supported Graphene, *Zbynek Novotny,* Pacific Northwest National Laboratory*, F.P. Netzer,* Karl-Franzens University, Austria*, Z. Dohnalek,* Pacific Northwest National Laboratory

Cerium oxide is an important catalytic material known for its ability to store and release oxygen, and as such, it has been used in a range of applications, both as an active catalyst and as a catalyst support. Using scanning tunneling microscopy and Auger electron spectroscopy, we investigated oxygen interactions with CeO_x clusters on a complete graphene monolayer-covered Ru(0001) at elevated temperatures (550 – 700 K). Under oxidizing conditions ($\sim 10^{-7}$ Torr of O_2), oxygen intercalation under the graphene layer is observed. Time dependent studies demonstrate that the intercalation starts in the vicinity of the CeO_x clusters and extends until a completely intercalated layer is observed. Atomically resolved images further show that oxygen forms $p(2 \times 1)$ structure underneath the graphene monolayer. Temperature dependent studies yield an apparent kinetic barrier for the intercalation of 0.9 eV. This value correlates well with the theoretically determined value for the reduction of small CeO_2 clusters reported previously. At higher temperatures, the intercalation is followed by a slower etching of the intercalated graphene (apparent barrier of 1.1 eV). The intercalated oxygen can also be released through the CeO_x clusters by annealing in vacuum. In agreement with previous studies, no intercalation is observed on a complete graphene monolayer without CeO_x clusters, even in the presence of a large number of point defects. These studies demonstrate that the easily reducible CeO_x clusters act as intercalation gateways capable of efficiently delivering oxygen underneath the graphene layer.

8:40am SS+AS+EN-TuM3 Dissociation Dynamics of Energetic Water Molecules on TiO$_2$(110): Combined Molecular Beam Scattering and Scanning Tunneling Microscopy Study, *Z.-T. Wang, Y.-G. Wang, R.T. Mu, Y. Yoon, G.A. Schenter, R. Rousseau, I. Lyubinetsky, **Zdenek Dohnalek**,* Pacific Northwest National Laboratory

Molecular beam scattering techniques have proven extremely useful in determining the dynamics of energy flow in the course of chemical reactions. We have successfully designed and constructed a unique, state of the art instrument combining a molecular beam scattering source coupled with a low temperature scanning tunneling microscope (STM). The combination of these techniques allows us to follow the same area during adsorption and image surface species as a function of incident energy of reacting molecules. Our first study focuses on reversible water dissociation on Ti rows of $TiO_2(110)$, which leads to the formation of pairs of terminal and bridging hydroxyl species, $H_2O \leftrightarrow HO_t + HO_b$. The results of our measurements show the onset of H_2O dissociation at 0.2-0.3 eV of incident energy, independent of whether the molecules impinge along or across the Ti rows at an incident angle of 60° relative to surface normal. Following the onset, the dissociation probability increases linearly with increasing incident energy. Ensembles of *ab initio* molecular dynamics (AIMD) simulations at several incident energies reproduce the product distribution seen in the STM. Additionally, these studies show that the dissociation occurs only for the impacts in the vicinity of surface Ti ions with an activation energy of 0.3 eV and that the O-H bond cleavage is accomplished within the time of a single vibration. The AIMD simulations were further used to construct a classical potential energy surface for water/$TiO_2(110)$ interactions and execute non-equilibrium classical MD simulations that closely reproduce the onset and linear energy dependence of the dissociation probabilities.

9:00am SS+AS+EN-TuM4 Tracking Site-Specific C-C Coupling of Formaldehyde Molecules on Rutile TiO$_2$(110), *Zhenrong Zhang, K. Zhu, Y. Xia,* Baylor University*, M. Tang,* Southern Illinois University Carbondale*, Z.-T. Wang, I. Lyubinetsky,* Pacific Northwest National Laboratory*, Q. Ge,* Southern Illinois University Carbondale*, Z. Dohnálek,* Pacific Northwest National Laboratory*, K. Park,* Baylor University

We report the direct visualization of molecular coupling of the smallest aldehyde, formaldehyde, on reduced rutile $TiO_2(110)$ surfaces using scanning tunneling microscope (STM). Images from the same area at viable temperatures (75 ~ 170 K) show that formaldehyde preferably adsorbs to bridging-bonded oxygen vacancy (V_O) defect site. V_O-bound formaldehyde couples with Ti-bound CH_2O form a diolate species, which stays stable at room temperature. In addition, two V_O-bound formaldehyde molecules can couple and form Ti-bound species, which desorbs above ~215 K. This coupling reaction heals both the V_O sites indicating formation and desorption of ethylene. We also directly observed the diffusion of methylene groups to nearby empty V_O sites formed upon dissociation of the C-O bond in V_O-bound formaldehyde, which suggests that the ethylene formation is via coupling of the methylene groups.

9:20am SS+AS+EN-TuM5 AVS 2014 Gaede-Langmuir Invited Talk: Models for Heterogeneous Catalysts: Complex Materials at the Atomic Level, *Hajo Freund**, Fritz Haber Institute of the Max Planck Society, Germany **INVITED**

Our understanding of catalysis, and in particular heterogeneous catalysis, is to a large extend based on the investigation of model systems. The enormous success of metal single crystal model surface chemistry, pioneered by physical chemists, is an outstanding example. Increasing the complexity of the models towards supported nanoparticles, resembling a real disperse metal catalyst, allows one to catch in the model some of the important aspects that cannot be covered by single crystals alone. One of the more important aspects is the support particle interface. We have developed strategies to prepare such model systems based on single crystalline oxide films, which are used as supports for metal, and oxide nanoparticles, which may be studied at the atomic level using the tools developed in surface science. However, those oxide films may also serve as reaction partners themselves, as they are models for SMSI states of metal catalyst. Using such model systems, we are able to study a number of fundamental questions of potential interest, such as reactivity as a function of particle size and structure, influence of support modification, as well as of the environment, i.e. ultra-vacuum or ambient conditions, onto reactivity. The thin oxide film approach allows us to prepare and study amorphous silica as well as 2D-zeolites. Those systems, in spite of their complexity, do lend themselves to theoretical modelling as has been demonstrated.

11:00am SS+AS+EN-TuM10 The Solid State Li-CoO Conversion Reaction Studied by ARXPS and STM, *Ryan Thorpe, S. Rangan,* Rutgers, the State University of New Jersey, *A. Howansky,* Stony Brook University, *R.A. Bartynski*, Rutgers, the State University of New Jersey

Cobalt (II) oxide is a promising electrode material for Li-ion conversion batteries, undergoing the following reversible redox reaction upon exposure to lithium:

$$2Li + CoO \leftrightarrow Li_2O + Co^0$$

In order to characterize the phase progression and morphology of the Li-CoO reaction, epitaxial CoO(100) and (111) films were exposed to lithium in an ultra-high vacuum chamber. The early stages of the reaction were then characterized with scanning tunneling microscopy (STM), while the diffusion of Li into the films and resultant reduction of CoO was quantified using angle-resolved x-ray photoemission spectroscopy (ARXPS). From these measurements, a model of the Li-CoO reaction was constructed for each orientation.

For CoO(111) films, the conversion reaction initiated at step edges and defect sites before proceeding across the surface of the film. STM images of CoO(111) after 0.2 ML of Li exposure suggest that the conversion reaction products initially assumed a periodic structure which was in registry with the CoO(111) surface. For larger Li exposures, ARXPS measurements indicated that the reaction proceeded in a layer-by-layer fashion into the bulk, maintaining a planar interface between reacted and unreacted CoO.

The reaction of the CoO(100) surface with 0.1 ML of Li resulted in the formation of 2-3 nm Co metal nanoparticles which decorated the CoO step edges. Upon further lithiation, the conversion reaction proceeded into the film preferentially at step edges. ARXPS measurements suggested that the reaction penetrated deep into the CoO film from these nucleation points before spreading across the rest of the surface. These combined results show the importance of crystallographic orientation in determining the reaction kinetics in a Li-ion battery.

11:20am SS+AS+EN-TuM11 Imaging Water Adsorption and Dissociation on RuO₂ (110) Surfaces, *Rentao Mu, D.C. Cantu, X. Lin, V.A. Glezakou, Z.-T. Wang, I. Lyubinetsky, R. Rousseau, Z. Dohnálek*, Pacific Northwest National Laboratory

Understanding water/solid interactions is a current critical scientific challenge with important implications for a variety of fundamental and applied processes. Here we study the interactions of water with RuO_2, which has a wide range of applications in photocatalytic water splitting, heterogeneous catalysis, electrochemistry and many other energy-related areas. We prepared stoichiometric (*s-*), reduced (*r-*) and oxidized (*o-*)$RuO_2(110)$ surfaces and studied water adsorption, dissociation, and diffusion using time-lapsed scanning tunneling microscopy and density functional theory calculations. On *s-*$RuO_2(110)$ we show that water monomers become mobile above 238 K and form dimers which are immobile below 273 K. More importantly, we find that the mobile water dimers dissociate readily to form Ru-bound H_3O_2 and hydroxyl species (HO_b) on bridging oxygen (O_b) rows. The onset for diffusion of H_3O_2 on *s-*$RuO_2(110)$ is observed at ~273 K, indicating a significantly higher diffusion barrier than that for water monomers. The experimentally determined

diffusion barriers are in agreement with those obtained from the DFT calculations. The observed behavior is compared and contrasted with that observed for water on isostructural rutile $TiO_2(110)$ where both molecularly-bound monomers and dimers are in equilibrium with their deprotonated states. In contrast with $TiO_2(110)$, the larger separation of Ru atoms induces the segmentation of water chains at high water coverages. On slightly oxidized *o-*$RuO_2(110)$, water molecules react with oxygen adatoms $(O_a$'s) on Ru rows and form pairs of terminal hydroxyl groups which can reversibly dissociate back to a water molecule and O_a. This process results in the displacement of O_a's along the Ru rows. Along- and across-row diffusion of isolated water molecules is tracked at room temperature on both slightly, and heavily oxidized *o-*$RuO_2(110)$ by following the position of hydroxyl pairs. On *r-*$RuO_2(110)$, we find that water molecules readily dissociate at bridging oxygen vacancies and form bridging hydroxyl groups. The mechanism of along- and across-row diffusion of the bridging hydroxyl protons is also studied at room temperature. The atomically-detailed, quantitative assessment of binding and diffusion of the surface species formed upon water adsorption on $RuO_2(110)$ represent a critical step in achieving fundamental level understanding of the role RuO_2 plays as H_2 and O_2 evolution co-catalysts in photocatalytic water splitting reactions.

11:40am SS+AS+EN-TuM12 Surface Reaction Kinetics during Low Temperature ALD of Al₂O₃ Studied by Broadband Sum-frequency Generation, *Vincent Vandalon, W.M.M. Kessels*, Eindhoven University of Technology, Netherlands

The nonlinear optical technique of broadband sum-frequency generation (BB-SFG) has been used to study the surface reactions during atomic layer deposition (ALD). Vibrational BB-SFG spectroscopy is excellently suited for *in-situ* studies of the surface chemistry governing ALD because of its inherent interface selectivity, submonolayer sensitivity, and short acquisition times. In contrast to BB-SFG, conventional absorption spectroscopy, based on the so called "differential" measurements, monitors only changes on the surface. On the other hand, due to its surface selectivity, BB-SFG reveals information about both *persistent* and *changing* surface groups. Therefore, with this technique, open questions can be addressed such as the origin of the decrease in growth per cycle (GPC) at low temperatures of the ubiquitous process of thermal ALD of Al_2O_3 from $Al(CH_3)_3$ and H_2O. So far, a complete picture of the surface chemistry explaining the reduced GPC is missing and the exact cause of the limited growth at low temperatures remains unclear.

More particularly, the surface chemistry of thermal ALD Al_2O_3 was followed by monitoring the density of the -CH_3 surface groups. In contrast to ALD at high temperatures, below 200^oC it was observed that a significant amount of -CH_3 could not be removed during the water half-cycle. The observed kinetics could not be explained by a thermally-activated first-order reaction with a constant cross section. We investigated the temperature dependence of the reaction kinetics further by measuring the -CH_3 coverage as a function of precursor and co-reactant exposure at different temperatures. It found that the absolute cross section obtained for the TMA half-cycle was independent of temperature, indicating that the chemisorption of TMA is not a thermally activated process. The behavior during the water half-cycle was found to be more complex showing a strong dependence on temperature; it cannot be described as a reaction simply obeying Arrhenius behavior. This is in line with the more complex behavior predicted by recent DFT work carried out by Shirazi and Elliott [Nanoscale 2015] where a so-called "cooperative" effect was observed leading to a coverage dependent reactivity. The observations presented in this work are direct experimental evidence of such a "cooperative" effect and were only possible due to the inherent surface selectivity of BB-SFG.

12:00pm SS+AS+EN-TuM13 The Preparation and Redox Properties of Cu/Al₂O₃/ZnO(0001) Model Surfaces, *J. Hu, J.J. Huang, H. Zhang, Mingshu Chen*, Xiamen University, China

The Cu/Al_2O_3/ZnO(0001)-Zn ternary model catalysts were prepared and characterized by XPS and LEISS. The Al_2O_3/ZnO was prepared by depositing Al onto the ZnO surface in O_2 atmosphere at 523 K, and Cu/ZnO was prepared by depositing Cu onto ZnO surface at room temperature. It was found that Al_2O_3 grew on the ZnO surface by a layer-by-layer model, while Cu formed two-dimensional islands only at low coverage and three dimensional clusters at high coverage. For Cu/Al_2O_3/ZnO(0001)-Zn, the XPS and LEIS spectra showed that the copper islands were preferred on the interfaces of Al_2O_3/ZnO. Comparing to the Cu/ZnO binary model catalyst, the addition of Al_2O_3 obviously slowed down the reduction of Cu/Al_2O_3/ZnO by H_2. More significantly, the existence of Al_2O_3 in the ternary model catalyst leaded to an increase of Cu^+ concentration. The enhancement of Al_2O_3 in Cu/Al_2O_3/ZnO(0001)-Zn for methanol synthesis may origin from that the Al_2O_3 helps to stabilize the surface Cu^+ which has been proposed as one of the active sites.

---

* Gaede Langmuir Award Winner

Tuesday Afternoon, October 20, 2015

2D Materials Focus Topic
Room: 212C - Session
2D+EM+MC+MI+NS+SP+SS+TF-TuA

Electronic and Magnetic Properties of 2D Materials
Moderator: Thomas Mueller, Vienna University of Technology, Austria, Xiaobo Yin, University of Colorado Boulder

2:20pm   2D+EM+MC+MI+NS+SP+SS+TF-TuA1   Direct Capacitive Probe of Isospin Order in Graphene Bilayers, *Andrea Young*, University of California at Santa Barbara   **INVITED**
Bilayer graphene is a highly tunable electronic system in which electric fields can be used to control both the carrier density as well as the electronic structure. Like its monolayer cousin, the bilayer graphene Landau levels are characterized by approximate spin and valley degeneracy; unlike monolayer, however, the three dimensional structure of the bilayer allows control of the sublattice splitting with a perpendicular electric field. This feature has been used extensively to probe the phase diagram of interacting electrons, particularly within the zero energy Landau level, revealing a number of interacting states characterized by spin and/or valley order. Typically, however, the spin or valley order is inferred indirectly by varying conjugate fields and inferring the order from the resulting changes in conductivity. Here I will describe a technique capable of resolving layer-polarization directly through high sensitivity capacitance measurements. The measurements confirm the known features of the bilayer graphene phase diagram, while revealing several new phases and a series of sharp features associated with phase transitions between states of different layer polarization. These features suggest a new mechanism for inversion symmetry breaking in Bernal stacked bilayer graphene.

3:00pm   2D+EM+MC+MI+NS+SP+SS+TF-TuA3   Patterning Hydrogenated Graphene via Electron Beam Irradiation, *Woo-Kyung Lee*, *K.E. Whitener, J.T. Robinson, P.E. Sheehan*, Naval Research Laboratory
We demonstrate that electron-beam irradiation selectively removes hydrogen atoms from hydrogenated graphene (HG) prepared by the Birch reduction.[1] Hydrogen removal can pattern the surface with two different functionalities. First, we show that partially-hydrogenated graphene (Phg) on a SiO_2 substrate is ferromagnetic, and that the local magnetic strength can be tuned using e-beam irradiation. An e-beam lithography system enables us to modulate or eliminate the permanent magnetization over a large area to produce a patterned magnetic array. Secondly, since removal of the hydrogens converts the highly electrically insulating HG back into conductive graphene, we can write chemically isolated, dehydrogenated graphene nanoribbons (GNR) as narrow as 100 nm. These GNRs have a low sheet resistance (≥ 31.5 K$\omega/\square$), only 10x that of the pristine graphene, and their Dirac points before and after e-beam irradiation appear at comparable gate voltages.

1. *W.K. Lee et al., Advanced Materials, 27, 1774 (2015).*

3:20pm   2D+EM+MC+MI+NS+SP+SS+TF-TuA4   Large-Area Low-Pressure Synthesis of Single-Layer MoS₂ Films and Schottky-Barrier Formation upon Metal Deposition, *Michael Gomez*, *J. Martinez, M. Valentin, L. Bartels*, UC Riverside
Using a high vacuum CVD process we are able to synthesize large are monolayer MoS_2 films. Organic chalcogen precursors are released into the growth chamber and react with a Mo filament creating films up to $2cm^2$ in size that are uniform and free of oxides. The films have pronounced photoluminescence intensity and are in Raman spectroscopy indistinguishable from exfoliated material. Metal contact formation to these films was investigated under UHV conditions utilizing X-Ray Photoelectron Spectroscopy . These measurements permit us to follow the formation of a Schottky Barrier with increasing metal film thickness on the Angstrom scale. We utilize core level spectroscopy to indicate the evolution of the MoS_2 valence band under metal deposition.

4:20pm   2D+EM+MC+MI+NS+SP+SS+TF-TuA7   Accelerating the Discovery of Alternative Fuel Catalysts through Intelligent Computational Framework, *Altaf Karim*, COMSATS Institute of Information Technology, Pakistan   **INVITED**
In today's modern world of high performance computing, properties of materials can be predicted with high accuracy before these materials are ever made. In this scenario my focus has been on the development of state of the art computational framework based on intelligent/ smart self-learning algorithms for the design and discovery of catalytic materials. By giving some examples, I will describe how this enterprise of the predictive multi-scale modeling/simulation has been passing through the stages of its evolution and how these complex algorithmic species integrated themselves into an intelligent python, which is helping scientists design & discover new materials for alternative fuel catalysis. In practice, our computational framework develops databases of candidate catalysts. Further this framework enables a set of algorithms to screen across a broad range of multi metallic catalytic materials with variable reactivity, selectivity, and stability while searching for materials with desired combination of properties required for the optimal catalytic performance for alternative fuel production. I would also explain that how our computational tools in catalyst design deal with the multi-component microstructures of catalysts composed of multi-element nano chunks. In order to tune up the rate limiting processes we can take advantage of the multi-element nano chunks. For example, on many catalytic surfaces the diffusion is rate limiting process for larger organic molecules. To enhance the diffusion such molecules on such surfaces, nano chunks of other materials (on which the diffusion of the organic molecules is comparatively higher) can be integrated in the catalyst's surface, which improves the overall performance of the catalyst in terms of overall reactivity and also selectivity. In addition to that our tools also help us to filter out, from the databases, stable multi-component microstructures of artificially engineered catalysts.

5:00pm   2D+EM+MC+MI+NS+SP+SS+TF-TuA9   Probing Massive Dirac Electrons in Bilayer Graphene, *Feng Wang*, University of California at Berkeley   **INVITED**
Electrons in monolayer graphene are described by massless Dirac electrons, which exhibit unique quantum phenomena due to the pseudospin and Berry phase of the massless electrons. In this talk, I will discuss our effort in probing massive Dirac electrons in gapped bilayer graphene. In particular, I will discuss the topologically protected 1D conducting channel at the domain boundary of AB-BA bilayers, which can be attributed to the quantum valley Hall edge states in gapped bilayer graphene.

5:40pm   2D+EM+MC+MI+NS+SP+SS+TF-TuA11   Combining Photoemission and Photoluminescence Microscopy to Study Substrate Transfer Process Effects in Chemical Vapor Deposited MoS₂ Monolayers, *Olivier Renault*, *M. Frégnaux*, Univ. Grenoble Alpes/ CEA, LETI, MINATEC Campus, France, *J. Bleuse*, Univ. Grenoble-Alpes & CEA-INAC, France, *H. Kim*, Univ. Grenoble Alpes/ CEA, LETI, MINATEC Campus, France, *D. Voiry, M. Chhowalla*, Rutgers University
Within the perspective of integrating two-dimensional transition metal dichalcogenides (2D TMDs) such as molybdenum disulfide (MoS_2), into devices, it becomes of utmost importance to assess the influence of each step of the device fabrication process on the optical and transport properties of the MoS_2 single layer (1L) domains. Particularly at the deposition stage the properties may be influenced by substrate effects [1], and later, transfer processes may further alter the desired properties of TMDs. This requires effective microscopic characterization techniques.

We present a characterization method combining photoemission microscopy (XPEEM and Kpeem) and photoluminescence microscopy to compare the structural, optical and electronic properties of both as-deposited and transferred MoS_2 1L domains onto different substrates. XPEEM is used with laboratory sources in both direct space imaging for work function and core-level mapping [2] and particularly in the momentum microscopy mode (k-PEEM) to perform parallel angular imaging and retrieve the band structure in a one shot experiment [3]. Micro-photoluminescence spectroscopy at low (5K) and room temperature is used to detect the specific radiative recombination that occurs in MoS_2 1L (direct band gap semiconductor behavior) and to evidence the eventual presence of midgap states caused by process-induced defects. The results of both characterization techniques will be presented for MoS_2 1L domains transferred onto silica and gold substrates highlighting the roles of substrate nature (metal or insulant), surface roughness, and the presence of structural defects whether induced by the preparation process or intrinsic such as grain boundaries.

[1] Jin et al. Phys. Rev. Lett. 111 (2013), 106801.

[2] Kim, Renault, et al. Appl. Phys. Lett. 105 (2014) 011605.

[3] Mathieu et al., PRB 83 (2011) 235436.

Energy Frontiers Focus Topic
Room: 211B - Session EN+EM+NS+SE+SS+TF-TuA

Batteries and Supercapacitors

Moderator: Elijah Thimsen, Washington University, St. Louis, Andrew C. Kummel, University of California at San Diego

2:20pm EN+EM+NS+SE+SS+TF-TuA1 Behavior of Layered Cathode Materials: A Route to Higher Energy Density for Li-Ion Batteries, *Marca Doeff*, *F. Lin,* Lawrence Berkeley National Laboratory, *I. Markus*, Lawrence Berkeley Lab, University of California, Berkeley **INVITED**
The most promising cathode materials for Li-ion batteries geared towards vehicular applications are the so-called NMCs ($LiNi_xMn_yCo_zO_2$), based on cost and performance considerations. NMCs exhibit a slightly sloping voltage profile in lithium half-cells, with typical utilizations significantly lower than the theoretical capacity of about 280 mAh/g. An attractive strategy for increasing the energy densities of devices meant for traction applications would be to cycle NMCs to a higher potential than is currently used (usually about 4.3V vs. Li^+/Li) so that more lithium can be extracted and cycled. For this approach to be viable, the cathodes must exhibit excellent structural stability and good reversibility over a wide composition range. Our recent work has been directed towards understanding the high-potential behavior of NMCs, using an array of synchrotron x-ray techniques as well as transmission electron microscopy. These techniques show that surface reconstruction to rock salt and spinel phases occur during high voltage cycling, and result in impedance rises and apparent capacity losses. The degree to which this occurs is a function of how the material is made and its electrochemical history. Partial substitution of Ti for Co in NMCs not only increases the capacities obtained during cycling to 4.7V in lithium half-cells compared to baseline materials, but appears to improve the cycling behavior as well. First principles calculations show that the aliovalent substitution lowers the voltage profile slightly. This allows a greater amount of lithium to be extracted and cycled below 4.7V, resulting in higher practical capacities. The Ti-substitution also delays the formation of rock salt during charging, resulting in better capacity retention. These observations suggest that optimizing the synthesis and judicious substitution can mitigate deleterious structural changes of the NMCs due to high potential operation in Li-ion cells. These strategies should be combined with those designed to prevent side reactions with electrolytic solutions during high potential operation, such as new electrolytic solutions with improved oxidative stability, or atomic layer deposition coatings on electrode surfaces, to further ensure stable cycling.

3:00pm EN+EM+NS+SE+SS+TF-TuA3 Next-Generation Electrolytes for Lithium-Ion Batteries, *Sarah Guillot*, University of Wisconsin - Madison, *M. Usrey, A. Pena-Hueso,* Silatronix, Inc., *R.J. Hamers*, University of Wisconsin-Madison and Silatronix, Inc.
Current-generation electrolytes for lithium-ion batteries are limited in electrochemical stability and thermal stability. Over the last several years, researchers at University of Wisconsin and at Silatronix, inc. have developed several new generations of electrolytes based upon incorporation of organosilane groups into the molecular structure. A recently developed class of compounds shows unprecedented enhancements in performance, including the ability to cycle full cells over 400 times at 70 degrees C, and the ability to reduce or eliminate "gassing" at cathode surfaces. In this talk we will discuss the molecular structure of these organosilane-based compounds, quantitative measurements of the decomposition pathways, and the resulting mechanistic insights into the molecular properties that gives rise to their outstanding performance characteristics.

3:20pm EN+EM+NS+SE+SS+TF-TuA4 Physico-Chemical Properties of Polyamidoamine Dendrimer-Based Binders for Carbon Cathodes in Lithium-Sulfur Batteries, *Manjula Nandasiri*, *P. Bhattacharya, A. Schwarz, D. Lu,* Pacific Northwest National Laboratory, *D.A. Tomalia,* NanoSynthons LLC, *W.A. Henderson, J. Xiao,* Pacific Northwest National Laboratory
Lithium-sulfur (Li-S) batteries are one of the most promising energy storage systems, offering up to five-fold increase in energy density as compared with state-of-the-art lithium-ion batteries to meet the growing demand for environmentally benign energy storage devices with high energy density, low cost, and long life time. For practical applications, high sulfur (active material) loading (> 2 mg/cm^2) within the carbon cathode in Li-S batteries is essential. Most reports on engineered cathode materials for Li-S batteries are based upon low sulfur loadings (typically ~1 mg/cm^2), which are impractical and often give misleading results. It is unknown how these novel engineered cathodes behave under high sulfur loading conditions. The binder is perhaps the most critical material in achieving a high sulfur loading in carbon cathodes. We have recently used dendrimers with various surface chemistries as functional binders in Li-S cells with SuperP-carbon/S as the cathode material. Even without engineering the cathode, very favorable cycling stability and electrolyte wetting were obtained with these binders. It was attributed to the high density of surface functional groups on the dendrimers, high curvature of the binder and its porosity, and the interactions between the large number of basic nitrogen and oxygen atoms on the dendrimers and lithium polysulfides.

Here, we will discuss the fundamental properties of dendrimers as aqueous binders for Li-S battery cathodes and compare their performance with other aqueous, commonly used linear polymeric binders such as styrene butadiene rubber (SBR) and sodium carboxyl methyl cellulose (CMC). Specifically, generation 4 polyamidoamine (PAMAM) dendrimers with hydroxyl (OH), 3-carbomethoxypyrrolidinone (CMP), and sodium carboxylate (COONa) surface functional groups served as good, electrochemically stable binders at high S loadings (~3-5 mg/cm^2) with high initial capacities (> 1000 mAh/g). In comparison to CMC-SBR binder-based electrodes which failed at high C-rates (0.2C) after 40 cycles, dendrimer-based binders showed a capacity retention of >85% for more than 100 cycles. It was also observed that acidic groups and all-NH_2 surface groups are poor binders, whereas binders with COO$^-$ and neutral surface groups (OH, CH_3) show better performance. X-ray photoelectron spectroscopy was used to identify different surface functional groups in these dendrimers and understand their interactions with SuperP-carbon/S cathode. In addition, a detailed physico-chemical characterization using IR spectroscopy and XANES/EXAFS will be presented to substantiate the superior dendrimer-carbon/S interactions.

4:20pm EN+EM+NS+SE+SS+TF-TuA7 The Road beyond Lithium Batteries is Paved — In Three Dimensions — With Rechargeable, Dendrite-Free Zinc, *Debra Rolison*, *J.F. Parker, C.N. Chervin, I.R. Pala, M.D. Wattendorf, J.W. Long,* U.S. Naval Research Laboratory **INVITED**
Lithium-ion batteries dominate the energy-storage landscape, but do so with the ever-present threat of thermal runaway and conflagration courtesy of flammable electrolytes and oxygen-releasing electrode materials. Fortunately, Zn-based batteries offer a compelling alternative grounded in the innate safety and cost advantages of aqueous electrolytes augmented by the high earth-abundance of Zn and the high energy density of Zn-based batteries (comparable to Li-ion). Traditional Zn-based batteries provide suboptimal utilization of the zinc (typically <60% of theoretical capacity) and poor rechargeability—thanks to the complex dissolution/precipitation processes that accompany Zn/Zn^{2+} cycling of conventional powder-bed Zn electrode structures in alkaline electrolyte. We address these limitations by redesigning the zinc anode as a porous, 3D-wired "sponge" architecture. Zinc sponge electrodes achieve >90% Zn utilization when discharged in primary Zn–air cells, retaining both the 3D framework of the Zn sponge and an impedance characteristic of the metal thanks to an inner metallic core of 3D zinc. When cycled in Ag–Zn and Ni–Zn cells, the Zn sponges retain monolithicity and reveal uniform deposition of charge/discharge products at the external and internal surfaces, even to deep depth-of-discharge of the zinc. These results show that all Zn-based chemistries can now be reformulated for next-generation rechargeable, Li-free batteries

5:00pm EN+EM+NS+SE+SS+TF-TuA9 Porous Silicon Electrochemical Capacitor Devices for Integrated On-Chip Energy Storage, *Donald Gardner*, *C.W. Holzwarth III, Y. Liu, S. Clendenning, W. Jin, B.K. Moon, Z. Chen, E.C. Hannah, T.V. Aldridge,* Intel Corp, *C.P. Wang, C. Chen,* Florida International University, *J.L. Gustafson,* Intel Corp
Integrated on-chip energy storage is increasingly important in the fields of internet of things (IoT), energy harvesting, and sensing. Silicon is already the materials of choice for the integrated circuits found in every IoT device; however, the efforts to integrate electrochemical (EC) capacitors on a silicon die have been limited. Unlike batteries, EC capacitors are electrostatic devices and do not rely on chemical reactions enabling cycle lifetimes of >1M. This is especially important for off-power-grid IoT devices where difficulty associated with regularly replacing the batteries of billions of devices is prohibitive. This work demonstrates electrochemical capacitors fabricated using porous Si nanostructures with extremely high surface-to-volume ratios and an electrolyte. Devices were fabricated with tapered channels sized from 100 nm at the top to 20 nm and with aspect ratios greater than 100:1. Surface coatings were necessary for long-term stability because unpassivated silicon structures react with the electrolytes. To obtain uniform coatings using stop-flow atomic layer deposition (ALD), efficient surface reactions are needed between high volatility, low molecular weight, small molecular diameter precursors without chemical vapor deposition side reactions. $TiCl_4$ and NH_3 precursors were found to coat porous Si with TiN uniformly. Measurements of coated P-Si capacitors reveal that an areal capacitance of up to 6 mF/cm^2 can be achieved using 2 µm deep pores, and scales linearly with depth with 28 mF/cm^2 measured for

12 μm deep pores. Three-terminal CV measurements with EMI-BF$_4$ ionic electrolyte were used to examine the stability of different pore sizes and TiN coating thicknesses. Pores with an average 50 nm width and 100:1 aspect ratio were stable to ±1.2 V when cycled at 10 mV/s and stable to ±1.0 V when cycled at 1 mV/s. Different ionic liquids were studied to determine the ionic liquid best suited to TiN coated porous Si including TEA-BF$_4$/AN, EMI-BF$_4$, EMI-Tf, and a 3M EMI-BF$_4$/propylene carbonate (PC) mixture. Using impedance spectroscopy, the time constant for a 2 μm deep porous Si EC capacitor with a high conductivity TiN coating was found to be 17.6 ms which is fast enough that this can be used for applications involving AC filtering for AC-DC conversion. Measurements of volumetric energy density versus power density of porous Si devices versus other devices show several orders of magnitude higher energy density than electrolytic capacitors with a similar voltage range. These results are also between one to two orders of magnitude higher than other studies utilizing porous silicon and are comparable to commercial carbon-based EC capacitors.

5:20pm EN+EM+NS+SE+SS+TF-TuA10 Investigations of Magnesium Stripping and Deposition using *Operando* Ambient Pressure X-ray Photoelectron Spectroscopy, *Yi Yu*, Lawrence Berkeley National Laboratory, *Q. Liu*, Shanghai Tech University, China, *B. Eichhorn*, University of Maryland, College Park, *E.J. Crumlin*, Lawrence Berkeley National Laboratory

Since the first demonstration of rechargeable magnesium battery, magnesium metal has been considered as an attractive battery anode due to its high volumetric energy density, high negative reduction potential, natural abundance in the earth crust, and relatively good safety features due to its dendrite-free formation. Although it is well accepted that the dissolution and plating of metal plays an important role in the electrochemical properties related to the discharge and charge of the battery, the nature of metal-electrolyte chemical and electrochemical interaction is still not fully established. In an effort to elucidate the interfacial electrochemical mechanisms, we present the studies of magnesium deposition and stripping using *operando* ambient pressure X-ray photoelectron spectroscopy (AP-XPS). Synchrotron X-rays at the Advanced Light Source, Lawrence Berkeley National Laboratory and our 'tender' X-ray AP-XPS endstation allow for probing the liquid-solid interface at pressures up to 20 Torr. Cyclic voltammetry is employed to examine the reversibility of electrochemical magnesium deposition. This talk will provide details on how *operando* AP-XPS coupled with electrochemistry allows for studying electrochemical processes of magnesium deposition and stripping at the liquid-solid interface and yields chemical information relevant to real-world applications.

5:40pm EN+EM+NS+SE+SS+TF-TuA11 Atomic Layer Deposition of Solid Electrolytes for Beyond Lithium–Ion Batteries, *Alexander Kozen*, *G.W. Rubloff*, University of Maryland, College Park **INVITED**
Solid Li-based inorganic electrolytes offer profound advantages for energy storage in 3-D solid state batteries: (1) enhanced safety, since they are not flammable like organic liquid electrolytes; and (2) high power and energy density since use of the 3D geometry can maximize the volume of active material per unit area, while keeping the active layer thickness sufficiently small to allow for fast Li diffusion. The quality of thin solid electrolytes is currently a major obstacle to developing these solid state batteries, restricting electrolyte thickness to >100 nm to control electronic leakage, consequently slowing ion transport across the electrolyte and impeding 3-D nanostructure designs that offer high power and energy.

Furthermore, the ion-conducting, electron-insulating properties of solid electrolytes are promising for their use as protection layers on metal anodes (e.g., Li, Na, Mg) and on cathodes in proposed "beyond-Li-ion" battery configurations such as Li-NMC, Li-O$_2$, and Li-S to prevent electrolyte breakdown.

Atomic layer deposition (ALD) is well suited to the challenge of solid electrolytes, providing ultrathin, high quality films with exceptional 3-D conformality on the nanoscale. We have developed a quaternary ALD processes for the solid electrolyte LiPON, exploiting *in-operando* spectroscopic ellipsometry and *in-situ* XPS surface analysis for process development. ALD LiPON has tunable morphology, and a nitrogen-dependent tunable ionic conductivity as high as 3.5×10^{-7} s/cm.

We explore the potential of ALD solid electrolytes for the fabrication of solid, 3D microbatteries, as we as the use of thin ALD solid electrolyte coatings on metal anodes to improve interfacial stability against organic electrolytes and thus prevent SEI formation. We demonstrate and quantify protection of lithium metal anodes with low ionic conductivity ALD Al$_2$O$_3$ coatings to prevent degradation reactions, and probe the surface chemistry and morphology of these anodes. Finally, we demonstrate that protection of Li metal using ALD protection layers can improve the capacity of

Li-S batteries by 60% by preventing anode corrosion by dissolved sulfur species in the electrolyte.

This work has implications beyond the passivation of lithium metal besides its focus and greatest impact on the Li-S battery system, as ALD protection layers could also be applied to other promising metal anode battery systems such as Mg and Na, and other beyond Li-ion technologies such as Li-NMC or- Li-Air where similar reactivity issues prevent adoption.

In-Situ Spectroscopy and Microscopy Focus Topic
Room: 211C - Session IS+AS+SS-TuA

Environmental TEM Studies for Catalytic and Energy Materials
Moderator: Franklin (Feng) Tao, University of Kansas, Judith Yang, University of Pittsburgh

2:20pm IS+AS+SS-TuA1 *In Situ* and *Operando* TEM of Thermal and Photocatalysts, *Peter Crozier*, B.K. Miller, L. Zhang, Q. Liu, Arizona State University **INVITED**
Heterogeneous catalysts play a vital role in the development of energy technologies. Understanding the fundamental relationships between catalyst activity and structure at the nanoscale will enable the improved design of catalyst nanostructures. *In-situ* and *operando* environmental transmission electron microscopy (ETEM) is a powerful technique for the investigation of structure-reactivity relationships in high surface area catalysts under reaction conditions. With current instruments, atomic resolution imaging and spectroscopy can be carried out in the presence of gas, liquid, light and thermal stimuli. The combination of mass spectrometry and electron energy-loss spectroscopy allow catalytic products to be detected and quantified directly in the electron microscope. Several specific applications of ETEM instrumentation and experiments to several heterogeneous catalysts will be presented.

Photocatalytic water splitting can be accomplished by a heterostructure of several materials, including a light absorbing semiconductor and one or more co-catalysts. Our group has focused on Ni-NiO co-catalysts on both TiO$_2$ and Ta$_2$O$_5$. In the Ni-NiO/TiO$_2$ system, deactivation occurs due to this Ni dissolution into water during illumination and H$_2$ is only produced by the oxidation of Ni metal[1]. For the Ta$_2$O$_5$ supported catalyst, H$_2$ was produced predominantly by a catalytic reaction [2] and the deactivation rate was found to be inversely proportional to the initial thickness of the NiO shell. In both systems, deactivation is observed only during light illumination, so that this deactivation is properly called photocorrosion.

Our group has also been pioneering the use of operando TEM to study CO oxidation over supported Ru nanoparticles [3]. There is uncertainty and debate in the literature regarding the most active form of this catalyst. Images of the Ru nanoparticles after reduction *in-situ* show a clean metal surface, but after only 0.5% O$_2$ is introduced into the cell, a thin oxide layer forms on the surface. Similar experiments are currently being performed under operando conditions.

References:

[1] L. Zhang, et al. The Journal of Physical Chemistry C, **119**, (2015), p. 7207–7214.

[2] Q. Liu, et al. Applied Catalysis B: Environmental, **172–173**, (2015), p. 58–64.

[3] B.K. Miller, P.A. Crozier Microscopy and Microanalysis **20**, (2014), p. 815–824.

[4] The support from the U.S. Department of Energy (DESC0004954), and the National Science Foundation (CBET-1134464), and the use of ETEM at John M. Cowley Center for HR Microscopy at Arizona State University is gratefully acknowledged.

3:00pm IS+AS+SS-TuA3 Environmental TEM Study of Gold and Platinum Nanoparticulate Catalysts, *H. Yoshida, Y. Kuwauchi, H. Omote, Seiji Takeda*, Osaka University, Japan **INVITED**
The catalytic activity of metal nanoparticles depends on their size, shape, and surface structure. It is well-known that the adsorption of gases induces changes in the shape and surface structure of metal nanoparticles. Thus, it is important to obtain structural information about metal nanoparticles under reaction conditions to elucidate the correlation between the catalytic activity and the morphology of the nanoparticles. Environmental transmission electron microscopy (ETEM) is one of the powerful methods for the study of catalytic materials under reaction conditions at atomic scale [1]. In this study, we have investigated the shape and surface structure of Au and Pt

nanoparticles that are supported on CeO_2 in reactant gases by a Cs-corrected ETEM.

We have found that the surface structure of a Au nanoparticle was reconstructed during CO oxidation at room temperature [2]. The {100} facets remain unreconstructed in vacuum. Under CO oxidation reaction conditions, the Au atomic columns on the topmost and second topmost {100} layers shift to peculiar positions. In the reconstructed surface the Au atoms on the topmost surface layer form an undulating hexagonal lattice, while those on the second topmost surface layer form a normal square lattice with slight distortion. This atomic-scale *in-situ* visualizing method provides us with insights into reaction mechanisms in heterogeneous catalysis.

We have observed the oxidation and reduction processes of the surface of Pt nanoparticles by ETEM. Atomic layers of Pt oxide were formed gradually in O_2 at room temperature during ETEM observations. In situ atomic resolution ETEM, combined with in situ electron energy-loss spectroscopy, showed that atomic layers of Pt oxides, including α-PtO_2 and Pt oxides of other forms, first started forming on the preferential facets of Pt nanoparticles at the early stage, entire oxidization on the whole surface of Pt nanoparticles then followed. The oxides were reduced promptly to Pt by adding a small amount of CO or H_2O vapor to the dominant O_2 gas. It is concluded that electron irradiation during ETEM observation activates the gases non-thermally, therefore promoting or suppressing the processes at room temperature [3].

[1] S. Takeda, Y. Kuwauchi, H. Yoshida, *Ultramicroscopy*, **151** (2015) 178.

[2] H. Yoshida, Y. Kuwauchi, J. R. Jinschek, K. Sun, S. Tanaka, M. Kohyama, S. Shimada, M. Haruta, S. Takeda, *Science***335** (2012) 317.

[3] H. Yoshida, H. Omote, S. Takeda, *Nanoscale*, **6** (2014) 13113.

4:40pm IS+AS+SS-TuA8 Environmental Study of the Reaction-driven Restructuring of Ni-Co Bimetallic Nanoparticles, *C.S. Bonifacio,* University of Pittsburgh, *H.L. Xin,* Brookhaven National Laboratory, *Sophie Carenco, M.B. Salmeron,* Lawrence Berkeley National Laboratory, *E. Stach,* Brookhaven National Laboratory, *J.C. Yang*, University of Pittsburgh

Bimetallic nanoparticles (NPs) possess novel catalytic, optical, and electronic properties compared to their monometallic counterparts. These catalytic properties can be controlled by fine-tuning the NP structure and dimension, surface oxidation, and chemical composition. For instance, bimetallic NPs with a core-shell structure can allow for fine tuning of reactivity, averting sintering issues in the core, and even increase tolerance to high temperature exposure. Above all, elemental segregation in the core-shell structure has been demonstrated as a potential route of modifying the NPs catalytic properties through *in situ* gas reaction studies. To confirm this hypothesis, we have used *in situ* imaging and spectroscopy techniques to study Ni-Co core-shell NPs under environmental conditions to provide direct evidence of elemental redistribution during reaction . Two pairs of oxidation and reduction reactions were performed in an environmental transmission electron microscope (ETEM) at 0.3 Torr in O_2 and H_2 gas at $220°C$ and $270°C$, respectively. Electron diffraction patterns and electron energy loss spectroscopy (EELS) maps showed a reaction-driven restructuring of the core-shell NPs with Ni species migrating to the NP surface by the 2nd reduction cycle. These results are in agreement with previous ambient-pressure x-ray photoelectron spectroscopy (AP-XPS) studies of the same NPs under identical reaction conditions. Furthermore, the ETEM results confirm the NP structure without erroneous interpretations that may result from post-mortem analysis of the samples. Quantitative analysis of the EELS results is underway to identify the valence states during the oxidation-reduction reactions. Correlation of the reaction-driven restructuring of NPs with the electronic structure changes from ETEM and AP-XPS will be provide insight into the optimum reaction conditions, i.e., catalytic properties, of the Ni-Co core-shell NPs in challenging reactions such as selective CO_2 reduction.

5:00pm IS+AS+SS-TuA9 *In situ* Vibrational Spectroscopy Investigation of the Surface Dependent Redox and Acid-base Properties of Ceria Nanocrystals, *Zili Wu*, Oak Ridge National Laboratory **INVITED**

Ceria is best known for its excellent redox property that makes it an important component in the three-way catalyst for auto exhaust cleanup. This is a result of its high oxygen storage capacity associated with the rich oxygen vacancy and low redox potential between Ce^{3+} and Ce^{4+} cations. Equally interesting yet less is known about ceria is its versatile acid-base properties. Either as a standalone catalyst, a modifier or a support, ceria and ceria-based catalysts can catalyze the transformation of a variety of organic molecules that makes use of the acid-base as well as the redox properties of ceria.

Recent advances in nanomaterials synthesis make it possible to achieve nanocrystals with crystallographically defined surface facets and high surface area, which can be considered as ideal model systems for catalytic studies under realistic conditions. In this work, I will showcase how we can make use of ceria nanoshapes as model systems to gain molecular level understanding of the shape effect on both redox and acid-base properties and catalysis of ceria nanocrystals *via in situ* IR and Raman spectroscopy. Insights have been gained into how the surface structure of ceria catalyst affects profoundly its redox and acid-base properties and consequently the catalytic behaviors. It is suggested that the surface structure of ceria controls the catalytic performance through the combination of various factors including structure-dependent surface sites geometry, lattice oxygen reactivity, surface vacancy formation energy, defect sites, and acid-base property on ceria.

5:40pm IS+AS+SS-TuA11 Direct Writing of sub-10 nm Structures from Liquid with Helium Ions, *V. Iberi, R.R. Unocic, **Nathan Phillip**, A. Belianinov, A.J. Rondinone, D.C. Joy, O.S. Ovchinnikova*, Oak Ridge National Laboratory

In-situ direct writing by electron beam from solutions opens a pathway for resistless fabrication of nanostructures at high throughput. However, when using electrons to direct write in solution the minimal size of the created structures is limited to the micron scale due to fundamental physics of the interactions between the electron beam and the liquid, including the lateral transport of solvated electrons and ionic species. Use of the helium beam with the opposite charge and shorter mean free path offers the potential for the localization of the reaction zone on the single digit nanometer scale. Here we will present our results demonstrating writing of platinum structures from liquid (beam induced electroplating) in a platinum chloride solution using helium ions with sub-10 nm resolution. Using data analytics on acquired in-situ growth movies we are able to elucidate the main statistical descriptors for helium ion beam initiated platinum structure growth. The possible mechanisms of beam induced growth and ultrahigh localization of reaction zone are discussed. Furthermore, we will discuss optimization of solution chemistry and instrumental parameters as they relate to the quality and thickness of structures and the extension to device fabrication on a single digit nanometer level.

This work was conducted at the Center for Nanophase Materials Sciences, which is a Department of Energy (DOE) Office of Science User Facility.

Nanometer-scale Science and Technology
Room: 212B - Session NS+EN+SS-TuA

Nanophotonics, Plasmonics, and Energy
Moderator: David Wei, University of Florida

2:20pm NS+EN+SS-TuA1 Subnanoscale Exciton Dynamics of C_{60}-based Single Photon Emitters Explored by Hanbury Brown Twiss Scanning Tunneling Microscope, *Pablo Merino Mateo, C. Grosse, A. Roslawska, K. Kuhnke, K. Kern*, Max-Planck-Institut für Festkörperforschung, Germany

Electron-hole pair (exciton) creation and annihilation by charges are crucial processes for technologies relying on efficient charge-exciton-photon conversion. Photoluminescence has been instrumental for this purpose with near-field techniques approaching 20 nm spatial resolution. However, molecular resolution is still out of reach and individual charge carriers cannot be addressed with these methods. In the present contribution we show how to overcome these limitations by using scanning tunneling microscopy (STM) to inject current at the atomic scale and Hanbury Brown-Twiss (HBT) interferometry to measure photon correlations in far-field electroluminescence.

Quantum systems like molecules or quantum dots cannot emit two photons at the same time which results in an antibunching of the emitted photon train and a dip in the photon-photon correlation function. Such single photon emitters are key elements for quantum cryptography and their miniaturization to the nanoscale would be desirable. This requires reproducible emitter separations typically below the optical diffraction limit and has imposed strong limitations on suitable structures and materials.

Using our HBT-STM setup on localized trap states in C_{60} multilayers we were able to study single photon emission at the ultimate molecular scale. Controlled injection allows us to generate excitons in C_{60} and probe them with charges one by one. We demonstrate electrically driven single photon emission and determine exciton lifetimes in the picosecond range. Monitoring lifetime shortening and luminescence saturation for increasing carrier injection rates provides access to charge-exciton annihilation dynamics with Ångstrom spatial resolution. Comparison with theory reveals exciton quenching efficiencies close to unity. Our approach introduces a unique way to study single quasi-particle dynamics on the ultimate molecular scale.

2:40pm NS+EN+SS-TuA2   Low-Damage Etching Process for the Fabrication of GaAs based Light-Emitting Devices, *Cedric Thomas, A. Higo,* Tohoku University, Japan, *T. Kiba,* Hokkaido University, Japan, *Y. Tamura,* Tohoku University, Japan, *N. Okamoto, I. Yamashita,* Nara Institute of Science and Technology, Japan, *A. Murayama,* Hokkaido University, Japan, *S. Samukawa,* Tohoku University, Japan

Fabrication of quantum dots (QD) and their use for optical devices are still facing big challenges, for instance a high-density and three-dimensional array of QDs is hardly achieved. We report here the fabrication of stacked layers of GaAs QDs (called nanodisks, NDs) of less than 20 nm in diameter by a top-down approach and their optical characteristics when embedding in light emitting device.

The fabrication process consists of a bio-template [1] used to create a high density etching mask coupled to a low-damage etching process using neutral beam (NB) [2]. The bio-template is realized by a self-assembled monolayer (SAM) of proteins called ferritins (cage like proteins) of 12 nm outside diameter with a 7 nm iron oxide core. The proteins are functionalized with poly-ethylene glycol (PEG) to control the ferritin-to-ferritin distance and avoid any ND coupling after fabrication. After removing the protein shell by oxygen based treatment, a high-density (ca. 1×10^{11} cm^{-2}) nano-pattern of cores is used as etching mask. The NB etching consists of an inductively couple plasma chamber separated from the process chamber by a carbon electrode with a high aspect-ratio aperture array. Therefore, the charged particles are efficiently neutralized and the UV photons from the plasma almost completely screened

Stacks of GaAs and AlGaAs layers were grown by metalorganic vapor phase epitaxy (MOVPE), with a GaAs cap layer of a few nanometer thick. SAM of ferritins was done by spin-coating. After removing protein shell by oxygen annealing in vacuum, a hydrogen radical treatment was performed to remove to remove the oxide layer. Etching was then realized by pure chlorine NB. Regrowth of AlGaAs barrier was done by MOVPE. Finally, temperature dependence of photoluminescence emission and ND light emitting diode were measured and results discussed [3].

[1] I. Yamashita et al., Biochim. Biophys. Acta 1800 (2010) 845

[2] S. Samukawa et al., Jpn. J. Appl. Phys. 40 (2001) L997

[3] A. Higo et al., Sci. Reports 5 (2015) 9371

3:00pm   NS+EN+SS-TuA3   Surface Plasmon-Mediated Selective Deposition of Au Nanoparticles on Ag Bowtie Nano-Antennas, *Jingjing Qiu, D. Wei*, University of Florida

Utilizing intrinsic surface properties to selectively direct and control nanostructure growth on a nanostructure is fundamentally interesting and holds great technological promise. We observed a surface plasmon resonance (SPR)-induced selective deposition of gold nanoparticles (Au NPs) at the tip of a silver (Ag) bowtie nanostructure using 532 nm laser excitation. Nanoscale secondary ion mass spectrometry (NanoSIMS) was applied to chemically image the distribution of elements after deposition, reaching a spatial resolution of ~50 nm and an elemental analysis sensitivity of 50 ppm. Possible mechanisms underlying this selective deposition were proposed based on the experimental evidence and theoretical discrete dipole approximation (DDA).

3:20pm   NS+EN+SS-TuA4   Broadband Light Trapping in Nanopatterned Substrates for Photovoltaic and Photonic Applications, *Carlo Mennucci,* Department of Physics, University of Genova, Genova, Italy, *C. Martella, M.C. Giordano, D. Repetto, F. Buatier de Mongeot,* University of Genova, Italy

Here we report on self-organised nanofabrication method applied to substrates of relevance in the field of optoelectronic and photonics in view of light trapping applications. We demonstrate the optical functionalization of glass [1], crystalline semiconductor (GaAS and Si [2]) and TCO substrates recurring to a self-organised pattern formation based on low-energy Ion Beam Sputtering (IBS). High aspect ratio nanoscale features are formed recurring to defocused IBS through a self-organised sacrificial Au nanowire stencil mask. Ion-beam irradiation at grazing angle leads to the formation of quasi-periodic one-dimensional nanostructures with a

characteristic lateral size in the range of 200nm and a root-mean-square roughness (σ) of the surface, measured by Atomic Force Microscope, ranging from 80 to 150nm.

These nanostructures confer broadband anti-reflective bio-mimetic functionality to crystalline semiconductor substrates (GaAs and Si [2]) as well as to glass and TCO substrates in the Visible and Near Infra-Red part of the spectrum. In fact, suppression of the reflected light intensity is due to high aspect ratio sub-wavelength features which leads to a progressive transition of the refractive index from the value of air to that of the substrate (index grading) analogous to that observed in the corneas of nocturnal moths. At the same time the patterned substrates have shown enhanced broadband light scattering due to the extended vertical dynamic of the surface corrugations with lateral size comparable or bigger than light wavelength. Moreover, Angular Resolved Scattering measurements has recently proved that nanostructured glasses can scatter light in the Visible and Near Infra-Red range of spectrum more efficiently and at wider angles with respect to standard Ashai-U substrates commonly used in optoelectronic device applications.

In order to asses the light trapping effect, identical amorphous thin film silicon solar cells (p–i–n single junctions) are grown on nano-patterned and on reference flat glass superstrates. Their performance is assessed by measuring their I–V characteristic and EQE under standard AM1.5g test conditions. The first encouraging results demonstrated that solar cells grown on patterned substrates with RMS roughness σ around 80 nm exhibit a 15% relative enhancement in photocurrent.

References:

[1] C. Martella, D. Chiappe, P. Delli Veneri, L.V. Mercaldo, I. Usatii, F.Buatier de Mongeot, Nanotechnology 24 (22), 225201 (2013).

[2] C. Martella, D. Chiappe, C. Mennucci, F. Buatier de Mongeot ,J.Appl.Phys. 115,194308 (2014).

4:20pm   NS+EN+SS-TuA7   *In Situ* Visualization of Intercalation-Driven Nanoparticle Phase Transitions using Plasmon-EELS, *Jennifer Dionne,* Stanford University   **INVITED**
A number of energy-relevant processes rely on nanomaterial phase transitions induced by solute intercalation. However, many of these phase transitions are poorly understood, since observing them in nanomaterials – and in particular in individual nanoparticles – can be extremely challenging. This presentation will describe a novel technique to investigate intercalation-driven phase transitions in individual nanoparticles, based on *in-situ* environmental transmission electron microscopy (TEM) and plasmon electron energy loss spectroscopy (EELS). As a model system, this presentation will focus on the hydrogenation of palladium nanoparticles. We use the plasmon-EEL signal at varying hydrogen pressures as a proxy for hydrogen concentration in the particle. First, we investigate the hydriding properties of single-crystalline particles, free from defects and grain boundaries, and free from elastic interactions with the substrate. We obtain single particle loading and unloading isotherms for particles ranging from approximately 10 nm to 100 nm, allowing us to address outstanding questions about the nature of phase transitions and surface energy effects in zero-dimensional nanomaterials. We find that hydrogen loading and unloading isotherms of single crystals are characterized by abrupt phase transitions and macroscopic hysteresis gaps. These results suggest that thermodynamic phases do not coexist in single-crystalline nanoparticles, in striking contrast with ensemble measurements of Pd nanoparticles. Then, we extend our single-particle techniques to explore the hydriding properties of polycrystalline and multiply-twinned nanoparticles, including Pd nanorods and icosahedra. In contrast to single crystalline nanoparticles, these particles exhibit sloped isotherms and narrowed hysteretic gaps. Based on these results, we develop a model to deconvolve the effects of disorder and strain on the phase transitions in nanoscale systems. Lastly, we describe techniques to generate high-resolution plasmon-EELS (and hence phase) maps of nanoparticles. These mapping studies promise unprecedented insight into the internal phase of nanomaterials, and can be complemented with diffraction and dark-field imaging studies. We will discuss how these results could be used to interpret the thermodynamics of Li-ion insertion in battery electrodes, hydrogen absorption in state-of the-art metal hydride catalysts, or ion exchange reactions in quantum dot syntheses.

5:00pm   NS+EN+SS-TuA9   Pulsed Laser-Induced Self-Assembly of Noble Metal Nanoparticles and an EELS Characterization, *Yueying Wu,* University of Tennessee, *G. Li,* University of Notre Dame, *C. Cherqui, N. Bigelow,* University of Washington, *J.P. Camden,* University of Notre Dame, *D. Masiello,* University of Washington, *J.D. Fowlkes,* Oak Ridge National Laboratory, *P.D. Rack,* University of Tennessee
Controlled nanoscale synthesis of plasmonic nanostructures based on noble metals is critical for realizing many important applications such as surface-enhanced Raman spectroscopy (SERS), subwavelength waveguides,

plasmonically enhanced photovoltaics, and photocatalysis. Recently pulsed laser induced dewetting (PLiD) has been shown to be an intriguing self and directed assembly technique for elemental and alloyed metallic nanoparticles. The liquid-phase assembly takes place in single to tens of nanoseconds and is governed by liquid phase instabilities and hydrodynamics of liquid thin films which produce arrays of random or highly ordered nanoparticles. In our recent studies, the PLiD of un-patterned, as well as nanolithographically pre-patterned thin films of various shapes and sizes was investigated for the purpose of understanding how initial boundary conditions facilitate precise assembly. The resultant ultra-smooth and metastable nanoparticles (~20nm to 1μm) are expected to be ideal building blocks for plasmonic applications. Based on this, we present a study on the self-assembly of gold and silver alloy thin films and also provide a comprehensive characterization of the resultant nanoparticles using electron energy loss spectroscopy (EELS) and through simulation using full-wave electron-driven discrete-dipole approximation (e-DDA). The study provides for the first time a thorough mapping of the plasmonic modes of synthesized Au-Ag alloy nanoparticles over a large size range.

5:20pm **NS+EN+SS-TuA10 Flexible, Adaptive Optoelectronic Camouflage Skins Using Concepts Inspired by Cephalopods**, *Cunjiang Yu*, University of Houston
Octopus, squid, cuttlefish and other cephalopods exhibit exceptional capabilities for visually adapting to or differentiating from the coloration and texture of their surroundings, for the purpose of concealment, communication, predation and reproduction. Long-standing interest in and emerging understanding of the underlying ultrastructure, physiological control and photonic interactions has recently led to efforts in the construction of artificial systems that have key attributes found in the skins of these organisms. In spite of several promising options in active materials for mimicking biological color tuning, such as cholesteric liquid crystals, electrokinetic and electrofluidic structures, colloidal crystals and plasmonics, existing routes to integrated systems do not include critical capabilities in distributed sensing and actuation.

The results reported here show that advances in heterogeneous integration and high performance flexible/stretchable electronics provide a solution to these critical sub-systems when exploited in thin multilayer, multifunctional assemblies. The findings encompass a complete set of materials, components, and integration schemes that enable adaptive optoelectronic camouflage sheets with designs that capture key features and functional capabilities of the skins of cephalopods. These systems combine semiconductor actuators, switching components and light sensors with inorganic reflectors and organic color-changing materials in a way that allows autonomous matching to background coloration, through the well-known working principle of each device.

Demonstration devices capable of producing black-and-white patterns that spontaneously match those of the surroundings, without user input or external measurement, involve multilayer architectures of ultrathin sheets of monocrystalline silicon in arrays of components for controlled, local Joule heating, photodetection and two levels of matrix addressing, combined with metallic diffuse reflectors and simple thermochromic materials, all on soft, flexible substrates. Systematic experimental, computational and analytical studies of the optical, electrical, thermal, and mechanical properties reveal the fundamental aspects of operation, and also provide quantitative design guidelines that are applicable to future, scaled embodiments.

5:40pm **NS+EN+SS-TuA11 Controlled Deposition of High Quality Nanocrystal Multilayer Structures for Optoelectronic Applications**, *Sara Rupich*, *A.V. Malko, Y.N. Gartstein, Y.J. Chabal*, University of Texas at Dallas
In order to meet the world's growing energy demand, harvesting energy from the sun is necessary. While silicon-based solar cells remain the industry standard, hybrid Si/nanocrystal (NC) structures exhibit significant promise for the development of the next generation of photovoltaic devices. In most current NC-based photovoltaics, photons are absorbed, separated and extracted in the NC layer; however, conversion efficiencies are limited by interface quality and carrier mobility. Hybrid Si/NC structures offer an alternative approach. In these structures, light is absorbed in the NC layer and transferred via efficient excitonic radiative (RET) and non-radiative (NRET) energy transfer into the underlying Si substrate where charge extraction and collection occurs. In order to utilize such structures, the controllable deposition of tens of layers of NCs needs to be realized where the composition of each layer can be varied. While many techniques exist to deposit NCs on substrates (i.e. spin coating, dropcasting), these methods result in thick films with limited control over the composition. Composition controlled structures need to be built up one layer at a time.

Here, we present the controllable deposition of dense, NC multilayer structures on Si and SiO₂ substrates via evaporation-driven self-assembly at the air-liquid interface. Using a layer-by-layer approach, CdSe/ZnS NC

multilayers were assembled, up to 15 layers in thickness. Extensive spectroscopic (UV-vis absorbance, photoluminescence (PL), ellipsometry) and microscopic (scanning electron microscopy and atomic force microscopy) characterization provided evidence for the successful deposition of high quality NC multilayers in each cycle. Additionally, the NCs were found to retain their quantum yields in the multilayers structures indicating that the deposition process does not introduce additional interface trapping centers and showing their promise for integration into optoelectronic devices. Using time-resolved PL measurements, a gradual increase in the average measured NC PL lifetime was observed as a function of layers for NC multilayers on Si surfaces. This behavior was confirmed by theoretical modeling and is indicative of the gradual reduction in ET efficiency as a function of distance and.

As this process is applicable to NCs of different size, shape and composition, the fabrication of band gap graded multilayers structures is possible, which would enable energy harvesting schemes based on directed energy flows.

6:00pm **NS+EN+SS-TuA12 Efficient Coupling of Visible Light to Thin Film Waveguides; FDTD Field Model Results for Nanometer Scale Graded Index/Waveguide Structures.**, *Adam Lambert*, *E. Demaray*, AVS
Previous work utilizing Finite Difference Time Domain (FDTD) models with 20 nm resolution demonstrated normal incident plane wave AM 1.5 solar light could be coupled and concentrated into modes of a lateral duct with ~ 91% efficiency for tapered concentrator with spatially uniform refractive index. However, for efficient coupling and mode compression into high index waveguides in advanced devices, continuously graded index films on the order of 150-200nm with nonlinear profiles have been shown to be near ideal anti-reflective coatings which Antropy Technology can now produce at high volume using modern sputter coating processes. Such devices could be revolutionary not only in the field of photonics, but could also open the path for an wide variety of green energy and advanced lighting applications. This presentation focuses on current advances in the parametric investigation of nonlinear refractive index profiles and related sputter coating production processes. The FDTD problem solving framework provides the fully resolved time dependent propagation of the electromagnetic field, accounting for the nonlinear influence of subwavelength structures and allowing for detailed design of the thin film product. We are reporting resolution capabilities are in the 1-5nm range depending on the relevant length scales for the process. Quantification of power, absorption/heat, and other variables relevant to R&D can easily be extracted during post processing. Parallel Monte Carlo simulations predict the refractive index profile resulting from dual source, inline, biased pulse DC sputter coating. The combination allows for highly accurate feasibility studies and front end process design. Both quantified numerical results as well as qualitative animations of the influence of the subwavelength devices are presented for both processes, as well as a detailed overview of the potential applications.

Surface Science
Room: 113 - Session SS+AS+EN-TuA

Mechanistic Insight of Surface Reactions: Catalysis, ALD, etc. - II
Moderator: Bruce D. Kay, Pacific Northwest National Laboratory

2:20pm **SS+AS+EN-TuA1 How does Absorbed Hydrogen Drive Olefin Hydrogenation on Pd?**, *Satoshi Ohno*, *M. Wilde, K. Fukutani*, The University of Tokyo, Japan
Pd-dissolved hydrogen is an essential ingredient in the highly selective hydrogenation of olefinic C=C double bonds catalyzed by Pd, yet the particular role played by H below the surface has long been debated controversially. Some proposed that absorbed H atoms become directly involved in hydrogenation reactions after they emerge from the metal interior onto the catalyst surface in an energetic state. Others considered that sizeable populations of subsurface sites by absorbed hydrogen indirectly activate surface-adsorbed hydrogen by altering the electronic structure of the catalyst.

To resolve this dispute we have studied the hydrogenation reaction of cis-2-butene to butane on a Pd(110) model catalyst surface with temperature-programmed desorption (TPD) and ^{1}H(^{15}N, ag)^{12}C nuclear reaction analysis (NRA) that reveals the hydrogen distribution on and beneath the surface. TPD demonstrates that the catalytic hydrogenation reaction proceeds efficiently between 160 and 250 K. NRA under the hydrogenation reaction condition, on the other hand, shows that the H concentration in the Pd

subsurface region is as small as 0.5 at. %. Thus, the scenario of indirect surface-hydrogen activation through large quantities of H in the subsurface sites appears rather unrealistic for our experimental conditions. We furthermore elucidate that the butane reaction yield scales linearly with the number of Pd-dissolved H atoms that reach the surface after diffusion from the Pd bulk. This observation clarifies that the Pd-catalyzed olefin hydrogenation is triggered by the emergence of bulk-dissolved hydrogen onto the Pd surface. Our NRA H profiles also demonstrate that the catalytic reaction proceeds on the Pd surface fully saturated with chemisorbed hydrogen. This surface hydrogen is considered important, as it possibly prevents deactivation of reactive surface hydrogen species in vacant chemisorption sites.

Finally, the TPD spectrum of butene shows four peaks at 140, 165, 190, and 225 K, suggesting multiple butene-adsorption modes onto Pd(110) surfaces. Reactive TPD experiments in presence of absorbed hydrogen exhibit a significant decrease in the 165 K peak, identifying this feature as the reactive butene species in the catalytic hydrogenation reaction.

2:40pm SS+AS+EN-TuA2 CO Oxidation over Pd Catalysts Supported on Different Low-Index Surfaces of CeO$_2$: A Combined Experimental and Computational Study, *Xiao Liu, Y.W. Wen, Z.Z. Chen, B. Shan, R. Chen*, Huazhong University of Science and Technology, China
Pd/CeO$_2$ has attracted much attention on the low temperature CO oxidation due to the strong metal-support interactions. In this study, we have systematically investigated the interface properties and CO oxidation activities of Pd catalysts supported on different low-index surfaces of CeO$_2$. The Pd/CeO$_2$ nanorods have been prepared by incipient wetness impregnation method and the exposed surfaces of CeO$_2$ nanorods have been controlled by changing the calcination temperature after their successful synthesis by hydrothermal method. Their catalytic activities in CO oxidation have been tested and the results show that Pd catalysts supported on CeO$_2$ nanorods exposed by (100) and (110) (calcined at 500 ºC) are more activated than that exposed by (111) (calcined at 700 ºC), which is related to the surface oxygen vacancies concentration and the strength of interface interaction. By performing density functional calculations, the surface oxygen activities and the binding strength of Pd clusters on these low-index surfaces of CeO$_2$ have been investigated. The results show that the oxygen vacancy formation energies of (100) and (110) are smaller than that of (111). The binding strength of Pd clusters on these surfaces follows the sequence: (100) > (110) > (111). Furthermore, CO oxidation routes on these surfaces proceeding through the LH, ER and MvK mechanism have been studied. Our studies not only reveal that the catalytic performance of Pd/CeO$_2$ can be tuned by controlling the exposed surface of oxide but also shed light on the interface structures and CO oxidation mechanism of Pd/CeO$_2$ system.

3:00pm SS+AS+EN-TuA3 *In Situ* Adsorption and Decomposition Studies of Dimethyl Methyl Phosphonate on Molybdenum Oxide Surfaces and Nanoparticles, *Ashley Head, L. Trotochaud, Y. Yu*, Lawrence Berkeley National Laboratory (LBNL), *Z. Hicks, X. Tang, K. Bowen*, Johns Hopkins University, *B. Eichhorn*, University of Maryland, College Park, *H. Bluhm*, LBNL
There is great interest in understanding the interaction between the nerve agent simulant dimethyl methyl phosphonate (DMMP) and metal oxide surfaces to further nerve agent filtration technology and decomposition methods. To this end, we have studied the room temperature adsorption of DMMP on MoO$_2$ and MoO$_3$ surfaces up to 30 mTorr using ambient pressure x-ray photoelectron spectroscopy (APXPS). On both surfaces, the majority of DMMP adsorbs intact, but differences in the behavior of DMMP on the two substrates are found upon heating. Two phosphorus species are seen on the MoO$_2$ surface and three are seen on the MoO$_3$; these species remain on both surfaces up to 450 ºC Additionally, carbon remains on the MoO$_2$ at high temperatures but is removed from MoO$_3$ by 420 ºC. The APXPS data were correlated with TPD measurements of DMMP adsorbed on MoO$_3$ clusters on HOPG, a model system closer to real filtration materials. Methanol was found as the major decomposition product in addition to trace amounts of dimethyl ether. The easily reducible MoO$_3$ is likely responsible for an oxidative cleavage of the P-CH$_3$ bond on both the surface and nanoparticles. These studies highlight how APXPS coupled with TPD yields chemical information relevant to real-world applications.

3:20pm SS+AS+EN-TuA4 Adsorption of Sterically Hindered Sulfur Containing Molecules on a Heterogeneous Model Catalyst, *Signe Sørensen, J.V. Lauritsen*, Aarhus University, Denmark
Cobalt promoted MoS2 nanoclusters (CoMoS) are the active phase of the hydrodesulfurization catalyst which enables sulfur removal from crude oil. New legislations on sulfur impurity levels in diesel in EU and US demands

still lower sulfur content which increases the requirements for even more effective catalysts.

Previously catalysts were improved by costly trial-and-error experiments. To target the improvements attempts, understanding of the catalytic mechanism is crucial. In the hydrodesulfurization catalysis the main source to residual sulfur content is the sterically hindered sulfur containing molecules, as the reactivity towards these is very low. To targeted enhance the catalytic activity, atomic scale understanding of this catalytic mechanism is essential.

Scanning tunneling microscopy (STM) is an outstanding tool for real space, atomic-scale imaging of supported nano-scale systems. This makes it the optimal tool for investigating the interaction between the sulfur containing molecules and metal-supported CoMoS, as it offers the unique and powerful ability to directly observe the catalytic active site by imaging single molecules adsorbing on the nanoparticles.

In this study STM is used on a model system of Co-promoted MoS2 on a gold substrate under ultrahigh vacuum conditions. To study the adsorption of the strongly steric hindered sulfur containing molecule 4,6-dimethyl-dibenzothiophene the molecule is dosed directly onto the nanoparticles which means that their location, orientation and the dynamics of single molecules can successfully be revealed through atom-resolved STM images and films. All observed adsorption modes are either associated with a sulfur vacancy on the corner site of the nanoclusters or with the one-dimensional metallic edge state associate with the edge of the Co-promoted MoS2 nanoclusters. These observations strongly indicate that these sites are important active sites of the catalyst and enable targeting the attempts for enhanced activity to optimization of the number of these apparent active sites in the industrial catalyst.

4:20pm SS+AS+EN-TuA7 Metal Nanoparticles on Thin Film Oxide Supports: Interaction and Reaction of Metals with Hydroxyls, *Martin Sterrer*, University of Graz, Austria INVITED
Water-oxide interaction is of great importance in a number of technologically relevant fields, among them heterogeneous catalysis. Several studies report on the promoting effect of water in catalytic reactions, the participation of surface hydroxyls in catalytic reactions, and the influence of hydroxylation on the binding of metals to oxide surfaces. Achieving a fundamental atomic scale understanding of water-oxide interaction at environmentally and catalytically relevant conditions (e.g. ambient pressure) represents, therefore, a challenge for surface science studies related to heterogeneous catalysis. In this contribution, I will present results of our recent studies related to the interaction of water with thin, single crystalline oxide films (Fe-oxides, alkaline earth oxides) carried out in a wide range of water chemical potential (from UHV to mbar water pressures). Topics that will be discussed are the characterization of ordered water monolayers, the dewetting of ice on oxide surfaces, hydroxylation of oxide surfaces at elevated pressure, the influence of hydroxyls on metal nucleation and sintering, and metal deposition onto oxide surfaces from aqueous solutions.

5:00pm SS+AS+EN-TuA9 Dynamics of Isolated Surface Complexes Formed Between a Chemisorbed Chiral Molecule and a Prochiral Reactant, *Jean-Christian Lemay, Y. Dong, P.H. McBreen*, Laval University, Canada
Adsorbed chiral molecules (chiral modifiers) can interact stereoselectively with prochiral co-adsorbates on reactive metal surfaces (1). This is used in one of the most common methods to perform asymmetric heterogeneous catalysis. The chiral modifier provides stereoselection through non-covalent assembly with a substrate, forming isolated complexes with well-defined geometries. We will present a variable temperature STM study of individual bimolecular complexes formed by enantiopure 1-(1-naphthyl)ethylamine and three representative prochiral substrates on Pt(111). The results reveal sub-molecularly resolved and time-resolved stereospecific data for competing complexation geometries. Time-lapsed STM measurements of individual substrate molecules sampling a set of interaction geometries provide new insight on the dynamics of stereocontrol. The results reveal that a single prochiral substrate can probe various sites on the surface due to diffusion and prochiral switching. This shows the importance of considering interconversion between complexation geometries to fully understand the stereocontrol operated by the chiral modifier. The results will be discussed in the context of proposed mechanisms for enantioselective hydrogenation.

5:20pm SS+AS+EN-TuA10 Density Functional Theory Study of CO Assisted Water Dissociation, *Liney Arnadottir, L. Halberstadt*, Oregon State University
Previous computational studies of methanol oxidation reaction intermediates (H-C=O and C-OH) have shown significant effects of water on both adsorbate adsorption energy as well as activation energies of interconversion between the two. On a clean Pt(111) surface the

interconversion between the two forms goes through a very stable COads and Hads intermediates and the activation barriers of CO + H to from HCO or COH are high or 1.3 and 1.8 eV respectively. In the presence of a single coadsorbed water molecule the activation barrier for this interconversion from HCO to COH was found to be much lower or 0.62 eV. These studies were motivated by experimental studies of methanol oxidation on Pt which found CO_2 formation at potentials lower then typically required for CO oxidation. Here we investigate Pt-water interactions and the effects of co-adsorbate CO on water dissociation as a possible CO assisted water dissection as an alternative reaction pathway on Pt surfaces.

6:00pm SS+AS+EN-TuA12 Crystalline Growth of Ice - Studying the Transition from the First Wetting Layer to Multilayers with Scanning Tunneling Microscopy, *Barbara Lechner, S. Maier, M.B. Salmeron*, Lawrence Berkeley National Laboratory

The growth of water layers on model substrates has been studied intensively, yet many questions still remain [1,2]. After many years of research, the structure of the first wetting layer on metal surfaces has been determined in comprehensive experimental and theoretical studies [3-5]. A surprisingly complex behavior was revealed, showing that the strain caused by the mismatch of the hexagonal planes in the ice crystal structure and the lattice of the substrate is released by forming structures that include rotated hexagons, pentagons and heptagons of molecules, in addition to strongly bound hexagonal rings commensurate with the substrate. A range of experimental and theoretical investigations showed that, on many substrates, the water monolayer does not expose any dangling hydrogen bonds as all water molecules adsorb either flat-lying or with a hydrogen atom pointing towards the surface [1,6]. Growth of multilayer water films that preserve the "down-pointing" average dipole orientation of water has been proposed to occur in some cases, resulting in the formation of "ferroelectric ice" [7]. However, the growth of the entropically more favorable, proton-disordered ice requires flipping some of the molecules in the first layer to expose dangling hydrogen bonds. Such molecular reorientation may be kinetically hindered, and has been invoked to be the reason for the hydrophobic character of many water monolayer films at low temperatures [6].

Here, we present high-resolution scanning tunneling microscopy (STM) measurements of water layers adsorbed on Pt(111) and Ru(0001) to study the transition from the first layer to multilayers. We observe that a second water layer initially grows in an amorphous structure when grown on the crystalline monolayer containing pentagons, hexagons and heptagons of water molecules. To facilitate the growth of ice in a bulk-like hexagonal arrangement, the first wetting layer needs to rearrange into a hexagonal structure commensurate with the surface.

[1] Hodgson, A.; Haq, S. *Surf. Sci. Rep.*2009, *64*, 381–451.

[2] Carrasco, J.; Hodgson, A.; Michaelides, A. *Nat. Mater.*2012, *11*, 667–674.

[3] Maier, S.; Stass, I.; Cerdá, J. I.; Salmeron, M. *Phys. Rev. Lett.*2014, *112*, 126101.

[4] Tatarkhanov, M.; Ogletree, D. F.; Rose, F.; Mitsui, T.; Fomin, E.; Maier, S.; Rose, M.; Cerdá, J. I. *J. Am. Chem. Soc.*2009, *131*, 18425–18434.

[5] Nie, S.; Feibelman, P. J.; Bartelt, N. C.; Thürmer, K. *Phys. Rev. Lett.*2010, *105*, 026102.

[6] Kimmel, G. A.; Petrik, N. G.; Dohnálek, Z.; Kay, B. D.; Kimmel, G. A.; Petrik, N. G.; Dohnálek, Z.; Kay, B. D. *J. Chem. Phys.*2007, *126*, 114702.

[7] Su, X.; Lianos, L.; Shen, Y. R.; Somorjai, G. A. 1998, 1533–1536.

Surface Science
Room: 112 - Session SS+EN-TuA

Photocatalysis, Photochemistry, and Chirality at Surfaces

Moderator: Arthur Utz, Tufts University

2:20pm SS+EN-TuA1 Photoemission of Electron from Diamond Into Water: Enabling Novel Electrochemical Reduction Reactions, *Robert Hamers, D. Zhu, L.H. Zhang,* University of Wisconsin-Madison*, J. Bandy,* University of Wisconsin-Madson*, G.M. Nathanson, J.R. Schmidt,* University of Wisconsin-Madison

Diamond's unusual property of negative electron affinity has long been used to enhance electron emission in vacuum. Recently we have demonstrated that diamond's facile electron emission properties can also be extended to solid-liquid interfaces. Electron photoemitted from diamond into water lead to formation of solvated electrons, widely regarded as the chemist's perfect reducing agent. We demonstrate the inexpensive diamond thin films and diamond powder can be used as solid-state sources of electrons able to induce the reduction of N2 to NH3 and the selective reduction of CO2 to CO. In this talk we will discuss the factors that influence electron emission into liquids, differences from emission into vacuum, and how electrons emitted into liquids can induce novel reduced chemistry not possible with traditional photocatalysts.

2:40pm SS+EN-TuA2 STM Tip-Induced Desorption of TMAA from TiO2(110): Model Study of a Photocatalytic Process, *Denis Potapenko, R.M. Osgood, Jr.*, Columbia University

Titanium oxide is a versatile photocatalytic material with numerous applications in the areas related to utilization of solar energy. Scanning Tunneling Microscopy (STM) allows explorations on the single molecule basis thus providing important insight into the physical phenomena involved in photocatalysis. Our experiments examine the tip-induced chemistry of trimethyl acetic acid (TMAA) molecules adsorbed on TiO2 rutile(110) surface;this systems was chosen as a model for light-driven catalysis since it is easily imaged with STM and since this system has been the subject of many earlier studies of photo and thermal chemistry. In present work we study the electrical hole-driven desorption of TMAA molecules, initiated by the charges, injected from the STM tip. Different values of the flux and the energy of the excitation charges were achieved by the simultaneous control of the setpoint current and the bias voltage of the STM tunneling junction. The dynamics of the tip-induced desorption of TMAA was compared with the photo-induced dynamics of the same reaction. In the latter experiments the monochromated light from a UV lamp was used as the source of excitation. We show that there is a threshold energy for a hot hole below the edge of the TiO_2 valence band that is required for TMAA photo-desorption.

3:00pm SS+EN-TuA3 Ultrafast Time-resolved Photoelectron Spectroscopy of Photocatalytic Surfaces, *Hrvoje Petek, S. Tan, A. Argondizzo*, University of Pittsburgh   **INVITED**

We investigate the ultrafast optical excitation and electron relaxation pathways for the clean and molecule covered rutile TiO2(110) surface. Using high power, broadly tunable (2.9-4.6 eV), 20 fs noncollinear parametric amplifier excitation source, we perform multiphoton photoemission (mPP) spectroscopy of TiO_2 surface. The energy, momentum, and pump-probe delay time resolved mPP spectra provide information on the occupied and unoccupied density of states that participate in photoemission from the valence band or the Ti-3d defect states on reduced TiO_2 surfaces. We find a new bulk transition between the Ti-3d bands of t_{2g} and e_g symmetry, which dominates the photoemission process form the Ti-3d defect states below the conduction band minimum of TiO_2.[1] The 3D mPP spectra provide information on the phase and energy relaxation of photoexcited electrons and holes.[2] Adsorption of molecules introduces adsorbate-induced resonances,[3,4] which can be excited by charge transfer excitation from the Ti-3d defect states. Metal nanoparticles grown on TiO_2 also open new photoemission pathways. We map out the energy and momentum distributions of the adsorbate and nanoparticle resonances as well as their relaxation dynamics.

1. Argondizzo, A.; Cui, X.; Wang, C.; Sun, H.; Shang, H.; Zhao, J.; Petek, H., Ultrafast multiphoton pump-probe photoemission excitation pathways in rutile TiO2(110). *Phys. Rev. B***91**, 155429 (2015).

2. Cui, X.; Wang, C.; Argondizzo, A.; Garrett-Roe, S.; Gumhalter, B.; Petek, H., Transient excitons at metal surfaces. *Nat Phys***10**, 505 (2014).

3. Onda, K.; Li, B.; Zhao, J.; Jordan, K. D.; Yang, J.; Petek, H., Wet Electrons at the H2O/TiO2(110) Surface. *Science***308**, 1154 (2005).

4. Li, B.; Zhao, J.; Onda, K.; Jordan, K. D.; Yang, J.; Petek, H., Ultrafast interfacial proton-coupled electron transfer. *Science***311**, 1436 (2006).

4:20pm SS+EN-TuA7 Surface and Interface Properties of Photoelectrocatalysts for Solar Fuels, *Bruce Koel, C.X. Kronawitter, P. Zhao, Z. Chen*, Princeton University

Experiments using well-defined model catalysts under controlled conditions and utilizing a range of spectroscopic techniques for characterization of surface and interface properties and the nature and reactivity of surface-bound species can greatly advance understanding of the structure and reactivity of photoelectrocatalysts for solar fuels. We report on several of our recent studies, which include investigations of the effects of dopant incorporation on the structural and chemical properties of the α-Fe2O3(0001) surface for water oxidation catalysis, facet-dependent activity and stability of Co3O4 nanocrystals towards OER, and the interaction of water with GaP(110), a semiconductor that is known to enable selective CO_2 reduction to methanol in aqueous solutions of CO_2 and nitrogen-containing heteroaromatics. For water oxidation on α-Fe2O3, we found that Ni doping in thin films of model catalysts caused a new termination for the

films and induced formation of more stable surface-bound OH groups. For the Co_3O_4 system, we used the well-defined morphologies of nanocubes and nanooctahedra to demonstrate that the (111) surfaces vastly out-perform the (100) surfaces for OER activity (overpotential and current density). Finally we have spectroscopically identified *in situ* the surface-bound species on GaP(110) associated with exposure to water using ambient pressure photoelectron spectroscopy (APPES). These observations on model systems afford further analysis and discussion of the role of surface-bound species in mechanisms for catalyzed water oxidation and CO_2 reduction.

4:40pm SS+EN-TuA8 Improving Hematite-Based Solar Water Splitting by Surface Modification with Sn, Ti, and FeOOH, *Anjli Patel, A.J. Abel*, Drexel University, *I. Garcia-Torregrosa*, Utrecht University, Netherlands, *B. Opasanont, J.B. Baxter*, Drexel University

Photoelectrochemical (PEC) water splitting with hematite (α-Fe_2O_3) photoanodes presents a promising route to sustainable energy production due to hematite's favorable bandgap, chemical stability, and widespread abundance. However, limitations arise from sluggish oxygen evolution reaction (OER) kinetics at the hematite-electrolyte interface, requiring a significant overpotential to induce photocatalysis. We report on the effects of Sn, Ti, and FeOOH surface treatments on hematite photoanodes to improve PEC performance by overcoming surface kinetic limitations. Thin film hematite photoanodes were fabricated by successive ionic layer adsorption and reaction (SILAR) of FeOOH on F:SnO_2–coated glass substrates, followed by annealing at 450 C to induce phase transition of FeOOH into hematite. Subsequent annealing at 775 C caused diffusion of Sn from the F:SnO_2 substrate through the hematite, resulting in 0.5at% Sn concentration at the photoanode surface. Current-voltage testing revealed that the presence of Sn in the hematite film significantly reduced the photocurrent onset potential, suggesting improved hole injection efficiency. Electrochemical impedance spectroscopy (EIS) revealed a reduction in the surface state charge transfer resistance ($R_{ct,ss}$) by 2 orders of magnitude, supporting the importance of interfacial kinetics. Hematite photoanodes doped with up to 10% Ti were also prepared by incorporating titanium into the SILAR deposition bath. Ti doping decreased the onset potential by 600 mV and significantly increased the plateau photocurrent density from 0.01 mA/cm^2 at 1.23 V vs. RHE for undoped hematite to nearly 0.6 mA/cm^2 for Ti-doped photoanodes. EIS showed that Ti-doping reduced the $R_{ct,ss}$ at applied potentials ranging from 0.8 to 1.6 V vs. RHE, indicating a possible catalytic effect on the OER reaction at the photoanode surface. FeOOH films were deposited on the hematite photoanodes by an additional SILAR step, which reduced the photocurrent onset potential and increased the plateau photocurrent density by 20%. Unlike Ti, the FeOOH surface treatment exhibited little to no effect on the $R_{ct,ss}$, suggesting that FeOOH does not directly catalyze the OER. However, both the FeOOH treatment and Ti doping significantly increased the peak surface state capacitance, which may be attributed to an increase in density of charged states at the hematite surface, resulting in higher plateau photocurrent. Together, these treatments yield photocurrents that are 3x larger than previous reports using SILAR-deposited planar hematite films, offering promising opportunities to overcome challenges in PEC water splitting with hematite photoanodes.

5:00pm SS+EN-TuA9 Metalation of a Polypyridine Macrocycle on Au(111): Preparation of a Water Reduction Catalyst on a Solid Substrate, *Gerson Mette, D. Sutter, S. Schnidrig, B. Probst, R. Alberto, J. Osterwalder*, Universität Zürich, Switzerland

Within the search for new materials and methods for renewable energy resources, photocatalytic water splitting is a very promising field of study. In this framework, a polypyridine macrocycle was investigated which was already described in 1984 but only superficially examined [1]. It shares some similarities to porphyrins but with pyridyl subunits instead of pyrrol, hence the given trivial name: *pyrphyrin*. A high stability of the pyrphyrin and corresponding complexes is indicated due to its conjugation, planarity and cyclic nature. Furthermore, metal complexes based on pyrphyrin show promise as water reduction catalysts.

In this study, we examined the preparation of a pyrphyrin metal complex on a single crystalline surface in ultrahigh vacuum. In a first step, pyrphyrin coverages of approximately one monolayer and less, as determined by XPS measurements, were obtained by sublimation of the molecules on a Au(111) surface at room-temperature. By means of Low-Energy Electron Diffraction (LEED) and Scanning Tunneling Microscopy (STM), two distinct phases depending on the surface coverage were identified and structurally characterized. In a second step, deposition of Co metal at the level of 5% of a monolayer and subsequent annealing led to the formation of an almost complete monolayer of Co-ligated pyrphyrin molecules.

[1] S. Ogawa et al., J. Am. Chem. Soc. **1984**, 106, 5760-5762.

5:20pm SS+EN-TuA10 Chiral Selective Chemistry Induced by Natural Selection of Spin-Polarized Electrons by DNA, *Richard Rosenberg*, Argonne National Laboratory, *D. Mishra, R. Naaman*, Weizmann Institute of Science, Israel

Most biomolecules can be synthesized in two different mirror-image (chiral) shapes, namely two enantiomers. The enantiomers are recognized by their ability to rotate the polarization of linear polarized light either to the left (L) or to the right (D). In bio-organisms, sugars are always D and amino acids are always L. How this enantiomeric preference originated remains a mystery. Investigations into possible avenues of prebiotic chiral selectivity have been pursued since the time of Pasteur. Many investigations in this area have been devoted to pathways that involve preferential destruction of a particular isomer in an initially racemic (equal quantities of both enantiomers) mixture, through the interactions of chiral particles such as circularly polarized UV radiation or longitudinally spin polarized electrons. It has been shown that low energy (0 – 10 eV) spin polarized secondary electrons, produced by irradiation of a magnetic substrate, can induce chiral-selective chemistry in an adsorbed adlayer.[1] Additional work has demonstrated that organized, double-stranded (ds) DNA, adsorbed on a gold substrate, acts as a natural spin filter for initially unpolarized, low energy (0 – 1.2 eV) electrons produced by UV irradiation of the substrate, resulting in net polarizations as high as 60%.[2] Experiment and theory indicates that this spin filtering effect should be effective for higher energy (E < 15 eV) electrons as well.[3] In the present study, we probe if low energy secondary electrons, produced by x-ray irradiation of a gold substrate, and transferred through the chiral monolayer, induce enantiomeric selective chemistry in an adsorbed adlayer. To test this, (R)- or (S)-epichloroydrin (C_3H_5ClO, Epi) was adsorbed on a self-assembled monolayer of 70 base pair long dsDNA. The secondary electron-induced reaction was monitored by following changes in the Cl 2p x-ray photoelectron spectroscopy spectra. By kinetic modeling of the reaction, quantum yields (QYs) were determined. For S-Epi the QY was ~16 % greater than for the (R) enantiomer, while the QYs were the same for the two enantiomers when they were adsorbed on bare Au.

[1] R. A. Rosenberg, M. Abu Haija, P. J. Ryan, Phys. Rev. Lett. **2008**, 101, 178301.

[2] a) B. Gohler, V. Hamelbeck, T. Z. Markus, M. Kettner, G. F. Hanne, Z. Vager, R. Naaman, H. Zacharias, Science **2011**, 331, 894-897; b) S. G. Ray, S. S. Daube, G. Leitus, Z. Vager, R. Naaman, Phys. Rev. Lett. **2006**, 96, 036101.

[3] R. A. Rosenberg, J. M. Symonds, V. Kalyanaraman, T. Markus, T. M. Orlando, R. Naaman, E. A. Medina, F. A. López, V. Mujica, J. Phys. Chem. C **2013**, 117, 22307-22313.

5:40pm SS+EN-TuA11 Creating Enantioselective Surfaces; Templating and One-to-one Interactions, *Wilfred Tysoe*, University of Wisconsin-Milwaukee

The mode of operation of heterogeneous chiral modifiers can be classified into those operating as templates, where several modifier molecules act in concert to define a chiral adsorption site, or one-to-one modifiers that form a docking complex between the modifier and a prochiral reactant.

Enantioselectivity is measured by adsorbing chiral probe molecules onto chirally modified surfaces. Templating is illustrated using aminoacids on Pd(111). Scanning tunneling microscopy (STM) reveals that some aminoacids form tetrameric units, and others form dimers. Only those aminoacids that form tetramers are enantioselective implying that the tetramers act as templates.

Naphthylethylamine (NEA) is proposed to acts as a one-to-one modifier. The interaction between NEA and a prochiral reactant, methyl pyruvate, is explored using STM. Possible docking complexes are identified using density functional theory and the simulated images are compared with experimental images. Finally, it is shown that tartaric acid on Pd(111) acts as a one-to-one modifier for glycidol and is controlled by hydrogen-bonding interactions.

6:00pm SS+EN-TuA12 Single-Molecule and Single-Active-Site Studies of Stereocontrol by Chemisorbed Chiral Molecules, *Peter McBreen, Y. Dong, J.C. Lemay, G. Goubert*, Laval University, Canada, *M.N. Groves, B. Hammer*, Aarhus University, Denmark

Isolated adsorbed chiral molecules can stereodirect prochiral co-adsorbates on reactive metal surfaces and the application of this phenomenon underpins a method to perform asymmetric heterogeneous catalytic reactions. Typically, the stereochemical action is attributed to intermolecular interactions in complexes formed by docking the prochiral substrate in a chiral pocket created by the chemisorbed chiral molecule. We will present results from combined variable temperature STM and optB88-vdW DFT studies of individual bimolecular docking complexes formed by enantipure 1-(1-naphthyl)ethylamine and selected prochiral molecules on

Pt(111). The experiments reveal sub-molecularly resolved and time-resolved site-specific and stereospecific data. The results show that a single chemisorbed enanantiomer simultaneously presents several chiral pockets, each displaying a specific prochiral ratio for a given substrate molecule. A hierarchy of metal-molecule and molecule-molecule interactions is found to control prochiral selection at each site. Time-lapsed STM measurements of individual substrate molecules sampling a set of chiral pockets provide new insight on the dynamics of stereocontrol.

Tuesday Evening Poster Sessions

Surface Science
Room: Hall 3 - Session SS-TuP

Surface Science Poster Session

SS-TuP1 Self-assembly and Thermally induced Conformational Changes of Ni(II)-*meso*-tetrakis (4-tert-butylphenyl) benzoporphyrin on Cu(111) Studied by STM, *Michael Lepper*, *M. Stark*, *L. Zhang*, FAU Erlangen-Nürnberg, *H.-P. Steinrück*, FAU Erlangen-Nürnberg, Germany, *H. Marbach*, FAU Erlangen-Nürnberg

A detailed scanning tunneling microscopy study of the self-assembly and thermally induced conformational changes of Ni(II)-meso-tetrakis (4-tert-butylphenyl) benzoporphyrin (Ni-TTBPBP) on Cu(111) will be presented. The coverage-dependent adsorption behavior at room temperature reveals that Ni-TTBPBP molecules can easily diffuse on the surface and self-assemble into islands with square order and a certain registry to the substrate.[1] The role of molecule-molecule and molecule-substrate interactions for the formation of the well-ordered supramolecular structure will be discussed. Interestingly, upon moderate heating two successive, irreversible intramolecular conformational changes are observed. This is explained comprehensively by a thermally induced dehydrogenative, intramolecular aryl-aryl coupling reaction. In addition this intramolecular structural change is coverage dependent, exhibiting a lower rate at higher initial coverage. This modification and the overall adsorption behavior of Ni-TTBPBP on Cu(111) will be discussed and compared to the very different behavior of the similar Ni(II)-tetraphenylbenzoporphyrin on the same substrate.

1. L. Zhang, M. Lepper, M. Stark, D. Lungerich, N. Jux, W. Hieringer, H.-P. Steinrück and H. Marbach, Phys. Chem. Chem. Phys., 2015, DOI: 10.1039/C5CP01490E.

SS-TuP3 Characterization of Pt-Re Bimetallic Clusters on TiO$_2$(110), *Randima Galhenage*, *K. Xie*, University of South Carolina, *H. Yan*, Brookhaven National Laboratory, *G. Seuser*, *D.A. Chen*, University of South Carolina

The study of metal clusters on single-crystal oxide supports as model systems has garnered much attention for fundamental investigations of catalytically active surfaces that can guide the rational design of new catalysts. For instance, Pt-based catalysts have been recently proposed for the aqueous phase reforming of alcohols but suffer from a lack of stability due to poisoning by CO and other carbonaceous species. The addition of a second metal, such as Re, to Pt has been shown to increase the stability and the activity of the catalyst, but the exact reason behind this enhanced activity is not well understood. To better understand this bimetallic system, we have prepared model catalysts consisting of bimetallic Pt-Re clusters on TiO$_2$ to investigate the growth of metals, metal-metal interactions, metal-support interactions and activity using Scanning Tunneling Microscopy (STM), X-ray Photoelectron Spectroscopy (XPS), Low Energy Ion Scattering Spectroscopy (LEIS) and Temperature Programmed Desorption (TPD). Re shows strong metal support interactions (SMSI) even at room temperature, resulting in highly dispersed 2D clusters. Encapsulation of Re by TiO$_x$ was observed due to SMSI effects. Pt-Re bimetallic clusters were prepared by depositing the less mobile Re first followed by deposition of Pt for submonolayer coverages. The surface composition of the bimetallic clusters was Pt-rich due to the lower surface free energy of Pt and the oxophillic nature of Re. CO adsorption behavior of the bimetallic clusters resembled the activity of pure Pt. At higher coverages (3.7 ML total metal coverage) bimetallic clusters were formed by both orders of deposition, Re on Pt and Pt on Re. When Re was deposited first, it resulted in a higher nucleation density for the bimetallic clusters with 100% Pt at the surface, and the activity resembled that of pure Pt. When Pt was deposited first, the initial seed cluster density was low, resulting in a lower density of bimetallic clusters, which led to a smaller number of active sites. In this order of deposition, the surface composition was a mixture of Pt and Re, and the activity studies suggest that both Pt and Re are active sites for the adsorption of CO. Pt-Re interactions were observed when Pt was deposited on titania followed by the deposition of Re.

SS-TuP4 Growth of Polymer Nanoparticles by Vapor Phase Polymerization onto Liquid Substrates, *Robert Frank-Finney*, *P. Haller*, *M. Gupta*, University of Southern California

The vapor phase deposition of polymers onto liquid substrates can result in the formation of polymer films or particles at the liquid–vapor interface. The initial polymer morphology at the interface is determined by the surface tension interaction between the liquid and polymer. Polymer particles form when it is energetically favorable for the polymer to aggregate rather than spread over the surface of the liquid as characterized by a spreading coefficient. The particles that are formed on the surface either remain partially protruding from the surface or submerge below the surface based on the engulfment energy of the polymer-liquid interaction. We systematically study the effects of deposition time, molecular weight, polymer accumulation, and liquid viscosity on the particle size and distribution to determine the mechanism of growth. Our results provide a fundamental understanding about polymer growth at the liquid–vapor interface that can be used to tailor the reaction conditions to produce particles of a desired size and improve upon the size distribution and can even offer insight into the growth of other materials on liquid surfaces. Vapor phase deposition onto liquid substrates is a rapid, one-step synthetic approach for fabricating functional polymer nanoparticles without the use of surfactants or volatile solvents.

SS-TuP6 Efficiency Improvement of Cu$_2$O/NiO/TiO$_2$ Solar Cells Prepared by Reactive Magnetron Sputtering, *Tomokazu Tsuchiya*, *I. Takano*, Kogakuin University, Japan

As one solution to the power shortage and global warming, a renewable energy such as solar cells is desired. Furthermore the high purity silicon that is the main raw material for solar cells is insufficient worldwide, and so new solar cells without silicon that are able to be replaced to silicon-based solar cells have been required. Practical application of oxide-based thin film solar cells is expected in reduction of the energy cost or the environmental load.

Generally a typical oxide-based thin film solar cell is a wet dye-sensitized solar cell composed of an electrolyte, an electrode of a titanium oxide and a sensitizing dye. Recently a solid-state dye-sensitized solar cell which uses metal oxides instead of an electrolyte has been studied. In our previous study on TiO$_2$/Cu$_2$O solid-state dye-sensitized solar cells, the main problem was Cu diffusion from the under layer Cu$_2$O. The diffusion of Cu to a titanium oxide layer induced the collapse of p-n junction.

The NiO thin film is used as a transparent oxide semiconductor. Most of the transparent oxide semiconductors are an n-type semiconductor, while NiO is a p-type semiconductor. In this study, we used NiO as a barrier layer between TiO$_2$ and Cu$_2$O for preventing the diffusion of Cu, and we investigated the characteristics of Cu$_2$O/NiO/TiO$_2$ solar cells.

Cu$_2$O/NiO/TiO$_2$ solar cells were fabricated by reactive magnetron sputtering. As substrates, the glass (Corning#1737) and an ITO-film coated glass were ultrasonically cleaned by acetone. The NiO thin film was deposited on those substrates by using pure metallic nickel (99.99%) as a sputtering target material in an oxygen gas atmosphere. The flow rate of an argon gas for sputtering was 20 sccm. The flow rate of an oxygen gas was 2.7 sccm. A thickness of the NiO layer was changed from 2 nm to 50 nm. On the other hand the fundamental preparations of the Cu$_2$O layer and the TiO$_2$ layer were performed by 200 nm in a thickness through 15 sccm and 20 sccm in an argon gas, and 10 sccm and 2.3 sccm in an oxygen gas, respectively.

Cu$_2$O/NiO/TiO$_2$ solar cells were successfully fabricated by reactive magnetron sputtering. The solar cell with the NiO layer of 4 nm thickness showed the maximum conversion efficiency of 5.6×10^{-3} % which was 9 times compared with the sample without the NiO layer.

SS-TuP7 Electrical Conductivity Control of Metal Doped DLC Films Prepared by N$_2^+$ Ion Beam Assistance, *Tsuyoshi Inoue*, *I. Takano*, Kogakuin University, Japan

DLC is amorphous carbon that contains a significant fraction of sp^2 and sp^3 bonds. It is known that their films show a low friction coefficient and are applied in a mechanical field such as cutting tools or frictional parts. DLC films were formed by the ion beam evaporation method in the early 1970's, and after that have been manufactured by various methods. In our experiment N$_2^+$ ion beam was used with metal evaporation to deposit metal doped DLC films. This deposition method has some independent parameters from the film formation condition in comparison with other dry process methods. Therefore this method is anticipated in appearance of superior characteristics such as a high adhesion. In our previous research, DLC thin films have been prepared by the N$_2^+$ ion beam assistance in a hydrocarbon gas. Their results showed that the films contained nitrogen of 8 % and mechanical properties were improved in hardness, friction and abrasion. On the other hand the electrical conductivity of metal doped DLC films prepared by this method is not clear.

In this study, the control of the electrical conductivity of DLC thin films was performed by the metal dope. Stainless steels (304SS) and slide glasses were used for sample substrates. The formation conditions of metal doped DLC films were changed with a metal evaporation rate from 0.01 nm/s to

0.05 nm/s and were an ultimate pressure of 6×10^{-4} Pa, an N_2 gas pressure of 4×10^{-3} Pa, a $C_7H_8+N_2$ gas pressure of 2×10^{-2} Pa in an ambient atmosphere. The ion beam irradiation was performed with 12 kV in an accelerating voltage and 5 μA/cm² in a current density, through an exposure time of 3600 s. The electrical conductivity and friction coefficient were determined by the four probe method and the tribotester of a ball-on-disk type, respectively. The tribotester was set with the conditions of an SUJ2 ball as a counter material and a constant load of 0.19 N until a sliding distance of 100 m.

The suitable electrical conductivity and mechanical property of the Ti or Cu doped DLC films were obtained by a Ti evaporation rate of 0.03 nm/s and a Cu evaporation rate of 0.05 nm/s respectively. The friction coefficient of Ti or Cu metal doped DLC films was about 0.24 - 0.23 at a distance of 100m. The electrical conductivity was 1.4×10^5 S/m in Ti doping and 5.17×10^6 S/m in Cu doping in comparison with the typical DLC film showing 1.0×10^{-7} S/m.

SS-TuP8 NEXAFS Studies of N_2O-N_2 Conversion on Reduced Ceria Surface, *Alexei Nefedov, C. Yang, F. Bebensee, C. Wöll*, Karlsruhe Institute of Technology, Germany

Ceria, one of the most reducible metal oxides, has proven to be a highly active catalyst for NO_x reduction to N_2. Here, we use synchrotron based photoemission spectroscopy (PES) and near edge X-ray absorption fine structure spectroscopy (NEXAFS) to monitor the conversion of N_2O to N_2 over reduced ceria surfaces ($N_2O + CeO_{2-x} \rightarrow N_2 + CeO_2$) in a time-resolved fashion. This enables us to determine the kinetics of this process.

The NEXAFS and PES measurements were carried out using the HE-SGM beamline at the synchrotron facility BESSY II operated by the Helmholtz-Zentrum Berlin. The clean and stoichiometric CeO_2(111) single crystal was annealed at 800 K for 15 min in vacuum to create surface oxygen vacancies prior to exposure to N_2O, whereas ceria powders were annealed at 1000 K for 30 min. Exposure to 50 Langmuir N_2O at sample temperatures typically below 120 K was achieved by backfilling the analysis chamber up to 10^{-9} mbar before NEXAFS spectra acquisition. The NEXAFS spectra were recorded in the partial electron yield mode for the π* resonance region of N K absorption edge. The Ce oxidation state was judged by PES before and after N_2O exposure.

In the NEXAFS spectra, two intense resonances (401.2 eV and 404.8 eV) are observed. The resonances are assigned to the transition from the 1s orbital into the lowest unoccupied molecular orbital (3π*) of the terminal and central nitrogen atom of N_2O, respectively. In agreement with previous experimental spectra for N_2O on CeO_2(111) thin films, both resonances exhibit equal intensity. Theoretical calculations for thin films indicate that N_2O is adsorbed with the oxygen-end towards a cation on the surface also on the CeO_2 single crystal. Moreover, these two resonances decrease in parallel over time and one may speculate at this point that the decrease is caused by conversion of N_2O to N_2 over reduced CeO_2(111). The difference in valence band photoemission spectra measured before and after the introduction of 50 Langmuir N_2O clearly demonstrate that the initial reduced CeO_2(111) surface is re-oxidized to some extent and thus confirms the speculation above that N_2O can interact with oxygen vacancies resulting in vacancy healing.

Annealing can easily reduce ceria, while N_2O can heal the oxygen vacancies on the reduced ceria surface, giving rise to a complete catalytic cycle. The first set of data on N_2O adsorption and reaction over ceria surface suggest the feasibility of the study of the conversion of N_2O to N_2 by using PES and NEXAFS, which gives us a chance to determine the kinetics of this reaction.

SS-TuP9 Photocatalytic Properties of TiO_2/NiO/Cu_2O Thin Films Prepared by Reactive Magnetron Sputtering, *Toshiya Souma, I. Takano*, Kogakuin University, Japan

In recent years, various characteristics of TiO_2 have attracted considerable attention. One of their characteristics is a photocatalytic effect. The photocatalytic effect of TiO_2 shows antifouling or antimicrobial activity, and has the ability to decompose environmental pollutants. Thus TiO_2 has superior characteristics in many metal oxides, because its photo-excited state is very stable and does not cause self-decomposition. Therefore, TiO_2 can perform the electrolysis of water by light, however, a light reaction region of TiO_2 is limited within the ultraviolet region corresponded with only about 3 % of sunlight.

In this study, to improve the photocatalytic property of TiO_2 the TiO_2/NiO/Cu_2O thin films were fabricated by laminating the TiO_2 layer with 3.0 - 3.2 eV and the Cu_2O layer with 2.2 eV in a band gap energy. In order to prevent the diffusion of Cu, the NiO layer was inserted between the TiO_2 layer and the Cu_2O layer. NiO has a high melting point, high hardness and has been used as a barrier layer. These three layers were prepared by reactive magnetron sputtering.

The film composition and microstructure were investigated by X-ray photoelectron spectroscopy and X-ray diffraction, respectively. Chromatic changes of a methylene blue solution were applied to the measurement of a photocatalytic property. Light irradiation to the TiO_2/NiO/Cu_2O thin films in a methylene blue solution was carried out using a commercial sterilizing lamp as ultraviolet light and an artificial sun lamp as visible light. Transmittance of a methylene blue solution was measured by a spectrophotometer.

On the XRD measurement for the crystal structure of TiO_2/NiO/Cu_2O thin films, the strong peaks of the anatase-rutile mixture from TiO_2 of the upper layer and the weak peaks of Cu_2O or NiO from the lower layer appeared. It was estimated that the diffusion of Cu from the Cu_2O layer was prevented by inserting the NiO layer. The suitable photocatalytic effect was obtained by inserting the NiO layer of 20 nm in a thickness and then the decomposition activity of a methylene blue solution showed about 57 % under an artificial sun light and about 77 % under a sterilization light. In the case of TiO_2/NiO/Cu_2O thin films, it was considered that the role of the NiO layer was not only the protection of the diffusion but also the electric effect as a p-type semiconductor.

2D Materials Focus Topic
Room: 212C - Session 2D+MN+NS+SP+SS+TF-WeM

Mechanical and Thermal Properties of 2D Materials
Moderator: Oleg Yazev, Ecole Polytechnique Fédérale de Lausanne (EPFL), Petra Reinke, University of Virginia

8:00am **2D+MN+NS+SP+SS+TF-WeM1 Mechanical Properties of Polycrystalline Graphene**, *Joseph Gonzales,* University of South Florida, *R. Perriot,* Los Alamos National Laboratory, *I.I. Oleynik,* University of South Florida
Experimental investigation of mechanical properties indicates that the polycrystalline graphene grown by chemical vapor deposition is as strong as pristine. The microscopic characterization of graphene samples using Atomic Force microscopy (AFM) nano-indentation is limited in the sense that the detailed mechanical characteristics such as stress and stain distributions under the indenter, elastic moduli and breaking strength are not available directly from experiment. Using accurate description of interatomic interactions provided by novel screened environment-dependent bond order, (SED-REBO) potential, we performed large-scale molecular dynamics investigations of mechanical properties of polycrystalline graphene under conditions mimicking nano-indentation AFM experiments. The atomically resolved characterization of the stress and strain distributions under indenter are used to understand detailed mechanisms of graphene strength and failure. The breaking strength, the crack initiation and propagation are investigated as a function of the grain boundary structure and the grain size distribution as well as the position of the indenter – at the center of the grain, at the a single grain boundary and at the junction of three or more grain boundaries.

8:40am **2D+MN+NS+SP+SS+TF-WeM3 Lévy Flights Found in Freestanding Graphene**, *Paul Thibado,* University of Arkansas, *M. Neek-Amal, F. Peeters,* University of Antwerp, Belgium
Local, long-time evolution measurements of the height fluctuations of a 2D membrane allows examination of the fundamental foundations of statistical mechanics in soft condensed matter. However, such measurements have proved elusive, thereby forcing critical theoretical assumptions in the best models. We report sub-nanometer, high-bandwidth height measurements of freestanding graphene using constant-current, point-mode scanning tunneling microscopy, as a follow-up to our previous related works [1-2]. By tracking atoms directly, the ability to measure dynamic events is increased by a factor of 1000 over the present state-of-the-art membrane imaging technology. Surprisingly, the membrane velocities follow the Cauchy-Lorentz distribution consistent with a Lévy process, rather than the expected Maxwell-Boltzmann distribution. We introduce a new theoretical approach using fractional-stochastic calculus.

Acknowledgements:

References:

[1] P. Xu, M. Neek-Amal, S.D. Barber, J.K. Schoelz, M.L. Ackerman, P.M. Thibado, A. Sadeghi, and F.M. Peeters, Nature Comm. **5**, 3720 (2014).

[2] M. Neek-Amal, P. Xu, J.K. Schoelz, M.L. Ackerman, S.D. Barber, P.M. Thibado, A. Sadeghi, and F.M. Peeters, Nature Comm. **5**, 4962 (2014).

9:00am **2D+MN+NS+SP+SS+TF-WeM4 Multilayer Graphene Strength Characterization**, *Joseph Rowley,* N. Boyer, K. Berry, R.C. Davis, Brigham Young University, *R. Creighton, J. Abbott, S. Cornaby, M. Harker,* Moxtek Inc., *R. Vanfleet,* Brigham Young University
Although there are many examples in the literature of multilayer graphene fabrication and electrical characterization, there is a lack of data on the mechanical properties of multilayer graphene, especially many layer. Conversely there is data about the mechanical properties of single layer graphene, and limited information about bilayer and few layer, but little about many layer. Multilayer Graphene was fabricated using chemical vapor deposition on a Nickel catalyst. Different flow rates and cooling rates were investigated to produce many layer films. Due to the high strength in graphene, these films were able to be suspended over millimeter size openings and have a differential pressure applied. This allowed for the characterization of the strength of these membranes using bulge testing.

9:20am **2D+MN+NS+SP+SS+TF-WeM5 Nanoelectromechanical Systems Based on 2D Materials beyond Graphene -- Effects from Geometry, Nonlinearity, and Anisotropy**, *Zenghui Wang,* Case Western Reserve University **INVITED**
Investigating and manipulating the mechanical degree of freedom in two-dimensional (2D) nanostructures present unique challenges and opportunities: such effort demands advanced fabrication and measurement schemes, and offers new insight into the physical properties of 2D materials. I will present our explorations and findings in mechanical processes at the nanoscale, through studying resonant nanoelectromechanical systems (NEMS) based on 2D materials beyond graphene (*e.g.,* molybdenum disulfide, black phosphorus, etc.). I will discuss the implications of geometrical irregularities on the nanomechanical responses of 2D-material-based resonators; impacts of device and material parameters on the mechanical nonlinearity and motional noise in 2D resonant transducers; and effects of material anisotropy in nanomechanical resonators based on new types of highly anisotropic 2D materials. These findings open new pathways towards nanomechanical coupling and tuning of the physical properties in 2D nanomaterials, and offer opportunities for building novel devices with new multimode functions.

11:00am **2D+MN+NS+SP+SS+TF-WeM10 Phonon Spectroscopy of Graphene Field Effect Devices with the STM**, *Fabian Natterer,* Y. Zhao, J. Wyrick, NIST/CNST, *W.Y. Ruan, Y.-H.C. Chan, M.-Y.C. Chou,* Georgia Institute of Technology, *N.B. Zhitenev, J.A. Stroscio,* NIST/CNST
Phonon spectroscopy of graphene by inelastic electron tunneling spectroscopy with the STM has been elusive in previous measurements [1–3]. The difficulty lies within the weak phonon signatures that are buried by other dominant spectral features that inhibit a clear distinction between phonons and miscellaneous excitations. Utilizing a back gated graphene device that permits continuous adjustment of the global charge carrier density, we employ an averaging method where individual tunneling spectra at varying charge carrier density are condensed into one representative spectrum [4]. This method improves the signal for inelastic transitions that appear at constant threshold, while it broadens and thereby suppresses dispersive spectral features. We use this method to demonstrate the mapping of the total graphene phonon density of states, in good agreement with density functional calculations. Using the knowledge about the phonons thusly obtained, we closely examine our gate resolved spectra and observe a surprising and abrupt change in the phonon intensity when the graphene charge carrier type is switched through a variation of the back gate electrode potential. This sudden variation in phonon intensity is asymmetric in carrier type, depending on the sign of the tunneling bias. We invoke a resonance mediated tunneling process that relies on the presence of tip-induced quasi-bound state resonances in graphene, resembling whispering gallery modes for electrons and holes [5]. Our tip-sample system thereby mimics a giant molecular state and shares analogies with resonant enhanced excitations of molecular vibrational or rotational modes [6–9].

[1] Y. Zhang, V. W. Brar, F. Wang, C. Girit, Y. Yayon, M. Panlasigui, A. Zettl, and M. F. Crommie, Nature Phys **4**, 627 (2008).

[2] V. W. Brar, S. Wickenburg, M. Panlasigui, C.-H. Park, T. O. Wehling, Y. Zhang, R. Decker, Ç. Girit, A. V. Balatsky, S. G. Louie, A. Zettl, and M. F. Crommie, Phys. Rev. Lett. **104**, 036805 (2010).

[3] G. Li, A. Luican, and E. Andrei, Phys. Rev. Lett. **102**, 176804 (2009).

[4] C. E. Malec and D. Davidović, Journal of Applied Physics **109**, 064507 (2011).

[5] Y. Zhao,, J. Wyrick, F. D. Natterer, J. F. Rodriguez-Nieva3, C. Lewandowski, K. Watanabe, T. Taniguchi, L. S. Levitov, N. B. Zhitenev, and J. A. Stroscio, Science **348**, 672 (2015).

[6] J. Gadzuk, Phys. Rev. B **31**, 6789 (1985).

[7] B. Persson and A. Baratoff, Phys. Rev. Lett. **59**, 339 (1987).

[8] A. Baratoff, Journal of Vacuum Science & Technology A: Vacuum, Surfaces, and Films **6**, 331 (1988).

[9] F. D. Natterer, F. Patthey, and H. Brune, ACS Nano **8**, 7099 (2014).

11:20am **2D+MN+NS+SP+SS+TF-WeM11 Edge-state-induced Stabilization of Dopants in Graphene**, *Yuuki Uchida,* A. Akaishi, J. Nakamura, The University of Electro-Communications (UEC-Tokyo) and JST CREST, Japan
Impurity doping is an efficient way to modify electronic properties of graphene. Several groups have reported the stability of dopants in graphene, especially near edges of graphene: Impurity atoms prefer to locate at the zigzag edge of graphene rather than the armchair one[1]. It has also been

reported that the electronic properties are strongly dependent upon the location of dopants, which is derrived from the non-equivalence of the two sublattice[2]. It is well-known that the edge-localized state emerges at the zigzag edge[3], which is specific for the so-called bipartite lattice. However, it has not been clarified yet how the edge-state affects the dopant stability depending on the sublattice. In this study, we investigate the role of the sublattice-dependent edge-state on the stabilization of impurities. We evaluate the dependence of the structural stability on the distance of impurity atoms from the zigzag edge using first-principles calculations within the density-functional theory. We have employed two types of graphene nanoribbons (GNRs) with the armchair- (AGNR) or the zigzag- (ZGNR) edge.

For AGNR, the formation energy of dopants does not change neither systematically nor monotonically as a function of the distance from the edge. On the other hand, for ZGNR, the formation energy is lower than that for AGNR and decreases with decreasing distance from the edge. In addition, two types of tendencies are confirmed for odd- and even-numbered sites from the zigzag edge, corresponding to the different sublattices of the bipartite lattice.

Such peculiar behavior as for of the formation energy can be explained as follows : The doped N atom donates its electron to the unoccupied-edge-state just above the Fermi level, resulting in the lowering of the one-electron energy of this state. The smaller the distance of N atoms from the zigzag edge is, the larger the electrostatic attraction between electrons of edge-localized states and positively-charged ion-shell at the N site becomes. Further, N atoms are much more stabilized at the odd-numbered site, because the edge-state has finite amplitude only at the odd-numbered sites.

[1] S. F. Huang et al., Phys. Rev. B. **80**, 235410 (2009)

[2] J. Jiang et al., J. Chem. Phys. **136**, 014702 (2012)

[3] M. Fujita et al., J. Phys. Soc. **65**, 1920 (1996)

11:40am 2D+MN+NS+SP+SS+TF-WeM12 Exploring the Thermal Stability of Two-Dimensional Black Phosphorus, *Xiaolong Liu, J.D. Wood, K.-S. Chen, E. Cho, M.C. Hersam,* Northwestern University
Two dimensional (2D) black phosphorus (BP) has attracted significant attention due to its superlative electronic and optical properties. Unlike graphene, its intrinsic and thickness-dependent band gap makes it feasible for direct application in electronic and optoelectronic devices.[1] However, before 2D BP can be effectively employed in such applications, it is necessary to establish the thermal stability of 2D BP since annealing is a key element in most device fabrication processes. Towards this end, we have utilized *in situ* scanning/transmission electron microscopy and spectroscopy methods to characterize the thermal decomposition process of mechanically exfoliated 2D BP.[2] The decomposition is observed to occur at ~400 °C in the form of sublimation, compared to the 550 °C of bulk BP. This decomposition initiates *via* eye-shaped cracks along the [001] direction and then continues until only a thin, amorphous red phosphorous-like skeleton remains. *In situ* electron energy loss spectroscopy, energy-dispersive X-ray spectroscopy, and energy-loss near-edge structure changes provide further quantitative insight into this chemical transformation process.

(1) Qiao, J.; Kong, X.; Hu, Z.-X.; Yang, F.; Ji, W. *Nature Comm.***2014**, *5*, 4475.

(2) Liu, X.; Wood, J. D.; Chen, K.-S.; Cho, E.; Hersam M. C. *J. Phys. Chem. Lett.***2015**, *6*, 773-778.

12:00pm 2D+MN+NS+SP+SS+TF-WeM13 Gas Permeation Through 1 nm Thick Carbon Nanomembranes, *A. Beyer, M. Ai,* Bielefeld University, Germany*, S. Shishatskiy, J. Wind,* Helmholtz-Zentrum Geesthacht, Germany*, X. Zhang, V. Chinaryan, Y. Yang,* **Armin Gölzhäuser**, Bielefeld University, Germany
The gas permeation characteristics of 1 nm thick carbon nanomembranes (CNMs) from self-assembled monolayers are reported. The assembly of CNMs onto polydimethylsiloxane (PDMS) support membranes allows determination of gas permeation characteristics. Single layer and triple layer CNMs were investigated in respect to permeation of hydrogen, helium, carbon dioxide, oxygen, nitrogen, argon, methane and ethane. In addition, the CNM-PDMS composites were characterized by X-ray photoelectron spectroscopy, helium-ion microscopy as well as atomic force microscopy. A careful analysis about the contribution of the PDMS support membranes to the gas permeation allowed an estimate of the intrinsic CNM permeances. These values indicate a molecular sieve-like property of CNMs which is attributed to molecular-sized channels in CNMs. As an example, hydrogen and carbon dioxide gas molecules display an order of magnitude higher permeance values for single layer CNMs in comparison to oxygen and nitrogen, which possess larger kinetic diameters.

In-Situ Spectroscopy and Microscopy Focus Topic
Room: 211C - Session IS+AS+SA+SS-WeM

In-situ Studies Using X-ray Absorption Spectroscopy and Vibrational Spectroscopy for Catalytic and Energy Materials
Moderator: Franklin (Feng) Tao, University of Kansas, Zili Wu, Oak Ridge National Laboratory

8:00am **IS+AS+SA+SS-WeM1** *In Situ* **X-ray Absorption Spectroscopy Technique for Metal/Water Interface Characterization**, *Chenghao Wu*,* University of California, Berkeley and Lawrence Berkeley National Laboratory*, J.-H. Guo, M.B. Salmeron,* Lawrence Berkeley National Laboratory
Most of the electrochemistry processes occur within the thin layer of electrolyte at the electrolyte/electrode interfaces, commonly denoted as the electrical double layer (EDL). Although some classic continuum theories about EDL have been established and widely accepted over the past century, very little experimental information is available regarding the molecular-level details at such solid/liquid interfaces. We have developed in-situ liquid cells to study such solid/liquid interfaces by means of soft x-ray absorption spectroscopy [1]. Because the fluorescence x-ray photon has much larger mean free path in condensed matters than the secondary electrons, by comparing the total fluorescence yield (TFY) and total electron yield (TEY) spectra, we can extract useful information about the compositional, structural or chemical difference between the bulk and the interfacial electrolyte. Under different bias, by modulating the incident x-ray, the TEY signal current becomes alternating and can be separated from the dominant faradaic current so that we can obtain surface-sensitive TEY signal under electrochemical conditions.

With this *in-situ* and *operando* XAS technique, we investigated the gold/water interface [1] and platinum/sulfuric acid solution interface. It was found that at gold/water interface, the interfacial water layer has significantly different hydrogen-bonding network structure compared to the bulk water. Under different bias, the polar water molecules respond to the external electrical field and reorient at the gold electrode surface, which significantly changes the amount of distorted or broken hydrogen bonds. First-principle simulations were able to corroborate the experimental results and qualitatively reproduce the change in the x-ray absorption spectra at different bias. In the platinum/sulfuric acid system, the charged solute species, such as SO_4^{2-} ions, hydronium ions, introduce extra complexity at the surface under different bias. Using the same *in-situ* technique, we were also able to identify some intermediate surface species in the potential window of OER reaction.

[1]. J.J. Velasco-Velez, C.H. Wu, T.A. Pascal, L.F. Wan, J.-H. Guo, D. Prendergast, and M. B. Salmeron, *Science*, **346**, 831-834 (2014).

8:20am **IS+AS+SA+SS-WeM2 Tip Enhanced Raman Spectroscopy (TERS) of Graphene Nano-Ribbons and Graphene on Au Surfaces: Imaging and Vibrational Spectroscopy of Surface Reaction Products**, *Delroy Baugh, S. Liu, T. Kumagai, M. Wolf,* Fritz-Haber-Institut der Max-Planck-Gesellschaft, Germany
Tip Enhanced Raman Spectroscopy (TERS) is currently one of the most powerful probe techniques available and could be used to study reactions on surfaces at the single molecule level. TERS combines two very well developed techniques scanning probe microscopy (SPM), used to image single molecules on surfaces, and surface enhanced Raman spectroscopy (SERS), used to characterize vibrational spectra also of single molecules on surfaces. TERS could therefore provide unique and heretofore unprecedented insight on adsorbate reactions at the single-molecule level, e.g., image a molecule while it evolves from reactant to product at well defined surface sites as well as monitor vibrational spectra to provide bond specific information about the reaction. However, in order to clarify the vibrational structure in TERS, the details of the enhancement mechanism and the issues regarding the plasmonic background that is almost always observed in TER spectra as well the "blinking" that occurs in the SERS part of TERS must be resolved. Towards this end here we will report studies of Graphene and Graphene Nanoribbons (GNR's) on Au surfaces as a model systems because their electronic and vibrational structure are clearly defined. Specifically, Near and Far-field Raman spectra will be reported for these systems and the above issues will be addressed experimentally and a simple theoretical model will be presented for the TERS observations.

---

* ASSD Student Award Finalist

8:40am IS+AS+SA+SS-WeM3 Isomerization of One Molecule Observed through Tip-Enhanced Raman Spectroscopy: Azobenzene Thiol on Au(111), *Joonhee Lee*, *N. Tallarida*, *L. Rios*, *V.A. Apkarian*, University of California, Irvine

The reversible *cis-trans* isomerization of a single azobenzene thiol (ABT) molecule is captured in tip-enhanced Raman trajectories in which the anti-correlated flip-flop between discrete, on and off-states of the two structural isomers is seen. The strongly blue-shifted spectra are recorded from a molecule that appears at the junction plasmon of a scanning tunneling microscope (STM), consisting of an atomically flat Au(111) surface and a silver tip. The variation in frequencies of switching events identifies heterogeneously photocatalyzed chemistry. The chemisorbed ensemble of ABT molecules lie flat on Au(111) surface with azobenzene headgroup strongly coupled to the surface. Nevertheless, we establish through STM imaging that the ABT molecules undergo both current driven and photoinduced *cis-trans* isomerization. Rather than decoupling from the surface, we suggest that strong coupling of the reaction coordinate to a vibrational energy sink is required for *cis-trans* isomerization of azobenzenes on metal surfaces.

9:00am IS+AS+SA+SS-WeM4 In Situ Characterization and Reaction Studies of MnO_x/Co_3O_4 Catalyst for CO and CO_2 Conversion, *Walter Ralston*, *G. Melaet*, University of California, Berkeley, *S. Alayoglu*, Lawrence Berkeley National Laboratory (LBNL), *G.A. Somorjai*, University of California, Berkeley

As the energy and fuel demands of our growing world continue to increase, non-fossil fuel carbon sources are increasingly attractive – especially if these carbon sources can be easily converted to transportable fuels and higher-value chemicals. Much attention has been focused on carbon dioxide, as capture and storage technology has emerged to mitigate emissions and CO_2 can be used to produce methanol.

Recently, we reported a catalyst for the low-pressure conversion of CO_2 to methanol[1]. Manganese oxide nanoparticles supported in mesoporous Co_3O_4 produced methanol in high yields and at significantly lower pressure conditions than typical Cu/ZnO catalysts used industrially. The advantage of this catalyst is in its lower pressure requirement, its high yield of methanol, and its evidence of carbon-carbon bond formation (10% ethylene production).

Catalytic testing of the material has shown the catalyst to be more than the sum of its parts; when each component is tested separately (MnO_x nanoparticles supported in SiO_2; mesoporous Co_3O_4 alone) CH_4 and CO are the major products. Preparation and testing of an inverse catalyst – CoO_x nanoparticles on a mesoporous MnO_2 support – proves the importance of the hybrid architecture in determining the selectivity of the catalyst, as the inverse catalyst is dominated by the selectivity of the support (>80% selective to CO).

Towards understanding this catalyst, in-situ X-ray Absorption Spectroscopy (XAS) utilizing both soft and hard x-ray energies has allowed for a detailed characterization of the catalyst under oxidation, reduction, and reaction conditions. In addition to CO_2, in-situ characterization under CO hydrogenation conditions was used to understand the Fischer-Tropsch activity of the catalyst for making longer chain hydrocarbons. The results of these in-situ studies are correlated with catalytic reaction data to help understand the nature of the active site/interface and guide future catalyst design.

References

(1) C. S. Li, G. Melaet, W. T. Ralston, *et al.* High-performance hybrid oxide catalyst of manganese and cobalt for low-pressure methanol synthesis. *Nature Communications,* 6:6538, **2015**.

9:20am IS+AS+SA+SS-WeM5 In Situ and Operando Raman Methodology to Understand the States of Oxide Catalysts and Alkane Oxidative Dehydrogenation and Ammoxidation Reactions, *Miguel A. Bañares*, Instituto de Catálisis y Petroleoquímica, Madrid **INVITED**

Operando methodology combines in situ spectroscopy during reaction with simultaneous performance measurement in a cell that behaves like a catalytic reactor. *Operando* methodology connects changes in the performance and in the structure in a simultaneous manner; this is fundamental to assess the structure-performance relationships at a molecular level.

Molecularly dispersed vanadia on oxide carriers is a key component in many catalytic formulations in environmental and selective oxidation and ammoxidation catalysis. The actual state of vanadia catalysts in specific environments depends on its surface density, the nature of the support and the presence of additives. We will summarize our experience on the state of supported vanadia paying particular attention to how the environment and reaction conditions finally shape the structure of vanadia catalysts. O*perando* Raman spectroscopy is an invaluable approach to fully

understand the actual state of the catalyst, its transformations during reaction and how these correlate with changes in catalytic performance.

A single technique, may no deliver the complete vista, thus collaboration with complementary talents and techniques is critical. We show the outcome of collaborations with theoretical chemistry approaches to bring the rationale behind structure-activity relationships inferred through *operando* Raman methodology. We also show the interaction with engineering approaches.

11:00am IS+AS+SA+SS-WeM10 Operando Studies of Dynamic Restructuring of Working Catalysts by Correlated Imaging and Spectroscopy Probes, *Anatoly Frenkel*, Yeshiva University **INVITED**

Understanding mechanisms of reactivity is often hindered by complexity of nanoscale supported metal catalysts. In the size range of 1-5nm, they feature a variety of structural motifs, sizes, shapes, compositions, degrees of crystalline order as well as multiple temporal scales. Hence, new experimental methodologies are called for, ones that are capable to capture not only the details of kinetic, dynamic and catalytic properties of metal clusters, but also their statistical distributions over ensemble of such clusters in a particular working catalyst, i.e., in reaction conditions. I will present our recent results obtained at the National Synchrotron Light Source, Advanced Light Source and Center for Functional Nanomaterials, where we combined x-ray absorption spectroscopy, high resolution transmission electron microscopy and micro-IR spectroscopy studies of a complex catalytic system *in operando*, using the same portable micro-reactor. This method will be illustrated on the example of supported Pt and Pd catalysts undergoing dynamic restructuring during ethylene hydrogenation reaction. Our results demonstrate a complexity of structures exhibited in this system and their dynamic, responsive transformations throughout changing reaction conditions. The new method is both general and generalizable to quantitative *operando* studies of complex material systems of broad interest to areas as diverse as catalysis science, applied physics and materials science, using a wide variety of x-ray and electron based experimental probes.

11:40am IS+AS+SA+SS-WeM12 A Correlation of Raman and Single and Multiple Layer Graphene Conductivity as Detected with a Cryogenic Multiprobe AFM with On-line Raman, NSOM and Other SPM Modalities, *Aaron Lewis*, The Hebrew University of Jerusalem and Nanonics Imaging Ltd, Israel, *O. Zinoviev*, *A. Komissar*, *E. Maayan*, *D. Lewis*, Nanonics Imaging Ltd, Jerusalem, Israel

It is a challenge to study 2D materials, such as Graphene, MoS_2, $WeSe_2$, etc. at temperatures down to 10^oK when one considers the wide variety of physical phenomena that have to be applied to get a full picture of the functionality of these materials. This involves questions of structure, nanometric photoconductivity, electrical properties, thermal properties, near-field optical in the apertured and scattering modes, Kelvin probe, and of course Raman. All of these phenomena are common not only to 2D materials but also to carbon nanotubes and related nanomaterials. This presentation will describe both the instrumental development of such a multiprobe cryogenic system that allows for state of the art on-line optical measurements and will also include a review of the probe developments that permit such multifunctional multiprobe operation with on-line full optical access. The system that will be described has a completely free optical axis from above and below that is not obscured by electrical or other probes that have been developed for this system for multiprobe operation. This permits on-line Raman and Tip Enhanced NanoRaman Scattering. With such a system we have investigated graphene and HfO2 using multiprobe electrical, Kelvin probe, NSOM and on-line Raman. The results have yielded new insights into the chemical changes that are correlated to the electrical conductivity.

12:00pm IS+AS+SA+SS-WeM13 Surface Structure and Chemistry of Rh(110)-1×2 Under Reaction Condition and During Catalysis explored with AP-XPS and HP-STM, *Franklin (Feng) Tao*, *L. Nguyen*, University of Kansas

High pressure scanning tunneling microscopy (HP-STM), ambient pressure X-ray photoelectron spectroscopy (AP-XPS), and computational studies were used to study the surface chemistry and structure of Rh(110)-1×2 and Rh(110)-1×1 at atomic scale in CO at different pressure and different temperature, and during CO oxidation at different pressure and different temperature. In gas of CO at a low pressure of 8×10^{-8} Torr, a Rh(110)-1×2 covered with CO is formed at 25C by replacing the adsorbed oxygen atoms adsorbed on Rh(110)-1×2 by CO molecules of gas phase. A pressure dependent structure of adsorbate layer of CO on Rh(110)-1×2 was revealed. In gas of CO at a high pressure of 0.08 Torr, the portion of CO molecules bound in atop configuration in the adsorbed layer increases along with the increase of pressure of CO gas though there is no restructuring of Rh(110)-1×2 at 25C in the pressure range of 8×10^{-8} to 0.8 Torr. This is supported by

the calculated coverage-dependent binding energy of CO on this surface. At a relatively high temperature of 55C, Rh(110)-1×2 in 0.08 Torr CO is restructured to Rh(110)-1×1 (Figure 1b). This temperature of surface restructuring is much lower than 153C for Rh(110)-1×2 in UHV. Theoretical simulation suggests that adsorbed CO molecules promote this restructuring compared to the restructuring in UHV since adsorption of CO on the intermediate structures of this restructuring in gas of CO lower the activation barrier of these intermediate structures. Rh(110)-1×2 is restructured to Rh(110)-1×1 during catalysis in the mixture of CO (0.08 Torr) and O_2 (0.02 Torr) even at 25C. Compared to the lack of restructuring in pure CO of 0.08 Torr at 25C, this restructuring during catalysis could result from a local heating of the catalyst surface by the exothermic reaction of CO oxidation. During CO oxidation, certain number of CO molecules are still remained on the catalyst surface. In the temperature range of 50-130C the active phase of catalysis is metallic Rh(110)-1×1. However, at 200C the active phase is surface rhodium oxide. These in-situ studies of surface structure and chemistry integrated with computational studies of Rh(110) in pure CO and in mixture of CO and O_2 clearly demonstrate the complexity of surface structure of a catalyst under reaction condition and during catalysis. The pressure-dependent structure of adsorbate layer, temperature-driven surface restructurings, generation of a new active surface phase of catalyst during catalysis, suggest the significance of in-situ studies of structure and chemistry of surface of a catalyst during catalysis.

Plasma Science and Technology
Room: 210A - Session PS+SS+TF-WeM

Atomic Layer Etching (ALE) and Low-Damage Processes I

Moderator: Geunyoung Yeom, Sungkyunkwan University, Republic of Korea

8:00am PS+SS+TF-WeM1 Atomic Layer Etching to Escape Process Tradeoffs for 7nm Technology and Beyond, *Alok Ranjan, M. Wang, S. Sherpa,* TEL Technology Center, America, LLC*, P. Ventzek,* Tokyo Electron America, Inc. **INVITED**
With shrinking critical dimensions, dry etch faces more and more challenges. Minimizing each of aspect ratio dependent etching (ARDE), bowing, undercut, selectivity, and within die uniformly across a wafer are met by trading off one requirement against another. The problem of trade-offs is especially critical for 10nm and beyond technology. At the root of the problem is that roles radical flux, ion flux and ion energy play may be both good and bad. Increasing one parameter helps meeting one requirement but hinders meeting the other. Self-limiting processes like atomic layer etching (ALE) promise a way to escape the problem of balancing trade-offs. ALE [1] was realized in the mid-1990s but the industrial implementation did not occur due to inherent slowness and precision loss from improper balance of self-limiting passivation and its removal processes. In recent years interest in ALE has revived and strides have been made by etch equipment manufacturers primarily through temporal, spatial or combination of these two pulsing approaches. Moderate success has been reported with some of the trade-offs purported to be managed. Difficulty meeting requirements is due to the inability of plasma technologies to control ion energy at low and precise values.

We overcome many of the practical implementation issues associated with ALE by precise passivation process control using plasmas with low electron temperature. Very low plasma potential, high radical flux and high bombardment flux are indispensable for achieving ALE. We demonstrate that ALE can achieve zero ARDE and infinite selectivity. Experimental results will highlight that careful consideration of surface process physics is required to achieve ALE and not simply "slow etching". Without profile control, ALE is not useful. Profile control will be shown to rely on careful management of the ion energies and angles. For ALE to be realized in production environment, tight control of IAD is a necessary. Experimental results are compared with simulation results generated using MCFPM [2] and theoretical scaling models to provide context to the work.

[1] S. Athavale and D. J. Economou, *J. Vac. Sci. Technol. B,* 14, 3702 (1996).

[2] M. Wang and M. J. Kushner, *J. Appl. Phys.,* 107, 023308 (2010)

8:40am PS+SS+TF-WeM3 Understanding of new processes for Atomic Layer Etching, *Florentin Chambettaz, L. Vallier, J. Dubois,* Univ. Grenoble Alpes-CNRS-CEA/Minatec-LTM,38000 Grenoble-France*, O. Joubert,* Univ. Grenoble Alpes-CNRS-CEA, France
In the pace of downscaling in microelectronic, current plasma etching processes show their limits. Actually for critical dimension smaller than 10

nm, atomic precision has to be reached during etching. In this study we are developing an Atomic Layer Etching (ALE) process by focusing on the induced damages related to the chemical and physical interaction(s) with hydrogen (This subject has already been broached in other studies on graphene [1] or carbon nanotubes [2]) and helium plasmas. Hydrogen plasmas have been used for years in the microelectronic industry and studied in the fields of deposition (PECVD, Plasma Enhanced Chemical Vapor Deposition), surface processing (surface passivation, hydrogenation) and plasma etching [3]. However the mechanisms related to these processes are not fully understood yet mainly because hydrogen is an element with peculiar characteristics such its low mass and its electronegativity. Helium plasmas have been also used for many years in the microelectronics industry. Helium is often employed in plasma processes as an additives gas due to its low chemical reactivity and low mass. Consequently ionic species present in the plasma and their effect are well known. To modify the surface of ultrathin layers without damaging the materials, a very low ion bombardment is required (conditions similar to those obtained in a pulsed ICP reactor [4]). At the same time, high energy plasmas are required to obtain satisfying etch rates when several nanometers have to be etched away. In this study we focus on plasma etching of silicon nitride by hydrogen plasma exposure in a commercially available 300 mm reactor, in order to develop an ALE process for spacer etching of future 10nm transistors. Several process conditions are achieved with different ion energies and ion densities, on thin silicon nitride blanket samples. The generated damages in the structure were quantified with an Electron Spin Resonance (ESR) spectroscopy and electrical characterization. The effect of these etching processes on silicon nitride will be discussed.

1. E.Despiau-Pujo, A.Davydova, G.Cunge, L.Delfour, L.Magaud, and D. B.Graves, Journal of Applied Physics, **113** (2013)

2. A.Hassanien, M.Tokumoto, P.Umek, D.Vrbanic, M.Mozetic, D.Mihailovic, P.Venturini, and S.Pejovnik, Nanotechnology, **16**, 278 (2005)

3. M.Sode, T.Schwarz-Selinger, and W.Jacob, Journal of Applied Physics, **113** (2013)

4. C. Petit-Etienne, M. Darnon, P. Bodart, M. Fouchier, G. Cunge, E. Pargon, L. Vallier, O. Joubert, and S.Banna, Journal of Vacuum Science & Technology B, **31** (2013)

9:00am PS+SS+TF-WeM4 Self-Limited Ion Implantation for Precise Low-k Spacer Etching, *Nicolas Posseme,* Cea-Leti, Minatec, France*, M. Garcia-Barros, C. Arvet,* ST Microelectronics*, O. Pollet,* Cea-Leti, Minatec*, S. Lagrasta, P. Maury,* ST Microelectronics*, F. Leverd,* ST Microlectronics*, C. Richard,* ST Microelectronics*, S. Barnola*, Cea-Leti, Minatec, France
With aggressive device shrinking, parasitic capacitances through the spacer become a greater contributor to the total device capacitance. This issue is exacerbated by the common use of SiN spacers. Since SiN has a relatively large dielectric constant (k~7.5), a simple approach to reduce capacitive coupling through the spacer is to supplant it with a low-k material [1]. Therefore, the reduction of spacer k value is a key for the high performance devices. In this context, Low-k films like SiCO, SiOCN or SiBCN have been proposed for the C014 technology node to replace the traditional silicon nitride investigated.

Today, the Low-k spacer etching is considered as one of the most challenging step in the high performance FDSOI devices realization. A trade-off has to be found between silicon germanium (or silicon) recess, foot formation and CD control impacting the device performances. The etch process must also be compatible with epitaxial step.

In a recent study, we proposed a new etch approach [2] for silicon nitride spacer etching. This new etching process is based on a Self-Limited Ion Implantation by plasma. In a first step, the film is modified in volume by a Hydrogen plasma performed in a conventional etch tool (CCP or ICP) followed in a second step by a 1%HF wet cleaning to remove the modified layer selectively to the non-modified material. We demonstrated that the silicon germanium recess was estimated to less than 6A with no foot formation, while a silicon germanium has grown by epitaxy without defects [2].

In this study, we propose to evaluate the compatibility of this new etch approach with low-k films like SiCO or SiCBN. By playing on plasma operating conditions performed in ICP etch tool, we will demonstrate that the Low-k films can accurately be etched with atomic layer control, stopping on SiGe or Si. The key parameters for such etch precision are identified as H ion energy and H ion dose implanted in the low-k film. The etch mechanisms to remove the modified layer by wet cleaning process will be understood on blanket wafers thanks to XPS and infrared spectroscopy analyses.

Finally the compatibility of this new Low-k spacer etching process with the epitaxial step will also be presented for C014 FDSOI integration.
References

[1] H. Niebojewski, C. Le Royer, Y. Morand, M-A. Jaud, O. Rozeau, E. Dubois, T. Poiroux, " Extra-low Parasitic Gate-to-Contacts Capacitance Architecture for sub-14nm Transistor Nodes", IEEE Euro SOI conference, 2013

[2] N.Posseme, O. Pollet, S.Barnola, "Alternative process for thin layer etching: Application to nitride spacer etching stopping on silicon germanium", Appl. Phys. Lett. 105, 051605 (2014)

9:20am PS+SS+TF-WeM5 Self-limiting Cyclic Etching of Silicon Nitride using Infrared Irradiation, *Nobuya Miyoshi*, Hitachi, Japan, *H. Kobayashi, K. Shinoda*, Hitachi, *M. Matsui*, Hitachi, Japan, *M. Miyake, K. Maeda*, Hitachi, *Y. Kouzuma*, Hitachi High-Technologies, Japan, *Y. Kudo, T. Kanekiyo, M. Izawa*, Hitachi High-Technologies

Advanced semiconductor device fabrication requires precise control of device dimensions down to the atomic level. Current efforts to achieve atomic level control are focused on cyclic etching that repeatedly forms and removes a reactive layer on a surface. The cyclic etching of SiO_2, for example, has been achieved by repeatedly forming and removing of ammonium hexafluorosilicate (($NH_4)_2SiF_6$) [1]. The essential point in realizing atomic level control is achieving a self-limiting process.

Fluorocarbon-based plasma produces a $(NH_4)_2SiF_6$ layer on silicon nitride surfaces [2]. We have reported the preliminary results of the cyclic etching of silicon nitride using the formation and removal of the $(NH_4)_2SiF_6$ layer [3]. An analysis using x-ray photoelectron spectroscopy (XPS) revealed that the $(NH_4)_2SiF_6$ layer formed on silicon nitride after exposure to fluorocarbon-based plasma and was desorbed by annealing the sample.

In this study, the removal of the $(NH_4)_2SiF_6$ layer using IR irradiation was investigated to achieve high-throughput cyclic etching. The reactive layer of $(NH_4)_2SiF_6$ was formed on a silicon nitride sample after exposure to radicals in fluorocarbon-based plasma. After formation of the reactive layer, IR light was irradiated to the sample for removal. The sample surface was analyzed by XPS, and the dependence of the etching depth on the radical exposure time was investigated. The temperature of the sample increased over 160°C under IR irradiation for 10 s. A nitrogen 1s peak at 402 Ev, which is attributed to $(NH_4)_2SiF_6$, disappeared after IR irradiation for 10 s. This result shows that IR irradiation is expected to result in fast removal of the reactive layer within 10 s. The etching depth after IR irradiation saturated at 1 nm as the radical exposure time was increased to over 300 s. Therefore, a self-limiting process for silicon nitride was obtained by forming and removing the $(NH_4)_2SiF_6$ layer. Finally, the cyclic etching was investigated by repeatedly forming and removing the reactive layer. The number of cycles was changed between 1 and 10. The total etching depth increased linearly with the number of cycles, demonstrating the cyclic etching of silicon nitride with high precision.

[1] H. Nishio, et al., J. Appl. Phys. **74**, 1345 (1993).

[2] W. R. Knolle et al., J. Electrochem. Soc. **135**, 2574 (1988).

[3] K. Shinoda et al., AVS Atomic Layer Etching workshop 2015 (2015).

9:40am PS+SS+TF-WeM6 Prospects for Thermal Atomic Layer Etching: Materials and Selectivity, *Steven George, Y. Lee, J.W. DuMont*, University of Colorado at Boulder

Thermal atomic layer etching (ALE) of Al_2O_3 and HfO_2 has recently been demonstrated using sequential, self-limiting reactions [1-3]. Al_2O_3 and HfO_2 ALE were performed using $Sn(acac)_2$ and HF as the reactants [1-3]. Recent work has also shown that Al_2O_3 ALE can be accomplished using $Al(CH_3)_3$ and HF as the reactants. The ALE reaction mechanism is believed to involve fluorination and ligand-exchange. For Al_2O_3 ALE using $Sn(acac)_2$ and HF, HF exposures convert Al_2O_3 to AlF_3. $Sn(acac)_2$ then accepts F from AlF_3 and donates acac to AlF_3 to produce volatile $Al(acac)_3$ or $AlF(acac)_2$.

The prospects for thermal ALE are very promising. Thermochemical calculations suggest that many materials should be etched with similar reactions. Metal oxides, metal nitrides, metal phosphides, metal arsenides and elemental metals can all be fluorinated with fluorine reactants such as HF or XeF_2 to form the corresponding metal fluoride. Ligand-exchange reactions can then be conducted with a variety of metal precursors that accept fluorine from the metal fluoride and donate one of their ligands to the metal in the metal fluoride. The metal reaction products then can leave the surface if they are stable and volatile. Preliminary results for GaN etching suggest that metal nitrides are good candidates for thermal ALE.

The metal fluoride reaction products produced by the ligand-exchange process provide pathways for selectivity during thermal ALE. Selectivity can arise depending on the stability of the metal reaction product. For example, $Sn(acac)_2$ is a metal beta-diketonate that donates acac ligands to the metal in the metal fluoride. Because most metals bind with acac ligands, $Sn(acac)_2$ may not lead to significant selectivity. In contrast, $Al(CH_3)_3$ is a metal alkyl that donates CH_3 ligands to the metal in the metal fluoride. Because some metals do not easily form sigma-bonds to bond to CH_3 ligands, more complete selectivity between different materials may be

expected for $Al(CH_3)_3$. The selectivity observed between Al_2O_3 and ZrO_2 etching will illustrate this concept.

1. Younghee Lee and Steven M. George, "Atomic Layer Etching of Al_2O_3 Using Sequential, Self-Limiting Thermal Reactions with $Sn(acac)_2$ and HF", *ACS Nano* **9**, 2061 (2015).

2. Younghee Lee, Jaime W. DuMont and Steven M. George, "Mechanism of Thermal Al_2O_3 Atomic Layer Etching Using Sequential Reactions with $Sn(acac)_2$ and HF" *Chem. Mater.* (In Press).

3. Younghee Lee, Jaime W. DuMont and Steven M. George, "Atomic Layer Etching of HfO_2 Using Sequential, Self-Limiting Thermal Reactions with $Sn(acac)_2$ and HF", *J. Solid State Sci. Technol.* **4**, N5013 (2015).

11:00am PS+SS+TF-WeM10 Atomic Layer Etching of Al_2O_3 Using Sequential, Self-Limiting Thermal Reactions with Trimethylaluminum and Hydrogen Fluoride, *Younghee Lee, J.W. DuMont, S.M. George*, University of Colorado, Boulder

A new approach for the atomic layer etching (ALE) of Al_2O_3 was demonstrated using sequential, self-limiting thermal reactions with trimethylaluminum (TMA) and hydrogen fluoride (HF) as the reactants. Previously, Al_2O_3 thermal ALE was reported using $Sn(acac)_2$ and HF as the reactants [1,2]. HfO_2 ALE was also demonstrated using $Sn(acac)_2$ and HF as the reactants [3]. This new approach using TMA expands the variety of ALE reactants and excludes the possibility that Sn could be left on the etched Al_2O_3 film.

Quartz crystal microbalance (QCM) experiments monitored Al_2O_3 ALE at temperatures from 275-325°C. The Al_2O_3 ALE was linear versus number of TMA and HF reaction cycles. The QCM studies showed that the sequential TMA and HF reactions were self-limiting versus reactant exposure. The QCM analysis measured a mass change per cycle (MCPC) of -16 ng/(cm^2 cycle) at 300°C. This MCPC corresponds to an Al_2O_3 etch rate of 0.53 Å/cycle. X-ray reflectivity analysis confirmed the linear removal of Al_2O_3 and etching rates. Fourier transform infrared spectroscopy measurements also monitored Al_2O_3 ALE by observing the loss of infrared absorbance from Al-O stretching vibrations.

Al_2O_3 ALE is believed to follow the reaction: $Al_2O_3 + 4Al(CH_3)_3 + 6HF \rightarrow 6AlF(CH_3)_2 + 3H_2O$. The proposed reaction mechanism involves fluorination and ligand-exchange. The HF exposure fluorinates Al_2O_3 and forms AlF_3 with H_2O as a reaction product. During ligand-exchange, $Al(CH_3)_3$ accepts F from AlF_3 and donates CH_3 to AlF_3 to produce volatile $AlF(CH_3)_2$ reaction products. Similar reaction mechanisms based on fluorination and ligand-exchange reactions may extend the range of thermal ALE to a wide variety of additional materials.

1. Younghee Lee and Steven M. George, "Atomic Layer Etching of Al_2O_3 Using Sequential, Self-Limiting Thermal Reactions with $Sn(acac)_2$ and HF", *ACS Nano* **9**, 2061 (2015).

2. Younghee Lee, Jaime W. DuMont and Steven M. George, "Mechanism of Thermal Al_2O_3 Atomic Layer Etching Using Sequential Reactions with $Sn(acac)_2$ and HF" *Chem. Mater.* (In Press).

3. Younghee Lee, Jaime W. DuMont and Steven M. George, "Atomic Layer Etching of HfO_2 Using Sequential, Self-Limiting Thermal Reactions with $Sn(acac)_2$ and HF", *J. Solid State Sci. Technol.* **4**, N5013 (2015).

11:20am PS+SS+TF-WeM11 Low Damage Etch Chamber for Atomic Layer Etching, *Leonid Dorf, S.R. Dorf, T.G. Monroy, K. Ramaswamy, K.S. Collins, Y. Zhang*, Applied Materials

The use of novel, ultra-sensitive materials requires low-damage plasma etching with atomic layer precision, which imposes progressively stringent demands on accurate control over ion energy and radical composition during plasma processing. Using electron sheet beam (e-beam) parallel to the substrate surface to produce plasma in a processing chamber provides an order of magnitude reduction in electron temperature T_e (~ 0.3 eV) and ion energy E_i (< 2 eV without applied bias) compared to conventional plasma technologies, thus making electron beam plasmas an ideal candidate for processing features at 5 nm and below. Furthermore, since dissociation is performed only by high-energy beam and not plasma electrons, and the dissociation cross-section drops off considerably at beam energies of about 1–2 keV, the beam created plasma is typically poor in radicals, which allows an independent control over plasma radical composition. In this presentation, we describe the Low Damage Etch Chamber (LoDEC) for atomic layer etching (ALE). The apparatus consists of (1) an e-beam source for creating radical-poor, low-T_e plasma in the processing chamber, (2) a remote plasma source (RPS) for producing and supplying radicals to the substrate, and (3) a bias generator for creating the voltage drop (with fine control in 0 – 50 V range) between the substrate and the plasma to accelerate ions over etch-threshold energies. Using patterned wafers, we have developed low-bias power (0 – 10 W) processes resulting in very high

selectivity (as per high-resolution TEM images) of Si_3N_4 to SiO_2 and poly-Si in fluorocarbon based chemistries. In application to ALE, we note that one existing approach to ALE of Si prescribes injecting Cl atoms to passivate the surface, and then replacing the processing gas with Ar and applying bias to the substrate to initiate the etching. Once the passivation layer is removed, the etch stops, provided Ar^+ ions have energies below sputtering threshold. By repeating passivation and etching steps, this scheme can be used to remove silicon in equally thick portions composed of one to a few atomic layers (few Amgstroms), without tight control over the duration of the bias part of the cycle. In LoDEC, this recent pulsed-ALE technique can be performed at ion energies much lower than that in conventional tools, thus minimizing damage to the processed materials. LoDEC also allows implementation of a unique, truly low damage, continuous-ALE technique by using electron beam to create plasma with very low ion energies (with or without an application of low-power bias to accelerate ions) and RPS to create radicals. The results of ALE experiments in LoDEC will be presented.

11:40am PS+SS+TF-WeM12 Modeling of Electron-Beam Generated Plasmas: Validation and System Design, *Shahid Rauf*, *A. Agarwal, L. Dorf, K.S. Collins,* Applied Materials, Inc.*, D.R. Boris, S.G. Walton*, US Naval Research Laboratory

Plasmas generated using energetic electron beams have unique properties that make them attractive for emerging plasma processing applications. In the work done at the Naval Research Laboratory, [1] it has been demonstrated that electron temperature (T_e) in the electron-beam plasmas generated in molecular gases is typically < 0.6 eV while electron densities are comparable to those obtained in radio-frequency (RF) inductively and capacitively coupled plasmas. In addition, the ions and radicals are primarily produced by highly energetic electrons (few keV) instead of electrons in the tail of a low energy distribution. The plasma chemistry in electron-beam generated plasmas is therefore significantly different than RF plasmas with a much higher ion to neutral radical density ratio in electron beam plasmas. As feature dimensions shrink below 20 nm in microelectronics devices with atomic level precision required during manufacturing, the unique properties of electron-beam generated plasmas (low T_e, low ion energy and unique chemistry) are becoming attractive for plasma processing in the semiconductor industry.

This paper focuses on a multi-dimensional computational model for electron-beam generated plasmas. A fluid model for the bulk plasma is coupled with a Monte Carlo kinetic model for beam electrons. The fluid plasma model uses the drift-diffusion approximation for electrons and negative ions. The momentum equation is solved for positive ions. The model includes the effect of magnetic field on charged species transport. The Monte Carlo model for beam electrons considers electron motion in the ambipolar electric field and externally imposed static magnetic field. Additionally, important collision processes including elastic collisions, ionization, excitation, dissociation and dissociative attachment are considered during the Monte Carlo simulation.

The computational model is validated in Ar, Ar/N_2 and O_2 plasmas using probe measurements over a range of gas pressures and electron beam properties. One factor that has important implications on quantitative accuracy of the model is the influence of magnetic field on electron transport properties. The paper will discuss the classical transport model as well as variations based on semi-empirical approximations. The validated model is applied to the design of electron beam based plasma processing systems.

This work was partially supported by the Naval Research Laboratory Base Program.

[1] S.G. Walton *et al.*, ECS Journal of Solid State Science and Technology, 4 (6) N5033-N5040 (2015)

12:00pm PS+SS+TF-WeM13 Enhanced Reaction Rate and Precursor Transport in Focused Electron Beam Induced Etching Via Pulsed Laser Assistance, *JooHyon Noh*, University of Tennessee*, J.D. Fowlkes,* Oak Ridge National Laboratory*, R. Timilsina, M.G. Stanford, B.B. Lewis, P.D. Rack*, University of Tennessee

Focused electron-beam-induced etching (FEBIE) is a versatile, selective or direct write nanomaterials etching technique, and is an alternative to focused ion beam (FIB) etching. FIB etching can cause collateral sub-surface damage due to knock-on collisions and ion implantation. FEBIE in contrast is minimally invasive because of the low electron mass and offers high etch selectivity between different materials. Additionally, the FEBIE process has better spatial resolution due to the smaller beam spot size. However, the low FEBIE etch rate has been a limiting factor for high-throughput applications.

The FEBIE process is governed by an electron-induced reaction with a precursor at the substrate surface, resulting in the volatile etch by-products. This complex process can be rate limited by different mechanisms

depending on the electron and precursor parameters, the electron stimulated reaction rates, and the by-product volatility (or residence time). While substrate heating can reduce the by-product residence time, the higher temperature concomitantly decreases the reactant residence time, which can reduce the reactant equilibrium coverage and result in the electron stimulated etching rate. In order to enhance the etch rate, we introduce a laser-assisted focused electron-beam-induced etching (LA-FEBIE) process which emulates an atomic layer etching process. The focused electron beam catalyzes the first half reaction which forms a pseudo-volatile byproduct. The periodic and appropriately synchronized pulsed laser can locally and briefly raise the surface temperature, which can affect the reactant and byproducts and facilitate the reaction kinetics. In this presentation we will overview the laser-assisted electron beam induced etching of Ti with a XeF_2 gas chemistry and will correlate the mechanisms to a selected area atomic layer etching process. We will show results that the Ti electron stimulated etch rate via the XeF_2 precursor can be enhanced up to 6 times with an intermittent pulsed laser assist. The etching evolution is correlated to in situ stage current measurements and scanning electron micrographs as a function of time. Other relevant work on conventional fluorine-based titanium plasma etching suggests the mechanism of Ti-F etching is attributed to the reaction of F radicals with Ti to form TiF_x products; where progressive fluorine incorporation drives x towards the volatile product of TiF_4. Notably TiF_3 is a stable solid at room temperature. The increased etch rate with laser assistance is attributed to photothermally enhanced Ti−F reaction and TiF_4 desorption and in some regimes enhanced XeF_2 surface diffusion to the reaction zone.

Scanning Probe Microscopy Focus Topic
Room: 212A - Session SP+AS+NS+SS-WeM

Advances in Scanning Probe Microscopy
Moderator: An-Ping Li, Oak Ridge National Lab, Saban Hus, Oak Ridge National Laboratory

8:00am SP+AS+NS+SS-WeM1 Designer Electrons: Quantum Information and New Particles in Atomically Assembled Matter, *Hari Manoharan*, Stanford University **INVITED**

The observation of massless Dirac fermions in monolayer graphene has propelled a new area of science and technology seeking to harness charge carriers that behave relativistically within solid-state materials. Using low-temperature scanning tunneling microscopy and spectroscopy, we show the emergence of Dirac fermions in a fully tunable condensed-matter system—molecular graphene—assembled via atomic manipulation of a conventional two-dimensional electron system in a surface state. We embed, image, and tune the symmetries underlying the two-dimensional Dirac equation into these electrons by sculpting the surface potential with manipulated molecules. By distorting the effective electron hopping parameters into a Kekulé pattern, we find that these natively massless Dirac particles can be endowed with a tunable mass engendered by the associated scalar gauge field, in analogy to the Higgs field. With altered symmetry and texturing of the assembled lattices, the Dirac fermions can be dressed with gauge electric or magnetic fields such that the carriers believe they are in real fields and condense into the corresponding ground state, as confirmed by tunneling spectroscopy. Using these techniques we ultimately fabricate a quantum Hall state without breaking time-reversal symmetry, in which electrons quantize in a gauge magnetic field ramped to 60 Tesla with zero applied laboratory field. We show that these and other chiral states now possible to realize have direct analogues in topological insulators, and can be used to guide or confine charge in nontrivial ways or to synthesize new particles [1,2].

[1] K. K. Gomes, W. Mar, W. Ko, F. Guinea, H. C. Manoharan, "Designer Dirac Fermions and Topological Phases in Molecular Graphene," *Nature* **483**, 306–310 (2012).

[2] M. Polini, F. Guinea, M. Lewenstein, H. C. Manoharan, V. Pellegrini, "Artificial Honeycomb Lattices for Electrons, Atoms, and Photons," *Nature Nanotechnology* **8**, 625–633 (2013).

8:40am SP+AS+NS+SS-WeM3 Scanning Quantum Dot Microscopy, *Ruslan Temirov*, *C.W. Wagner, M.F.B.G. Green, P.L. Leinen,* Forschungszentrum Juelich GmbH, Germany*, T.D. Deilmann, P. Krueger, M.R. Rohlfing,* Muenster University, Germany*, F.S.T. Tautz,* Forschungszentrum Juelich GmbH, Germany

Interactions between atomic and molecular objects are to a large extent defined by the nanoscale electrostatic

potentials which these objects produce. Consequently, a tool for nanometre scale imaging and quantification of

local electrostatic fields could help in many areas of nanoscience research. In this contribution we introduce a

scanning probe technique that for the first time enables truly three-dimensional imaging of local electrostatic

potential fields with sub-nanometre resolution. Registering single electron charging events of a molecular

quantum dot attached to the tip of a tuning fork atomic force microscope operated at 5 K, we image the

quadrupole field of a single molecule adsorbed on a metal surface. To demonstrate quantitative measurements,

we investigate the Smoluchowski dipole field created by a single metal adatom adsorbed on a metal surface. We

show that because of its high sensitivity the technique can probe electrostatic potentials at large distances from

their sources, which should allow for the imaging of samples with increased surface roughness.

Reference

[1] C. Wagner, M. F. B. Green, P. Leinen, T. Deilmann, P. Krüger, M. Rohlfing, R. Temirov, F. S. Tautz

arXiv:1503.07738 (2015)

9:00am SP+AS+NS+SS-WeM4 Local Probing of the Photo-carrier Lifetime by Kelvin Probe Force Microscopy, *Nicolas Chevalier, S. Pouch, D. Mariolle,* Univ. Grenoble Alpes/ CEA, LETI, MINATEC Campus, France*, B. Grevin,* Univ. Grenoble Alpes/ CEA, INAC, SPrAM, LEMOH, France*, Ł. Borowik*, Univ. Grenoble Alpes/ CEA, LETI, MINATEC Campus, France

The photo-carrier lifetime plays a major role in the overall efficiency of a solar cell because it limits the proportion of photo-generated charges collected at the electrodes. This lifetime, which should be ideally as large as possible in an organic or inorganic solar cell, is rather difficult to measure in nanostructured materials or in more complex hybrid systems, indirect band-gap semiconductors, and ultra-thin layers. Identifying the losses mechanisms is one of the main objectives for increasing the performances of solar cells. Most of the experimental approaches developed so far consist in studying recombination by techniques such as transient photovoltage measurements or charge extraction. All these techniques average sample properties over macroscopic scales, making them unsuitable for directly assessing the impact of local heterogeneity on the recombination process. In this paper, we propose a steady method to measure the photo carrier lifetime by photo-modulated techniques based on Kelvin probe force microscopy (KPFM). [1] Additionally, KPFM technique provides a spatially resolved measurement, which is applicable on the overall of solar cells.

We will present the principle of this original method based on the measurement of the surface potential by KPFM under an illumination with a rectangular waveform light modulation. Photo-carrier lifetime down to µs scale is reachable with our experimental setup. The modulation-dependent surface potential is plotted as a function of the frequency. Assuming an immediate generation time under illumination and an exponential decay of the surface potential during the dark condition, the averaged surface potential over a cycle can be fitted as a function of the frequency by simple equation where the only fit parameter is the photocarrier-lifetime. [2] Instrumental aspects as well as data treatment will be reviewed. Measurements obtained on silicon nanocrystals embedded in 30 nm film of silicon dioxide [3] and on organic donor-acceptor blend (PBTFB and PCBM) [4] will be presented to illustrate the potential of the technique.

This work was supported by the French "Recherche Technologique de Base" Program and performed in the frame of the trSPV Nanoscience project. The measurements were performed on the CEA Minatec Nanocharacterization Platform (PFNC).

1. Ł. Borowik *et al.* Phys. Rev. B 82, 073302 (2010).

2. Ł. Borowik *et al.* Nanotechnology 25, 265703 (2014).

3. D. Asakura *et al.* Phys. Rev. Lett. 93, 247006 (2004).

4. N. Delbosc et al. RSC Adv 4, 15236 (2014).

9:20am SP+AS+NS+SS-WeM5 Nanoscale Capacitance-Voltage (C-V) Curves: Using Scanning Microwave Impedance Microscopy (sMIM) to Characterize Local Electrical Properties of Linear and Non-Linear Materials, *Stuart Friedman, Y. Yang, O. Amster,* PrimeNano, Inc.

Understanding and optimizing advanced materials frequently requires detailed knowledge of nanoscale electrical properties. Scanning probe techniques such as scanning tunneling microscopy (STM), conductive AFM (cAFM), scanning capacitance microscopy (SCM), and Kelvin probe force microscopy (KPFM) provide such nano-electrical measurements, but are generally limited in the classes of materials they can characterize or the properties they can measure. Scanning microwave impedance microscopy (sMIM) uses GHz frequency microwaves and shielded AFM probes to directly measure the impedance (capacitance and conductance) of the tip sample interface. As such sMIM is sensitive to the permittivity and conductivity of a wide variety of samples including dielectrics, conductors, and semiconductors.

When sMIM is applied to non-linear materials, changing the tip sample bias changes the local electric field thereby changing the local electrical properties of the sample just under the AFM tip. The electric field induced changes in the sample create changes in the tip-sample impedance that can be measured by sMIM. For example, when imaging doped semiconductor samples, the tip sample interface forms either a metal-semiconductor junction or a metal-insulator-semiconductor junction. Plotting the sMIM measured capacitance as a function of the tip sample bias voltage produces the equivalent of a typical capacitance-voltage curve, but from nanoscale regions selected from an AFM image. C vs V results from doped silicon samples that closely match theoretical calculations will be discussed. The talk will also present results from advanced and novel materials and devices, such as III-V semiconductors, 2D materials and 1D structures where sMIM data has been used to assess non-linear behavior and characterize dopant type and distribution.

9:40am SP+AS+NS+SS-WeM6 STM Study of the Correlation between Structural, Magnetic, and Electronic Properties of Co Nano-Islands on Cu(111), *Jewook Park, C. Park, M. Yoon, Z. Gai, A.P. Baddorf, A.-P. Li,* Oak Ridge National Laboratory

An epitaxially grown Co nano-island on Cu(111) surface is a model system to study the correlation between structural, magnetic, and electrical properties of nanophase materials. We carried out an extensive study on Co islands by using spin-polarized scanning tunneling microscopy and spectroscopy (SP-STM/S) at low temperatures (130 K and 38 K). Two structurally different island types are clearly distinguished, rotated by 180 about the surface normal due to a stacking fault in one type of the islands. The triangular Co islands are 5-20 nm wide and 4 Å high. Regardless of the structural asymmetry, both faulted and un-faulted Co islands possess two distinctive spin orientations. With Cr-coated W-tip as a spin-polarized probe, bias-dependent tunneling conductance maps are measured on Co islands. An antiparallel spin-orientation between magnetized tip and Co islands display higher conductance compared to a parallel relation at -400 meV and *vice versa* at around Fermi-level, which is verified by density functional theory calculations. Furthermore, by recording 23 hours of time-lapse images from the same Co islands, we demonstrate a time-dependent correlation between structural, magnetic, and electrical behaviors. We find that a contamination-induced structural change modifies the magnetic properties of Co islands and is confirmed by theoretical calculations.

11:00am SP+AS+NS+SS-WeM10 Probing Electrostatic Field Effect in Quantum Materials by Microwave Impedance Microscopy, *Keji Lai*, University of Texas at Austin **INVITED**

The research of complex quantum materials, in which a dazzling number of emergent phenomena take place in the nanoscale, is a major theme in modern condensed matter physics. For real-space imaging of complex systems, electrical impedance microscopy fills an important void that is not well represented by the existing local probes. Using shielded cantilever probes and sensitive microwave electronics, we can now perform non-invasive electrical imaging with sub-100nm resolution and sub-aF sensitivity.

Combining the cryogenic microwave impedance microscopy (MIM) and a spin-coated thin ionic gel layer, we are able to visualize the metal-insulator transition of functional materials in electrolyte-gated electric double-layer transistors. The microwave images acquired at different gate voltages clearly show the spatial evolution of channel conductivity and its local fluctuations through the transition. By applying a large source-drain bias above the glass transition temperature of the gel, an uneven conductance profile is established across the EDLT channel, which can be visualized by the MIM and further investigated by transport measurements and numerical simulations. The combination of ultra-thin ion-gel gating and microwave microscopy paves the way for studying the microscopic evolution of phase transitions in complex materials induced by electrostatic field effects.

11:40am SP+AS+NS+SS-WeM12 Subsurface Visualization of Soft Matrix using 3D-Spectroscopic Atomic Force Acoustic Microscopy, *Kuniko Kimura*, K. Kobayashi, A. Yao, H. Yamada, Kyoto University, Japan

Nondestructive visualization of subsurface features of various materials with nanometer-scale spatial resolution is strongly demanded in a wide variety of scientific research fields such as nanoelectronics, nanomechanics and life science. Recently, many research groups have demonstrated the visualization of nanometer-scale subsurface features using various techniques based on atomic force microscopy (AFM) [1-4]. (All references and figures are given in Supplement.) We recently demonstrated the imaging of Au nanoparticles buried under 900 nm from the surface of a polymer matrix by atomic force acoustic microscopy (AFAM), as shown in Fig. 1 [5]. In AFAM, the amplitude and phase of the cantilever vibration at the contact resonance frequency induced by the sample excitation are measured, which allows us the quantitative evaluation of surface stiffness [6]. The AFAM images in Fig. 1 show that the surface viscoelasticity of the soft matrix is affected by subsurface hard objects such as the Au nanoparticles buried even roughly 1 micro-meter below the surface. However, only from AFAM images, it is difficult to determine which the dominant mechanism for the subsurface imaging is viscosity variation or elasticity variation, because AFAM images were taken at a single excitation frequency near contact resonance.

In this presentation, we discuss the origin of the visualization of subsurface features in soft matrix based on spectroscopy of AFAM [7]. We recorded the amplitude and phase spectra at every pixel of the AFAM image as represented in Fig. 2, which we call 3-dimensional spectroscopic atomic force acoustic microscopy (3D-spectroscopic AFAM). A schematic diagram of the 3D-spectroscopic AFAM is shown in Fig. 3. After the tip was brought into contact with the surface, we first measured the contact resonance frequency (fc). Then we recorded the amplitude and phase spectra measured by a lock-in amplifier, while the tip was raster-scanned with the contact mode. At each scanning pixel, the excitation frequency was swept with the span of 25 kHz which was centering around fc, whose sweep time was 35 msec. The total acquisition time for 128 x 128 pixels took about 20 min.

Using this method, we can compare the frequency spectrum measured on the subsurface Au nanoparticle with that on another position having no subsurface particle, as shown in Fig. 4. We can also reconstruct AFAM images of arbitrary frequencies within the sweep frequency range, which is the meaning of "3-dimensional". Moreover, the 3D-spectroscopic AFAM enables us to characterize the amplitude and phase spectra and to detect the variation that may be caused by the nonlinear tip-sample interactions.

12:00pm SP+AS+NS+SS-WeM13 Quantifying the Effects of Cantilever Modes Shapes on Studies of the Liquid-Solid Interface, *Aleks Labuda*, M. Viani, D. Walters, R. Proksch, Asylum Research, an Oxford Instruments company

At the core of most AFM measurements is the assumption that the motion of the cantilever probe can be well quantified. However, most AFM systems use a "beam bounce" optical beam deflection (OBD) method which, because it is fundamentally an angular measurement, only provides accurate tip position information when the mode shape of the cantilever matches the calibration conditions. For example, if the OBD sensitivity is calibrated with a force curve, the calibration holds true only for experiments where the mode shape is similar to an end-loaded cantilever. This assumption is quickly violated when the cantilever is oscillated at frequencies different from the calibration. This is especially true in liquids, where Q~1 and the combination of significant base motion and hydrodynamic effects lead to a variety of different mode shapes that are strongly frequency dependent (see Figure). This clearly demonstrates that the sensitivity (nm/V) is actually a frequency dependent quantity. Worse, it may also drift with time. Another consequence is that the effective stiffness of the cantilever, which depends on mode shape, is also highly frequency dependent. Both of these effects cause quantitative misinterpretation of the tip-sample interaction and artifacts in imaging contrast. These problems affect both dynamic AFM modes (such as AM-AFM and FM-AFM) as well as sub-resonance modes such as fast force mapping and force modulation.

To quantify this effect, we present measurements based on Ref [1-2] using a modified commercial AFM that combines a standard OBD detector with an integrated laser Doppler vibrometer (LDV) system that directly measures displacement. As shown in the Figure, The OBD and LDV can be used simultaneously, such that the cantilever base motion or tip motion can be accurately monitored with the LDV during an AFM experiment – independent of the OBD and any feedback loops. In the Figure, the ~2 μm LDV laser spot was scanned along the cantilever for high-resolution in situ mapping of its dynamics across a wide spectrum of frequencies and showing significant deviations from ideal mode shapes over the entire frequency range.

The effects of these frequency-dependent mode shapes are then quantified by appropriate modeling for a variety of experimental conditions, and demonstrated experimentally using stiff levers for AM-AFM at the calcite-water interface and soft levers for fast force mapping of polymeric materials.

Surface Science
Room: 113 - Session SS+AS+NS-WeM

Metals, Alloys & Oxides: Reactivity and Catalysis
Moderator: John Russell, Jr., Naval Research Laboratory

8:00am SS+AS+NS-WeM1 Surface Chemistry of Single-Layer MoS₂, *Koichi Yamaguchi*, E. Li, L. Bartels, University of California - Riverside

Molybdenum disulfide (MoS_2) is a semiconducting transition metal dichalcogenide (TMD) that forms a stable monolayer 2D crystal structure similar to graphene. It is the key material for industrial hydrodesulfurization (alloyed with cobalt) and has shown promise in electrocatalytic water splitting. We present a study of MoS_2's ability to bind small reactants and its stability when exposed to them at elevated temperature. We utilize a combination of thermally programmed desorption measurements and in-situ PL imaging. The latter permits us to study the film activity over a wide pressure range (high-vacuum to ambient).

8:20am SS+AS+NS-WeM2 On the Adsorption Behavior of a Porphyrin on Different Cu Surfaces: A Comparative Scanning Tunneling Microscopy Study, *Liang Zhang*, Universität Erlangen-Nürnberg, Germany, *M. Lepper*, Universität Erlangen-Nürnberg, Germany, *M. Stark, S. Ditze, H.-P. Steinrück, H. Marbach*, Universität Erlangen-Nürnberg, Germany

Self-assembly of functional molecular building blocks on well-defined surfaces is a promising approach for the bottom-up fabrication of two-dimensional nanostructures with outstanding properties. In this respect, porphyrins are particularly attractive because of their distinct chemical and physical properties.[1,2]

In this presentation, we investigate and compare the adsorption behaviour of 2H-5,10,15,20-Tetrakis-(3,5-di-tert-butyl)-phenylporphyrin (2HTTBPP) on different substrates, i.e., Cu(111),[3-5] Cu(110) and Cu(110)-(2X1)O, under ultra-high vacuum conditions by scanning tunneling microscopy (STM). At room temperature, supramolecular arrangements of 2HTTBPP are observed on Cu(111) and Cu(110)-(2X1)O, while on Cu(110) individual 2HTTBPP molecules are observed in a disorderd layer. Interestingly, the intramolecular conformations of the molecules are quite different on the investigated substrates, as determined by STM.[4] The corresponding findings are interpreted by accounting for specific molecule-molecule and molecule-substrate interactions. In addition, the so-called self-metalation of 2HTTBPP with Cu atoms will be reported and discussed.[4,5]

References:

1. Auwärter, *et al.*, Nat. Chem., 2015, 7, 105.

2. Gottfried, Surf. Sci. Rep., 2015, doi:10.1016/j.surfrep.2015.04.001.

3. Ditze *et al.*, J. Am. Chem. Soc., 2014, 136, 1609.

4. Stark *et al.*, Chem. Commun., 2014, 50, 10225.

5. Marbach *et al.*, Chem. Commun., 2014, 50, 9034.

8:40am SS+AS+NS-WeM3 Redox-Active On-Surface Assembly of Metal-Organic Chains with Single-Site Transition Metals, *Steven Tait*, Indiana University **INVITED**

Programming the specific chemistry of single-site transition metal centers at surfaces by organic ligand design is a promising route to improve selectivity in surface catalysts. The chemical behavior of the surface and redox chemistry happening at the surface need to be further developed and understood. These studies benefit from interdisciplinary research into the programming of the growth, reactivity, and functionality of nano-scale systems in general and metal-organic complexes as surface catalysts in particular. Our group has recently demonstrated the formation of structurally ordered and chemically uniform single-site centers at surfaces by on-surface redox chemistry of metallic precursors including platinum, chromium, iron, and vanadium with organic ligands on a gold surface (*J. Am. Chem. Soc.* 2014, **136**, 9862-9865; *J. Chem. Phys.* 2015, **142**, 101913; and newly submitted work). The on-surface redox process relies on straightforward vapor deposition protocols and takes advantage of the catalytic role of the surface to show promise as an approach for the growth of inorganic complexes at surfaces. The ability to tune the reactivity and catalysis of these systems is a central question in this field. We report new results here that probe the extent of oxidation state control in these systems

using tailored tetrazine-based ligands and vanadium metal; vanadium is an excellent candidate for probing access to a variety of oxidation states. The oxidizing power of the tetrazine species is tuned by peripheral functional groups to access two and three electron oxidation processes, as determined by X-ray photoelectron spectroscopy (XPS). Platinum(II) centers have also been formed with these ligands. In each of these cases, the metal-ligand complexes take the form of nearly identical one-dimensional polymeric chains, resolved by molecular-resolution scanning tunneling microscopy (STM). These structures provide highly uniform quasi-square-planar coordination sites for the metal, which contributes to the well-defined chemical state of the metal. This strategy is also applied to earth-abundant metals such as iron and chromium using commonly available phenanthroline ligands and is allowing us to develop understanding of how to control and program single-site metal centers on surfaces for next-generation catalysis.

9:20am **SS+AS+NS-WeM5 Ultra-thin Bi(110) Films on Si(111)√3x√3-B Substrates**, *I. Kokubo, Y. Yoshiike, K. Shishikura, K. Nakatsuji, **Hiroyuki Hirayama***, Tokyo Institute of Technology, Japan

Bismuth (Bi) takes the rhombohedral (A7) crystalline structure in bulk. However, it also takes the black phosphorous (BP) structure in ultrathin films. Theoretically, a few bilayer thick Bi(110) films with the BP structure were predicted to be a nontrivial two-dimensional topological insulator by removing the buckling at the surfaces [1]. In the meantime, ultrathin Bi(110) films with the A7 structure was suggested to realize the Dirac electron system at the surfaces [2]. From these viewpoints, the growth, structure, and electronic states of the Bi(110) ultra-thin films are of great interest. In this study, we investigated the details of the atomic arrangements and electronic states at the Bi(110) islands on the Si(111)√3 × √3-B substrate experimentally using scanning tunneling microscope (STM) [3] and angle-resolved photoelectron spectroscopy (ARPES) in a synchrotron radiation facility.

In the study, we found that atomically flat, long, narrow Bi(110) islands grew along specific orientations on the Si(111))√3 × √3-B substrate. The orientations belonged to one of the two sets of three-fold rotational axes, which differed by 26° each other. The preference of the specific orientations were reasonably attributed to the commensuration of the diagonal of the rectangular Bi(110) lattice to the √3 × √3 substrate unit cell. The islands grew as to make their edges parallel to the short side of the Bi(110) rectangular unit cell. The combination of the Bi domains of different orientations caused various types of boundaries on the wide terraces of the Bi(110) islands. In particular, the domains along ±87° from the {1-10} direction were found to be connected perfectly on the atomic scale at the straight boundary by inserting a local switching of the bond direction to the zigzag chains of the in-plane bonds. On the Si(111))√3 × √3-B substrate, both the odd layer thick A7 and even layer thick BP Bi(110) islands appeared. The dispersive surface bands and their Fermi surface mapping with characteristic electron and hole pockets were observed in ARPES spectra. Details will be reported in the presentation.

[1] Y. Lu, W. Xu, M. Zeng, G. Yao, L. Shen, M. Yang, Z. Luo, F. Pan, K. Wu, T. Das, P. He, J. Jiang, J. Martin, Y. P. Feng, H. Lin, X. Wang, Nano Lett. 15, 80 (2015).

[2] G. Bian, X. Wang, T. Miller, T. -C. Chiang, P. J. Kowalczyk, O. Mahapatra, S. A. Brown, Phys. Rev. B 90, 195409 (2014).

[3] I. Kokubo, Y. Yoshiike, K. Nakatsuji, H. Hirayama, Phys. Rev. B 91, 075429 (2015).

}

9:40am **SS+AS+NS-WeM6 STM Study of Growth Processes for Ir/Ge(111)**, *M.S. van Zijll, B.H. Stenger, C.H. Mullet, E.S. Huffman, D. Lovinger, W.F. Mann, **Shirley Chiang***, University of California, Davis

Using scanning tunneling microscopy (STM), we have characterized the surface of clean Ge(111) dosed with 0.66 to 2.0 monolayers (ML) of Ir and then annealed to temperatures between 550 K and 800 K. We observed a broad range of surface formations, including Ir adatom clusters and various stages of island formation. Islands with winding, wormy shapes formed around 580K. As the annealing temperature increased above 650K, round islands formed. In addition, a new type of growth is observed in which the Ir gathers along the antiphase domain boundaries between competing surface domains of the Ge surface reconstruction; this gives the appearance of the Ir forming pathways interconnecting different Ir islands. The low energy electron diffraction (LEED) pattern for this surface shows domains with (√3 x √3)R30° reconstruction and becomes sharper as the temperature is increased. In the STM images, the Ge top layer reconstruction, the Ir adatom clusters, the pathways, and the Ir round islands all have √3-spacing between features. X-ray photoemission spectroscopy (XPS) was used to determine that the IR coverage was ~ 2.0 monolayers when low energy electron microscopy (LEEM) images showed completion of 1 overlayer of Ir grown on Ge(111) at 600C. We present a model consistent with our XPS

and LEEM data that suggests that each Ir adatom cluster observed in STM images corresponds to three Ir adatoms. To model the surface-adsorption processes for the Ir/Ge(111) system, we used simple Monte Carlo simulations with pair-wise surface potentials and random walks of atoms to imitate surface diffusion. Particular parameter choices yielded growth along pathways between domain boundaries of the substrate, in agreement with the experimental data.

11:00am **SS+AS+NS-WeM10 Gas Sensor Resistance Changes for Ar/O₂ and H₂O Plasma Modified SnO₂ Nanomaterials**, ***Erin Stuckert***, *C.J. Miller, E.R. Fisher*, Colorado State University

Although steps have been made to decrease toxic gas emissions globally, these emissions persistently cause detrimental health effects worldwide. Current household gas sensors are limited in their abilities to detect sensitively and selectively at or below relevant toxicity levels for many gases. Tin(IV) oxide (SnO_2) nanomaterials are well-equipped to address some of these limitations as a result of dual valency (Sn^{2+} and Sn^{4+}) and high surface area, thus creating diverse surface chemistry. These properties are advantageous for gas sensing devices because SnO_2 functions as a sensor via gas-surface interactions, facilitated by adsorbed oxygen species. By measuring changes in resistance upon gas exposure, sensitivity and selectivity are observed. To increase sensitivity through maximizing gas surface interactions, chemical vapor deposition-grown SnO_2 nanowires and commercial nanoparticles were treated with an Ar/O_2 and $H_2O_{(v)}$ plasma resulting in increased oxygen adsorption. Surface and bulk characterization throughout the plasma treatment process demonstrate an increase in adsorbed oxygen content over a 30 - 150 W applied power range regardless of plasma precursor, in addition to showing that tin reduction occurs upon $H_2O_{(v)}$ plasma treatment. Gas sensing performance was initially explored by exposing SnO_2 sensors to air at temperatures of 25-300° C to determine base resistance of the materials in an ambient atmosphere. The data show changes in resistance that are dependent upon nanomaterial architecture, plasma treatment conditions, and sensor temperature. Base resistance changes for specific plasma and sensor conditions will be discussed as well as sensor responses and selectivity upon exposure to toxic gases including benzene and carbon monoxide. By combining materials characterization with gas sensor responses, we can optimize sensor sensitivity and selectivity by tuning plasma modification conditions with aims for targeted gas sensing applications.

11:20am **SS+AS+NS-WeM11 Enhanced Adsorption of CO₂ at Steps of Planar ZnO(0001) Grown on Au(111)**, ***Xingyi Deng***, *D. Sorescu, J. Lee*, National Energy Technology Laboratory

In this work, we study the energetics of CO_2 adsorbed on the bi- and tri-layer ZnO(0001) grown on Au(111) using temperature programmed desorption (TPD) and calculations based on density functional theory (DFT). Both bi- and tri-layer ZnO(0001) on Au(111) adopt a planar, graphite-like structure via an inter-layer relaxation to minimize the surface dipole arising from alternating Zn^{2+} and O^{2-} layers. CO_2 is adsorbed weakly on these planar ZnO(0001) surfaces, desorbing between 125-130 K in TPD. Two other desorption peaks were also observed in TPD at ~ 150 and 280-320 K and are attributed to the CO_2 adsorption at the steps between the bi- and tri-layer ZnO(0001) surfaces. This enhanced adsorption of CO_2 at the steps is supported by DFT calculations: the computed energetics of CO_2 adsorbed on surfaces and at steps is indeed consistent with that estimated from the TPD experiments via the Redhead method. Implications of our fundamental results for ZnO based catalysts will be discussed.

11:40am **SS+AS+NS-WeM12 Characterization of Band Gap and Lattice Constant of Ultrathin ZnO Layers on Au(111)**, ***Junseok Lee***, *D. Sorescu, X. Deng*, National Energy Technology Laboratory

Ultrathin layers of ZnO grown on the Au(111) substrate have been characterized using low-temperature scanning tunneling microscopy (STM). Under reactive deposition condition, the ZnO layers have been found to grow by forming islands. Detailed analysis of electronic structure have been conducted using scanning tunneling spectroscopy (STS) and the density functional theory (DFT) calculations. The band gap of ultrathin layers of ZnO is found to be larger compared to the bulk ZnO wurtzite structure. The density functional theory calculations provides understanding of the increased band gaps of thin ZnO layers. The lattice constants of ultrathin ZnO layers on Au(111) are also found to be larger than that of the bulk lattice constant, which could be explained by the formation of graphitic-like ZnO layers.

12:00pm SS+AS+NS-WeM13 Submonolayer Water Adsorption on Stepped and Planar Pt Surfaces, *Rachael Farber*, Loyola University Chicago, *M.J. Kolb*, Leiden Institute of Chemistry, *J. Derouin*, Loyola University Chicago, *M.T.M. Koper, L.B.F. Juurlink*, Leiden Institute of Chemistry, *D.R. Killelea*, Loyola University Chicago

The adsorption of water onto metal surfaces yields a host of intricate adsorbate structures at

coverages less than a single layer. Complex adsorption structures arise due to the delicate balance

of hydrogen bonding between water molecules as well as attractive forces between water molecules

and the metal surface. Therefore, the complexity of the system provides an excellent opportunity to

refine models of water-water and water-surface interactions. Water molecules are largely confined

to a single plane and, as a result, the geometry of aligned water molecules gives rise to frustrated

hydrogen bonding. At low coverages of water on metal surfaces, these frustrated intermolecular

interactions result in the formation of structures other than the classic hexagons of bulk water. We

will report the results of a combined theory-experiment study of water adsorption on planar Pt(111)

and stepped Pt(553). Experimentally, temperature programmed desorption (TPD) and ultra-high

vacuum scanning tunneling microscopy (UHV-STM) were used to quantify water coverage and to

image the resultant surface structures. On Pt(111), 5, 6, and 7-membered rings were found to form

across the Pt surface, in agreement with previously reported experimental results and electronic

structure calculations. On Pt(553), however, tetragonal structures that have not been previously

observed were found to form across monatomic steps. These observations confirm DFT

calculations for submonolayer water coverage on Pt(553) and provide fine details as to how water-

water and water-surface interactions are balanced on active metal surfaces.

Surface Science
Room: 112 - Session SS-WeM

Environmental Interfaces, Ambient Surfaces, In-Operando Studies and Adsorption on 2D Materials
Moderator: Peter Sutter, University of Nebraska - Lincoln

8:00am SS-WeM1 Liquid-Jet Ambient Pressure Photoelectron Spectroscopy Studies of the Liquid/Vapor Interface of 1-Propanol and 2-Propanol Aqueous Solutions, *Michael Makowski*, *J.M. Langford, D. Tobias, J.C. Hemminger*, University of California Irvine

The liquid/vapor interface of aqueous 1- and 2-propanol solutions for a broad range of concentrations was studied using a liquid-jet ambient pressure X-ray Photoelectron Spectroscopy system at the Advanced Light Source synchrotron in the Lawrence Berkeley National Laboratory. At low concentrations, 1-propanol displays a clear propensity to lie at the solution surface, evidenced by an enhanced carbon 1s XPS signal for electrons of low kinetic energy. Near a concentration (mole fraction) of 0.01 mf, a surface layer of 1-propanol appears to saturate, as evidenced by the saturation of the carbon 1s to oxygen 1s XPS signal ratio. Furthermore, over increasing concentrations carbon and oxygen 1s binding energies show a sharp redshift of 1 eV, until reaching a concentration of approximately 0.01 mf. This suggests an increasing 1-propanol density at the surface, with the resulting surface dipole layer causing a shift in the observed C1s and O1s binding energies for the condensed species.

These results of aqueous 1-propanol are compared and contrasted to similarly obtained aqueous 2-propanol carbon and oxygen spectra. Moreover, experimental results were corroborated with classical molecular dynamics simulations. Density profiles relative to an instantaneous interface were calculated for aqueous 1-propanol solutions. MD simulations indicate that 1-propanol accumulates at the surface at very low concentrations an a surface layer saturates at approximately 0.01 mf in agreement with the experimental results.

8:20am SS-WeM2 Near Ambient Pressure XPS at the SLS – *In Situ* Cell Design for Solid/Vapor Interfaces and First Results in Environmental TiO₂ Photocatalysis, *Fabrizio Orlando*, Paul Scherrer Institut, Switzerland, *A. Waldner*, Paul Scherrer Institut and ETH Zürich, Switzerland, *M.-T. Lee*, Paul Scherrer Institut and University of Bern, Switzerland, *M. Birrer, T. Bartels-Rausch*, Paul Scherrer Institut, Switzerland, *C. Proff*, Paul Scherrer Institut and ETH Zürich, Switzerland, *T. Huthwelker, A. Kleibert*, Paul Scherrer Institut, Switzerland, *J. van Bokhoven*, Paul Scherrer Institut and ETH Zürich, Switzerland, *M. Ammann*, Paul Scherrer Institut, Switzerland

Near ambient pressure X-ray photoelectron spectroscopy (NAPP) is a powerful tool to investigate elemental composition and chemical specificity of surfaces under reaction conditions that offers tremendous opportunities in environmental science and heterogeneous catalysis research. In the first part of this contribution I will provide a brief outlook on a new analysis chamber for the NAPP endstation at the Swiss Light Source that is designed for in situ XPS and NEXAFS at solid/vapor interfaces under environmentally relevant conditions of temperature and pressure (up to 20 mbar and 100% relative humidity) [1]. The flow-tube design of this new chamber allows to perform in situ measurements at high pressure and UHV conditions one after the other in the same analysis cell, while at the same time reducing the exposed volume and surface area of the analysis cell. Moreover, this chamber features (i) a direct access from a gas dosing system down to the sample, allowing for the admission of sticky gases with reduced wall effects, and (ii) a UV laser setup, providing the opportunity to investigate photoactive materials under atmospherically relevant conditions of pressure and light with reduced extent of gas phase photochemistry induced by the UV-light. We have used this novel chamber to investigate photocatalysis on TiO₂, which is a component of natural mineral dust that represents an important reactive aerosol in the atmosphere affecting the ozone budget and the climate. In this context, adsorption of water and hydroxylation of the surface, which are key aspects to understand TiO₂ photocatalysis in the environment, offer still major open questions. Earlier NAPP studies have provided important insight into the nucleation of water on this surface [2]. In a recent study we have quantified the effect of humidity on ozone-induced band bending on the TiO₂(110) surface [3], and found interesting changes in XPS and NEXAFS spectra indicative of changes in the hydrogen bonding structure in multilayers of water [4]. I will discuss our most recent NAPP investigation on the influence of UV light and humidity on the adsorption of water on a TiO₂ powder sample surface. Our results indicate an enhancement of water adsorption under UV irradiation, which might be the basis to explain light-induced superhydrophilicity previously observed on TiO₂-based nanomaterials. I will also briefly illustrate an application study on the uptake of trace gases on ice surface.

References

[1] F. Orlando et al., submitted.

[2] G. Ketteler et al., J. Phys. Chem C 111, 8278 (2007).

[3] M. Lampimäki et al., ChemPhysChem 14, 241 (2013)

[4] M. Lampimäki et al., J. Phys. Chem. C 119, 7076 (2015).

8:40am SS-WeM3 Ambient Pressure XPS Observation of Electrode Surfaces During Electrochemical Reactions, *Hirohito Ogasawara*, *S. Kaya, H.S. Sanchez Casalongue, M.L. Ng, D. Friebel, A. Nilsson*, SLAC National Accelerator Laboratory

We have been focusing on identifying the surface electronic structure and chemical nature of catalytic electrodes during electrochemical reactions through the use of synchrotron-based ambient pressure photoemission spectroscopy (APXPS) [1]. One of the crucial factors that limit electrochemical water splitting is the large overpotential required for the oxygen evolution reaction. Iridium oxide, which is one of the most widely used anode catalyst, has been shown to have high activity and stability in water electrolysis. APXPS studies indicate both oxide and hydroxide species on the catalyst surface. Under electrochemical oxygen evolution conditions, iridium undergoes a change in oxidation state, which takes place predominantly at the surface of the catalyst [2]. Molybdenum sulfides are promising materials in the search for cost-effective cathode catalyst. We tracked the transformation of amorphous MoS₃ nanoparticles during electrochemical hydrogen evolution reactions. We observed that surface sites are converted from MoS₃ to MoS₂ increasing MoS₂ edge-like sites with high activity [3]. The sluggish kinetics in oxygen reduction reaction is one of the key challenges in polymer electrolyte membrane fuel cells. We established that the species on the platinum catalytic electrode change drastically depending on the oxygen pressures. We used this knowledge to clarify that the reaction pathway is dependent on the operating conditions [4].

References

[1] S. Kaya, H. Ogasawara, L.-Å. Näslund, J.-O. Forsell, H. Sanchez Casalongue, D.J. Miller, A. Nilsson, *Catalysis Today* **205** (2013) 101

[2] H. Sanchez Casalongue, M.L. Ng, S. Kaya, D. Friebel, H. Ogasawara, A. Nilsson, *Angewandte Chemie* **126** (2014) 7297

[3] H. Sanchez Casalongue, J.D. Benck, C. Tsai, R.K.B. Karlsson, S. Kaya, M.L. Ng, L.G.M. Pettersson, F. Abild-Pedersen, J.K. Nørskov, H. Ogasawara, T.F. Jaramillo, A. Nilsson, *J. Phys. Chem. C* **118** (2014) 29252

[4] H. Sanchez Casalongue, S. Kaya, V. Viswanathan, D.J. Miller, D. Friebel, H.A. Hansen, J.K. Nørskov, A. Nilsson, H. Ogasawara, *Nature Communications* **4** (2013) 2817

9:00am SS-WeM4 Formation of Heterogeneous Multiple-Oxide/Hydroxide Species on a GaP(111) Surface Tracked by *In Situ* Near-Ambient Pressure XPS, *Xueqiang Zhang, S. Ptasinska*, University of Notre Dame

A photoelectrochemical (PEC) solar cell for water splitting converts solar energy into chemical energy and store it in the form of hydrogen, which is a promising candidate of sustainable and clean fuels. PEC solar cells consisted of phosphide-based III-V semiconductors are known to have a higher solar to hydrogen conversion efficiency than other materials. They are, however, usually limited by technological drawbacks such as photocorrosion or decreased electron extraction efficiency due to the formation of surface oxide species. The formation of surface oxides becomes critical when operating electrodes are exposed to aqueous electrolytes or to ambient conditions. Therefore, it is desirable to understand the interfacial processes of water interactions with semiconductors, and to elucidate possible oxidation and reduction mechanisms at the H_2O/semiconductor interface, especially under near realistic conditions.

In this study, water dissociative adsorption onto a GaP (111) surface was investigated using near ambient pressure X-ray photoelectron spectroscopy (NAP XPS) at various pressures and temperatures [1]. This advanced technique allowed us to monitor the H_2O/semiconductor interfacial chemistry under *operando* conditions, which would not be feasible to be investigated by traditional surface sensitive techniques. The interfacial chemistry was tracked by recording high-resolution photoemission spectra of Ga $2p_{3/2}$, O 1s, and P 2p. In the pressure-dependent study conducted at room temperature, ~300 K, the enhancement of surface Ga hydroxylation and oxidation was observed with an increase in H_2O pressures. This finding was also confirmed by changes observed in the photoemission spectra of O 1s. In the temperature dependent study, surface Ga hydroxylation and oxidation were further enhanced at temperatures below 673 K. While a large-scale conversion of surface O-Ga-OH species into Ga hydroxide, along with surface P oxidation, were observed at 773 K. Moreover, the formation of Ga and P oxide/hydroxide networks was suggested and a "phase diagram" that demonstrates the distribution of different chemical species under various experimental conditions has been generated (supplemental document). Our results led to a better understanding of the H_2O/semiconductor interfacial chemistry and the water splitting mechanism in the PEC solar cells.

Reference

1. Zhang, X., Ptasinska, S. Distinct and dramatic water dissociation on GaP(111) tracked by near-ambient pressure X-ray photoelectron spectroscopy. Phys. Chem. Chem. Phys., 2015, 17, 3909-3918.

9:20am SS-WeM5 Investigation of Liquid/Solid Interfaces using Photoelectron Spectroscopy, *Hendrik Bluhm*, Lawrence Berkeley Lab, University of California, Berkeley **INVITED**

Solid/vapor, liquid/vapor and liquid/solid interfaces govern many processes in the environment, heterogeneous catalysis, and technology. Ambient pressure photoelectron spectroscopy is an excellent method for the characterization of these interfaces under operating conditions, in particular since it affords to correlate the elemental and chemical composition at the interface with the electrical potentials. This talk will focus on the application of APXPS to the investigation of liquid/solid surfaces under realistic conditions, which is arguably the next frontier in surface science. We will highlight the application of ambient pressure XPS in combination with standing waves for the investigation of the electric double layer at solid liquid interfaces in environmental science and corrosion chemistry.

11:00am SS-WeM10 Surface and Bulk Crystallization Kinetics of Amorphous Solid Water Nanoscale Films, *R. Scott Smith, C. Yuan, R.A. May, B.D. Kay*, Pacific Northwest National Laboratory

We investigate the crystallization kinetics of nanoscale amorphous solid water (ASW) films using temperature-programmed desorption (TPD) and reflection absorption infrared spectroscopy (RAIRS). ASW is a metastable form of water created by vapor deposition on a cold substrate (T < 130 K). In prior work, we reported the episodic release of trapped gases in concert with the crystallization of ASW, a phenomenon that we termed the "molecular volcano." The observed abrupt desorption is due to the formation of cracks that span the film to form a connected pathway for

release. In a recent study we used the selective placement of an inert gas layer is used to show that cracks form near the top of the film and propagate downward into the film. Those experiments showed that, after some induction time, cracks propagate linearly in time with an Arrhenius dependent velocity consistent with the crystallization growth rates reported by others. This suggested a direct connection between the crystallization growth and the crack propagation rate. In the present study we directly measure the surface (using TPD) and bulk (using RAIRS) ASW crystallization kinetics as a function of film thickness. These results show that nucleation and crystallization begins at the ASW/vacuum interface and then the crystallization growth front propagates linearly into the bulk. The details of the experiment and the interpretation of the results will be discussed in detail.

11:20am SS-WeM11 Environmental Effects on Oxidative Surface Passivation Across $Al_xFe_yNi_{1-x-y}$ Composition Space, *Matthew Payne, J.B. Miller, A.J. Gellman*, Carnegie Mellon University

Alloys that derive robust oxidation resistance by the preferential formation of a passivating Al_2O_3 scale are commonly used for structural applications in thermochemically harsh operating environments. Often, one of the primary design concerns is to determine the lowest Al content required to induce passivation, so as to minimally impair the mechanical properties of the material. This "critical Al concentration" is kinetically dictated and can depend strongly on both multicomponent composition and the nature of the oxidizing environment. We have previously developed high-throughput methodology to study oxidation using composition spread alloy films (CSAFs), combinatorial sample platforms with continuous lateral composition gradients. Behavior related to oxidative corrosion and passivation can be characterized continuously across an entire ternary composition space with a single CSAF, using a combination of spatially resolved techniques including optical imaging, scanning electron microscopy, energy-dispersive X-ray spectroscopy, Raman spectroscopy, and X-ray photoemission depth profiling. We have used this methodology to compare the oxidation of $Al_xFe_yNi_{1-x-y}$ alloys at 700 K in dry-air and humid-air environments. The critical Al concentration in the Fe-rich region of composition space was found to be significantly higher for exposure to the humid air. The continuous nature of the results provides valuable fundamental insight into the interplay of composition and environment on alloy oxidation kinetics.

11:40am SS-WeM12 Hydrogen-Bonded Self-Assembled Molecular Structures on Hexagonal Boron Nitride, *Vladimir Korolkov, S. Svatek, L. Yang, J. Kerfoot, A. Summerfield, N. Champness,* University of Nottingham, UK*, T. Taniguchi, K. Watanabe,* The National Institute for Materials Science, Japan*, N. Besley, P. Beton*, University of Nottingham, UK

Hexagonal boron nitride (h-BN) is a layered material and a wide-gap semiconductor with a band gap of 5.2 e.V. The latter property makes it highly attractive as a support to study optical and electrical properties of monolayered molecular assemblies stabilized by non-covalent interactions. Although h-BN has been known since 1940s it is a relatively new substrate in the area of molecular self-assembly. In part this is due to the widespread use of scanning tunneling microscopy to acquire images of molecules, but this technique is not compatible with h-BN.

The adsorption of a range of molecules on BN and other layered materials has been investigated using using high resolution atomic force microscopy (AFM). We have observed several arrangements of molecules which are stabilized by hydrogen bonding including a bimolecular layer formed by perylene tetracarboxylic di-imide (PTCDI) and melamine which form an open nanporous array in which the planar PTCDI molecules are adsorbed parallel to the substrate. The networks are deposited from solution by immersion of BN substrate and the ordering may be improved by post-annealing in an inert atmosphere. We have also investigated the adsorption of 5,10,15,20-tetrakis(4- carboxylphenyl)porphyrin (TCPP), a dye molecule with a planar porphyrin macrocycle as its core. This molecule forms an open square array, also stabilized by hydrogen bonding through carboxlic acid pendant groups which steer the arrangement so that macrocycle lies parallel to the surface. In this arrangement the molecular layer is strongly fluorescent showing lines which are red-shifted from solution. When molecules are adsorbed on MoS2 they form similar structures but the resulting islands are smaller and less ordered, and, due to the smaller band gap of MoS2, fluorescence is quenched. We also present density functional theory calculations of the conformation of adsorbed molecules and numerical estimates of the hydrogen bonding and adsorption energies. We

discuss this approach as a route to the molecular functionalization of two-dimensional materials and the formation of hybrid molecular devices.

The work will present an outstanding examples of single molecule and submolecular resolution achieved in the ambient on standard Atomic Force Microscopes. Most of the presented results will be on level with the published UHV-STM studies.

12:00pm SS-WeM13 Suppression of the Topological Surface State of Bi$_2$Te$_3$ by the Organic Molecule Manganese Phthalocyanine, *Andrew Hewitt, J. Boltersdorf, P.A. Maggard, D.B. Dougherty*, North Carolina State University

Organic molecules coupled to the spin-textured topological surface states of a topological insulator (TI) are expected to result in an interface ideal for organic spintronic devices.[1] Exploiting interfacial control at molecule-functionalized TI surface is a crucial step in realizing the potential of these new materials. It has been shown[2] that such a coupling may exist, along with a new hybrid-interface state above the Fermi level, between the magnetic molecule Manganese Phthalocyanine (MnPc) and the TI Bi$_2$Te$_3$. We report the suppression of the topological surface state by the adsorption of MnPc molecules as measured by Ultraviolet Photoelectron Spectroscopy. We show a new state emerging below the Fermi level at less than a monolayer coverage of MnPc molecules. The new interface state is different than the topological surface state and the molecular orbitals of the MnPc molecules as evidenced by the modified dispersion with Angle-Resolved Photoelectron Spectroscopy. We also observe an *n*-doping effect as charge is transferred from the molecule to the TI substrate in agreement with recent work.[2,3] We suggest that this interface system may have important implications for understanding the role of local time reversal symmetry breaking in TI's and in controlling spin injection into these novel materials.

[1] Jakobs *et al.* DOI: 10.1021/acs.nanolett.5b02213

[2] Sessi *et al.* Nano Lett. 2014, 14, 5092−5096

[3] Bathon *et al.* Nano Lett. 2015, 15, 2442−2447

Thin Film
Room: 114 - Session TF+SS-WeM

ALD Surface Reactions and Precursors
Moderator: Sean Jones, National Science Foundation (NSF), Paul Poodt, Solliance/TNO

8:00am TF+SS-WeM1 High Performance Precursors for Atomic Layer Deposition of Silicon Containing Films, *Anu Mallikarjunan*, Air Products and Chemicals, Inc. **INVITED**

Conformal and continuous silicon containing films produced by Atomic Layer Deposition (ALD) are enabling novel processing schemes and integrated device structures. The increasing drive towards lower temperature processing requires new precursors with even higher reactivity. A systematic method for identification of high performance precursors is thus very desirable, and needs to incorporate fundamental understanding of precursor chemistry, surface reactions; and relationships between precursor structure and deposited films. The overall approach accordingly relies on integrating molecular and surface reaction modeling, the ability to synthesize stable precursors with reactive groups, in-situ surface studies, and thin film deposition testing. To illustrate this approach, two case-studies will be discussed in this presentation: silicon oxide and silicon nitride ALD. In both cases, a representative monoaminosilane (R^1 R^2 N)SiH$_3$ called di - sec- butylaminosilane (DSBAS) will be studied. The impact of changing the precursor structure will also be discussed.

8:40am TF+SS-WeM3 Amorphous In$_2$O$_3$ and Sn-doped In$_2$O$_3$ Layers by ALD Prepared using Trimethyl Indium and Ozone, *Anil Mane, A. Allen*, Argonne National Laboratory, *R. Kanjolia*, SAFC Hitech, *J. Elam*, Argonne National Laboratory

Abstract:

Among the transparent conducting oxides (TCOs), Indium oxide (In$_2$O$_3$) possesses a wide band gap of 2.9 Ev at room temperature yielding high optical transparency and also exhibits good chemical stability. When doped with tin to form Indium tin oxide (ITO), the electrical conductivity increases greatly allowing this material to be used in a wide range of applications including touch screens displays, light-emitting diodes, liquid crystal displays, and sensors. Further amorphous TCOs have several advantages over their crystalline microstructures e.g. lower temperatures deposition which tend to simplify the deposition methods for mainly for plastics for flexible electronics. The lack of grain boundaries in amorphous materials, isotropic nature allows a simpler scheme for uniform etching with

lower surface roughness. Unlike crystalline TCOs, the amorphous TCOs electrical and optical are also strongly influenced by the oxygen content of the films. As ALD offers the potential to deposit ITO over large areas at low temperature with high uniformity to address some of these applications, but the viability of this method hinges on developing a robust In$_2$O$_3$ ALD process. Trimethyl indium (TMIn) is an attractive economical precursor for In$_2$O$_3$ ALD because it offers the advantages of a high vapor pressure and availability in high volume.

In this study we examined the ALD of In$_2$O$_3$ using alternating exposures to TMIn and different oxygen sources: O$_3$ (ozone), O$_2$, H$_2$O, and H$_2$O$_2$. We first used in situ quartz crystal microbalance (QCM) and mass spectrometry measurements to evaluate the effectiveness of the different oxygen sources and found that only ozone yielded sustained growth. These measurements also provided details about the In$_2$O$_3$ growth mechanism and enabled us to verify that both the TMIn and the O$_3$ surface reactions were self-limiting. Next, we prepared ALD In$_2$O$_3$ films on a variety of substrates and characterized them using X-ray diffraction, UV-vis. Spectrometry, spectroscopic ellipsometry, X-ray photoelectron spectroscopy, Hall probe measurements, scanning electron microscopy, and atomic force microscopy. We found that at deposition temperatures of 100-200ºC the amorphous growth per cycle was nearly constant at ~0.4 Å/cycle and the films were dense and pure. At higher growth temperatures the In$_2$O$_3$ growth rate increased due to thermal decomposition of the TMIn. We succeeded in doping the amorphous In$_2$O$_3$ films with tin by substituting tetrakis-(dimethylamino) tin for the TMIn in a fraction of the growth cycles and observed that the electrical conductivity improved substantially in these films.

9:00am TF+SS-WeM4 Towards Organic Electronics: Atomic Layer Like Deposition of ZnS and ZnO on Organic Thin Films, *Z. Shi, Amy Walker*, University of Texas at Dallas

We discuss our recent studies of atomic layer like deposition (ALLD) of ZnS and ZnO on organic thin films using diethyl zinc (DEZ) as the zinc source. This work has important applications in photovoltaics, molecular and organic electronics, sensing, photonics and other technologies. We show that a detailed understanding of the reaction pathways is critical for controlling the properties of ZnO and ZnS films grown by ALD. For both ZnO and ZnS ALLD, the growth rates on –COOH terminated SAMs are approximately 10 % lower than on –OH terminated SAMs. As expected on −OH terminated SAMs, the DEZ reacts with the hydroxyl group. However, on –COOH terminated SAMs DEZ reacts with both the carbonyl and hydroxyl bonds present leading to the formation of a ketone rather than deposition. Further, the composition of the deposited layer and its growth can be affected by the functionality of the surface. For ZnO ALLD, on-COOH terminated SAMs XPS indicates that the initial composition of the layer is similar to Zn(OH)$_2$. In contrast on –OH terminated SAMs the deposited layer is always composed on ZnO. The growth of the layer also appears to be different. On –COOH terminated SAMs, the layer growth is more two dimensional (layer-by-layer) while on –OH terminated SAMs, the growth appears to proceed via the formation of islands.

9:20am TF+SS-WeM5 AlF$_3$ Atomic Layer Deposition or Al$_2$O$_3$ Atomic Layer Etching from Sequential Exposures of Trimethylaluminum and HF, *Jaime DuMont, Y. Lee, S.M. George*, University of Colorado at Boulder

Sequential exposures of Al(CH$_3$)$_3$ [trimethylaluminum (TMA)] and HF can lead to either AlF$_3$ atomic layer deposition (ALD) or Al$_2$O$_3$ atomic layer etching (ALE). The observation of AlF$_3$ ALD or Al$_2$O$_3$ ALE depends on temperature and pressure. AlF$_3$ ALD occurs at lower temperatures and higher pressures. Al$_2$O$_3$ ALE of an initial Al$_2$O$_3$ film occurs at higher temperatures and lower pressures. The AlF$_3$ ALD or Al$_2$O$_3$ ALE were investigated using *in situ* Fourier transform infrared (FTIR) spectroscopy and quartz crystal microbalance (QCM) measurements.

The FTIR analysis observed AlF$_3$ ALD or Al$_2$O$_3$ ALE by measuring the absorbance gain of Al-F stretching vibrations in AlF$_3$ or the absorbance loss of Al-O stretching vibrations in Al$_2$O$_3$. At lower temperatures, the HF exposures react with the underlying Al$_2$O$_3$ surface to form AlF$_3$ and HF molecules on the surface. TMA molecules subsequently react with HF on the surface to yield AlF(CH$_3$)$_2$ surface species. AlF(CH$_3$)$_2$ is then converted to AlF$_3$ with the next HF exposure producing AlF$_3$ ALD. At higher temperatures, the HF exposures react with the underlying Al$_2$O$_3$ surface to form AlF$_3$ and fewer HF molecules absorb on the surface. TMA then accepts fluorine from AlF$_3$ to form AlF(CH$_3$)$_2$ which desorbs from the surface and leads to etching of the initial Al$_2$O$_3$ film.

The effect of pressure was also explored by adjusting the N$_2$ carrier gas flow from 0-150 sccm to vary the background pressure from 30 mTorr to 1.6 Torr. These FTIR experiments revealed that the transition from AlF$_3$ ALD to Al$_2$O$_3$ ALE occurred at higher temperatures for higher background pressures. The higher pressures apparently produce a "cage effect" and

increase the lifetime of the AlF(CH$_3$)$_2$ surface species that leads to AlF$_3$ ALD. The QCM experiments measured an AlF$_3$ ALD growth rate that progressively decreased at higher temperatures and went negative at >250°C when TMA and HF etched the AlF$_3$ or Al$_2$O$_3$ films.

9:40am TF+SS-WeM6 A Comparison of Water Delivery Methods for Atomic Layer Deposition, *Tariq Ahmido, W.A. Kimes, B.A. Sperling, J.E. Maslar*, NIST

Water is frequently used as an oxygen source for atomic layer deposition (ALD) of metal oxides. However, water exhibits a relatively high vapor pressure at room temperature and readily adsorbs on reactor surfaces. These characteristics can make it difficult to reproducibly control water delivery during ALD, particularly when small quantities are desired. The focus of this work is characterizing and comparing three different methods of water vapor delivery in an effort to identify techniques for ensuring reproducible delivery of water vapor quantities. For this investigation, three methods of water injection were compared. The first method utilizes a needle valve between the water reservoir and the water injection valve (the valve that controls the water allowed into the delivery line to the reactor). This method is commonly employed for research grade reactors as the use of an adjustable orifice permits the water flow rate to be varied. However, control of small water quantities can be difficult due to the buildup of water vapor between the needle valve and the water injection valve. The second method overcomes this control limitation by utilizing a pump to vent water vapor from the volume between the needle valve and injection valve prior to injection into the delivery line. This method provides a high degree of control at the cost of added complexity and expense. The third method utilizes a laser-drilled orifice in a VCR gasket as the flow-controlling orifice. This method is simple and inexpensive, however, water flow rates cannot be adjusted without changing the orifice. The performance of these three water injection methods was characterized using an optical water mass flow meter (MFM) that has been developed to rapidly quantify water vapor. This MFM was based upon a wavelength modulation spectroscopic technique utilizing a near-infrared diode laser. This MFM permits quantitative comparison of the performance of these three water injection methods, allowing a potential user to identify method suited to a particular application.

11:00am TF+SS-WeM10 Stoichiometric Dependence of the Interface of HfO$_2$ ZrO$_2$, TiO$_2$, Ta$_2$O$_5$ and La$_2$O$_3$ on Si (100) by ALD, *Pierre Mani*, Universidad Autónoma de Ciudad Juárez-IIT, Mexico, *E. Lopez*, Universidad Autónoma de San Luis Potosí, Mexico, *H. Leos*, Universidad Autónoma de Ciudad Juárez-IIT, Mexico, *H. Hernandez*, Universidad Autónoma de San Luis Potosí, Mexico, *J.A. Hernandez, J.R. Farias, J.T. Elizalde*, Universidad Autónoma de Ciudad Juárez-IIT, Mexico, *M.A. Melendez*, CINVESTAV, Mexico, *M.A. Vidal*, Universidad Autónoma de San Luis Potosí, Mexico

A systematic analysis was performed to determine the characteristic times of surface coverage of oxidant-agent on silicon substrates (100) by the atomic layer deposition (ALD) method in order to ensure the saturation of the surface substrate for growth. The aperture-times of the precursors have been studied due to stoichiometric impact of the layers and also at the interface. The numbers of cycles were critical for the interface formation at the early stage growth. This work emphasizes in the study and analysis between interface of high k dielectric layer and amount of cycles as function of layers and stoichiometric interface. Previous works complement with results obtained in study the growth of hafnium oxide and titanium oxide by atomic layer deposition (ALD) demonstrating the close relationship between the thickness and composition of the interface layer with the number of cycles performed by the ALD and with the aperture-time of the precursors. This analysis shows a base that will allow create HfO2 ZrO2, TiO2, Ta2O5, La2O3 nanofilms with optimal characteristics.

11:20am TF+SS-WeM11 In-situ Infrared Study of Atomic Layer Deposition of Molybdenum Nitride using Bis(tert-Butylimido)-Bis(dimethylamido) Molybdenum and Hydrazine, *Abraham Vega, C.E. Nanayakkara*, The University of Texas at Dallas, *G. Liu, R. Kanjolia*, SAFC Hitech, *Y.J. Chabal*, The University of Texas at Dallas

Molybdenum nitride films have properties such as high hardness, high melting point, good chemical stability and high conductivity, which makes them suitable for a wide range of technological areas, as diffusion barriers or interconnections in microelectronics and even as catalysts in fuel cells. Molybdenum nitride films have been deposited by variety of techniques, such as chemical vapor deposition, magnetron sputtering, and atomic layer deposition among others.

For atomic layer deposition of molybdenum nitride, molybdenum complexes containing alkylamido and alkylimido ligands are being considered as potential molybdenum precursors. A notable advantage is that they do not produce corrosive byproducts compared to halide based

transition metal precursors.[1] A uniform growth has been achieved in the range 260 – 300 ^{0}C with bis(tert-butylimido)-bis(dimethylamido)molybdenum when used with NH$_3$ as a co-reactant.[1]

In this study, *in-situ* IR and X-ray photoelectron spectroscopies are used to investigate ALD of bis(tert-butylimido)-bis(dimethylamido)molybdenum and hydrazine an alternative for NH$_3$ as co-reactant for molybdenum nitride deposition on pre-annealed, oxidized and OH-terminated Si(100) surfaces. While bis(tert-butylimido)-bis(dimethylamido) molybdenum is expected to react with two surface OH groups leaving one amino groups with further reaction with hydrazine leading to a NH$_x$-terminated surface, the details of the reactions have not been explored, hence the importance of *in-situ* IR spectroscopy.

Bis(tert-butylimido)-bis(dimethylamido) molybdenum reacts with surface Si-OH groups (loss at 3740 cm^{-1}) to form the expected (O)$_2$-Mo=(N-tBu)$_2$structure, as evidenced by broad band from various CH$_x$ stretch bands in the 2900 cm^{-1} region and stretching of CN bonds at 1240 cm^{-1}, respectively. The first hydrazine pulse leads to a loss of tBu vibrational bands [at 2900 and 1240 cm^{-1}]. The steady state ALD process is characterized by tBu removal by hydrazine and formation of NH$_x$ groups driving the ALD process. A clear ligand exchange is observed at deposition temperatures of 225, 250 and 275 $^\circ$C for 30 cycles. The ALD window for this process was found to be between 225 and 275 $^\circ$C, with low carbon content determined by XPS, which is lower than the window when using NH$_3$ (260-300 °C) instead of hydrazine. No growth is observed above 300 °C, and very poor quality films are obtained at 200°C.

This work confirms the reactivity of bis(tert-butylimido)-bis(dimethylamido) molybdenum with OH-terminated surfaces at low temperatures and illustrates the role of the co-reactant on the thermal window and the quality of the resulting molybdenum nitride films.

1. Chem. Mater., Vol. 19, No. 2, 2007

11:40am TF+SS-WeM12 Atomic-Layer-Deposited In$_2$O$_3$:H Transparent Conductive Oxides: How to Achieve the Best Possible Carrier Mobility, *Bart Macco**, Eindhoven University of Technology, Netherlands, *H.C.M. Knoops*, Oxford Instruments Plasma Technology, UK, *M.A. Verheijen, W.M.M. Kessels*, Eindhoven University of Technology, Netherlands

Recently, we have reported on an atomic layer deposition (ALD) process to prepare H-doped indium oxide (In$_2$O$_3$:H) transparent conductive oxides (TCOs) with an extremely high carrier mobility (138 cm^2/Vs) and low resistivity (0.27 mΩcm) at low processing temperatures (<200 $^\circ$C) [1]. This high carrier mobility is especially promising for silicon heterojunction solar cell applications, as it allows for a low resistivity at low carrier density, thereby nullifying parasitic free carrier absorption in the infrared. Here we focus on new insights into the physical mechanisms during the preparation process and explain how such high mobility can be obtained through analysis of the electron scattering and doping mechanisms.

The preparation starts with ALD of In$_2$O$_3$:H at 100 ^{o}C using InCp, H$_2$O and O$_2$ as growth precursors. The films are amorphous, although a low density of very small crystallites is present. Subsequently the films are crystallized by annealing at 150-200 ^{o}C. Electron microscopy reveals that crystallization proceeds from grain growth from the pre-existing crystallites without additional nucleation, which makes the final grain size and optoelectronic properties independent of annealing temperature. The resulting crystals extend over the film thickness of 75 nm and have a typical lateral size of a few hundred nm. Analysis of the grain growth by electron microscopy shows a thermally activated behavior, with an activation energy of 1.4 eV.

A combination of temperature-dependent Hall measurements and spectroscopic ellipsometry has been employed to distinguish between the various scattering mechanisms and dopants in crystallized In$_2$O$_3$:H films. Key results include the fact that carrier mobility is only limited by ionized impurity and phonon scattering processes and that other extrinsic defect scattering such as neutral impurity and grain boundary scattering can be neglected. Since only unavoidable scattering processes play a role, this means that this TCO has the highest possible mobility at this carrier density. The analysis also excludes a significant contribution from doubly charged donors (i.e. oxygen vacancies), and the source of doping is confirmed to be singly charged H. Furthermore, by comparison of the absolute H-concentration and the carrier density in crystallized films, it is deduced that <4 % of the incorporated H is an active dopant in crystallized films. Therefore, it can be concluded that inactive H atoms do not contribute to defect scattering, which explains why In$_2$O$_3$:H films are capable of achieving a much higher carrier mobility than conventional In$_2$O$_3$:Sn films.

[1] Macco et al., *P.S.S. - Rapid Res. Lett.*, DOI: 10.1002/pssr.201409426

---

* TFD James Harper Award Finalist

12:00pm TF+SS-WeM13 Mechanical Property and Corrosion Resistance Evaluation of CrVN and CrSiN Thin Films Grown by a Hybrid High Power Impulse Magnetron Sputtering and Radio Frequency Sputtering Technique, *Jyh-Wei Lee*, *C.Y. Cheng, P.W. Chang,* Ming Chi University of Technology, Taiwan, Taiwan, Republic of China*, B.S. Lou,* Chang Gung University, Taiwan, Taiwan, Republic of China

High power impulse magnetron sputtering (HIPIMS) is a novel coating technology, which is characterized for its high peak power density to achieve unique thin film properties, such as high hardness, good adhesion and tribological performance. The aim of this work was to systematically study the microstructure, mechanical properties and corrosion resistance of CrVN and CrSiN coatings fabricated by a hybrid high power impulse magnetron sputtering and radio frequency sputtering technique. The experimental results showed that the peak power density increased linearly as the duty cycle decreasing from 5% to 2.5%. As compared with the CrVN coating, the higher hardness and better corrosion resistance were obtained for the CrSiN coatings, which can be attributed to their denser microstructures fabricated using the HIPIMS technology under optimal duty cycle and pulse frequency in this work. Effects of Vanadium and Silicon elements on the microstructure, mechanical and electrochemical properties of CrVN and CrSiN coatings were also discussed.

2D Materials Focus Topic
Room: 212C - Session 2D+EM+IS+MC+NS+SP+SS-WeA

Dopants and Defects in 2D Materials

Moderator: Daniel Gunlycke, Naval Research Laboratory, Zenghui Wang, Case Western Reserve University

2:20pm 2D+EM+IS+MC+NS+SP+SS-WeA1 The Effect of Defect Density on the Mechanical Properties of Graphene, *Jonathan Willman*, *J.M. Gonzales,* University of South Florida*, R. Perriot,* Los Alamos National Laboratory*, I.I. Oleynik,* University of South Florida

Recent experiments involving nanoindentation of graphene have demonstrated counterintuitive weakening of Young's modulus with increasing concentrations of point defects in graphene in contradiction to previous investigations. To fully resolve these inconsistencies we perform large-scale molecular dynamics simulations of nanoindentation under conditions of Atomic Force Microscopy (AFM) nanoindentation experiments. The reliable description of interatomic interactions is achieved by using recently developed screened environment-dependent bond order (SED-REBO) potential. The elastic properties of the defective graphene, the breaking strength and the mechanisms of fracture under indenter are investigated as a function of type of point defects as well as their concentration.

2:40pm 2D+EM+IS+MC+NS+SP+SS-WeA2 Investigation of Grain Boundaries in CVD Grown MoS$_2$, *Kolyo Marinov*, *D. Ovchinnikov, D. Dumcenco, A. Kis*, Ecole Polytechnique Fédérale de Lausanne (EPFL), Switzerland

We present the characterization of grain boundaries in polycrystalline CVD-grown MoS$_2$ films. Epitaxial growth on sapphire substrates is achieved leading to preferred orientation of the domains, which is confirmed by transmission electron microscopy experiments. Using Scanning Kelvin probe microscopy the local potential drop across the three predominant types of grain boundaries in field effect transistors is investigated. These measurements demonstrate that the interfaces between single grains do not degrade the electrical conductivity, which is due to the well aligned growth of the single domains. Furthermore, the relatively high mobility of electrons in the polycrystalline material stays constant even in devices with channels of 80 µm containing multiple grains, separated by grain boundaries. Our approach is a step forward to fabrication of large-area, uniform and high quality single-layer CVD MoS$_2$.

3:00pm 2D+EM+IS+MC+NS+SP+SS-WeA3 Polycrystalline 2D Materials: Atomic Structure and Electronic Transport Properties, *Oleg Yazyev*, Ecole Polytechnique Fédérale de Lausanne (EPFL), Switzerland **INVITED**

Grain boundaries and dislocations are intrinsic topological defects of polycrystalline materials, which inevitably affect their physical properties. In my talk, I will discuss the structure of topological defects in two-dimensional (2D) materials such as graphene and monolayer transition metal dichalcogenides (TMDCs) [1].

I will first introduce a general approach for constructing dislocations in graphene characterized by arbitrary Burgers vectors and grain boundaries covering the complete range of possible misorientation angles. By means of first-principles calculations we address the thermodynamic properties of grain boundaries revealing energetically favorable large-angle configurations as well as dramatic stabilization of small-angle configurations via the out-of-plane deformation, a remarkable feature of graphene as a two-dimensional material [2]. Both the presence of stable large-angle grain-boundary motifs and the out-of-plane deformation of small-angle configurations have recently been observed by scanning tunneling microscopy [3].

In the rest of my talk, I will focus on the electronic transport properties of polycrystalline 2D materials. Ballistic charge-carrier transmission across periodic grain boundaries is governed primarily by momentum conservation. Two distinct transport behaviors of such grain boundaries in graphene are predicted − either perfect reflection or high transparency with respect to low-energy charge carriers depending on the grain boundary periodicity [4]. It is also shown that certain periodic line defect structures can be engineered and offer opportunities for generating valley polarized charge carriers [5]. Beyond the momentum conservation picture we find that the transmission of low-energy charge carriers can be dramatically suppressed in the small-angle limit [6]. Unlike graphene, TMDCs combine a two-valley electronic band structure with strong spin-orbit effects. The

latter can be employed for creating spin-polarized currents and adds yet another conservation law in the electronic transport across regular defects such as the frequently observed inversion domain boundaries [7,8].

[1] O. V. Yazyev and Y. P. Chen, Nature Nanotechnology **9**, 755 (2014).
[2] O. V. Yazyev and S. G. Louie, Phys. Rev. B **81**, 195420 (2010).
[3] Y. Tison *et al.,* Nano Lett. **14**, 6382 (2014).
[4] O. V. Yazyev and S. G. Louie, Nature Materials **9**, 806 (2010).
[5] J. H. Chen *et al.,* Phys. Rev. B **89**, 121407(R) (2014).
[6] F. Gargiulo and O. V. Yazyev, Nano Lett. **14**, 250 (2014).
[7] A. Pulkin and O. V. Yazyev, s*ubmitted.*
[8] O. Lehtinen *et al.,* ACS Nano **9**, 3274 (2015).

4:20pm 2D+EM+IS+MC+NS+SP+SS-WeA7 Defects Compensation and Refining Optical Luminescence in Organic/Transition Metal Dichalcogenide Heterostructure, *J.H. Park*, UC San Diego, *A.M. Sanne, H.C.P. Movva*, UT-Austin, *S. Vishwanath*, Cornell University, *Il Jo Kwak*, UC San Diego, *H. Xing*, Cornell University, *J. Robertson*, University of Cambridge, UK, *S.K. Banerjee*, UT-Austin, *A.C. Kummel*, UC San Diego

Since layered transition-metal dichalcogenides(TMD) have demonstrated novel electronic and optoelectronic property, intense research has focused synthesis and integration into future electronic devices. Unlike graphene, TMD materials have band gaps, and these band structures can be tuned by thickness. However, in many cases, unintentional defects can be observed on TMD giving rise to the degradation of performance in the devices. Even for mechanical exfoliated TMD, there is a high density of defects, such as vacancies. For successful integration of TMD into devices, proper passivation of defects on TMD requires high stability in ambient conditions. In this study, a TiOPc monolayer was employed for passivation of defects to improve electrical and optical properties in TMD devices. Multilayer MoS$_2$ flakes were cleaved in ambient condition and transferred into the UHV chamber; afterwards. TiOPc monolayers were deposited on the MoS$_2$ surfaces by organic molecular beam epitaxy. After deposition, TiOPc forms a monolayer with only few defects, and the TiOPc monolayer structure has square lattice in a 1.5x1.5 nm grid. This crystal structure indicates that each TiOPc in the monolayer is directed outward to vacuum. The deposited TiOPc layer has very high thermal stability on MoS$_2$; the TiOPc layer on MoS$_2$ requires annealing above of 673K for desorption. This high thermal stability indicates there are strong interaction between TiOPc and MoS$_2$ surface. STS shows the band gap of the monolayer is 1.8 eV, while bulk MoS$_2$ has a 1.3eV band gap. Moreover, the Fermi level of TiOPc/bulk MoS$_2$ is shifted to the valence band, consistent with a P type shift. However, bulk MoS$_2$ surface, where less than monolayer of TiOPc was deposited, has Fermi level shifted towards the conduction band, consistent with N type doping. In the single layer MoS$_2$ deposited TiOPc monolayer, threshold bias is shifted from -30 V to near O V, indicating P-doping of MoS$_2$. It can be hypothesized that the work function transition of MoS2 is changed as a function of thickness. Before deposition of the TiOPc monolayer, the defects peak corresponded to S vacancy is displayed at 1.7 eV in photoluminescence. Conversely, the deposition of TiOPc monolayer almost completely suppresses S vacancy peak located 1.7 eV. Moreover, in the single layer MoS$_2$ FET, the on/off ratio is enhanced more than 2 orders magnitude. The similar charge transfer behavior also can be observed in TiOPc/WSe$_2$; on the bilayer WSe$_2$/HOPG, the TiOPc monolayer deposited on the first layer of WSe$_2$ shows the a conduction band shifted Fermi level, while a TiOPc monolayer deposited on the second layer of WSe$_2$ shows a valence band shifted Fermi level.

4:40pm 2D+EM+IS+MC+NS+SP+SS-WeA8 Reactivity and Wettability of PVD Metals on 2D Transition Metal Dichalcogenides, *Christopher Smyth*, *S. McDonnell, R. Addou, H. Zhu, C.L. Hinkle, R.M. Wallace*, University of Texas at Dallas

Transition metal dichalcogenides (TMDs) have been studied for years due to their tribological properties, but recent discoveries have illuminated unique opportunities for the use of single or few layer TMDs in electronics, specifically tunnel field effect transistors (TFETs). The properties of FETs fabricated with single and few layer TMDs have been investigated with some degree of success, but it has been shown via in-situ chemical analysis that interface interactions between certain contact metals and the underlying TMD are not fully understood[1,2].

In this study, the wettability and reactivity of various metals with a number of bulk TMDs (MoS$_2$, HfSe$_2$, SnSe$_2$, etc.) were investigated. Multiple samples were processed in parallel to ensure that all sample sets saw

identical metal depositions. The metal-TMD interface was monitored in-situ using X-ray photoelectron spectroscopy (XPS) and metal film topography was imaged using atomic force microscopy (AFM). For some low work function metals, noticeable differences in interface chemistry were found between samples that saw high vacuum rather than UHV metal e-beam depositions.

Significant variations in compatibility between contact metal and TMD were discovered. These variations were dependent upon the metal-TMD pair and the base pressure of the chamber prior to metal deposition. Au exhibits far superior wettability on $MoSe_2$, where uniform thin films were achieved, compared to $ReSe_2$, on which Au grows as clusters. Au wettability varies between that of thin films and clusters for the other TMDs studied. An Au thin film deposited on $SnSe_2$ results in the formation of reaction products such as Sn metal, as evidenced by the evolution of different chemical states in the Sn $3d$ spectrum after deposition. Reactions between MoS_2 and Sc producing Mo metal occur when Sc is deposited in UHV instead of HV. These results provide further understanding for the critical interface between Sc and TMD in high performance TFETs.

[1] McDonnell, S.; Addou, R.; Buie, C.; Wallace, R. M.; Hinkle, C. L. Defect Dominated Doping and Contact Resistance in MoS_2. *ACS Nano* **2014**, *8*, 2880-2888.

[2] Das, S.; Chen, H.Y.; Penumatcha, A. V.; Appenzeller, J. High Performance Multi-Layer MoS_2 Transistors with Scandium Contacts. *Nano Lett.* **2012**, *12*, 100-105.

5:00pm 2D+EM+IS+MC+NS+SP+SS-WeA9 Defects and Boundaries in 2D Materials: Correlating Electronic Properties to Atomic Structures, *An-Ping Li*, Oak Ridge National Laboratory **INVITED**

The quest for novel two-dimensional (2D) materials has led to the discovery of hybrid heterostructures of graphene and other 2D atomic films, which provide us fascinating playground for exploring defects and boundaries in a variety of atomic layers. Even in graphene itself, there usually exist large amount of extended topological defects, such as grain boundaries and changes in layer thickness, which divide graphene into grains and domains. These interfaces and boundaries can break the lattice symmetry and are believed to have a major impact on the electronic properties, especially the transport, in 2D materials.

Here, we report on the electronic and transport properties of two types of defects studied by STM and multi-probe scanning tunneling potentiometry with a focus on the correlations to their atomic structures. The first type of defect is the monolayer-bilayer (ML-BL) boundaries in epitaxial graphene on SiC. By measuring the transport spectroscopy across individual ML-BL graphene boundaries, a greater voltage drop is observed when the current flows from monolayer to bilayer graphene than in the reverse direction, displaying an asymmetric electron transport upon bias polarity reversal [1, 2]. Interestingly, this asymmetry is not from a typical nonlinear conductance due to electron transmission through an asymmetric potential. Rather, it indicates the opening of an energy gap at the Fermi energy. Another type of defect is 1D interface in hexagonal boron nitride (hBN) and graphene planar heterostructures, where a polar-on-nonpolar 1D boundary is expected to possess peculiar electronic states associated with edge states of graphene and the polarity of hBN [2]. By implementing the concept of epitaxy to 2D space, we grow monolayer hBN from fresh edges of monolayer graphene with lattice coherence, forming a 1D boundary [3]. STM/STS measurements reveal an abrupt 1D zigzag oriented boundary, with boundary states about 0.6 eV below or above the Fermi level depending on the termination of the hBN at the boundary [4]. The boundary states are extended along the boundary, and exponentially decay into the bulk of graphene and hBN. The origin of boundary states and the effect of the polarity discontinuity at the interface will be discussed.

1 K. W. Clark, et al., *ACS Nano* **7**, 7956 (2013).

2 K. W. Clark, et al., *Phys. Rev. X* **4**, 011021 (2014).

3 L. Liu, et al., *Science* **343**, 163 (2014).

4 J. Park et al., *Nature Commun.* **5**, 5403 (2014).

5:40pm 2D+EM+IS+MC+NS+SP+SS-WeA11 Metal Ion Intercalated 2D Materials as Transparent Electrodes, *Jiayu Wan**, *W. Bao, F. Gu*, University of Maryland, College Park, *M. Fuhrer*, Monash University, Malaysia, *L. Hu*, University of Maryland, College Park

Transparent electrode materials are critical for optoelectronic devices such as touch screen and solar cells. Graphene has been widely studied as transparent electrodes for its unique physical properties. To further boost the performance of graphene based transparent electrodes, we novelized Li-ion intercalation in graphene, and achieved highest performance of carbon based transparent electrodes.[1] Transmission as high as 91.7% with a sheet resistance of 3.0 ohm/sq is achieved for 19-layer LiC_6, which corresponds to a figure of merit ($Sigma_{dc}/Sigma_{opt}$) at 1,400, significantly higher than any other continuous transparent electrodes. The unconventional modification of ultrathin graphite optoelectronic properties is explained by the suppression of interband optical transitions and a small intraband Drude conductivity near the interband edge. To achieve low cost, large scale graphene-based transparent electrodes, we further developed Na-ion intercalated printed reduced graphene oxide (RGO) film[2]. Unlike pristine graphene that inhibits Na-ion intercalation, the larger layer-layer distance of RGO allows Na-ion intercalation, leading to simultaneously much higher DC conductivity and higher optical transmittance. The typical increase of transmittance from 36% to 79% and decrease of sheet resistance from 83 kohms/sq to 311 ohms/sq in the printed network was observed after Na-ion intercalation. Compared with Li-intercalated graphene, Na-ion intercalated RGO shows much better environmental stability, which is likely due to the self-terminating oxidation of Na ions on the RGO edges. This study demonstrated the great potential of metal-ion intercalation to improve the performance of graphene-based materials for transparent conductor applications.

Reference

1. Jiayu Wan[a], Wenzhong Bao[a], et al., Nature communications, 2014,5, 4224. ([a] equally contribution)

2. Jiayu Wan, Feng Gu, Wenzhong Bao, et al. Nano Letters, 2015, DOI: 10.1021/acs.nanolett.5b00300.

6:00pm 2D+EM+IS+MC+NS+SP+SS-WeA12 Oxygen Reduction Reaction on Nitrogen-doped Graphene, *Jun Nakamura*, The University of Electro-Communications (UEC-Tokyo), Japan, *A. Ichikawa, H. Matsuyama, A. Akaishi*, The University of Electro-Communications (UEC-Tokyo)

Recently, several groups have reported high oxygen reduction reaction (ORR) activities in nitrogen-doped carbon nanomaterials which are candidates of metal-free catalysts for ORR [1]. Lee et al. have successfully fabricated nitrogen-doped graphene with the high ORR activity in acid media [2]. It has been confirmed that local atomic configurations of dopants in nitrogen-doped graphene are classified into three functional groups (pyrrole-like, pyridine-like, and graphite-like configurations) [3,4]. However, the mechanism of the ORR on the nitrogen-doped graphene has not fully understood.

In this work, we examine the ORR on the nitrogen-doped graphene containing the graphite-like N in a basal plane using first-principles calculations. In general, the ORR occurs mainly two pathways: The two-electron pathway (2e-) that is reduced to hydrogen peroxide ($H2O2$), and the direct four-electron pathway (4e-) that reduces to water ($H2O$). Thermodynamic electrode potentials of each process at standard conditions are about 0.68V (2e-) and 1.23V (4e-), respectively. In case of the associative mechanism for the two- and four- electron reduction pathways, the electrocatalytic activity is governed by the stability of reaction intermediates like OOH*, OH*, and O* (where "*" refers to a surface site). Free energies of the reaction intermediates have been calculated based on the computational hydrogen electrode model suggested by Nørskov et al. [5]. We have taken account of effects of electrode potential, Ph of a solution, a local electric field in double layer, and water environment.

We have constructed energy diagrams at several electrode potentials on the basis of the first-principles calculations. It has been shown that the 2e- and 4e- reduction processes proceed at potentials up to about 0.5V and 0.8V, respectively. This means that we can control the reduction pathway for the nitrogen-doped graphene with the graphite-like N. Proton-electron transfer to OOH* (the 2e- pathway), and the formation of OOH* (the 4e- pathway) are confirmed to be the rate-limiting steps, respectively. Density dependence of N on the ORR activity will also be discussed in the presentation.

References

[1] J. Ozaki, N. Kimura, T. Anahara, and A. Oya, Carbon **45**, 1847 (2007).

[2] K. R. Lee et al., Electrochem. Commun. **12**, 1052 (2010).

* NSTD Student Award Finalist

[3] H. Niwa et al., J. Power Sources **187**, 93 (2009).

[4] T. Umeki, A. Akaishi, A. Ichikawa, and J. Nakamura, J. Phys. Chem. C **119**, 6288 (2015).

[5] J. K. Nørskov et al., J. Phys. Chem. B **108**, 17886 (2004).

Applied Surface Science
Room: 212D - Session AS+SS-WeA

Characterization of Buried Interfaces
Moderator: Xia Dong, Eli Lilly and Company, James Ohlhausen, Sandia National Laboratories

2:20pm   AS+SS-WeA1   ASSD 30th Anniversary Speaker: Characterization of Sub-surface Interfaces using SIMS, TEM, and FIB or: How Much will it Cost me to Fix that Interface?, *Fred Stevie*, North Carolina State University **INVITED**
Characterization of interfaces between layers or between layer and substrate has always been of interest. Interface issues include visible problems, such as delamination or corrosion, and contamination that can affect product quality, such as electrical properties in semiconductors. The information desired includes the physical quality of the interface and identification and quantification of contaminants. This presentation summarizes multiple approaches to interface analysis, particularly with use of SIMS, FIB, and TEM.

Common approaches for analysis of a buried interface involve a depth profile or cross section. Depth profiling by SIMS is often used because of good sensitivity and depth resolution. Matrix, dopant and contaminant species in the structure can be characterized with a single SIMS depth profile. Quantification of contamination at an interface is highly desired but can be difficult to obtain. Once an element has been identified as a contaminant, quantification at interfaces may be possible with ion implantation. Significant improvements have been made with the species used for depth profiling. C_{60} and argon cluster beams are used to depth profile organic materials. These high mass ion beams provide better sensitivity for high mass species and do not affect the chemical composition, so it is possible to obtain interfacial chemistry.

The FIB has revolutionized sample preparation and lift-out methods can routinely prepare cross section specimens for TEM analysis. A sample polished to provide an edge can rapidly be trimmed with FIB to provide a surface 50 to 100μm in height that is suitable for high resolution analysis. Optimization of beam conditions such as dwell and overlap can increase removal rate by several times. Plasma ion sources dramatically increase material removal rates and make possible the study of 100μm deep interfaces which will cover most layers of interest. Plating coatings are commonly less than 5μm thick and paint coatings 100 to 150μm.

3:00pm   AS+SS-WeA3   FIB-TOF Tomography Characterization of Organic Structures, *David Carr, G.L. Fisher,* Physical Electronics USA, *S. Iida, T. Miyayama*, ULVAC-PHI
1. Introduction
There are practical limitations to the use of ion beam sputtering for probing the sample chemistry beyond the surface region which include preferential sputtering and accumulated sputter beam damage. Both effects result in a distortion or complete loss of the true 3D chemical distribution as a function of depth

An alternative approach to achieve 3D chemical imaging of complex matrix chemistries is to utilize *in situ* FIB milling and sectioning in conjunction with TOF-SIMS chemical imaging, or 3D FIB-TOF tomography [1]. This can minimize or eliminate artifacts caused by sputter depth profiling such as differential sputtering and accumulated ion beam damage.

However, even with FIB polishing there remains some FIB beam-induced chemical or molecular damage that may or may not limit the detection of characteristic molecular signals. For certain specimens, it is an advantage to follow FIB polishing with cluster ion polishing to recover the characteristic molecular signals.

2. Method
The 3D chemical characterization of pure organic and metal-organic mixed composition structures was achieved utilizing 3D FIB-TOF tomography on a PHI TRIFT *nanoTOF* II (Physical Electronics, USA) imaging mass spectrometer. The spectrometer's large angular acceptance and depth-of-field maintain high mass resolution and high mass scale linearity even in this challenging geometry. This provides the highly desirable ability to perform artifact-free chemical imaging of high aspect ratio features.

3. Results

The present study investigated samples from two classes of materials: one metal-organic mixed matrix composition and one mixed organic phase comprised of two polymer moieties. Since there was no preferential sputtering, an immediate result of the FIB-TOF imaging was the accurate determination of the depth scale. We have collected characteristic molecular information from each sample for the purposes of 2D and 3D imaging. Cluster ion beam polishing (e.g. $C_{60}{}^{+}$ or $Ar_{2,500}{}^{+}$) was necessary to remove the FIB beam-induced damage, and the new instrument configuration allows cluster ion polishing to be accomplished with ease. We will highlight certain aspects of the studies for presentation.

4. References
[1] A. Wucher, G.L. Fisher and C.M. Mahoney, Three-Dimensional Imaging with Cluster Ion Beams (p. 207-246) in *Cluster Secondary Ion Mass Spectrometry: Principles and Applications*, C.M. Mahoney (Ed.), Wiley & Sons, N.J. (2013).

4:20pm   AS+SS-WeA7   Interface Characterization using Ballistic Electron Emission Microscopy and Spectroscopy: Recent Results and Related Techniques, *Douglas Bell*, Jet Propulsion Laboratory, California Institute of Technology **INVITED**
Ballistic electron emission microscopy (BEEM) is a microscopy and spectroscopy based on scanning tunneling microscopy (STM), developed as a scanning probe of subsurface interface properties. By monitoring the fraction of tunneling current between STM tip and sample that traverses a subsurface heterostructure, BEEM can probe hot-carrier transport as well as heterostructure and material properties. Because BEEM uses an STM tip to inject a highly localized carrier distribution, high-resolution imaging of interface electronic structure can be performed. Control of tunnel voltage polarity allows injection of either holes or electrons into the sample structure, thus enabling characterization of electronic structure both above and below the Fermi level.

Since its inception, BEEM has found many applications such as studies of interface heterogeneity, carrier scattering, band structure, transport in oxides, and interface chemistry. A wide range of structures have been probed, including metal/semiconductor, metal/oxide/semiconductor, quantum wells, and quantum dots. Researchers have measured quantized energy levels and spatial variations of Schottky barrier height. BEEM has also provided a new means for studying fundamental characteristics of interface transport such as conservation of momentum parallel to an interface.

More recently, BEEM has been applied to the investigation of other novel materials and structures. Organic materials, graphene layers, and nanowires have received attention, and research has been done on molecular vibrational spectroscopy. Related techniques for magnetic materials, and measurements of BEEM-induced luminescence, have been further developed and demonstrated.

This talk will discuss some of these recent advances and extensions, as well as further developments in more traditional areas. Some comparisons with results from other characterization techniques will also be presented.

5:00pm   AS+SS-WeA9   Using XPS to Study Electrochemical Solid-Liquid Interfaces In-Operando: Standing-Wave Ambient-Pressure XPS (SWAPPS), *Osman Karslioglu*, Lawrence Berkeley National Laboratory, *S. Nemsak,* Forschungszentrum Juelich GmbH, Germany, *I. Zegkinoglou, A. Shavorskiy, M. Hartl, C.S. Fadley, H. Bluhm,* Lawrence Berkeley National Laboratory
Accessing the chemical and electrical potential information at a solid/liquid interface is an important capability for investigating a process like corrosion where electrochemical transformations are at work. Here we report the first results of a combination of techniques, where we use X-ray standing waves to enhance the photoemission signal from the solid-liquid interface during an ambient-pressure XPS experiment, investigating the oxidation of Ni. X-ray standing waves were generated by a Si/Mo multilayer mirror, on which the sample is prepared as a thin layer (~8 nm Ni in this case). A thin liquid layer was formed on the surface by dipping the sample into an electrolyte (KOH(aq), 0.1 mol/L) and pulling back partially. The solid-liquid interface was probed through this thin liquid layer using hard X-rays (3100 eV). The sample was the working electrode in a 3-electrode cell, and it was oxidized by applying a positive potential using the potentiostat. Comparing the experimental rocking curves for Ni 3p and O 1s with theory provided thickness and roughness information for solid and liquid layers with ~1 nm resolution.

5:20pm   AS+SS-WeA10   Exploring the Usefulness of Monochromatic Ag Lα X-rays for XPS, *Sarah Coultas, J.D.P. Counsell, S.J. Hutton, A.J. Roberts, C.J. Blomfield*, Kratos Analytical Limited, UK
High energy X-ray sources have been used in XPS analysis for some time to access more core-levels and probe deeper into the sample surface. Lab

based sources such as Zr and Ti have been offered in the past but the broad X-ray line widths produced by such sources limit their applications for chemical analysis. This problem is mitigated by the use of an Ag Lα X-ray source. The source energy is 2984 eV, conveniently approximately twice that of Al Kα, hence the same quartz crystal mirror may be used to monochromate the Ag Lα X-ray line producing a narrow, high energy source of X-rays for XPS. Modern X-ray photoelectron spectrometers may be fitted with automated Al / Ag X-ray monochromators which greatly improve the usability of Ag Lα X-rays allowing Al and Ag X-ray generated spectra to be recorded from the same sample as part of automated data acquisition. Highlights of the source's characteristics include:

• Good sensitivity and energy resolution provide useful chemical information

• Enhanced surface compositional information from approximately twice the analytical depth as Al Kα radiation for same core line

• Higher excitation energy allows deeper core levels and additional Auger lines to be explored

• Large energy range of Ag Lα allows exploitation of "depth dimension" for surface segregation studies

Here we investigate the practical uses of these characteristics. This includes using the Auger parameter for aluminium and silicon containing compounds where the higher energy radiation can excite the 1s core lines and the KLL Auger series. Earlier studies [1] have shown the usefulness of higher excitation energies in elucidating structure via Auger parameters.

We also illustrate the usefulness of Ag Lα as an additional tool for the surface analyst by way of examples of spectroscopy, ARXPS, depth profiling and imaging.

1. References

[1] J.E. Castle, L.B. Hazell & RH West, *J. Electron Spectrosc. Relat. Phenom.* ., 1979, **16**, 97

5:40pm AS+SS-WeA11 Optimizing the TOF-SIMS CsM⁺ Depth Profile of a Tunnel Magneto Resistance (TMR) Structure, *Alan Spool*, HGST, a Western Digital Company

Used now for many years in modern magnetic recording devices, TMR sensors consist at their heart of a complicated series of layers, mostly metallic, ranging in thickness from less than a nm to several nm. In order to use the potentially better depth resolution and sensitivity of a SIMS depth profile over other surface analytical techniques, CsM⁺ profiles were obtained using a variety of conditions. The ratio of the sputter ion to primary ion fluences, the sputter ion beam energy, and the % of Cs in a combined Cs/Xe sputter ion beam were all varied, and the results for a single wafer compared. In addition to changes in various CsM⁺ ion intensities and therefore their signal to noise, the Cs/Xe ratio sometimes had unexpected effects on the profile shapes. The primary ion beam fluence was lessened by increasing its raster size over more than the crater bottom. Depth profiles were then created retrospectively from the raw data, using the results themselves to select the flattest portion of the crater bottom.

6:00pm AS+SS-WeA12 Interface and Composition Analyses versus Performances: How to Improve Perovskite Solar Cells, *Y. Busby*, University of Namur, B-5000 Namur, Belgium, *F. Matteocci*, University of Rome "Tor Vergata", Italy, *G. Divitini, S. Cacovich*, University of Cambridge, UK, *C. Ducati*, University of Cambridge, *A. di Carlo*, University of Rome "Tor Vergata", Italy, **Jean-Jacques Pireaux**, University of Namur, Belgium

Hybrid halide perovskite solar cells (PSCs) have received much attention during the very last years because of their very promising cost/performance ratio. Different architectures and preparation methods have been tested, but still some general guidelines for their optimization are missing. In particular, the interfaces are now well known to play a dominant role in the device performances but have been so far poorly studied.

In this work, we correlated the solar cell characteristics to their interface composition and morphology in PSCs deposited by different procedures (single-step, double-step by dipping, double-step by a vacuum assisted technique) and different conversion environments (air, vacuum and nitrogen atmosphere). The interface quality is found to be affected by the perovskite conversion method and in particular from the environment where the conversion is performed. Power conversion efficiencies between 7 and 14.5% have been measured from the characteristics of the differently prepared cells. The morphology, crystal size and interdiffusion have been fully characterized by scanning transmission electron microscopy (STEM), equipped with high resolution energy-dispersive X-ray spectroscopy (EDX). Interfaces have been further characterized by depth profile techniques by combining ion beam sputtering with atomic and molecular composition analysis with X-Ray photoelectron spectroscopy (XPS) and Time of Flight Secondary Ion Mass Spectroscopy (ToF-SIMS). In particular

these techniques allowed detecting and evaluating the diffusion of metals into the hole transport material (SpiroOMetAD) and iodine and chlorine diffusion in the TiO₂ back contact. Interestingly, the higher oxygen content perovskite formed in air is not associated to a sensibly lower (short term) efficiency of the solar cell.

Electronic Materials and Processing
Room: 211C - Session EM+AS+MS+SS-WeA

Surface and Interface Challenges in Wide Bandgap Materials
Moderator: Aubrey Hanbicki, U.S. Naval Research Laboratory, Rachael Myers-Ward, U.S. Naval Research Laboratory

2:20pm EM+AS+MS+SS-WeA1 Effects of Nitrogen and Antimony Impurities at SiO₂/SiC Interfaces, *Patricia Mooney*, Simon Fraser University, Canada **INVITED**

4H-SiC is an attractive material for devices operating at high power and high temperatures because of the large bandgap energy, 3.23 eV, the high critical breakdown field, 2.0 MVcm⁻¹, and high electron mobility,

850 cm²V⁻¹s⁻¹. Commercialization of 4H-SiC MOSFET technology was long delayed due to the high density of defects near the SiO₂/SiC interface. Post oxidation annealing in NO ambient, the process that enabled the commercialization of SiC Power ICs in 2011, significantly reduces the density of near-interface traps and results in typical effective MOSFET channel electron mobility (μ_{FE}) values of ~20 cm²V⁻¹s⁻¹ [1]. The relatively high density of near-interface traps having energy levels within 0.5 eV of the SiC conduction band was investigated using constant capacitance transient spectroscopy (CCDLTS). These measurements showed that NO annealing reduced the density of the two near-interface oxide trap distributions, attributed to Si interstitials and substitutional C pairs in SiO₂, by as much as a factor of 10 [1,2].

It has also been shown that introducing impurities such as Na, P, or Sb near the SiO₂/SiC interface further increases μ_{FE}, to peak values of 104 cm²V⁻¹s⁻¹ and to 50 cm²V⁻¹s⁻¹ at high electric field for Sb [3]. The much higher value of μ_{FE} in Sb-implanted MOSFETs was attributed to counter-doping by Sb in SiC near the interface. To investigate the effects of Sb at SiO₂/SiC interfaces, Sb ions were implanted near the surface of the 4H-SiC epitaxial layer and the wafer was annealed at 1550℃ in Ar to activate the Sb donors. Dry thermal oxidation was done at 1150℃ and the sample was then NO-annealed at 1175℃ for 30 or 120 min. CCDLTS results of Sb-implanted MOS capacitors were compared with those having no Sb implant but with similar dry oxidation and NO-annealing processes. The density of near-interface oxide traps was similar in samples with and without Sb, indicating that Sb has little effect on those defects. However, CCDLTS spectra taken at bias and filling pulse conditions that reveal defects in the SiC depletion region, show both the deeper of the two N donor levels at E_C - (0.10±0.01) eV and a second energy level only in Sb-implanted samples at E_C - (0.12±0.01) eV. To our knowledge this is the first measurement of Sb donors in SiC and it confirms counter doping of SiC by Sb near the SiO₂/SiC interface.

[1] P.M. Mooney and A.F. Basile, in *Micro and Nano-Electronics: Emerging Device Challenges and Solutions*, Ed. T. Brozek (CRC Press, Taylor and Francis, 2014) p. 51.

[2] A.F. Basile, et al., J. Appl. Phys. **109**, 064514 (2011).

[3] A. Modic, et al., IEEE Electron Device Lett. **35**, 894 (2014).

3:00pm EM+AS+MS+SS-WeA3 Hydrogen Desorption from 6H-SiC (0001) Surfaces, *Sean King*, Intel Corporation, *R. Nemanich, R. Davis*, North Carolina State University

Due to the extreme chemical inertness of silicon carbide (SiC), *in-situ* thermal desorption is commonly utilized as a means to remove surface contamination prior to initiating critical semiconductor processing steps such as epitaxy, gate dielectric formation, and contact metallization. *In-situ* thermal desorption and silicon sublimation has also recently become a popular method for epitaxial growth of mono and few layer graphene. Accordingly, numerous thermal desorption experiments of various processed silicon carbide surfaces have been performed, but have ignored the presence of hydrogen which is ubiquitous throughout semiconductor processing. In this regard, we have performed a combined temperature programmed desorption (TPD) and x-ray photoelectron spectroscopy (XPS) investigation of the desorption of molecular hydrogen (H₂) and various other oxygen, carbon, and fluorine related species from *ex-situ* aqueous hydrogen fluoride (HF) and *in-situ* thermal and remote hydrogen plasma

cleaned 6H-SiC (0001) surfaces. Using XPS, we observed that temperatures on the order of 700 - 1000°C are needed to fully desorb C-H, C-O and Si-O species from these surfaces. However, using TPD, we observed H_2 desorption at both lower temperatures (200 – 550°C) as well as higher temperatures (> 700°C). The low temperature H_2 desorption was deconvoluted into multiple desorption states that, based on similarities to H_2 desorption from Si (111), were attributed to silicon mono, di, and trihydride surface species as well as hydrogen trapped by sub-surface defects, steps or dopants. The higher temperature H_2 desorption was similarly attributed to H_2 evolved from surface O-H groups at ~ 750°C as well as the liberation of H_2 during Si-O desorption at temperatures > 800°C. These results indicate that while *ex-situ* aqueous HF processed 6H-SiC (0001) surfaces annealed at < 700°C remain terminated by some surface C-O and Si-O bonding, they may still exhibit significant chemical reactivity due to the creation of surface dangling bonds resulting from H_2 desorption due from previously undetected silicon hydride and surface hydroxide species.

3:20pm **EM+AS+MS+SS-WeA4 Chemical and Microstructural Characterization of Interfaces between Metal Contacts and β-Ga₂O₃**, *Lisa M. Porter*, *Y. Yao, J.A. Rokholt, R.F. Davis,* Carnegie Mellon University, *G.S. Tompa, N.M. Sbrockey, T. Salagaj,* Structured Materials Industries, Inc.

β-Ga₂O₃ is a promising alternative to traditional wide bandgap semiconductors, as it has a wider bandgap (~4.9 eV) and a superior figure-of-merit for power electronics and other devices; moreover, β-Ga₂O₃ bulk single crystals have recently been grown commercially using melt-growth methods. While several groups have demonstrated Ga₂O₃-based devices such as Schottky diodes and MOSFETs, understanding of contacts to this material is limited. In this study, we investigated a variety of metal contacts (Ti, In, Mo, W, Ag, Au, and Sn) to both (-201) β-Ga₂O₃ single crystal substrates (from Tamura Corp.) and β-Ga₂O₃ epitaxial layers grown by MOCVD on various substrates (sapphire and single crystal β-Ga₂O₃) by co-authors at Structured Materials Industries. We have characterized these substrates and epilayers using techniques such as X-ray diffraction and transmission electron microscopy (TEM), which show that the epitaxial layers are oriented (-201) with respect to the substrates. We found that the electrical characteristics of the metal contacts to the Ga₂O₃ epilayers and substrates are highly dependent on the nature of the starting surface and the resulting interface, and less dependent on the work function of the metal than expected. For example, both Ti and bulk In readily form ohmic contacts to Ga₂O₃, whereas other low-workfunction metals, such as Sn, did not form ohmic contacts even after annealing to 800 °C. For Ti ohmic contacts on Sn-doped Ga₂O₃ substrates the optimal annealing temperature was ~400 °C: the electrical characteristics continually degraded for annealing temperatures above ~500 °C. Thermodynamics predicts that Ti will reduce Ga₂O₃ to produce Ti oxide, therefore indicating that the Ti/Ga₂O₃ interface is unstable. In correspondence with this prediction, high-resolution cross-sectional TEM images of 400 °C-annealed samples show the formation of an ultra-thin (~2 nm) interfacial amorphous layer. TEM samples at higher annealing temperature have also been prepared for analysis; electron energy loss spectroscopy will be used to characterize the interfacial composition profiles in these samples to determine the relationship between composition and thickness of the interfacial layer and the electrical degradation of the contacts. Schottky diodes with Au, Mo, W and Sn as the Schottky metal were also fabricated. The Schottky barrier heights (SBHs) showed a weak dependence on the metal workfunction. An overview of the electrical behavior of different metals as ohmic or Schottky contacts to Ga₂O₃ and the interfacial chemistry and microstructure will be presented.

4:20pm **EM+AS+MS+SS-WeA7 Regrown InN Ohmic Contacts by Atomic Layer Epitaxy**, *Charles Eddy, Jr.,* U.S. Naval Research Laboratory, *N. Nepal,* Sotera Defense Solutions, *M.J. Tadjer, T.J. Anderson, A.D. Koehler, J.K. Hite, K.D. Hobart,* U.S. Naval Research Laboratory

For the past 25 years, compound semiconductors comprised of elements from group III-B of the periodic table and nitrogen have attracted a sustained, high-level of research focus. More recently they have found growing application to rf and power electronics in the form of advanced transistor structures such as the high electron mobility transistor (HEMT) with and without insulated gates. Key performance parameters for such devices (cut-off frequency for rf transistors and on-resistance for power transistors) are often dominated by the contact resistance. The current best approach to contact resistance minimization involves aggressive processing requirements that challenge device fabrication, especially when insulated gates are required. A potential solution is the regrowth of highly conducting semiconductor contact layers where ohmic contacts are needed.

Here we report on initial efforts to employ regrown indium nitride (InN) contact layers by atomic layer epitaxy (ALE) as a low temperature solution to the ohmic contact challenge for III-N transistors. Recently, we have

reported that good crystalline quality InN can be grown at less than 250°C by ALE [1]. Here we employ such conditions to grow very thin layers and assess them morphologically and electrically.

InN regrown contact layers of 5nm thickness grown on sapphire are very smooth (rms roughness < 0.17nm) and possess sheet resistances as low at 3.6 kΩ/sq, corresponding to electron sheet carrier densities of 2-3 x10¹³ cm⁻² and mobilities of 50 cm²/V-s. These electron mobilities are higher than previously reported (30 cm²/V-s) for much thicker films (1.3 μm) [2]. Similarly grown 22.5 nm thick InN layers on highly resistive silicon were processed with mesa isolation regions and 20/200 nm thick titanium/gold contact metals. Without any contact annealing, an ohmic contact resistance of 9.7x10⁻⁷ Ω-cm² (1.2 Ω-mm) was measured, comparable to the best high temperature alloyed contact to an AlGaN/GaN HEMT.

In our initial non-alloyed ohmic contact process, contact regions were recessed down to the GaN buffer layer to establish physical contact between the highly-conductive InN layer and electrons in the HEMT channel. A 25 nm thick InN layer was then grown by ALE, and the InN-filled ohmic regions were then capped with a Ti/Al/Ti/Au layers. Using the metals as an etch mask, the InN outside of the ohmic regions was etched away. We will report on initial results of application of ALE InN regrown contact layers and the modified fabrication approaches to AlGaN/GaN HEMTs.

1. N. Nepal, et al., *J Cryst. Growth and Design*, **13**, 1485-1490 (2013).

2. Kuo et al., *Diamond & Related Materials* **20**, 1188 (2011).

4:40pm **EM+AS+MS+SS-WeA8 High-Temperature Characteristics of Ti/Al/Pt/Au Contacts to GaN at 600°C in Air**, *Minmin Hou*, *D.G. Senesky*, Stanford University

The high-temperature characteristics (at 600°C) of Ti/Al/Pt/Au contacts to gallium nitride (GaN) in air are reported. GaN is a wide bandgap semiconductor material being developed for high-temperature electronics and micro-scale sensors. Ti/Al/Pt/Au metallization is frequently used for forming ohmic contacts to GaN. However, few studies have been devoted to studying the electrical characteristics of the Ti/Al/Pt/Au metallization at elevated temperatures and even fewer in oxidizing environments. It is not practical to obtain a hermetic sealing at elevated temperatures and a number of sensing applications may require non-hermetic packages. Therefore, the electrical characteristics of Ti/Al/Pt/Au contacts in a hot oxidizing ambient instead of an inert ambient or vacuum can provide new insights. In this work, the electrical and microstructural properties of Ti/Al/Pt/Au contacts to GaN upon exposure to 600°C in air are presented.

In this work, microfabricated circular-transfer-line-method (CTLM) patterns were used as the primary test structure. Ti/Al/Pt/Au were patterned through a standard lift-off process on unintentionally-doped GaN epitaxial layer grown by metal organic chemical vapor deposition (MOCVD) on sapphire. After lift-off, the samples were subject to a rapid thermal annealing (RTA) process at 850°C for 35 seconds in a nitrogen ambient.

To observe the impact of thermal exposure on the electrical and microstructural properties, the test structures were subject to a 10-hour thermal storage test in a furnace (air ambient), during which time the test structures were taken out of the furnace every two hours and their I-V characteristics were measured at room temperature. After the initial 2-hour "burn-in" period, the contact resistance remained stable over the entire reminder thermal storage test, with the variance within less than 3% and the specific contact resistivity remained on the order of 10^-5 Ω-cm^2.

In addition, the samples were subject to in-situ high-temperature I-V tests at 600°C in air both before and after the thermal storage using a high-temperature probe station. The linear I-V response confirms that the contacts remained ohmic after the thermal storage. The contact resistance at 600°C showed minimal change (approximately 9%) for a 20-μm-wide gap CTLM test structure, before and after thermal storage.

The microstructural analysis with atomic force microscopy (AFM) showed minimal changes (less than 0.1%) in surface roughness after thermal storage. The results support the use of Ti/Al/Pt/Au metallization for GaN-based sensors and electronic devices that will operate within a high-temperature and oxidizing ambient.

5:00pm **EM+AS+MS+SS-WeA9 Schottky Contacts and Dielectrics in GaN HEMTs for Millimeter-Wavelength Power Amplifiers**, *Brian Downey*, Naval Research Laboratory **INVITED**

Although GaN RF transistor technology has begun to enter commercial markets, there are still several active research efforts aimed at extending the operating frequency of GaN devices to the millimeter-wavelength (MMW) frequency range of 30 – 300 GHz. In order to facilitate power gain at MMW frequencies, both geometric device scaling and novel heterostructure/device design are required, which present interesting materials and processing challenges. In this talk, an overview of NRL's approaches to MMW GaN high-electron-mobility transistor (HEMT) technology will be presented. In one approach, N-polar GaN inverted HEMT structures are employed, which

places the GaN channel at the surface of the device. In this case, Schottky gate contacts are made directly to the N-polar GaN channel. The effect of GaN crystal polarity on Schottky barrier height will discussed along with strategies to increase the Schottky barrier height of metals to N-polar GaN. In a second approach, Ga-polar GaN HEMTs with vertically-scaled barrier layers are utilized to reduce the surface-to-channel distance in order to maintain electrostatic control of the channel in short gate length devices. The high electric fields in these vertically-scaled barrier devices can create large tunneling-related gate leakage currents, leading to high off-state power dissipation and soft breakdown characteristics. The use of gate dielectrics in these scaled structures will be discussed including their effect on device electrical performance.

5:40pm EM+AS+MS+SS-WeA11 Nitrogen as a Source of Negative Fixed Charge for Enhancement Mode Al2O3/GaN Device Operation, *MuhammadAdi Negara, R. Long, D. Zhernokletov, P.C. McIntyre*, Stanford University

In recent years, significant research efforts have focused on developing enhancement mode (E-mode) GaN-based devices fueled by many potential applications. Simpler power amplifier circuits using a single polarity voltage supply and increased safety using a normally-off device can be achieved using E-mode devices leading to lower cost and an improvement of system reliability. Using the combination of E-mode and depletion mode (D-mode) devices in direct coupled logic open up also new applications for nitride semiconductors. To realize normally-off operation of GaN transistors, several approaches have been reported in the past including recessed gate structures [1], p-type gate injection [2], fluorine plasma treatment [3], surface channel GaN [4], thermally oxidized gate insulator [5] and oxide charge engineering [6]. In this report, nitrogen impurities introduced during atomic layer deposition of an Al_2O_3 gate dielectric are investigated as a means of modifying the threshold voltage (V_{th})/flat band voltage (V_{fb}) of GaN MOS devices. As reported in reference [7], nitrogen may incorporate on either cation or anion substitutional sites or on interstitial sites in Al_2O_3 and become a source of negative fixed charge within Al_2O_3. The effectiveness of this approach for fixed charge modification of ALD-grown Al_2O_3 compared to several alternative approaches will be presented.

References:

[1] W. B. Lanford, et al., Electron. Lett. 41, no. 7, 449 (2005).

[2] Y. Uemoto, et al., IEEE Trans. Elect. Dev. 54, no. 12, 3393 (2007).

[3] Zhang et al., Appl. Phys. Lett. 103, 033524 (2013).

[4] W. Huang, et al., IEEE Elect. Dev. Lett. 27, no. 10, 796 (2006).

[5] K. Inoue et al., Elect. Dev. Meet., IEDM Technical Digest. International, pp. 25.2.1 (2001).

[6] B. Lu, et al., in Proc. Int. Workshop Nitride Semicond. Abstr.,536 (2008)..

[7] Choi et al., Appl. Phys. Lett. 102, 142902 (2013).

6:00pm EM+AS+MS+SS-WeA12 Activation of Mg-Implanted GaN Facilitated by an Optimized Capping Structure, *Jordan Greenlee, B.N. Feigelson, T.J. Anderson, K.D. Hobart, F.J. Kub*, Naval Research Laboratory

For a broad range of devices, the activation of p and n-type implanted dopants in GaN is needed. The activation of implanted ions by annealing requires post-implantation damage removal and the arrangement of implanted ions in their proper lattice sites. Post-implantation activation of Mg via annealing requires high temperatures (>1300 °C). At these high annealing temperatures, GaN decomposes, leaving behind a roughened surface morphology and a defective crystalline lattice, both of which are detrimental for GaN device applications. To combat decomposition, either a high pressure environment, which is prohibitively expensive and not easily scalable, or a capping structure combined with short exposure to T >1300°C is required to preserve the GaN. In this work, we explore the effects of different capping structures and their ability to protect the GaN surface during a high temperature pulse, similar to those used in the Multicycle Rapid Thermal Annealing (MRTA) process.

It was determined that the sputtered cap provides sufficient protection for the underlying GaN during a rapid heat pulse. The in situ MOCVD-grown AlN cap, although it should have a better interface and thus provide more protection for the GaN layer, is inferior to the sputtered cap as determined by Nomarski images. After etching the surface with AZ400k developer, it was determined that the GaN underneath the MOCVD-grown cap has pits as-grown. Since both GaN layers were grown with the same recipe, we attribute these pits to the HT MOCVD AlN growth process. Atomic force microscopy was used to determine the as-grown and post annealing surface morphologies of the samples. The as-grown sample covered with MOCVD AlN does not exhibit the same smooth step flow growth as the as-grown

sample without the MOCVD AlN cap. After annealing and etching off the AlN caps, the surface that was capped with MOCVD AlN shows evidence of pitting while the sample that was protected with only sputtered AlN no longer exhibits step flow growth like the as-grown sample. Since we are above 2/3 of the melting point of GaN, we expect that bulk diffusion is occurring and causing this rearrangement at the surface. This implies that sputtered AlN can provide sufficient protection of the underlying GaN surface, which will facilitate mid-process implantation and activation of Mg in GaN.

In-Situ Spectroscopy and Microscopy Focus Topic
Room: 211B - Session IS+SS+NS+BI+VT+MN+AS-WeA

In situ Imaging of Liquids using Microfluidics
Moderator: Xiao-Ying Yu, Pacific Northwest National Laboratory, Stephen Nonnenmann, University of Massachusetts - Amherst

2:20pm IS+SS+NS+BI+VT+MN+AS-WeA1 *In Situ* Multimodal Biological Imaging using Micro- and Nanofluidic Chambers, *James Evans, C. Smallwood*, Pacific Northwest National Laboratory **INVITED**
Biological organisms have evolved a number of spatially localized and highly orchestrated mechanisms for interacting with their environment. Since no single instrument is capable of probing the entire multidimensional landscape, it is not surprising that one of the grand challenges in biology remains the determination of how dynamics across these scales lead to observed phenotypes.

Therefore, there is a need for in-situ correlative multimodal and multiscale imaging to fully understand biological phenomena and how chemical or structural changes at the molecular level impact the whole organism. We have been advancing new methods for both cryogenic and in-situ correlative analysis of biological samples using electron, ion, optical and x-ray modalities. Central to this work is the development of new micro- and nanofluidic chambers that enable in-situ observations within precisely controlled liquid-flow environments. In this talk I will review the design of these new chambers, highlight current science applications and outline our future goals for adding additional functionality and expanding the versatility of the devices to other disciplines.

3:00pm IS+SS+NS+BI+VT+MN+AS-WeA3 Glyoxal Aqueous Surface Chemistry by SALVI and Liquid ToF-SIMS, *Xiao Sui, Y. Zhou, Z. Zhu*, Pacific Northwest National Laboratory*, J. Chen,* Shandong University, China, *X.-Y. Yu,* Pacific Northwest National Laboratory
Glyoxal, a ubiquitous water-soluble gas-phase oxidation product in the atmosphere, is an important source of oxalic acid, a precursor to aqueous secondary organic aerosol (SOA) formation. Many recent laboratory experiments and field observations suggest that more complex chemical reactions can occur in the aqueous aerosol surface; however, direct probing of aqueous surface changes is a challenging task using surface sensitive techniques. The ability to map the molecular distribution of reactants, reaction intermediates, and products at the aqueous surface are highly important to investigate surface chemistry driven by photochemical aging. In this study, photochemical reactions of glyoxal and hydrogen peroxide (H_2O_2) were studied by a microfluidic reactor, System for Analysis at the Liquid Vacuum Interface (SALVI), coupled with Time-of-Flight Secondary Ion Mass Spectrometry (ToF-SIMS). Aqueous surfaces containing glyoxal and hydrogen peroxide were exposed to UV light at variable lengths of time and were immediately analyzed in the SALVI microchannel by in situ liquid ToF-SIMS. In addition, various control samples were conducted to ensure that our findings were reliable. Compared with previous results of bulk solutions using ESI-MS, our unique liquid surface molecular imaging approach provided observations of glyoxal hydrolysis (i.e., first and secondary products, dimers, trimers, and other oligomers) and oxidation products (i.e., glyoxylic acid, oxalic acid and formic acid) with sub-micrometer spatial resolution. We potentially provide a new perspective and solution to study aqueous surface chemistry as an important source of aqueous SOA formation of relevance to atmospheric chemistry known to the community.

3:20pm IS+SS+NS+BI+VT+MN+AS-WeA4 Investigating *Shewanella Oneidensis* Biofilm Matrix in a Microchannel by *In Situ* Liquid ToF-SIMS, *Yuanzhao Ding*, Nanyang Technological University, Singapore, *X. Hua, Y. Zhou, J. Yu, X. Sui, J. Zhang, Z. Zhu*, Pacific Northwest National Laboratory, *B. Cao*, Nanyang Technological University, Singapore, *X.-Y. Yu*, Pacific Northwest National Laboratory

Biofilms consist of a group of micro-organisms attached onto surfaces or interfaces and embedded with a self-produced extracellular polymeric substance (EPS) in natural environments. The EPS matrix, like the "house of the cells", provides bacteria cells with a more stable environment and makes them physiologically different from planktonic cells. *Shewanella oneidensis* MR-1 is a metal-reducing bacterium, forming biofilms that can reduce toxic heavy metals. This capability makes *S. oneidensis* biofilms very attractive in environmental applications. To better understand the biofilm EPS matrix composition at the interface, in situ chemical imaging with higher spatial resolution and more molecular level chemical information is strongly needed. Traditionally, electron microscopy and fluorescence microscopy are common imaging tools in biofilm research. However, the bottlenecks in these imaging technologies face the limitations that it is difficult for them to provide chemical information of small molecules (e.g., molecule weight <200). In this study, we use an emerging technology liquid Time-of-Flight Secondary Ion Mass Spectrometry (ToF-SIMS) to observe *S. oneidensis* biofilm cultured in a vacuum compatible microchannel of the System for Analysis at the Liquid Vacuum Interface (SALVI) device. Chemical spatial distributions of small organic molecules that are considered to be the main building components of EPS in live biofilms are obtained. Principal component analysis is used to determine differences among biofilms sampled along the microchannel. This new approach overcomes previous limitations in live biofilm analysis and provides more chemical information of the EPS relevant to biofilm formation. Better understanding of the biofilm matrix will potentially fill in the knowledge gap in biofilm surface attachment and detachment processes and improve the engineering and design of *S. oneidensis* biofilms with high efficiencies in heavy metal reduction.

4:20pm IS+SS+NS+BI+VT+MN+AS-WeA7 Ultrafast Proton and Electron Dynamics in Core-Level Ionized Aqueous Solution, *Bernd Winter*, Helmholtz-Zentrum Berlin für Materialien und Energie/Elektronenspeicherring BESSY II, Germany **INVITED**

Photo- and Auger electron spectroscopy from liquid water reveals a novel electronic de-excitation process of core-level ionized water in which a pair of two cations forms, either $H_2O^+ \cdot H_2O^+$ or $OH^+ \cdot H_3O^+$. These reactive species are the delocalized analogue to H_2O^{2+}, formed in a localized on-site Auger decay, and are expected to play a considerable role in water radiation chemistry. Both cationic pairs form upon autoionization of the initial ionized water molecule, and we are particularly interested in the situation where autoionization occurs from a structure that evolves from proton transfer, from the ionized water molecule to a neighbor molecule, within a few femtoseconds. The actual autoionization is either through intermolecular Coulombic decay (ICD) or Auger decay. Experimental identification of the proton dynamics is through isotope effects. A question that arises is whether such so-called proton-transfer mediated charge separation (PTM-CS) processes occur in other and similarly hydrogen-bonded solute molecules as well. This is indeed the case, and is illustrated here for ammonia and glycine in water, as well as for hydrogen peroxide in water, where characteristic differences are detected in the Auger-electron spectra from the light *versus* heavy species, *i.e.*, NH_3 in H_2O *versus* ND_3 in D_2O, glycine(H) in H_2O versus glycine(D) in D_2O, and H_2O_2 in H_2O versus D_2O_2 in D_2O. The important spectral feature here is the high-kinetic energy tail of the Auger spectrum, which has no gas-phase analogue, and hence reflects the participation of solvent water in the relaxation process. The probability of the proton dynamics, judged from the intensities of the electron signal and inferred from methods of quantum chemistry and molecular dynamics, is found to depend on hydrogen-bond strength and hence on the specific hydration configuration. Favorable configurations for hydrogen peroxide(aq) occur due to the molecule's flexible structure. In ammonia(aq) the PTM processes are found to be less probable than for water(aq), which is attributed to the planarization of the ammonia molecule upon core-level ionization. The effect is smaller for the neutral $-NH_2$(aq) group of glycine at basic pH, where intramolecular dynamics is less likely. Nature and chemical reactivity of the initial transient species and their role for radiation chemistry and for local reactions relevant for biological molecules in an aqueous environment are discussed for the different molecular hydrogen-bonded systems.

5:00pm IS+SS+NS+BI+VT+MN+AS-WeA9 Water Dissociation in Metal Organic Frameworks with Coordinatively Unsaturated Metal Ions: MOF-74, *Kui Tan*, The University of Texas at Dallas, *S. Zuluaga*, Wake Forest University, *E. Fuentesf*, The University of Texas at Dallas, *H. Wang*, Rutgers University, *P. Canepa*, Wake Forest University, *J. Li*, Rutgers University, *T. Thonhauser*, Wake Forest University, *Y.J. Chabal*, The University of Texas at Dallas

Water dissociation represents one of the most important reactions in catalysis, essential to the surface and nano sciences. However, the dissociation mechanism on most oxide surfaces is not well understood due to the experimental challenges of preparing surface structures and characterizing reaction pathways. To remedy this problem, we propose the metal organic framework MOF-74 as an ideal model system to study water reactions. Its crystalline structure is well characterized; the metal oxide node mimics surfaces with exposed cations; and it degrades in water. Combining *in situ* IR spectroscopy and first-principles calculations, we explored the MOF-74/water interaction as a function of vapor pressure and temperature. Here, we show that, while adsorption is reversible below the water condensation pressure (~19.7 Torr) at room temperature, a reaction takes place at ~150 ˚C even at low water vapor pressures. This important finding is unambiguously demonstrated by a clear spectroscopic signature for the direct reaction using D_2O, which is not present using H_2O due to strong phonon coupling. Specifically, a sharp absorption band appears at 970 cm^{-1} when D_2O is introduced at above 150 ˚C, which we attribute to an O-D bending vibration on the phenolate linker. Although H_2O undergoes a similar dissociation reaction, the corresponding O-H mode is too strongly coupled to MOF vibrations to detect. In contrast, the O-D mode falls in the phonon gap of the MOF and remains localized. First-principles calculations not only positively identify the O-D mode at 970 cm^{-1} but derive a pathway and kinetic barrier for the reaction and the final configuration: the D (H) atom is transferred to the oxygen of the linker phenolate group, producing the notable O-D absorption band at 970 cm^{-1}, while the OD (or OH) binds to the open metal sites. Experimental data and theoretical modeling further shows that the reaction is facilitated by a cooperative effect of several H_2O molecules. This finding explains water dissociation in this case and provides insight into the long-lasting question of MOF-74 degradation. Overall, it adds to the understanding of molecular water interaction with cation-exposed surfaces to enable development of more efficient catalysts for water dissociation.

Ref: K. Tan, S. Zuluaga, Q. Gong, P. Canepa, H. Wang, J. Li, Y. J. Chabal and T. Thonhauser, *Chem. Mater.*, 2014, **26**, 6886-6895.

5:20pm IS+SS+NS+BI+VT+MN+AS-WeA10 Competitive Co-Adsorption of CO_2 with H_2O, NH_3, SO_2, NO, NO_2, N_2, O_2, and CH_4 in M-MOF-74 (M= Mg, Co, Ni): The Role of Hydrogen Bonding, *K. Tan*, The University of Texas at Dallas, *Sebastian Zuluaga*, Wake Forest University, *H. Wang*, Rutgers University, *Y. Gao*, The University of Texas at Dallas, *J. Li*, Rutgers University, *T. Thonhauser*, Wake Forest University, *Y.J. Chabal*, The University of Texas at Dallas

The importance of co-adsorption for applications of porous materials in gas separation has motivated fundamental studies, which have initially focused on the comparison of the binding energies of different gas molecules in the pores (i.e. energetics) and their overall transport. By examining the competitive co-adsorption of several small molecules in M-MOF-74 (M= Mg, Co, Ni) with *in-situ* infrared spectroscopy and *ab initio* simulations, we find that the binding energy at the most favorable (metal) site is not a sufficient indicator for prediction of molecular adsorption and stability in MOFs. Instead, the occupation of the open metal sites is governed by kinetics, whereby the interaction of the guest molecules with the MOF organic linkers controls the reaction barrier for molecular exchange. Specifically, the displacement of CO_2 adsorbed at the metal center by other molecules such as H_2O, NH_3, SO_2, NO, NO_2, N_2, O_2, and CH_4 is mainly observed for H_2O and NH_3, even though SO_2, NO, and NO_2, have higher binding energies (~70-90 kJ/mol) to metal sites than that of CO_2 (38 to 48 kJ/mol) andslightly higher than water (~60-80 kJ/mol). DFT simulations evaluate the barriers for H_2OàCO_2 and SO_2àCO_2 exchange to be ~ 13 and 20 kJ/mol, respectively, explaining the slow exchange of CO_2 by SO_2, compared to water. Furthermore, the calculations reveal that the kinetic barrier for this exchange is determined by the specifics of the interaction of the second guest molecule (e.g., H_2O or SO_2) with the MOF ligands. Hydrogen bonding of H_2O molecules with the nearby oxygen of the organic linker is found to facilitate the positioning of the H_2O oxygen atom towards the metal center, thus reducing the exchange barrier. In contrast, SO_2 molecules interact with the distant benzene site, away from the metal center, hindering the exchange process. Similar considerations apply to the other molecules, accounting for much easier CO_2 exchange for NH_3 than for NO, NO_2, CH_4, O_2, and N_2 molecules. In this work, critical parameters such as kinetic barrier and exchange pathway are first unveiled and provide insight into the mechanism of competitive co-adsorption, underscoring the need of combined studies, using spectroscopic methods and *ab initio* simulations to

uncover the atomistic interactions of small molecules in MOFs that directly influence co-adsorption.

Ref: K. Tan, S. Zuluaga, Q. Gong, Y. Gao, N. Nijem, J. Li, T. Thonhauser and Y. J. Chabal, *Chem. Mater.*, 2015, **27**, 2203-2217.

6:00pm IS+SS+NS+BI+VT+MN+AS-WeA12 *In Situ* **STM Observation of Pd(110) Under the Hydrogen Pressure Between 10^{-6} Pa and 10^{-3} Pa**, *Jun Yoshinobu, H. Kikuchi, T. Koitaya, K. Mukai, S. Yoshiomoto*, University of Tokyo, Japan

Hydrogen adsorption and absorption on/in Pd and Pd alloys are vital processes for the hydrogen storage and hydrogen permeation materials. We investigated the Pd(110) surface under the hydrogen pressures between 10^{-6} Pa and 10^{-3} Pa at room temperature using in-situ atom-resolved scanning tunneling microscopy (STM). We observed missing-atom, missing-row and added-row structures and the number of atoms in these structures were quantitatively analyzed as a function of exposure time. Note that adatoms were not detected probably because they were mobile in the present experimental conditions. At 10^{-6} Pa, the numbers of missing-row and added-row atoms increased up to ~20 L (langmuir) and after that they were gradually reaching the saturation (steady-state). On the other hand, the number of missing-atoms decreased gradually from the initial stage. With increasing the hydrogen pressures the number of missing-row atoms and added-row atoms increased, and the whole surface was covered with these reconstructed structures after large exposures (>1000 L). It has been known that not only hydrogen adsorption but also hydrogen absorption occur in such conditions. Thus, the missing-row and added-row reconstructed structures are inevitable for hydrogen absorption on Pd(110).

Nanometer-scale Science and Technology
Room: 212B - Session NS+EN+MG+SS+TF-WeA

Nanoscale Catalysis and Surface Chemistry
Moderator: Sidney Cohen, Weizmann Institute of Science, Israel

2:20pm NS+EN+MG+SS+TF-WeA1 Effects of γ-Al$_2$O$_3$ Support on the Geometry and Electronic Structure of H-covered Pt Nanoparticles, *Sampyo Hong, G. Shafai, T.S. Rahman*, University of Central Florida

We have studied the effects of γ-Al$_2$O$_3$(110) support on the geometry and electronic structures of H-coveredPt$_x$ (x=22,44) nanoparticles (NP) using density functional theory (DFT). We find that the unoccupied d-band center of γ-Al$_2$O$_3$(110) supported Pt NPs exhibits a blue shift with decreasing Pt size similarly as the measured XANES absorption peak energy of Pt NP samples. In fact, our DFT results reveal that the shift of the unoccupied d-band center of Pt NPs is dependent of surface hydroxylation level on γ-Al$_2$O$_3$(110). At higher hydroxylation the calculated unoccupied d-band center can even show red shift. Thus, consideration of hydroxylation level on γ-Al$_2$O$_3$(110) is needed to properly interpret support effect from XANES spectra. Overall, the strength of Pt- γ-Al$_2$O$_3$(110) binding seems to be a reasonable measure of the shift of unoccupied d-band center as a result of metal-support interaction: the stronger the interaction the more the blue shift. In the light of these results, it is plausible to postulate that the adsorption energy shift of XANES spectra represent the strength of metal-support interaction (support effect). A remarkable example of such hydroxylation tuned metal-support interaction is structural transition of Pt$_{22}$ from a biplanar to a 3D-like geometry as a function of support hydroxylation.

This work is supported in part by DOE Grant DE-FG02-07ER15842.

3:00pm NS+EN+MG+SS+TF-WeA3 Fabrication and SERS Activity of Metal-loaded TiO$_2$ Nanometer ScaleParticles, *Paolo Reyes, J.C. Hemminger*, University of California Irvine

Our current research focuses on the fabrication and study of metallic loaded titanium dioxide (TiO$_2$) nanoparticles supported by highly oriented pyrolitic graphite (HOPG). Highly dispersed TiO$_2$ particles are formed via physical vapor deposition (PVD) under high vacuum settings with an average pseudo-diameter of 11.6 ± 2.65 nm. Metallic loading is completed by an ex-situ photo-deposition method by exposure to precursor metal salt solutions under TiO$_2$ bandgap UV irradiation. We have attempted to fabricate Pt-, Ag-, Au-, and Pt-Au-TiO$_2$ particles and observed photocatalytic enhancement with the inclusion of Pt nanoparticles deposited onto TiO$_2$ surfaces. We believe this enhancement is a result of Pt nanoparticles harboring free excited electrons and preventing electron-hole recombination. We have developed a technique to increase the density of TiO$_2$ particles by creating site defects on the surface of HOPG through plasma mild oxygen plasma exposure. Highly dispersed TiO$_2$ nanoparticle

distributions allow an increase of metal nanoparticle formation on TiO$_2$ for surface and intrinsic property observations. Ag nanoparticles have been fabricated in order to observe Surface Enhanced Raman Spectroscopy (SERS) Ag nanoparticles were observed to be an average pseudo-diameter of 2.6 ± 1.4 nm. A probe molecule was used to determine Raman intensity enhancement factor (EF) and we believe that the EF can be affected by the spacing and size of Ag-TiO$_2$ nanoparticles. We will present our studies of bi-metallic loading of TiO$_2$.

4:20pm NS+EN+MG+SS+TF-WeA7 Pyridine Coordination Chemistry for Molecular Assemblies, *Milko Van der Boom*, Weizmann Institute of Science, Israel **INVITED**

Many types of metal-ligand interactions have creatively been used in the chemical sciences since the description of coordination complexes. The rich coordination chemistry of pyridine-type ligands has contributed significantly to the incorporation of metal ions into functional materials on surfaces. We will discuss molecular assemblies formed with a variety of pyridine-based compounds. These assemblies are formed by layer-by-layer deposition from solution that allows for precise fitting of the assembly properties. The degree of intermolecular interactions can be controlled by varying the degree of π-conjugation and the availability of coordination sites. Unlike molecular assemblies that are constructed with organic ligands, assemblies with polypyridyl complexes are active participants in their own formation and amplify the growth of the incoming molecular layers. Such a self-propagating behavior for molecular systems is rare and the mechanism of their formation will be presented. Incorporating multiple metal complexes into a single assembly give rise to composite materials that exhibit unique electrochemical and electrochromic properties that are dependent on the arrangement of these metal complexes. We will also discuss the coordination chemistry of pyridine-based compounds with nanoparticles, the formation of metal-organic frameworks and their practical applications.

5:00pm NS+EN+MG+SS+TF-WeA9 Atomic Scale Iron Carbide Films on Au(111) and Cu(111) as a Iron Fischer-Tropsch Model Catalyst, *Gilbère Mannie, X. Wen, Y.W. Li*, SynCat@Beijing, China, *J.V. Lauritsen*, Interdisciplinary Nanoscience Center (iNANO), Denmark, *H.J.W. Niemantsverdriet*, SynCat@Beijing, China

Iron-based Fischer-Tropsch synthesis (FTS) is one of the most investigated catalytic systems in the world due to the ability to convert any form of hydrocarbons like coal, natural gas or biomass into diesel, gasoline and chemicals [1]. Although investigated for more than 50+ years, fundamental surface reactions involved in this process are not known or fully understood. Within the FTS community, iron carbide is seen as the active phase in the catalytic process but the atomic-scale surface structure and even the stoichiometry of the bulk phase is a matter of debate [1,2]. In order to fundamentally investigate the active phase, to for example verify molecular modeling studies on iron carbide surfaces (like [3,4]), we successfully synthesized highly-crystalline iron carbide monolayer islands (on Au(111)) and multilayer islands (on Cu(111)). Obtained carbidic films are suitable for analysis with scanning tunneling microscopy (STM) and other surface science techniques. Our atomically-resolved STM results, together with preliminary density functional theory (DFT) results show that we can characterize our iron carbide (Fe$_x$C$_y$) islands as iron layer with interstitial carbon atoms, based on the increase of the inter-atomic Fe-Fe distance [5]. During the synthesis of the Fe$_x$C$_y$ islands we were able to record some STM movies showing the formation of the carbidic phase out of the metallic phase but we could also record movies during dosing experiments of several gasses (H$_2$, O$_2$) to the pure iron carbide islands. During the presentation we will explain how we synthesized these crystalline iron carbide films and how these films can act as a model system for fundamental Fischer-Tropsch catalyst research.

[1] E. de Smit, B. M. Weckhuysen, *Chem. Soc. Rev.,***2008,** *37,* 2758

[2] J. W. Niemantsverdriet, A. M. van der Kraan, W. L. van Dijk, H. S. van der Baan, *J. Phys.,* **1980,** *84,* 3363

[3] J. M. Gracia, F. F. Prinsloo, J. W. Niemantsverdriet, *Catal. Lett.,***2009,** *133,* 257

[4] M. O. Ozbek, J. W. Niemantsverdriet, *J. Catal.,***2014,** *317,* 158

[5] G. J. A. Mannie, L. Lammich, Y. W. Li, J. W. Niemantsverdriet, J. V. Lauritsen, *ACS Catal.,***2014,***4,* 3255

5:20pm NS+EN+MG+SS+TF-WeA10 Fullerene Interaction with W Surfaces: Synthesis of Nanospheres with Tunable Bandgap, *Ehsan Monazami*, University of Virginia, *J.B. McClimon*, University of Pennsylvania, *P. Reinke*, University of Virginia

The interaction of f C_{60} molecules with metal surfaces is a topic of considerable interest and discussed in the context of molecular electronics and organic solar cell applications. Our work focuses on the interaction of C_{60} with W, which is a carbide forming transition metal. It has generally been assumed that the C_{60} cage breaks up readily on a W surface, but our observations reveal a more complex, temperature induced reaction sequence leading to the formation of nanospheres with variable bandgap, which has been studied with in-situ STM and STS analysis.

The nanospheres are synthesized by initiating the reaction between C_{60} deposited on a W-thin film surface grown on MgO(001) at about 450 K. In contrast to previous reports, the molecules do not collapse but the spherical shape is retained up to 800 K and the electronic structure changes gradually from wide bandgap C_{60} to fully metallic nanospheres. The size distribution of the nanospheres is centered at 1.5 nm (600 K) and shifts for higher temperatures to about 2 nm with a concurrent decrease in height resulting in an ellipsoidal shape. These nanosheres present an exceptional resistance to sintering which is a unique feature for metallic nanoparticles. The densely packed C_{60} and isolated C_{60} molecules show the same transition in shape and electronic structure which confirms that the transformation is controlled by the reaction with the W substrate.

The transition in the electronic structure progresses gradually from the wide-bandgap molecule (2.3 eV) to a bandgap of ~1eV at 700 K, and a metallic surface at 800 K. We will illustrate this progression with a series of ST spectra and maps. The bandgap variation offers for the first time a pathway to the formation of nanoscale clusters (nanospheres) with variable bandgap while retaining the surface curvature in narrow range. The detailed structure of the nanospheres is, however, still subject to discussion. We currently favor, based on our experimental results, a substitution model where the W-atoms from the substrate react with the C_{60} cage which acts as a scaffold. The W atoms are incorporated substitutionally forming a carbide type bonding, whose presence is indicated by XPS analysis. The variation in bandgap is then driven by the degree of substitution and the fullerene molecule acts as a scaffold. We predict that other carbon scaffolds such as nanotubes and carbide forming transition metals can react in the same manner leading to a new class of nanostructures with unique adaptability of the electronic structure. The nanospheres are an excellent testbed for the physics and chemistry of highly curved surfaces.

Supported by NSF-DMR Ceramics DMR-100580.

5:40pm NS+EN+MG+SS+TF-WeA11 Enantiomeric Separations of Chiral Pharmaceuticals using Chiral Tetrahexahedral Au Nanoparticles, *Nisha Shukla*, *D. Yang, A.J. Gellman*, Carnegie Mellon University

Chiral tetrahexahedral (24-sided) Au nanoparticles are tested for their use as chiral separators of pharmaceutical drugs in solution phase. Tetrahexahedral Au nanoparticles were chirally modified with either D- or L-cysteine. They show enantioselective adsorption of pharmaceuticals such as propranolol hydrochloride (used for anxiety and high blood pressure) from a solution of racemic propranolol hydrochloride, thus leaving an enantiomeric excess in the solution phase. This work suggests that chiral nanoparticles can be used for enantiomeric separation of real pharmaceutical drugs. A simple robust model has also been developed that allows extraction of the enantiospecific equilibrium constants for R- and S-propranolol hydrochloride adsorption on the chiral tetrahexahedral Au nanoparticles. The model obviates the need for experimental determination of the surface area of absorbent Au nanoparticles which is extremely difficult to measure.

6:00pm NS+EN+MG+SS+TF-WeA12 Electroreduction Catalysis with Defect-Rich Metal Nanoparticles, *Xiaofeng Feng*, *M. Kanan*, Stanford University

New design principles for electroreduction catalysts are essential for CO_2 recycling using renewable electricity. Au is one of the most active catalysts for CO_2 reduction to CO, and numerous efforts have been made to optimize Au catalysts by tuning the size, composition, and shape of Au nanostructures. Here we show that grain boundaries (GBs) in Au nanoparticles create highly active surface sites for CO_2 electroreduction (1). Defect-rich Au nanoparticles were synthesized by vapor deposition of Au onto a carbon nanotube thin film, which enables direct TEM characterization without further processing. We compared the CO_2 reduction activity of the as-deposited catalysts to those annealed at different temperatures. While the annealing process has little impact on the distribution of Au surface facets, it reduces the GB density, which is quantified by measuring GB lengths and particle areas from high-resolution TEM images. We found that the surface-area-normalized activity for CO_2 reduction is linearly correlated with GB density in Au nanoparticles in the

low overpotential regime. Similarly, GB-density was also found to correlate with catalytic activity for the electroreduction of CO to multi-carbon oxygenates on Cu nanoparticles. Our studies show that grain boundary engineering is a general strategy for improving electrocatalytic activity for carbon fuel synthesis.

References:

(1) Feng, X.; Jiang, K.; Fan, S.; Kanan, M. W. *J. Am. Chem. Soc.***2015**, *137*, 4606–4609.

Plasma Science and Technology
Room: 210B - Session PS+AS+SS-WeA

Plasma Surface Interactions
Moderator: Steven Vitale, MIT Lincoln Laboratory

2:20pm PS+AS+SS-WeA1 *In Situ* FTIR Diagnostics and Characterization of Etch By-Product Deposition on Chamber Walls and Wafer Surface during Halogen Etching of Silicon, *Neema Rastgar*, *S. Sriraman, R. Marsh, A. Paterson*, Lam Research Corporation

Plasma etching is a critical technology for nanoelectronics fabrication, but the use of a vacuum chamber limits the number of in situ, real-time diagnostics measurements that can be performed during an etch process. Byproduct deposition on chamber walls during etching can affect the run-to-run performance of an etch process if there is build-up or change of wall characteristics with time. Knowledge of chamber wall evolution and the composition of wall-deposited films are critical to understanding the performance of plasma etch processes, and an in situ diagnostics measurement is useful for monitoring the chamber walls in real time.

In this talk, we report the use of attenuated total reflectance Fourier transform infrared spectroscopy (ATR-FTIR) to perform in situ diagnostics of a vacuum chamber's walls during plasma etching. Using ATR-FTIR, the relative thickness and makeup of chamber wall deposits in real time is monitored. This information is then used to develop a chamber wall cleaning process in order to maintain reproducible etching conditions from wafer to wafer. In particular, we report mid-IR (4000-650 cm^{-1}) absorption spectra of chamber wall-deposited silicon byproducts formed during halogen etching of silicon wafers. Preliminary results demonstrating measurements of on-wafer etch byproduct evolution as well as its correlation to chamber wall deposits will be discussed.

2:40pm PS+AS+SS-WeA2 Particle as a Temperature Probe: Thermal Effects in Non-Thermal Plasmas, *Thomas Lopez*, *L. Mangolini*, University of California Riverside

Silicon nanocrystals are currently under investigation for several applications including nanoelectronics, light emitting devices, photovoltaics, thermal electric devices, and energy recovery and storage. Continuous flow nonthermal plasmas reactors are ideal for silicon nanaparticle production for many reasons; continuous flow non thermal plasma reactors are a scalable system, they readily produce completely amorphous to completely crystalline samples, and they have the ability to control size and size distributions of produced particles [1]. Extensive *in-situ* and *ex-situ* characterization on continuous flow non-thermal plasma reactors has been carried out characterizing nucleation, growth, and structural evolution [2]. Particle size, structure, and surface termination are all particle properties that are directly correlated to the particles' interactions with ions and other plasma produced radicals during their creation [2]. It has been shown that the interactions between particles, ions and other radicals in non-thermal plasmas leads to a thermal annealing process [3], meaning particles in non-thermal plasmas are heated well above the temperatures of their respective carrier gases. We probe the temperature of silicon nanoparticles produced via continuous flow non-thermal plasma reactors by monitoring their surface termination. *In-situ* FTIR has been utilized to track changes in the surface chemistry of particles, which have then been correlated to the particle temperature as a function of plasma power. FTIR data shows that hydrogen termination of silicon nanoparticles as they flow through a plasma is power dependent, with higher power leading to a decrease in hydrogen surface termination. We attribute this behaviour to thermally induced desorption from the particle surface. A discussion on the characterization of nanoparticle interactions with the plasma based on *in-situ* FTIR, optical emission spectroscopy and ion density measurements will be presented.

1. Lopez, T. and L. Mangolini, *Low activation energy for the crystallization of amorphous silicon nanoparticles*, Nanoscale, 2014. **6**(3): p. 1286-1294

2. Lopez, Thomas, and Lorenzo Mangolini. Journal of Vacuum Science & Technology B 32.6 (2014): 061802.

3. Kramer, N.J., R.J. Anthony, M. Mamunuru, E.S. Aydil, and U.R. Kortshagen, *Plasma-induced crystallization of silicon nanoparticles*, Journal of Physics D: Applied Physics, 2014. **47**(7): p. 075202.

3:00pm PS+AS+SS-WeA3 Plasma-Surface Interactions at Low and High Pressure, *Vincent Donnelly*, University of Houston **INVITED**
This talk will review studied of the interactions of low pressure Cl₂, HBr, and O₂ inductively-coupled plasmas with reactor chamber walls, with and without Si etching, using the "spinning wall" technique. The spinning wall is part of the reactor chamber walls, allowing near-real-time analysis of the composition of surface layers via Auger electron spectrometry, and determination of species desorbing off the walls by mass spectrometry. Langmuir-Hinshelwood (L-H) reactions, with surface residence times > 0.5 ms can be studied by this technique. Many commonalities were found for the different source gas plasmas. For example, when the walls were coated with SiO_x or AlO_x layers, A + B recombination reactions including O + O, O + Cl, Cl + Cl and H + Br are detected, provided that the surface contains a level of oxygen above some critical value. During Si etching, surfaces coated with Si-halide products tend to be less catalytic toward L-H recombination reactions, while Si-oxyhalides films formed on chamber walls when oxygen is present in the plasma are much more active in promoting L-H recombination, as well as adsorption and delayed desorption of Cl₂. At most sites, O is believed to be in the inactive form of Si-O-Si. In relatively few cases, O cannot coordinate to a second Si and the active Si-O- forms. This quickly forms Si-O-A and then mobile B on the surface forms Si-O-AB, followed by desorption of AB, which could also be delayed. For all of the products observed, formation and desorption of AB is exothermic. Si etching with small oxygen addition leads to "sticky" products with a range of masses up to at least the limit of our mass spectrometer (m/e = 500) that desorb from chamber wall surfaces in ms to min after plasma exposure. Gaseous products contain -O-Si-O- linkages are prominent, in addition to Si-mono and tri-halides. In HBr-containing plasmas, products contain little or no H. Experiments have also begun to study plasma-surface interactions at atmospheric pressure. Species present within one mean free path of a quartz substrate exposed to a He jet plasma in ambient air and in a sealed chamber with gas additives are spatially resolved using a new near-field optical emission spectroscopy method.

4:20pm PS+AS+SS-WeA7 Measurements of IIEE Emitted Electrons from Chemically-Cleaned and Sputtered-Cleaned Semiconductor Surfaces, *D. Urrabazo*, *Lawrence Overzet*, University of Texas at Dallas
Plasma-surface interactions with semiconductors comprise a variety of interesting phenomena in addition to etching and deposition. One such phenomenon is ion induced electron emission (IIEE). IIEE has historically been viewed as extremely surface sensitive; but recent measurements have suggested that the IIEE yield from semiconductors, unlike metals, may in fact depend on the sub-surface properties as well. We investigated the effects of the surface and sub-surface properties (doping type, Fermi level, cleanliness level) on the relative IIEE yields from Si and Ge. Our measurements indicate that the relative IIEE yields did not depend on the doping type to a significant degree independent of the level of cleanliness. This result is consistent with IIEE theory. We further explored the sensitivity of the IIEE yield to surface cleanliness by making XPS and UPS measurements on the surface chemistry and approximate surface density of states (sDOS) of the semiconductors. By combining the theoretical IIEE model with the sDOS, we were able to replicate the changes in the IIEE emitted electron distribution functions due to surface cleanliness changes. Thus, we confirmed that the IIEE yield is affected by the cleanliness of the surface primarily through the change in the surface density of states.

4:40pm PS+AS+SS-WeA8 Effects of Hydrogen on Etching Processes for Transparent Conducting Films, *Hu Li**, *K. Karahashi*, Osaka University, Japan, *M. Fukasawa, K. Nagahata, T. Tatsumi*, Sony Corporation, Japan, *S. Hamaguchi*, Osaka University, Japan
The market demand for high-resolution optoelectronic devices such as head-mounted displays has accelerated the development of micro pattern formation technologies for transparent conducting oxides (TCOs) with a pattern resolution of sub-microns or even nanometers. Reactive ion etching (RIE), which has been widely used in the fabrication of semiconductors, is also a promising technology for patterning of TCOs. Tin-doped indium oxide (ITO) and Zinc oxide (ZnO) are widely used TCOs in the industry. The goal of this study is therefore to establish RIE technologies for ITO and ZnO for high-resolution patterning.

---

* Coburn & Winters Student Award Finalist

Typical RIE processes for ITO and ZnO use plasmas based on organic gases such as CH₄ and CH₃OH. CH₄ and CH₃OH are non-corrosive gases and RIE processes with such gases are expected to achieve high etching rates with less process damages. In this study, we have mostly focused on ZnO etching processes and evaluated sputtering yields and analyzed surface reaction characteristics of ZnO by various chemically reactive species such as CH_x^+, H^+, and H^*, using a mass-selected ion beam system. The mass-selected ion beam system allows one to examine surface reactions caused by specific ion species with a given incident energy incident upon the sample substrate set in an ultra-high vacuum (UHV) reaction chamber. Simultaneous injection of hydrogen radicals have been also performed with a hydrogen radical source. Surface chemical composition after such beam injections have been analyzed by *in-situ* X-ray Photoelectron Spectroscopy (XPS) installed in the reaction chamber.

Our previous study [1] found that the sputtering yield of ZnO strongly depends on the number of hydrogen atoms contained in each incident molecular ions. In this study, we have clarified the effects of incident hydrogen ions and radicals. When ZnO is etched by simultaneous injection of energetic CH^+ ions and abundant hydrogen radicals, it has been found that etching proceeds with no carbon deposition and the sputtering yield of ZnO is closed to that of the corresponding physical sputtering. This result suggests that hydrogen radicals prevent carbon accumulation on ZnO and energetic hydrogen ion incidence leads to the formation of a surface damage layer, which is more easily sputtered by incident energetic ions. Therefore the presence of CH_3^+ ions is not indispensable in such a RIE process and the embrittlement of ZnO by hydrogen is more crucial to the achievement of efficient etching processes for ZnO.

[1] H. Li, K. Karahashi, M. Fukasawa, K. Nagahata, T. Tatsumi, and S. Hamaguchi, AVS61st Int. Symp. Exh. Abst. 4892, PS-TuM11.

5:00pm PS+AS+SS-WeA9 Mechanisms of Hydrocarbon Based Polymer Etch using Pulsed Plasmas, *Barton Lane*, *P. Ventzek, M. Matsukuma, A. Suzuki, A. Koshiishi*, Tokyo Electron Limited
Dry etch of hydrocarbon based polymers is important for semiconductor device manufacturing. The etch mechanisms for oxygen rich plasma etch of hydrocarbon based polymers has been studied but the mechanism for lean chemistries has received little attention. We report on an experimental and analytic study of the mechanism for etching of a hydrocarbon based polymer using an Ar/O2 chemistry in a single frequency 13.56 MHz test bed. The experimental study employs an analysis of transients from sequential oxidation and Ar sputtering steps using OES and surface analytics to constrain conceptual models for the etch mechanism. The conceptual model is consistent with observations from MD studies and surface analysis performed by Vegh, et al. and Oehrlein, et al. [1,2] and other similar studies. Parameters of the model are fit using published data and the experimentally observed time scales. [1] J.J. Vegh, D. Nest, D. B. Graves, R. Bruce, S. Englemann, T. Kwon, R. J. Phaneuf, G. S. Oehrlein, B. K. Long, and C. G. Willson, Jour. of Applied Physics **104**, 034308 (2008), [2] G.S. Oehrlein, R. J. Phaneuf, D. G. Graves, J. Vac. Sci. Tech. B 29, 010801-1 (2011).

5:20pm PS+AS+SS-WeA10 Role of Plasma Density in Damage Characterization and its Impact on Low-Damage Plasma Process Design, *Koji Eriguchi*, *M. Kamei, Y. Nakakubo, K. Ono*, Kyoto University, Japan
Plasma process-induced damage (PID) is one of critical issues in designing metal−oxide−semiconductor field-effect transistors (MOSFETs) with higher performance and reliability. The damage creation mechanisms—plasma-induced physical damage (PPD) and charging damage (PCD) [1]—have been characterized by various techniques so far [2] to design low plasma processes. In this study, conflicting results leading to erroneous conclusions in designing future plasma processes are presented, where ion flux and charge injection from plasma (~ plasma density) play a key role in these conventional characterizations. Firstly, regarding PPD, n-type (100) Si wafers were exposed to Ar-based ICP and CCP discharges [3] and the localized defects were created in the Si substrates by ion bombardment. It is found that, although the average energy of incident ions (E_{ion}) is larger for the case of CCP, the latent defect density (n_{dam}) of CCP-damaged samples is smaller than that of ICP, even after the damaged-layer removal. This observation is in sharp contrast to previous pictures, i.e., the larger E_{ion} leads to the larger PPD. Secondary, MOSFETs with "high-k" (HfSiO$_x$) gate dielectric were damaged by the Ar-based ICP plasma and the high-k damage (~ carrier trap site generation) by PCD is evaluated by time-dependent dielectric breakdown (TDDB) measurement [4]. We identify that

the TDDB lifetime becomes longer under a certain amount of charge injection by plasma-induced current. This finding implies that one might be misled to an erroneous design rule of future LSIs. We propose a model explaining these conflicting results, where both ion flux and charge injection from plasma and the nature of the analysis techniques are taken into account. Since modern FinFETs with high-k dielectrics [5] are susceptible to PPD and PCD, the present model should be intensively implemented in designing future "low-damage" plasma processes.

[1] For example, K. Eriguchi and K. Ono, J. Phys. D 41, 024002 (2008).

[2] M. Fukasawa et al., Dry Process Symposium, 183, (2013).

[3] Y. Nakakubo et al., ECS J. Solid State Sci. Technol., 4 N5077 (2015).

[4] M. Kamei et al., IEEE Int. Integrated Reliability Workshop Final Report, 43 (2014).

[5] For example, I. Ferain et al., Nature 479, 310 (2011).

5:40pm PS+AS+SS-WeA11 Dry Deep Etching Of Bulk Titanium By Plasma Processes, *Edouard Laudrel, T. Tillocher, P. Lefaucheux,* GREMI CNRS/Université d'Orléans, France, *B. Boutaud,* Sorin Crm, France, *R. Dussart*, GREMI CNRS/Université d'Orléans, France

Bio-MEMS have emerged these last years with applications for biosensors, drug delivery, etc. The biocompatibility, the mechanical strength and the hydrophilicity properties have made titanium a widely used material with a great interest in the biomedical field. This element was chosen to fabricate body implantable devices with the help of microfabrication methods from microelectronics technologies in order to pattern structures with vertical sidewalls and smooth surfaces. Most of the literature with an interest in titanium deep etching relies on chlorine plasma processes. They are performed at room temperature of the substrate with typical etch rates close to 1 $\mu m.min^{-1}$ and provide rather smooth surfaces. TiO_2 or Ni are typically used as hard mask. However, a thick (several 10s of microns) SU8 layer, which is a negative photoresist, has also been reported as an alternative mask because it can be easily patterned and stripped.

Samples used in our experiments consist of coupons of a patterned titanium wafer glued on a silicon carrier wafer. The titanium wafer is 300 μm thick with a 15 μm thick backside thermal TiO_2 layer and the mask is a 15 μm electrochemically deposited thick nickel layer. The samples were processed in two different ICP reactors. Two different chemistries can be used to etch titanium. A chlorine-based chemistry at low pressure can be used to obtain anisotropic profiles but with reduced etch rates at room temperature. With the first reactor, equipped with a diffusion chamber, titanium etch rate was 1 $\mu m.min^{-1}$. A fluorine-based chemistry admits higher etch rate (as 4 $\mu m.min^{-1}$) at higher pressure (few Pa) with isotropic profiles if the sample temperature is sufficient to form volatile etch by-products. Both chemistries, as well as $Cl_2/Ar/SF_6$ mixture, produced non-reproducible results and a high roughness. These observations were attributed to the redeposition of etch by-products (like $SiOCl_x$) on the sample surface. It induces a micro-masking effect which generates a high roughness and leads to reproducibility issues. The so-called APETi (Alternated Process for the deep Etching of Titanium) process has been developed to prevent this roughness and increase the reproducibility. An average etch rate of 1.4 $\mu m.min^{-1}$ has been achieved with reproducible features.

Comparative experiments have started on a second ICP reactor which enables higher etch rates due to a higher self-bias voltage and higher density species. The substrate holder temperature can also be higher, which should help to enhance chemical etching processes with a fluorine chemistry.

6:00pm PS+AS+SS-WeA12 Particle Transport with Wafer Potential Controlled by Dipole Electrostatic Chuck Electrodes, *Masaki Ishiguro, M. Sumiya*, Hitachi High-Technologies Corp., Japan

In plasma etching for semiconductor manufacturing, it is important to prevent particle attachment on the wafer during processing to maintain high yield rate. As the device size continue to be scaled down, smaller particles should be taken care not to attach onto the wafer. It is said that 10 nm particles will be critical for semiconductor manufacturing in 2019 [1]. One important approach to prevent particle attachment on the wafer is controlling particle transport. Electrostatic force is one of the suitable forces to control particle transport. In the case that particle charge and wafer potential polarity is opposite, large number of small particles can be attracted onto the wafer. In plasma etching process, plasma on and off periods are periodically repeated. Kobayashi *et. al.* revealed that in plasma on period, the particles are trapped at the plasma sheath boundary and there is a less-risk of particle attachment to the wafer [2]. It suggested that, in plasma off period, there is a large-risk of particle attachment to the wafer if the wafer and the particles have opposite charge respectively.

In this study, the relationship between particle attachment to the wafer and wafer potential in plasma off period was investigated. Particle count on the wafer was measured at different wafer potential during plasma-off period by changing voltage settings of dipole electrostatic chuck electrodes (ESC) in Ar, O_2 and N_2 plasma. In the case of negative wafer potential, particle counts increased as the plasma off time was prolonged. On the other hand, in the case of positive or 0 wafer potential, particle count was relatively low level and it did not increase even if plasma off time was prolonged. This result suggests that, in our experimental condition, the particles charge positive during plasma off period and they are continuously generated from inner chamber wall. If the wafer has negative potential, the particles are attracted by electrostatic force. The numerical simulation result will also be shown to understand the effect of electrostatic force on small particle attachment.

In plasma on period, wafer has plasma floating potential and the potential remains on the wafer even after plasma discharge is finished. It leads to increase of particle attachment risk as mentioned above. In this time, newly developed wafer potential control sequence with ESC electrodes to reduce wafer potential during plasma off period will be reported. This sequence enables to reduce particle attachment during plasma off period.

[1] International Technology Roadmap for Semiconductors 2013.

[2] H. Kobayashi, *et al.*, IEEE trans. Semicond. Manuf., **22**, 462 (2009).

Scanning Probe Microscopy Focus Topic
Room: 212A - Session SP+2D+AS+NS+SS-WeA

Probing Electronic and Transport Properties
Moderator: Tae-Hwan Kim, Pohang University of Science and Technology, Jewook Park, Oak Ridge National Laboratory

2:20pm SP+2D+AS+NS+SS-WeA1 Geometric and Electronic Structures of Epitaxially Grown Pnictide 122, 111 and Cu$_x$Bi$_2$Se$_3$ Samples, *Young Kuk*, Seoul National University, Republic of Korea
INVITED

Order parameters were measured mainly on low-temperature cleaved, superconductor surfaces from their measured topographic images (constant current maps) and Fourier-transformed, measured density of states (energy dependent *dI/dV* map) in previous scanning tunneling microscopy (STM) studies. However, no direct evidence of coupling mechanisms has been given for these *high temperature* superconductors by these STM studies. We intend to study how homogeneity of a doped sample influences the superconducting property in an STM study. We were able to grow pnictide 111, 122, and Cu$_x$Bi$_2$Se$_3$ samples by molecular beam epitaxy. We found that surfaces of these grown samples are often terminated by alkali or alkaline atomic plane or non-superconducting metallic planes. These surfaces reveal distorted superconducting or non-superconducting properties. We adopted various ways to expose the superconducting planes in these samples. At the same time, we tried to grow samples homogeneously doped over the coherence lengths. Nodal structures were observed on these samples in their quasiparticle interference patterns. In this talk we will discuss the properties of the s±, s, d states as likely candidates pairing states for these materials.

3:00pm SP+2D+AS+NS+SS-WeA3 Direct Measurement of Conductance from Topological Surface States in Topological Insulators, *Corentin Durand, X. Zhang, S. Hus, M. McGuire, I. Vlassiouk, A.-P. Li*, Oak Ridge National Laboratory

Topological insulators (TI) with characteristic topological surface states (TSS) attract great interest for both fundamental physics and device applications. However, the unavoidable presence of defects in bulk single crystals usually dopes the material leading to a metallic behavior. Thus, the direct measurement of the TSS electronic transport properties is hard to achieve due to the dominant contribution from the bulk states. Here, we measure the transport properties of Bi$_2$Se$_3$ crystals by Four Probe Scanning Tunneling Microscopy (4P-STM) technique at different temperatures on fresh surfaces obtained by cleavage in Ultra-High Vacuum (UHV) (base pressure = 2×10^{-10} Torr). In contrast to conventional models that assume two resistors in parallel to count for both the TSS and bulk conductance channels, we show that this technique can be used to differentiate the 2D contribution of TSS to the transport from the 3D contribution (bulk) by considering the potential profiles across the interface. Our method allows quantitative determination of conductivities from both channels. We also compare our results with samples exhibiting pure 2D and 3D transport behaviors. Our results shows that our approach enables direct distinguishing and accessing electronic transport of TI surfaces surface states, which can

be applied to the studies of 2D to 3D crossover of conductance in other complex systems.

3:20pm SP+2D+AS+NS+SS-WeA4 Chiral Edge States of Topological Insulator in 1D, *Tae-Hwan Kim*, Pohang University of Science and Technology, Republic of Korea, *S. Cheon, S.-H. Lee,* Institute for Basic Science, Republic of Korea, *H.W. Yeom*, Pohang University of Science and Technology and Institute for Basic Science, Republic of Korea

Chiral edge states are one of the most fascinating hallmark of topological insulators [1-4]. While chiral edge states are the vitally important feature of 2D and 3D topological insulators, no correspondence has yet been found in 1D. On the other hand, in 1D, a Peierls-distorted atomic chain such as polyacetylene has two topologically different ground states and a topological edge state or so-called a topological soliton connecting between them [5,6]. The topological edge states in 1D show many interesting properties such as charge-spin separation, fractional charge, and so on [7,8]. However, they do not exhibit chirality as 2D or 3D topological insulators do. In this talk, we report that the 1D topological edge states, solitons, of the charge-density wave (CDW) system of indium atomic wires self-assembled on a silicon surface have the chiral property [9,10]. Our system can be well described by a coupled double Peierls-distorted atomic chain with zigzag interchain coupling, which induces dynamical sublattice symmetry breaking. This subtle change ensures a dynamically generated topological structure with four-fold symmetric ground states and has topological edge states with a new degree of freedom, chirality, which is absent in the case of a single Peierls atomic chain. We have performed scanning tunneling microscopy and spectroscopy in order to obtain experimental evidences of the chiral edge states in the 1D CDW. Individual right- and left-chiral edge states are directly identified from non-chiral ones, which are similar to the topological solitons found in a single Peierls atomic chain. Furthermore, we found that chiral edge states can produce quantized charge pumping across the chain that is topologically protected and controllable by their chirality. Thus, these topological chiral edge states or solitons can be utilized for future single-electron-level data storage devices or logic circuits, which are topologically protected.

B. A. Bernevig, T. L. Hughes, and S.-C. Zhang, *Science* **314**, 1757 (2006).

M. König, S. Wiedmann, C. Brüne, A. Roth, H. Buhmann, L. W. Molenkamp, X.-L. Qi, and S.-C. Zhang, *Science* **318**, 766 (2007).

M. Z. Hasan, C. L. Kane, *Rev. Mod. Phys.* **82**, 3045 (2010).

X.-L. Qi, S.-C. Zhang, *Rev. Mod. Phys.* **83**, 1057 (2011).

W. P. Su, J. R. Schrieffer, A. J. Heeger, *Phys. Rev. Lett.* **42**, 1698 (1979).

R. Jackiw, C. Rebbi, *Phys. Rev. D* **13**, 3398 (1976).

T. Giamarchi, *Quantum Physics in One Dimension* (Oxford University Press, Oxford : New York, 2004).

T. Dauxois, M. Peyrard, *Physics of Solitons* (Cambridge University Press, 2006).

T.-H. Kim, H. W. Yeom, *Phys. Rev. Lett.* **109**, 246802 (2012).

S. Cheon, T.-H. Kim, S.-H. Lee, H. W. Yeom, under review.

4:20pm SP+2D+AS+NS+SS-WeA7 Electronic Properties of Quasi-one-dimensional Defects in Monolayer h-BN, *Chuanxu Ma, J. Park,* Oak Ridge National Laboratory, *L. Liu, G. Gu,* The University of Tennessee, *A.P. Baddorf, A.-P. Li*, Oak Ridge National Laboratory

Two-dimensional (2D) hexagonal boron nitride (h-BN) monolayers have wide promising applications in nanoelectronics. The presence of defects could greatly impact its electronic properties. Here, we present experimental results about two types of line defects in h-BN monolayers, prepared on Cu foils by chemical vapor deposition (CVD) method.

Using scanning tunneling microscopy/spectroscopy (STM/STS), the structural and electronic properties of two types of quasi-1D defects are characterized in monolayer h-BN. An energy gap ~4 Ev is observed for h-BN monolayers on Cu foils. The first type of quasi-1D defects is the worm-like defects with length 3~30 nm, and width ~1.5 nm. Nano-ripples with modulation λ ~ 5.2 Å, which is about double the size of h-BN lattice, are observed both from the topographic images and Di/Dv mappings along the worm-like defects. The modulation is in phase at negative bias and out of phase at positive bias between the topographic images and Di/Dv mappings. The defects also show higher tunneling conductance than the h-BN sheet in the Di/Dv mappings. The observed nano-ripples in the defects might indicate interesting electronic properties, such as charge density wave (CDW).

The other type of defcts are the linear boundaries of h-BN. The tilting angle between the two domains at the both sides of the boundary is about 90°, which is well in line with our simulations. From the Di/Dv mapping, the boundary shows lower tunneling conductance than the h-BN sheet, which is different from the first type of quasi-1D defects.

Our experimental results demonstrate that the existence of quasi-1D defects tramendously affect the structure and electronic properties of h-BN, thus could be used to tune the transport properties in h-BN-based nanodevices.

4:40pm SP+2D+AS+NS+SS-WeA8 Real-Space Imaging of the Multiple Scattering in Single Layer Graphene: FT-STM/STS Studies, *M. Jung, S.-D. Sohn, J. Park, K. Lee, Hyung-Joon Shin*, Ulsan Natioanl Institute of Science and Technology, Republic of Korea

The electrons in graphene exhibit unusual two-dimensional behaviors, which can be described by massless Dirac quasiparticles. In order to understand the fundamental electronic properties of graphene, extensive studies have been focused on graphene both experimentally and theoretically. Undoubtedly, however, not only the electronic property of graphene itself but also that of graphene on metallic substrates is of great importance for the further applications. In this study we investigated the scattering behaviors of electrons in single layer graphene (SLG) on a Cu(111) substrate by means of low-temperature scanning tunneling microscopy (LT-STM) and scanning tunneling spectroscopy (STS). When there is a defect in graphene, we can observe the scattering of electrons in the form of interference pattern by STM. In previous STM studies, the energy level of Dirac point has been assigned by the position of a dip in dI/dV curve. It is very difficult, however, to determine the exact position of Dirac point from STS for the graphene on metallic substrates, because surface states of the substrate is too close to Dirac point of graphene in energy level. Here, we could successfully deconvolute and identify the electronic dispersion relations in graphene and in Cu(111) by applying Fourier transformation to one-dimensional and two-dimensional STS maps, which enables us to resolve surface states of Cu(111) and Dirac point of graphene respectively. We will also present our first observation of the defect-induced intravalley scattering, which has not been observed experimentally to date for SLG. Our results show that the careful examination of interference pattern can provide valuable information regarding intravalley, intervalley, and interband scatterings of electrons in graphene/Cu(111).

5:00pm SP+2D+AS+NS+SS-WeA9 Tunability of Single-Atom Electron Spin Relaxation Times and Their Characterization by Pump-Probe STM, *William Paul, S. Baumann,* IBM Research - Almaden, *K. Yang,* Chinese Academy of Sciences, *N. Romming,* University of Hamburg, Germany, *T. Choi, C.P. Lutz, A. Heinrich*, IBM Research - Almaden

A single atomic spin constitutes the ultimate limit to the miniaturization of magnetic bits. Can the state of such a spin be made stable against the quantum mechanical tunneling of magnetization? The energy relaxation time, T1, of single spins on surfaces can be measured by spin-polarized pump-probe STM [1]. To date, the relaxation times reported for Fe-Cu dimers on Cu$_2$N insulating films have been of the order ~100 ns [1]. A three-order-of-magnitude enhancement of lifetime, to ~200 μs, was recently demonstrated for Co on a single-monolayer of MgO [2]. This was accomplished by choosing a less conductive decoupling layer to electronically separate the atom from a metal substrate, along with the careful design of the symmetry of orbital states. Here, we report on the tailoring of the T1 lifetime of single Fe atoms on single- and multi- layer MgO films grown on Ag(001). We focus on the characterization of intrinsic lifetimes for the atom-substrate system which are independent of the STM tip used to probe them, that is, without influence of the nearby STM tip which can be a strong source of electronic de-excitation. We also report on new advances in pump-probe techniques which were necessary to carry out these measurements. These advances extend lifetime detection to the femto-ampere and many-millisecond regimes demanded by the Fe on MgO system.

[1] Loth *et al.*, Science **329**, 1628 (2010)

[2] Rau *et al.*, Science **344**, 988 (2014).

5:20pm SP+2D+AS+NS+SS-WeA10 Imaging and Spectroscopy of Graphene Heterostructures, *Brian LeRoy*, University of Arizona
INVITED

The ability to create arbitrary stacking configurations of layered two-dimensional materials opens the way to the creation of designer band structures in these materials. Graphene on hexagonal boron nitride is an example of such a van der Waals heterostructure where the electronic properties of the composite material can be different from either individual material [1]. These van der Waals heterostructures can be formed using a

wide variety of layered materials including from transition metal dichalcogenides, graphene and topological insulators. This talk will focus on devices consisting of graphene coupled to other layered materials. The lattice mismatch and twist angle between the layers produces a moiré pattern and affects their electronic properties. In double layer graphene systems, we find a van Hove singularity whose energy depends on the rotation angle [2]. This singularity in the density of states leads to a strong enhancement of the absorption at a particular wavelength. In graphene on transition metal dichalcogenides, the interaction between the materials leads to the possibility of commensurate stackings and the presence of new states in graphene [3].

[1] M. Yankowitz et al., *Nature Physics* **8**, 382 (2012).

[2] S. Huang et al., arXiv:1504.08357 (2015).

[3] M. Yankowitz et al., *Nano Letters* **15**, 1925 (2015).

6:00pm SP+2D+AS+NS+SS-WeA12 Correlated STM and Electron Transport Study of Individual Nanowires down to Atomic Scale, *Shengyong Qin*, University of Science and Technology of China, *T.H. Kim*, Oak Ridge National Laboratory, *Y. Zhang, R. Wu*, University of California, Irvine, *H.H. Weitering*, The University of Tennessee, Knoxville, *C.K. Shih*, The University of Texas at Austin, *A.-P. Li*, Oak Ridge National Laboratory
The electronic conductance in quantum wires is often dictated by quantum instabilities and strong localization at the atomic scale. We present a novel nano-transport technique which combines local nano-contacts and four-probe STM. The approach allows for correlated study of electron transport and scanning tunneling spectroscopy in individual nanowires. We first apply it to the GdSi$_2$ quantum wires, which show that isolated nanowires exhibit a metal-insulator transition upon cooling, driven by the defect-induced localizations, while wire bundles maintain a robust metallic state, stabilized by interwire electronic coupling. We then demonstrate applications of this transport technique with cabon nanotubes and copper wires in situ. The method bridges the gap between the transport and the local electronic and structural properties down to the atomic scale.

Surface Science
Room: 113 - Session SS+AS+EN-WeA

Metals, Alloys & Oxides: Reactivity and Catalysis
Moderator: Daniel Killelea, Loyola University Chicago

2:20pm SS+AS+EN-WeA1 Understanding Chemical Activity in Pt-Re Bimetallic Systems, *Donna Chen*, *R.P. Galhenage, K. Xie, A.S. Duke*, University of South Carolina, *H. Yan*, Brookhaven National Laboratory
INVITED
The nucleation, growth and chemical activity of bimetallic Pt-Re clusters on titania have been investigated as model systems for understanding Pt-Re catalysts for oxidation reactions. Scanning tunneling microscopy studies demonstrate that exclusively bimetallic clusters can be grown from the sequential deposition of Pt on Re or Re on Pt, provided that the deposition of the first metal creates a high enough cluster density for the nucleation of the second metal. Low energy ion scattering experiments indicate that the bimetallic clusters are Pt-rich regardless of the order of deposition. However, X-ray photoelectron spectroscopy (XPS) suggest that a Pt-Re alloy is formed from deposition of Re on Pt but not from Pt on Re. Furthermore, Re interacts more strongly with the titania support than Pt, resulting in reduction of titania. Temperature programmed desorption studies for CO desorption and methanol reaction confirm that the Re clusters have lower activity than Pt despite their higher surface area, and this behavior is attributed to oxidation of Re by the titania support. The alloyed clusters exhibit new activity for CO and H$_2$ evolution that is not observed for the pure or unalloyed clusters. Methanol oxidation activity of these model surfaces are studied in a microreactor attached to an ultrahigh vacuum chamber so that the surfaces can be characterized by XPS before and after reaction. Specifically, changes in the oxidation states of Re in the bimetallic and pure Re clusters are investigated.

3:00pm SS+AS+EN-WeA3 Removal of Surface Carbon from Pt(111) by Hydrogenation via an Ethylidyne Intermediate, *J.D. Krooswyk, C.M. Kruppe, Michael Trenary*, University of Illinois at Chicago
Transition metals that are used to catalyze reactions of hydrocarbons are often deactivated by the deposition of unreactive carbon on the catalyst surface. The structure and properties of the deposited carbon are often poorly defined. We have investigated the reactivity of carbon deposited onto a Pt(111) surface through exposure to acetylene at 750 K. At this temperature the acetylene is completely dehydrogenated leaving only carbon the surface. Earlier work had shown that the carbon deposited in this

way largely consists of C$_2$ molecules. We have used reflection absorption infrared spectroscopy (RAIRS) to characterize the reactivity of the deposited carbon under ambient pressures of H$_2$(g) up to 10 torr. The results show that C$_2$ can be hydrogenated to ethylidyne (CCH$_3$) and that the ethylidyne is slowly hydrogenated to ethane, which desorbs thus removing carbon from the surface. The maximum coverage of the C$_2$ molecules can be deduced from comparison with the peak areas measured with RAIRS for ethylidyne formed from ethylene exposure, which is known to give an ethylidyne coverage of 0.25 monolayer. Auger electron spectroscopy confirms that surface carbon is removed by hydrogenation under these conditions. In separate experiments based on comparisons of s- and p-polarized RAIR spectra in which both surface and gas phase species can be simultaneously monitored, we have shown that surface ethylidyne is a spectator species as gas phase acetylene is converted first to gas phase ethylene and then to gas phase ethane. Although ethylidyne is a spectator species in the hydrogenation of ethylene and acetylene to ethane over Pt(111), in the case of C$_2$ hydrogenation, ethylidyne plays the role of a reaction intermediate.

3:20pm SS+AS+EN-WeA4 Density Functional Study of the Oxygen Chemistry and NO Oxidation Mechanism on Low-index Surfaces of SmMn$_2$O$_5$ mullite, *X. Liu, Z.Z. Chen*, Huazhong University of Science and Technology, China, *K.J. Cho*, The University of Texas at Dallas, *R. Chen, Bin Shan*, Huazhong University of Science and Technology, China
SmMn$_2$O$_5$ mullite has recently been reported to be a promising alternative to traditional Pt-based catalysts for environmental and energy applications. By performing density functional calculations, we systematically investigated lattice oxygen reactivity and oxygen adsorption/dissociation/migration behaviors on low index surfaces of SmMn$_2$O$_5$ mullite with different terminations. The (001), (010) and (100)surfaces have lowest barriers against exchanging O species with environments and thus are expected to be active surfaces.Furthermore, we have calculated the reaction routes along different channels on these three surfaces. Our results show that both ER and MvK mechanisms co-exist in NO oxidation by SmMn$_2$O$_5$. The most active surface is the (010) facet with Mn^{4+} ions in the surface layer where oxidation can be realized by a synergetic mechanism involving ER processes along bridge-MnO channels. The (001) surface with Mn^{4+} ions in the surface layer is also expected to be active for oxidation via the MvK mechanism. On the other hand, despite the low oxygen vacancy formation energy, the (110) surface could easily undergo surface reconstruction and quickly lose active sites. Our calculations also suggest that the rate determining step of oxidation reaction on SmMn$_2$O$_5$ surfaces is the desorption of NO$_2$ on both (010) and (001) facets. Our study presents systematic pictures on catalytic activities of SmMn$_2$O$_5$, which are important to the full understanding and improvement of SmMn$_2$O$_5$ performance. The comprehensive micro-kinetic model on the reaction dynamics of SmMn$_2$O$_5$ is under construction.

4:20pm SS+AS+EN-WeA7 Medard W. Welch Award Lecture - Thermodynamics and Kinetics of Elementary Reaction Steps on Late Transition Metal Catalysts, *Charles Campbell**, University of Washington
INVITED
Experimental and theoretical results concerning the thermodynamics and kinetics of surface chemical reactions of importance in late transition metal catalysis will be reviewed. Topics include: (1) calorimetric measurements of the adsorption energies of small molecules and molecular fragments on single crystal surfaces, and their comparison to different DFT methods; (2) measurements of the entropies of adsorbates and their trends, (3) using these together with elementary-step rate measurements to build microkinetic models for multi-step catalytic reactions, and a method for analyzing these that quantifies the extent to which each elementary step and intermediate controls the net rate; and, (4) measurements of the energies of transition metal atoms in nanoparticle catalysts as a function of particle size and support, which correlate with catalytic activity and sintering rates.

· Work supported by NSF and DOE-OBES Chemical Sciences Division.

5:00pm SS+AS+EN-WeA9 Bridging Hydroxyl Formation from Water on Reduced TiO$_2$(110), *Nikolay Petrik, G.A. Kimmel*, Pacific Northwest National Laboratory
TiO$_2$ is an important photocatalyst with many practical applications. It is also a good model system for fundamental studies of thermal and non-thermal reactions, including photocatalytic water splitting. Our understanding of water's reactions on TiO$_2$ surface is limited. In this paper, we have investigated temperature-dependent reaction of water molecules with bridging oxygen vacancy (V$_O$) on rutile TiO$_2$(110) surface using three independent methods: i) infrared reflection absorption spectroscopy (IRAS) to monitor the bridging hydroxyl (OH$_B$ or OD$_B$) formation, ii) electron-

---

* Medard W. Welch Award Winner

stimulated desorption (ESD) of molecular water to monitor the water coverage,[1] and iii) photon-stimulated desorption (PSD) of CO_2 – which is a product of CO photooxidation – to monitor the unoccupied V_O coverage. [2] Narrow, distinct peaks for isolated OD_B and OH_B at ~2736.5 cm^{-1} and ~3711.5 cm^{-1} are detected in P-polarized mode for the samples exposed to D_2O and H_2O, respectively. If water is dosed at low temperature and annealed, bridging hydroxyl peaks appear above 150 K, growing with temperature until ~ 250 K, then saturate. In the same temperature range, molecular water and V_O coverages from the ESD and PSD data decrease in correlated fashion according to the reaction $H_2O_{Ti} + V_O \rightarrow 2OH_B$. The temperature range for this conversion appears to be too broad to be fitted with a single Arrhenius term and a reasonable pre-factor. On the other hand, the data can be fitted well using a "normal" prefactor ($v = 10^{12}$ s^{-1}) and a distribution of activation energy (E_a) centered at 0.545 eV with ΔE_a(FWHM) = 0.125 eV. These parameters are close to those obtained from STM data[3] and theory[4] for the water monomer diffusivity on Ti sites, which most likely controls the water – vacancy reaction. This work was supported by the US Department of Energy, Office of Science, Office of Basic Energy Sciences, Division of Chemical Sciences, Geosciences & Biosciences.

(1) Zhang, Z.; Du, Y.; Petrik, N. G.; Kimmel, G. A.; Lyubinetsky, I.; Dohnalek, Z. Water as a Catalyst: Imaging Reactions of O_2 with Partially and Fully Hydroxylated TiO$_2$(110) Surfaces. *J. Phys. Chem. C* 2009,113, 1908-1916.

(2) Petrik, N. G.; Kimmel, G. A. Off-Normal CO_2 Desorption from the Photooxidation of CO on Reduced TiO$_2$(110). *J. Phys. Chem. Lett.* 2010,1, 2508-2513.

(3) Matthiesen, J.; Hansen, J. O.; Wendt, S.; Lira, E.; Schaub, R.; Laegsgaard, E.; Besenbacher, F.; Hammer, B. Formation and Diffusion of Water Dimers on Rutile TiO$_2$(110). *Phys. Rev. Lett.* 2009, 102, 226101.

(4) Hammer, B.; Wendt, S.; Besenbacher, F. Water Adsorption on TiO$_2$. Top. Catal. 2010, 53, 423–430.

5:20pm SS+AS+EN-WeA10 The Adsorption and Desorption of Small Hydrocarbons on Rutile TiO$_2$(110), *Long Chen*, R.S. Smith, B.D. Kay, Z. Dohnalek, Pacific Northwest National Laboratory

The interaction of small hydrocarbons with metal and metal oxide surfaces is important for a wide range of applications including heterogeneous catalysis, atmospheric chemistry, geochemistry and chemical sensing. In this work, temperature programmed desorption (TPD) and molecular beam techniques are used to study the adsorption and desorption kinetics of small hydrocarbons (C$_1$ - C$_4$) on rutile TiO$_2$(110) surface. In addition to n-alkanes, 1-alkenes (ethylene, propylene and 1-butylene) and 1-alkynes (acetylene, propyne and 1-butyne) were included to follow the effect of the nature of the carbon-carbon bond on hydrocarbon binding. We show that the sticking coefficients for all the hydrocarbons studied here are close to unity (> 0.95) at an adsorption temperature of 60 K. Similar to previous studies on metal and metal oxide surfaces, for n-alkanes on TiO$_2$(110) we find a linear increase in desorption energy with chain length. In contrast, for 1-alkenes and 1-alkynes, a roughly linear relationship between desorption energy and chain length is also observed at low coverages, but with a much smaller slope, suggesting that the additional CH$_x$ segments either interact less efficiently with the substrate or destabilize the bonding of the unsaturated carbon-carbon bond. Further, we also determined the absolute saturation coverages of each hydrocarbon on the five-fold coordinated titanium sites (Ti$_{5c}$). We show that except for CH$_4$, the saturation coverages of the same type of hydrocarbons on Ti$_{5c}$ sites are nearly independent of the chain length, and that the saturation coverages of 1-alkynes consistently exceed those of n-alkanes and 1-alkenes, contrary to what one would expect based on their sizes.

5:40pm SS+AS+EN-WeA11 Pd-Au *Single Atom Alloys* for the Activation of Diatomic Molecules, *Felicia Lucci*, E.C.H. Sykes, Tufts University Department of Chemistry

Pd-Au alloys are known to catalyze a wide range of hydrogenation and oxidation reactions; however, the size of Pd ensembles in Au required for small molecule activation is not well understood. On the atomic scale, we investigate size effects of Pd atoms in Au for the catalytic activation of H$_2$ and O$_2$. We show that isolated Pd atoms are capable of catalyzing the dissociative adsorption of H$_2$, a process which was previously thought to require contiguous Pd sites. H spillover from active Pd sites to the Au surface can be induced the adsorption of CO. Conversely, single Pd atoms are not capable of O$_2$ dissociation. Small Pd clusters on Au enable O$_2$ activation and adsorption at Pd-Au interface sites. Since weakly bound H and O atoms are capable of enhancing reaction selectivity on Au substrates, this Pd-Au system serves as an ideal model system with which to probe selective hydrogenation and oxidation reactions at both single and ensemble active sites.

6:00pm SS+AS+EN-WeA12 Pt/Cu Single Atom Alloys for Highly Selective Formic Acid Dehydrogenation, *Matthew Marcinkowski*, C.J. Murphy, M.L. Liriano, N.A. Wasio, F.R. Lucci, E.C.H. Sykes, Tufts University Department of Chemistry

Selective decomposition on metal catalysts is a critical step in formic acid's application as a hydrogen storage molecule and for its use in direct formic acid fuel cells. Depending on the metal, formic acid can decompose via a dehydrogenation pathway to produce CO$_2$ and H$_2$, or a dehydration pathway to produce CO and H$_2$O. For most applications, very high selectivity to dehydrogenation is preferred as reactively formed CO from dehydration can poison the catalyst. The Cu(110) surface is known to selectively decompose formic acid via dehydrogenation, however, despite being the most dominate facet of nanoparticles, Cu(111) has received little study. Pt surfaces exhibit greater reactivity to decomposition, but are not as selective resulting in increased catalyst poisoning. We report that formic acid on Cu(111) and Pt/Cu(111) selectively decomposes via dehydrogenation. We find the bare Cu(111) surface to be 100% selective towards dehydrogenation, but not very active. Substitution of 1% of a monolayer of Pt into the Cu(111) surface results in a single atom alloy (SAA) that maintains this high selectivity and is ~six times more reactive than Cu(111). Higher coverages of Pt improve reactivity further, but beyond the single atom regime the selectivity towards dehydrogenation decreases and dehydration is observed. Our results show that Pt/Cu SAAs significantly improve the reactivity of Cu, while also maintaining high selectivity towards dehydrogenation, therefore avoiding catalyst poisoning by CO. Based on our results, real nanoparticle catalysts designed on the SAA principle are expected to be promising candidates for formic acid dehydrogenation.

Surface Science
Room: 112 - Session SS+AS-WeA

Surface Dynamics, Non-Adiabaticity, and Single Molecule Phenomena
Moderator: Eddy Tysoe, University of Wisconsin-Milwaukee

2:20pm SS+AS-WeA1 Benchmarking Theory with Vibrational State Resolved Reactivity Measurements, *Arthur Utz*, E. Peterson, E. Dombrowski, E. Nicotera, E. High, Tufts University

Electronic structure calculations provide predictions of energy thresholds for a wide range of surface chemical reactions, and they are the basis for significant advances in our understanding of surface reactivity. Despite the central role these calculations and their predictions play, testing the absolute accuracy of these calculations with direct experimental measurements has proven to be challenging.

The presentation will focus on using the results of state-resolved beam-surface scattering measurements to benchmark theoretical predictions. We find that when these measurements are performed on a cold surface, we observe sharp energetic thresholds for reaction. These observations result from our ability to control and vary precisely all energetic degrees of the system. These experimentally measured threshold energies can be compared directly with both electronic structure calculations, as well as with quantum dynamics predictions of chemical reactivity. We will compare experimental results for methane dissociation on Ni(111) with recent computational predictions from the Jackson group to illustrate this approach. We will also provide an update on our work extending this approach to other molecule-surface systems.

2:40pm SS+AS-WeA2 Confirming the role of Hydrogen Bonding in Electron-promoted Desorption at Water Ice Surfaces., *D. Marchione, A.G.M. Abdulgalil, M.P. Collings, Martin McCoustra*, Heriot-Watt University, UK

We have previously reported observations of large (>10^{-16} cm^2), low-energy (<500 eV), electron-promoted desorption cross-sections for benzene (C$_6$H$_6$) molecules adsorbed on the surface of amorphous solid water [1]. We will now report on the extension of this work to other molecular solids exhibiting varying degrees of hydrogen bonding within the molecular solid itself and between the solid surface and adsorbed benzene; specifically we have repeated our measurements employing substrates comprised of solid methanol (CH$_3$OH) and diethyl ether (CH$_3$CH$_2$OCH$_2$CH$_3$). Our report will detail our studies of the structure of adsorbed layers of C$_6$H$_6$ on the molecular solids and demonstrate the crucial role of hydrogen bonding in propagating electronic excitation to the solid-vacuum interface where C$_6$H$_6$ desorption can occur. Competitive electron-promoted chemistry in the form of H$_2$ formation will also be reported. Conclusions related to the impact of

these observations on the early phase of icy interstellar grain chemistry will be discussed.

[1] Highly efficient electron-stimulated desorption of benzene from amorphous solid water ice, J. D. Thrower, M. P. Collings, F. J. M. Rutten, and M. R. S. McCoustra, *Chem. Phys. Lett.*, 2011, **505**, 106–111.

3:00pm SS+AS-WeA3 Strategic Applications of the Vibrational Dynamics of the Outer Layer of Metal Nanoparticles, *Marisol Alcantara Ortigoza*, University of Central Florida **INVITED**
The structure characterization, stability and thermal properties of nanoparticles (NPs) are topics of fundamental and technological significance. This information, however, is not always readily available from experiment. Moreover, the vibrational density of states VDOS of small (<2 nm) metal NPs definitely does not have a quadratic decay at the low-frequency end, for which the thermal properties cannot be obtained from the VDOS as Debye proposed in 1912. The features particular to the VDOS of NPs will be rationalized in terms of the charge density distribution around low-coordinated atoms, the quasi-radial geometric distribution of NPs, force constant variations, degree of symmetry of the nanoparticle, discreteness of the spectrum, and the confinement of the eigenmodes. I will present an explanation and application of the enhanced low- and high energy tails of the vibrational density of states (VDOS) of nanoparticles with respect to their bulk counterparts, as well as show that the eigenmodes defining the two extremes of the VDOS are not that alien to widely studied surface phonons. I will show that the high- and low-energy tails of the VDOS of NPs may be a powerful tool to reveal information about their chemical composition and geometric structure of small NPs. For example, the size of the confinement gap at the low-frequency end of the VDOS and the extent by which the high-frequency end surpasses the bulk limit may indicate whether a NP is bulk-like or non-bulk-like and the extent to which it is disordered or segregated. Regarding thermal properties, I will also show that for NPs with a largely discrete VDOS, the frequency of their fundamental mode may largely determine their thermal properties.

4:20pm SS+AS-WeA7 An Accurate Full-Dimensional Potential Energy Surface for H at Au(111): The Importance of Nonadiabatic Electronic Excitation in Energy Transfer and Adsorption, *S.M. Janke, A. Kandratsenka*, **Daniel Auerbach**, *A.M. Wodtke*, Max Planck Institute for Biophysical Chemistry, Germany
We have constructed a potential energy surface (PES) for H atoms interacting with *fcc* gold based on the form of the PES in Effective Medium Theory. The PES was adjusted to match energies calculated by DFT in many configurations, including many with the Au atoms displaced from their lattice positions. It describes both the interatomic forces and electron densities in *full dimension* with the accuracy of the *ab initio* energies used in its construction. Calculations describing the motion of H and Au atoms using this full dimensional adiabatic PES agree with results obtained previously using Ab Initio Molecular Dynamics, demonstrating the accuracy of the PES for configurations occurring in the scattering of H atoms from a surface at finite temperature.

The analytic expression for the total energy contains the embedded electron density leading to a self-consistent approach to simulating nonadiabatic trajectories. We find that nonadiabatic electron-hole pair excitation is the most important energy loss pathway for the H atom. The calculated energy distributions for scattered H atoms are in reasonable agreement with experimental results that are just becoming available. and determines the probability and mechanism for its adsorption. Analysis of trajectories calculated with and without nonadiabatic energy dissipation shows the adsorption or sticking probability as well as the mechanism of H atom adsorption is changed dramatically by nonadiabatic energy transfer

4:40pm SS+AS-WeA8 STM Characterization of Quasi-one Dimensional C_{60} Nanostructures on Rippled Graphene, *C. Chen, H. Zheng, A. Mills*, **Chenggang Tao**, Virginia Tech
Highly ordered one-dimensional (1D) molecular configurations are excellent model systems and prototypes of 1D quantum confinement of electronic states, and thus have potential importance in electronic nanodevices, spintronics and solid-state quantum computation. Due to the spherical geometry of C_{60} molecules, it has been challenging to experimentally realize quasi-1D C_{60} nanostructures, a highly anisotropic configuration. We will present our recent scanning tunneling microscopy (STM) characterization of novel quasi-1D C_{60} nanostructures on rippled graphene. Through careful control of the subtle balance between the linear periodic potential of rippled graphene and the C_{60} surface mobility, C_{60} molecules can be arranged into a 1D C_{60} chain structure with widths of two to three molecules. At a higher annealing temperature, the chain structure transitions to a more compact hexagonal close packed quasi-1D stripe structure. We will also discuss our scanning tunneling spectroscopy (STS) measurements on this hybrid system.

5:00pm SS+AS-WeA9 Classical and Quantum Description of Ion Desorption from Ionic Crystals, *Leszek Markowski*, University of Wroclaw, Poland
It is well known that irradiation of the solid with electrons or photons can cause its decomposition. This process, or, more adequately processes, is very fast (typically finalized within a time shorter than 10^{-14} s) and is realized mainly by desorption of atoms or ions.Unfortunately, until now, existing models still do not give a proper value of the desorption yield and, simultaneously, a correct kinetic-energy distribution of emitted particles, as compared to the experimental observations.

In this talk a classical, quasi-quantum and quantum description of the positive ion desorption from ionic crystal surface, in which three potentials are involved, will be discussed and compared. It will be shown that the quantum description allows to explain some effects observed experimentally, such as a periodicity of small oscillations on the kinetic energy distribution (KED) curves (predicted by Wave-Packet Squeezing model) and emission through a temporarily existing potential barrier from the temporary bounded states located above the vacuum level. Moreover, analysis method of the ion KED oscillation and the fitting procedure which allows to determined a final effective desorption potential will be presented.

For two examples discussed, Li^+ desorption from LiF and Na^+ desorption from NaCl, desorption from two desorption sites can be distinguished – dominating ion desorption channel from adatom sites (more than 95%) and marginal one from the sites in the first surface layer. For the second desorption channel neighboring negative ions, due to surface relaxation lying in the first surface layer slightly above positive one, can act as a two-dimensional array of rosette-like apertures. In consequence, positive ions after passing through them may form diffraction pattern.

Finally, it appears that when desorption process is described using three potentials both the ions desorption efficiency and their kinetic-energy distribution are in agreement with the experimental results.

5:20pm SS+AS-WeA10 Spin and Isotope Effects on Molecular-Hydrogen Adsorption on Pd(210), *H. Kobayashi, S. Ohno, M. Wilde*, University of Tokyo, Japan, *M. Matsumoto*, Tokyo Gakugei University, Japan, *S. Ogura*, **Katsuyuki Fukutani**, University of Tokyo, Japan
Molecular hydrogen is physisorbed on flat metal surfaces via van der Waals interaction. By taking advantage of the fact that molecular hydrogen exists in nuclear-spin isomers of ortho and para species [1], we have shown the interaction potential on Ag(111) is anisotropic with a slight perpendicular preference [2]. The Pd(210) surface has a step-like structure consisting of alternately aligned (100) and (110) terraces, and it has been shown that H_2 is rather strongly adsorbed on H-covered Pd(210) with a significant contribution of orbital hybridization [3]. On the other hand, it has been suggested that molecularly adsorbed species could be important for hydrogen absorption into the interior of Pd surfaces [4]. In the present study, we have investigated the adsorption of H_2 and D_2 on the Pd(210) with temperature-programmed desorption (TPD) combined with resonance-enhanced multi-photon ionization (REMPI).

When Pd(210) was exposed to H_2 at 115 K, TPD revealed a desorption peak at 180 K (α-peak) originating from the absorbed state as well as a peak at 280-320 K (b-peak) due to chemisorbed H. From the uptake rate of the α-peak, the absorption probability of H on Pd(210) was estimated to be 3×10^{-3}. When the surface was exposed to either H_2 or D_2 at 45 K, on the other hand, an additional TPD peak was observed at about 70 K (γ-peak), which was attributed to molecular adsorption. While a small difference between H_2 and D_2 was observed for the b-peak, the γ-peak temperature of D_2 was found to be higher than that of H_2 by 9 K, which corresponds to the difference in the adsorption energy of about 20 meV. Assuming that this difference is due to the zero-point energy difference in the adsorption potential, the adsorption potential was analyzed in terms of the Morse potential. By applying REMPI-TPD, furthermore, the TPD spectra of ortho-H_2 in the rotational state of J=1 and para-H_2 in J=0 were state-selectively measured. The desorption temperature of ortho-H_2 was found to be higher than that of para-H_2 by about 4 K, which corresponds to a difference in the adsorption energy of about 10 meV. We discuss that this large energy difference between the ortho and para species originates from the potential anisotropy on the basis of the first-order perturbation.

[1] K. Fukutani, T. Sugimoto, Prog. Surf. Sci. 88, 279 (2013).

[2] T. Sugimoto, K. Fukutani, Phys. Rev. Lett. 112, 146101 (2014).

[3] P. K. Schmidt et al., Phys. Rev. Lett. 24 87, 096103 (2001).

[4] S. Ohno et al., J. Chem. Phys. 140, 134705 (2014).

5:40pm SS+AS-WeA11 Eley-Rideal Typed Mechanism of Formate Synthesis by Hydrogenation of Carbon Dioxide on Cu Surfaces, *J. Quan,* University of Tsukuba, Japan*, T. Ogawa,* Universityy of Tsukuba, Japan*, T. Kondo,* University of Tsukuba, Japan*, G. Wang,* Nankai University, China*, **Junji Nakamura**,* Univerisity of Tsukuba and ACT-C, Japan

Methanol synthesis by hydrogenation of CO_2 using Cu catalysts is one of the promising reactions to convert CO_2 into useful chemicals. Formate species is the pivotal intermediates formed as the initial step of CO_2 hydrogenation ($CO_2 + H_a \rightarrow HCOO_a$). The reaction rate of formate synthesis is very low and the reaction probabilities are about 10^{-12} at 340K. Our previous kinetic measurements have suggested that formate is synthesized via Eley-Rideal typed mechanism, in which CO_2 molecules directly attack adsorbed hydrogen atoms on Cu surfaces. The structure insensitivity observed for formate synthesis experiments on Cu(111), Cu(100), and Cu(110) were well explained by the Eley -Rideal mechanism based on DFT calculations. In addition, sharp angular desorptions of CO_2 have been observed for formate decomposition as the reverse reaction of formate synthesis, indicating thermal non- equilibrium reaction. In the present study, we performed molecular beam experiments to prove the Eley-Rideal typed mechanism, in which CO_2 molecules with controlling vibrational and translational energies were reacted with adsorbed hydrogen on cold Cu(111) and Cu(110) surfaces (T_S =150-215 K). We confirmed the formation of formate species on Cu(111) and Cu(110) with reaction probabilities of 10^{-5} by heating nozzle above 1000 K, while no formate is formed at nozzle temperatures below 1000 K. The results indicate the Eley-Rideal typed mechanism with thermal non-equilibrium character. DFT calculations also reproduce the Eley-Rideal typed mechanism, in which vibrational excitations of CO_2 are required to overcome the barrier of formate synthesis.

2D Materials Focus Topic
Room: 212C - Session
2D+EM+MG+NS+SE+SM+SS+TF-ThM

Emergent 2D Materials
Moderator: Paul Sheehan, Naval Research Laboratory

8:00am **2D+EM+MG+NS+SE+SM+SS+TF-ThM1 CVD Growth and Characterization of 2D MoS$_2$, MoSe$_2$, MoTe$_2$, WS$_2$, WSe$_2$, and MoS$_{2(1-x)}$Se$_{2x}$ Alloys**, *David Barroso, T. Empante, A. Nguyen, V. Klee, I. Lu, E. Preciado, C. Lee, C. Huang, W. Coley, S. Naghibi, G. von Son, A. Brooks, J. Kim, L. Bartels*, University of California, Riverside
Transition Metal Dichalcogenides (TMDs) have been of increasing interest over the past years due to their exciting semiconducting properties. In the bulk, TMDs possess a native indirect bandgap and transition to a direct bandgap as they approach the monolayer limit. The bandgaps range from 1.15 eV to 1.95 eV depending on composition. Using organic liquids and/or inorganic powders as precursors, CVD growth techniques have been realized for MX$_2$ TMDs (M = Mo, W; X = S, Se, Te) and their alloys at tunable compositions. We achieved consistent synthesis of these TMDs materials. The films can either be made homogeneous in bandgap or exhibiting a linear bandgap gradient. Characterization of the films include Raman and photoluminescence spectroscopy, as well as AFM. Device fabrication allows for transport measurements. Depending on the composition, the materials show n- or p-doping in a consistent fashion.

8:20am **2D+EM+MG+NS+SE+SM+SS+TF-ThM2 Investigation of Manganese Dioxide Nanosheets by STM and AFM**, *Loranne Vernisse, S. Afsari, S.L. Shumlas, A.C. Thenuwara, D.R. Strongin, E. Borguet*, Temple University
Interest in ultrathin two-dimensional nanosheets has grown exponentially thanks to their unique and diverse electronic properties. As they possess atomic or molecular thickness and infinite planar dimension, they are expected to have different properties than the bulk of the material from which they originate. This offers opportunities for the development of devices in various areas, ranging from catalysis to electronics. Using the exfoliation approach, it is possible to investigate 2D nanosheets of different materials in search of new phenomena and applications. Bearing this mind, we focused on manganese dioxide (MnO$_2$), and more specifically δ-MnO$_2$ (Birnessite). This mineral has the advantage to present a low surface enthalpy[1], which results in weak water binding. Moreover, the presence of defects, e.g., oxygen vacancies has a dopant effect on water oxidation. These properties make MnO$_2$ a perfect candidate as a catalytic surface for water splitting and pave the way to the design of clean and renewable energy system. Furthermore, MnO$_2$ can be easily exfoliated into ultrathin nanosheets owing to the layered structure of the manganese oxide precursors.

Our goal is to investigate the catalytic activity of ultrathin MnO$_2$ nanosheets using scanning probe microscopy techniques, especially atomic force microscopy (tapping mode) and scanning tunneling microscopy (ambient and electrochemical conditions). In this perspective, we have first improved the deposition processes and find the imaging conditions to observe MnO$_2$ nanosheets with an average thickness of one or two layers. We have also showed that MnO$_2$ single layer nanosheets exhibit an expected hexagonal atomic pattern and present some defects. We will now resolve and identify the different defects and investigate the evolution of the conductivity as a function of the defect concentration and the number of layers.

This work was supported as part of the Center for the Computational Design of Functional Layered Materials, an Energy Frontier Research Center funded by the U.S. Department of Energy, Office of Science, Basic Energy Sciences under Award #DE-SC0012575.

[1] M. M. Najafpour, E. Amini, M. Khatamian, R. Carpentier, S. I. Allakhverdiev, Journal of Photochemistry and Photobiology B: Biology (2014), 133, 124.

8:40am **2D+EM+MG+NS+SE+SM+SS+TF-ThM3 Two-Dimensional Early Transition Metal Carbides and Carbonitrides "MXenes": Synthesis, Properties and Applications**, *Michael Naguib*, Oak Ridge National Laboratory **INVITED**
Ternary layered carbides and nitrides with formula of M$_{n+1}$AX$_n$ (M stands for early transition metal, A for group A element, X is carbon or nitrogen, and n=1, 2, or 3), so called MAX phases, are known for their unique combinations properties of ceramics and metals. It was found recently that etching atomically thin layers of aluminum from the MAX phases results in

forming weakly bonded stacks of two-dimensional (2D) layers of early transition, coined as *MXenes*. The etching was carried out in fluoride contained aqueous systems. Thus MXenes surfaces are terminated with a mixture of groups including OH, O, and F. Sonicating MXenes in water results in delaminating few layers of MXenes from each other. However, to achieve a large-scale delamination, intercalation of a large compound between the layers prior to delamination is needed. MXenes were found to be a very interesting family of 2D materials since they are electrically conductors and hydrophilic. They also showed an excellent performance as electrodes for electrochemical super capacitors and Li-ion batteries. Here the recent progress in MXenes research from the synthesis to properties and applications will be covered, and in more details, large-scale delamination of MXenes will be discussed. Also, light will be shed on the performance of MXenes as electrode materials for electrochemical energy storage systems.

9:20am **2D+EM+MG+NS+SE+SM+SS+TF-ThM5 Molecular Beam Epitaxy of Large area HfSe2(ZrSe$_2$)/MoSe$_2$ van der Waals Heterostructures on AlN(0001)/Si substrates**, *Athanasios Dimoulas, P. Tsipas, E. Xenogiannopoulou, D. Tsoutsou, K.E. Aretouli, J. Marquez-Velasco, S.A. Giamini, N. Kelaidis*, NCSR DEMOKRITOS, Greece
Two dimensional (2D) semiconductor van der Waals heterostructures (HS) made of group IVB (Zr, Hf) and group VIB (Mo, W) metal dichalcogenides are predicted [1] to have type II or type III band alignments mainly because of a large difference in their workfunctions and band gaps, which makes them candidates for novel 2D staggered, or broken gap tunneling field effect transistors (TFET). We use molecular beam epitaxy (MBE) to grow high quality large area HfSe$_2$ [2,3], ZrSe$_2$ [4] and MoSe$_2$ [5] films directly on AlN(0001)/Si(111) substrates. We confirm by RHEED and HRTEM that atomically thin layers (1-6 ML) are grown in single crystal form with a well-defined in-plane orientation on AlN. The films are continuous with smooth surface morphology (0.6 nm RMS roughness) and abrupt interfaces with no detectable reaction as verified by in-situ XPS and HRTEM. Micro Raman mapping for all layers confirms their structural integrity down to one monolayer and reveals very good uniformity on a cm-scale wafer and excellent stability of MoSe2 over a period of at least two weeks in air. Strong room temperature PL signal of 1 ML MoSe$_2$ indicate high quality direct gap semiconductor in agreement with valence band structure details imaged by our in-situ ARPES [3, 5]. In a second step, MoSe2/HfSe$_2$ [3] and MoSe$_2$/ZrSe$_2$ [4] HS were grown. Despite the large lattice mismatch, all layers are grown epitaxially as evidenced by RHEED with no detectable defects at the interfaces as confirmed by HRTEM suggesting good quality VdW epitaxy [6]. Using UPS the workfunctions (WF) were estimated to be 5.2, 5.5 and 5.4 eV for MoSe$_2$, HfSe$_2$ and ZrSe$_2$ respectively [3,4]. The last two differ substantially from theoretical values (~ 6 eV). Based on our STM and DFT calculations [3], we conclude that this difference is due to an ordered Se adlayer which lowers the HfSe$_2$ and ZrSe$_2$ WF bridging the WF gap between them and MoSe2. As a result, small valence band offsets of 0.13 and 0.58 eV were found for the HfSe$_2$/MoSe$_2$ and ZrSe$_2$/MoSe$_2$ HS, respectively leading to type II band alignments. The availability of low cost wide-gap-AlN/Si wafers in 300 mm wafer sizes defines a manufacturable route for single crystal 2D semiconductor technology.

We acknowledge financial support from ERC Advanced Grant SMARTGATE-291260. We thank IMEC for providing the AlN/Si substrates.

[1] C. Gong et al., *APL.* **103**, 053513 (2013)

[2] R. Yue et al., *ACS Nano***9**, 474 (2014)

[3] K. E. Aretouli et al., *APL***106**, 143105 (2015)

[4] P. Tsipas et al., *Microelectron. Eng.* (2015), http://dx.doi.org/10.1016/j.mee.2015.04.113

[5] E. Xenogiannopoulou et al, *Nanoscale* **7**, 7896 (2015)

[6] F.S. Ohuchi et al., *JAP***68**, 2168 (1990)

9:40am **2D+EM+MG+NS+SE+SM+SS+TF-ThM6 Surface Investigation of WSe$_2$ Atomically Thin Film and Bulk Crystal Surfaces**, *Rafik Addou, H. Zhu*, University of Texas at Dallas, *Y.-C. Lin, S.M. Eichfeld, J.A. Robinson*, Penn State University, *R.M. Wallace*, University of Texas at Dallas
Heterogeneous fabrication of semiconducting two-dimensional layered materials presents a promising opportunity to develop highly tunable electronic and optoelectronic materials.(1-2) An example of crystalline monolayer of WSe$_2$ grown by chemical vapor deposition on epitaxial graphene (EG) grown from silicon carbide had been investigated at nanoscale level. The WSe$_2$ surface was characterized using atomic force microscopy (AFM) scanning tunneling microscopy/spectroscopy (STM/STS) and X-ray photoelectron spectroscopy (XPS).(3,4) AFM and

large STM images show high-quality WSe_2 monolayers. The sharpness of the W *4f* and Se *3d* core levels confirms the absence of any measurable reaction at the interface and oxide formation. The photoemission measurements of WSe_2-Graphene interface suggest p-type doping due to charge transfer (EG withdraws electrons from WSe_2) at the interface and formation of Schottky-type contact,(5) suggesting possible applications of such heterostructures as diodes and photodetectors. High-resolution STM images reveal atomic-size imperfections induced by Se vacancies and impurities. Additionally, the investigation of bulk $WSe_2(0001)$ surface shows spatial variation attributed to the presence of two components in W $4f_{7/2}$ core level attributed to the presence of both n- and p-type behavior. STM images exhibit also various types of defect induced by vacancies and dopants. The STS spectra reveal two main characteristics i) expected p-type conductivity where the Fermi level located at the valence band edge, and ii) zero conductivity at negative bias explained by defect-induced band bending as reported on geological MoS_2 crystal surfaces.(4) In conclusion, the spatial variation (topography and electronic structure) is more noticeable in bulk WSe_2 grown by chemical vapor transport than in CVD thin films.

(1) Yu-Chuan Lin et al., Nano Lett., **14** (2014) 6936-6941.

(2) Yu-Chuan Lin et al., Nature Comm. arXiv:1503.05592v1.

(3) Robert M. Wallace, *ECS Trans*. **64** (2014) 109-116.

(4) Rafik Addou, Luigi Colombo, and Robert M. Wallace, ACS Appl. Mater. Interfaces (Accepted, 2015).

(5) Horacio Coy Diaz, Rafik Addou, and Matthias Batzill, Nanosclae **6** (2014) 1071-1078.

11:00am 2D+EM+MG+NS+SE+SM+SS+TF-ThM10 A Kinetic Study on the Adsorption of Polar (Water) and Non-Polar (Benzene) Molecules on CVD Graphene, *Nilushni Sivapragasam*, *U. Burghaus*, North Dakota State University
The adsorption kinetics of water and benzene at ultrahigh vacuum conditions were studied. Two different chemical vapor deposited graphene samples (graphene/SiO_2 and graphene/Cu) were utilized. Different surface analytical techniques (Auger electron spectroscopy, X-ray photoelectron spectroscopy, and Raman spectroscopy) were used to characterize the surface. Subsequently, a kinetics study - to understand the adsorption of water and benzene- using thermal desorption spectroscopy (TDS) was conducted. The TDS results revealed the hydrophobicity of water on graphene. However, the adsorption kinetics of water on graphene did not mimic the bare substrate, i.e., graphene is non-transparent for water adsorption. In contrast, graphene was transparent for benzene adsorption. Furthermore, the adsorption kinetics of both, water and benzene were substrate dependent.

11:20am 2D+EM+MG+NS+SE+SM+SS+TF-ThM11 Epitaxial Ultrathin $MoSe_2$ Layers Grown by Molecular Beam Epitaxy, *Ming-Wei Chen*, *M.B. Whitwick, O. Lopez-Sanchez, D. Dumcenco, A. Kis*, Ecole Polytechnique Fédérale de Lausanne (EPFL), Switzerland
Two-dimensional transition metal dichalcogenides (TMDs) have attracted widespread attention recently, and the focus is specifically on ultrathin layers due to the strong spin-orbit coupling and direct band-gap transition of single-layers. The unique properties of various TMDs also enable the possibilities for future optoelectronic applications. However, the synthesis of TMDs with uniform large-area and high-quality still remains challenging. While chemical vapour deposition has been demonstrated as a promising technique, the complexity of chemical precursors and the lacking of *in-situ* observation technique strongly hinder the progress.

Here, We propose to use ultra-high vacuum molecular beam epitaxy (MBE) to grow $MoSe_2$ ultrathin layers, down to single-layer in a controllable way. Epitaxial $MoSe_2$ layers were successfully grown on different crystalline substrates via van der Waals epitaxy mechanism, benefited from the weak interlayer interaction and the lacking of dangling bonds. Reflection high energy electron diffraction (RHEED) was used to *in-situ* monitor the initial growth stage and revealed a clear transition of the streaks, demonstrating the formation of $MoSe_2$ layer. Sharp streaks were obtained in the growth end, with the streak spacing corresponding to $MoSe_2$ lattice constant, and no significant strain effect was observed. In order to demonstrate the validity of van der Waals epitaxy, different crystalline substrates with lattice mismatch up to 30 % have been tested. The epitaxial layers showed a smooth and uniform surface in atomic force microscopy, and the quality was further confirmed in Raman spectrum and transmission electron

microscopy. Furthermore, photoluminescence of the single-layer $MoSe_2$ showing a sharp peak of ~1.58 eV at room temperature demonstrates the direct band-gap feature and indicates the potentials of photovoltaic applications. In the end, the growth of two-dimensional van der Waals heterostructures has also been addressed and the results pave way for heterostructure studies.

In summary, molecular beam epitaxy has been proved to be a reliable route to grow large-area and high-crystalline transition metal chalcogenides, and is promising to facilitate the integration of other two-dimensional materials in the future.

11:40am 2D+EM+MG+NS+SE+SM+SS+TF-ThM12 A Two-Dimensional Oxide Quasicrystal, *Stefan Förster*, Institute of Physics, Martin-Luther-Universität Halle-Wittenberg, Germany, *J.I. Flege,* Institute of Physics, Univerisity of Bremen, Germany, *K. Meinel, R. Hammer, M. Trautmann,* Institute of Physics, Martin-Luther-Universität Halle-Wittenberg, Germany, *J. Falta,* Institute of Solid State Physics, University of Bremen, Germany, *T. Greber,* Physik-Institut, University of Zürich, Switzerland, *W. Widdra,* Institute of Physics, Martin-Luther-Universität Halle-Wittenberg, Germany **INVITED**
With the recent discovery of the first oxide quasicrystal (QC) aperiodicity is entering the field of two-dimensional materials [1]. Aperiodicity means that the system exhibits long-range order as expressed by sharp diffraction spots but since the ordering follows an aperiodic function the system is lacking translational symmetry. We report here on the complex growth process of the oxide QC involving a high-temperature wetting process and periodic approximant structures.

The QC is derived from $BaTiO_3$ thin films on a hexagonal Pt(111) substrate and exhibits a sharp twelve-fold diffraction pattern [1]. Based on scanning tunneling microscopy the aperiodic atomic structure had been resolved [1]. It is formed by surface atoms arranged in forms of squares, triangles, and rhombi with a next-neighbour distance of 0.69 nm. In addition to this dodecagonal atomic arrangement, building blocks of squares, triangles, and rhombi are also found on $(2+\sqrt{3})$ and $(2+\sqrt{3})^2$ larger scales indicating the characteristic self-similarity of an ordered QC [1]. The high-resolution STM measurements allow furthermore to identify atomic flips in the structure indicating lattice excitations in the quasicrystal called phasons. Using low-energy electron microscopy (LEEM) the preparation and the growth of the QC films on top of the hexagonal Pt(111) is monitored in all details from room temperature up to about 1200 K. LEEM shows that upon high-temperature annealing large $3DBaTiO_3$ islands are formed with bare Pt(111)-(1x1) in between. At temperatures above 1020 K a wetting layer spreads on the free Pt area. This wetting process can be reversed by annealing in an oxygen atmosphere. In-situ LEEM measurements show that under these conditions the QC decays into small $BaTiO_3$ islands. The observed interface-driven formation of a 2D QC from a perovskite oxide in contact with a hexagonal substrate is expected to be a general phenomenon.

1. S. Förster, K. Meinel, R. Hammer, M. Trautmann, and W. Widdra, *Nature* **502**, (2013) 215.

Helium Ion Microscopy Focus Topic
Room: 211B - Session HI+AS+SS+NS-ThM

Focused Ion Beam Technology (08:00-10:00)/Fundamentals of Helium Ion Microscopy (11:00-12:20)
Moderator: Gregor Hlawacek, Helmholtz-Zentrum Dresden - Rossendorf, Leonidas Ocola, Argonne National Laboratory

8:00am HI+AS+SS+NS-ThM1 Ga+ Ion Beam Nanofabrication Techniques of 3D Micro- and Nano- Fluidic Devices, *Leonidas Ocola*, Argonne National Laboratory
Three-dimensional (3D) fluidic geometries have been fabricated in the past by using several layers of Polydimethylsiloxane (PDMS) molds or double-sided Si etch steps [1], which require highly accurate chip bonding to complete the fluid path and multiple process steps. An alternative to this method is the use of direct write ion beam micromachining as a means to fabricate key components of a microfluidic device that require variations in depth as well as variations in width. 3-D microfabrication currently is mainly constrained to excimer lasers [2-3] and therefore is inherently diffraction limited. Grey scale lithography is also used for 3D structures but has limited capability. On the other hand, ion beam micromachining can scale down below the diffraction limit with no change in the technique and almost unlimited depth bandwidth. The focused ion beam / scanning electron microscope (FIB/SEM) is a powerful tool used for sample analysis

and characterization. When equipped with a sophisticated pattern generator and lithography technology it can expand its use to new applications in nano- and micro-fabrication. Ion beam micromachining is akin to electron beam lithography, where a beam of charged particles are steered to draw structures contained in a computer aid design (CAD) file. Unlike electron beam lithography, one can program arbitrary depths by manipulating the dwell time, or dose, of a particular structure. In this paper the work reported previously [4-5] has been expanded to large and complex geometries to place emphasis on the applicability of ion beam micromachining to practical microfluidic applications, such as straight 3D mixers and serpentine 3D mixers with sections as deep as 70 microns and channel widths as large as 30 microns. We have found that these devices can achieve full mixing of aqueous solutions in about an order of magnitude faster than traditional devices. The challenges encountered and overcome to fabricate these mixers will be described and the scalability of different fabrication techniques to nano-fluidics will be revisited.

References:

1. R. H. Liu et al., J. MEMS 9 (2000) 190

2. Y. Liao et al., Lab Chip, 12 (2012) 746

3. A. Ródenas et al., Proc. SPIE 8542 (2012) 854217

4. A. Imre et al., J. Vac. Sci. & Technol. B 28 (2010) 304

5. E. Palacios et al., J. Vac. Sci. Technol. B 28 (2010) C6I1

8:20am HI+AS+SS+NS-ThM2 Adding 3D to Conventional SEM or FIB Surface Imaging Information - *In situ* **Surface Sensing and Nanoprofilometry for Focused Electron and Ion Beam Induced Processes Verification**, *Andre Linden*, Raith America, Inc., *A. Rudzinski, M. Levermann, T. Michael*, Raith GmbH, *E. Maynicke*, RWTH Aachen
Nanopatterning processes and corresponding parameters are typically well understood for standard nanofabrication applications using resist based electron beam lithography (EBL) or FIB milling processes (e.g. for TEM lamella preparation).

Recently however, the bandwidth of nanofabrication applications for dedicated nanopatterning tools has significantly broadened and is no more limited to resist based EBL and mere, standard FIB milling tasks. Some latest generation multi-technique electron and ion beam nanolithography tools even facilitate additional *in situ* processes such as resistless focused electron or ion beam induced processes - e.g. material deposition or gas enhanced etching. The number of variable parameters for such complex processes involving e.g. new gas chemistry or ion species is nearly "infinite". Moreover, smart and flexible patterning strategies, e.g. by using loops in conjunction with various multi-directional patterning modes, have significant impact on the final nanostructure´s definition and performance, so that a straight *in situ* characterization of e.g. material deposition, milling or etching rates becomes crucial for most efficient understanding and subsequent optimization of such processes.

In contrast to elaborately using additional analytical equipment outside the vacuum and subsequently re-introducing the sample for further processing and optimization, we have implemented a distance sensitive nanomanipulator with nanoprofilometric capabilities into our professional multi-technique nanofabrication tools, which allows *in situ* characterization of nanostructures in 3D with ~10nm resolution by collecting topographic sample surface information.

First results of direct *in situ* growth rate determination of focused electron beam induced material deposition (FEBID) for process calibration as well as 3D surface topographic information of challenging milling applications will be presented.

8:40am HI+AS+SS+NS-ThM3 Nanofabrication Using Gas-Assisted Focused Ion Beams, *Chad Rue*, FEI Company **INVITED**
A brief introduction to gas-assisted etching for Focused Ion Beams (FIBs) is given, including typical chemical precursors for various applications, and appropriate beam control parameters such as pixel overlap, dwell time, and refresh time. These factors are reasonably well-understood for pattern dimensions that are large compared to the size of the ion beam. However, for applications such as nanofabrication, which require high milling precision over small areas, the limiting size of the ion beam and its associated activated volume begin to influence the milling performance. The remainder of the discussion will focus on the relatively-unexplored regime in which the size of the pattern dimension is comparable to the size of the ion beam itself. The influence of various beam control parameters, particularly refresh time, becomes critically important to the milled profile of the desired structure. Redeposition effects, peripheral erosion, and mill rate trends are discussed. Operating tips and tricks are described, including

the use of drift compensation strategies. The minimum physically achievable via size is examined. For a 10 pA Ga^+ beam at 30 keV, used to mill a via in a SiO_2 substrate with XeF_2-assist, the minimum achievable via size (FWHM) is found to be 50 ± 10 nm, and is relatively independent of depth or aspect ratio. Implications for nanofabrication are discussed and examples are shown.

9:20am HI+AS+SS+NS-ThM5 The Psychology and Applications of a Bipolar Plasma Focused Ion Beam, *Rod Boswell*, ANU, Australia, *N. Smith, P. Tesch, N. Martin*, Oregon Physics
A new high brightness ion source has been developed using bi-polar power supplies that can be used with either positive or negative ions. This has involved a redesign of the plasma source and the acceleration optics to allow high currents to be focused with an energy of up to 30kV. We expect to make significant advances in Ultra High Resolution SIMS with a negative oxygen beam; a second application is the milling of structures in glass with a O- beam, such as a microfluidic set of channels. At the higher voltages mentioned above, it should be possible to cut cross sections of Through Silicon Vias in glass substrates. The challenges encountered in creating and extracting the negative ions will be discussed along with some performance and application data.

9:40am HI+AS+SS+NS-ThM6 Advanced FIB Applications with New Ion Species and Large Area Capabilities, *Sven Bauerdick, L. Bruchhaus*, Raith GmbH, Germany, *J. Fridmann*, Raith America, Inc., *P. Mazarov, A. Nadzeyka, R. Jede*, Raith GmbH, Germany
Focused ion beam (FIB) systems are applied to a wide range of applications in R&D nanofabrication, both for creating functional devices as well as for preparing sample imaging and analysis. With different ion species on one hand and very sophisticated patterning approaches on the other hand it is possible to improve results and provide solutions for more advanced applications. Here we show and discuss the capabilities of Ga and new ion species like Au or Si with high resolution, long-term stability and easy handling, which is combined with an instrument design enabling large area or elongated patterns by write field stitching or truly continuous writing, respectively.

The type of ion defines the nature of the interaction mechanism with the sample and has significant consequences on the resulting nanostructures or samples. Therefore, we have extended the FIB technology towards the delivery of multiple ion species selectable into a nanometer-scale focused ion beam by employing a liquid metal alloy ion source (LMAIS). A mass separation filter is incorporated into the column to allow for fast and easy switching between different ions. The respective capabilities of mainly Ga, Au and Si have been investigated (resolution, milling rate, imaging, implantation) and according results and applications will be presented.

Moreover we investigated, optimized and tested milling approaches for pattern (write field) stitching and for truly continuous patterning based on precise stage movement while milling/ cutting with the ion beam. An improved beam pattern needs to mimic the looping strategy of conventional milling, so that grooves with defined depth, steep sidewalls and minimum re-deposition can be achieved. This combination of functionality enables applications like nanofabrication of micro-fluidic mixers, zone plates, large area gratings, or wafer-level nanopore devices as well as sample investigation e.g. imaging, X-sectioning and preparation in an automated way. Examples for new nanofabrication techniques like large area hard masking by implantation, both for reducing and increasing the rate in standard etching processes, or seamless direct milling of nano-fluidic channels over cm's will be discussed.

11:00am HI+AS+SS+NS-ThM10 SIMS on the Helium Ion Microscope : a Powerful Tool for High-resolution High-sensitivity Nano-Analytics, *Tom Wirtz, D. Dowsett*, Luxembourg Institute of Science and Technology (LIST), Luxembourg, *S. Sijbrandij*, Carl Zeiss Microscopy **INVITED**
While the ORION Helium Ion Microscope NanoFab has become an ideal high resolution imaging and nanofabrication tool, its analysis capability is currently limited. By contrast, Secondary Ion Mass Spectrometry (SIMS) is an extremely powerful technique for analysing surfaces owing in particular to its excellent sensitivity, high dynamic range, very high mass resolution and ability to differentiate between isotopes. The combination of He/Ne microscopy and SIMS would not just offer the prospect of obtaining SIMS information limited only by the size of the probe-sample interaction (~10 nm) but also of directly correlating such SIMS images with high resolution (0.5 nm) secondary electron images of the same zone taken at the same time. We have therefore investigated the feasibility of combining SIMS with Helium Ion Microscopy from a fundamental and instrumental point of view.

In order to reach good detection limits when probing very small voxels in imaging applications, the ionization probability of the sputtered atoms and molecules needs to be maximized. When using He^+ and Ne^+ bombardment,

the intrinsic yields are low compared to the ones found in conventional SIMS. However, the yields may be drastically increased by using reactive gas flooding during analysis, namely O_2 flooding for positive secondary ions and Cs flooding for negative secondary ions. Our results show that both negative and positive ion yields obtained with He^+ and Ne^+ bombardment may be increased by up to 4 orders of magnitude when using such reactive gas flooding. This optimization of secondary ion yields leads to detection limits varying from 10^{-3} to 10^{-6} for a lateral resolution between 10 nm and 100 nm.

The prototype instrument we developed during this feasibility study contains extraction optics allowing the emitted secondary ions to be extracted with a maximized efficiency and without negatively impacting the focusing of the incoming He^+ or Ne^+ ion beam (broadening or distortion of the ion beam due to the electric fields). These extraction optics are coupled to a specially designed compact high-performance magnetic sector double focusing mass spectrometer that we developed for the purpose of HIM-SIMS. The specifications of this mass spectrometer include high mass resolution with optimized transmission ($M/\Delta M > 1000$ at 100% transmission or $M/\Delta M > 3000$ at 50% transmission), full mass range (H-U) and parallel detection of several masses.

The results are very encouraging and the prospects of performing SIMS on the Helium Ion Microscope are very interesting. In this paper we will present the main findings of our feasibility study, including fundamental, instrumental and application aspects.

11:40am HI+AS+SS+NS-ThM12 Nanometer TOF-RBS and TOF-SIMS in a Helium/Neon Ion Microscope, *Nico Klingner*, *R. Heller, G. Hlawacek, S. Facsko, J. von Borany*, Helmholtz-Zentrum Dresden - Rossendorf, Germany

Helium ion microscopes (HIM) have become powerful imaging devices within the last decade. Their excellent lateral resolution down to 0.3 nm and their high field of depth make them a unique tool in surface imaging [1]. So far the the analytical capabilities of a HIM are rather limited or need complex detection setups. In addition we will discuss major challenges and physical limitations of ion beam analysis in the HIM.

We will present a new and relatively easy to implement method for ion beam analysis in the HIM by means of time of flight spectrometry to obtain elemental information from the sample. We will demonstrate the flexibility and applicability of the method to image samples with target mass contrast, to analyze the target compositions, and to measure depth profiles of films with few tens of nm thickness.

Pulsing the primary helium or neon ion beam and measuring the time of flight of ejected particles allows to obtain the energy of the backscattered particles as well as the mass of the ionized, sputtered target atoms. This has been achieved by chopping the primary ion beam down to pulse widths of 18 ns by use of the built-in beam blanker and a customized plug-on beam blanking electronics. The secondary particles are detected by means of a multi channel plate mounted on a flange of the HIM.

We will show TOF-RBS and TOF-SIMS measurements for different materials, which can give complementary information. Lateral resolved TOF-SIMS allows to quickly obtain qualitative elemental mapping while the TOF-RBS gives the standard-free quantitative sample composition of regions of interest. We will also show, that with TOF-RBS depth profiling of nm-thick layers is possible.

[1] G. Hlawacek, V. Veligura, R. van Gastel, and B. Poelsema, J. Vac. Sci. Technol. B 32(2), 2014

12:00pm HI+AS+SS+NS-ThM13 Improving Pattern Fidelity in Helium Ion Beam Lithography using Pixel Dose Optimization, *N. Kalhor*, TU Delft, Netherlands, *W. Mulckhuyse*, TNO Technical Sciences, Netherlands, *Paul Alkemade*, TU Delft, Netherlands, *D. Maas*, TNO Technical Sciences, Netherlands

Scanning Helium ion beam lithography (SHIBL) with a sub-nanometer beam probe size at the sample surface is a promising technology for high-resolution lithography with high pattern density.[1] The advantages of SHIBL compared to e-beam lithography are higher sensitivity and a lower proximity effect. Remarkably, there are unique similarities in the activation response of resists to He-ions and extreme-ultraviolet (EUV) photons in EUV lithography (EUVL). Both primary beams produce low energy secondary electrons (SEs) and are not hindered by proximity effect. Recently Maas et al. experimentally demonstrated these similarities and suggested SHIBL as a promising method for pre-screening chemically amplified resists (CARs) prior to their final performance evaluation in an EUV scanner.[2]

However, unlike an EUV photon which only interacts with one resist molecule, an He-ion scatters inelastically in the resist and causes a chain of collisions with resist molecules, producing one or more SEs per collision.

Also, a small dose-to-clear of 0.085 ions/nm^2 for SHIBL in a CAR was measured.[2] Hence, Maas et al. hinted at ion shot noise as a limiting factor in pattern fidelity in SHIBL.[2]

Here, we present a heuristic resist activation model for single-pixel dose SHIBL. The model employs a point-spread function (PSF) to account for all contributing factors in the resist activation. Ion shot noise impact is modeled with Poisson statistics. We show a good agreement between the model and our experimental single-pixel dose SHIBL results for line-and-space (LS) and contact hole patterns. Our model indicates pattern fidelity in sensitive CAR is not only limited to ion shot noise; instability of the He-ion source emission and post-exposure resist processing can also play important roles. Moreover, we introduce optimized-pixel-dose SHIBL to improve critical dimension uniformity (CDU), line width roughness (LWR), exposure latitude and throughput gain. In this approach, we calculate an optimum ion dose map for a given binary pattern such that the pattern's edges are exposed at the steepest part of the PSF to improve resist-pattern contrast and to minimize ion shot noise effect. Pixel dose optimization is advantageous to single-pixel exposure when the feature size is larger than the FWHM of the PSF. We discuss this by comparing our modeling results for single-pixel and optimized-pixel-dose SHIBL exposure modes for a desired LS pattern. We show that pixel-dose optimization could reduce LWR by ~45% (~1.3 nm) with a concurrent 20% dose reduction.

[1]V. Sidorkin et al., J. Vac. Sci. Technol. B **27**, L18 (2009)

[2]Maas et al., SPIE Proc. **9048**, 90482Z (2014)

Scanning Probe Microscopy Focus Topic
Room: 212A - Session SP+AS+NS+SS-ThM

Probing Chemical Reactions at the Nanoscale
Moderator: Stephen Nonnenmann, University of Massachusetts - Amherst, Shengyong Qin, University of Science and Technology of China

8:40am SP+AS+NS+SS-ThM3 Adsorption of Trimethyl Acetic Acid on (1x2) Reconstructed TiO$_2$(110), *Kenneth Park*, *K. Zhu, Y. Xia, Z. Zhang*, Baylor University

The adsorption of trimethyl acetic acid on (1x2) reconstructed $TiO_2(110)$ is investigated using scanning tunneling microscopy (STM) with the same area analysis. After de-protonation, trimethyl acetate (TMA) molecules preferentially adsorb in the troughs between two adjacent 1x2 strands. The nearest neighbor distance between TMA molecules is about 5.9 Å, twice the lattice constant along [001], corresponding to the bridging bidentate configuration over two 5-coordinated Ti^{4+} sites. With increasing coverage, they form linear chains, separated by (1x2) strands leading up to the nominal saturation coverage of 0.25 ML. Upon further adsorption, the second-layer of TMA molecules start clustering on top of 1x2 strands. The coverage-dependent TMA adsorption structures on (1x2) reconstructed $TiO_2(110)$ will be compared and discussed with the reported TMA adsorption on (1x1) $TiO_2(110)$, and relative reactivity of TMA with other defect sites including cross-links will be presented.

9:00am SP+AS+NS+SS-ThM4 Anticorrelation between Surface and Subsurface Point-Defects and Influence on Redox Chemistry at TiO$_2$(110), *Igor Lyubinetsky*, *Y. Yoon, Y. Du*, Pacific Northwest National Laboratory, *J.C. Garcia*, Worcester Polytechnic Institute, *Z. Zhu, Z.-T. Wang, N.G. Petrik, G.A. Kimmel, Z. Dohnalek, M.A. Henderson, R. Rousseau*, Pacific Northwest National Laboratory, *N.A. Deskins*, Worcester Polytechnic Institute

The atoms at the surface that constitute reactive sites clearly govern surface chemistry. But subsurface atoms, particularly substitutional and/or interstitial defects, can also influence surface chemistry, though a detailed understanding is still emerging. Here we report the interplay and relative impact of surface vs. subsurface defects on the surface chemistry of rutile TiO$_2$, a prototypical metal oxide. Importantly, it contains both surface and subsurface intrinsic point-defects in the reduced state (along with residual extrinsic defects). Our scanning tunneling microscopy results show that O vacancies (V_O's), the dominant surface defects, are virtually absent in the vicinity of positively-charged subsurface point-defects. Such anticorrelation of defects is consistent with density functional theory (DFT) calculations of the impact of subsurface defect proximity on V_O formation energy, which narrows down the possible candidates to certain interstitial defects, of both intrinsic and extrinsic nature. To monitor the influence of such (electron-donor type) defects on surface redox chemistry, a test reaction of the electron-mediated dissociative adsorption of O_2 is employed, which is observed to be suppressed around these defects. DFT results attribute this to a perceived absence of the intrinsic (Ti) (and likely extrinsic) interstitials in

the nearest subsurface layer beneath "inhibited" areas, while the underlying energetic driver is largely repulsive electrostatics. Finally, we postulate that the entire subsurface region up to several atomic layers deep could be voided of any charged point-defects, whereas such defects are proposed to exist beyond the subsurface region. Subsequently, prevalent V_O's are largely responsible for both the surface/subsurface reduction and mediation of the redox chemistry at reduced $TiO_2(110)$ surface. Overall, this work provides new fundamental insights into the relation between surface and subsurface defects. In a broader perspective, the uncovered effects may prove to be general for other reducible oxides, and thus have potential implications in such diverse research fields as environmental remediation or microelectronics.

9:20am SP+AS+NS+SS-ThM5 Dissociation of Water on Oxygen Pre-Covered Cu(110) Observed with Scanning Tunneling Microscopy, *Zongqiang Pang*, Lawrence Berkeley National Laboratory (LBNL)
The dissociation of water on the oxygen pre-covered Cu(110) surface has been studied with Scanning Tunneling Microscopy (STM). At low temperature (77K), water reacts with pre-covered oxygen to produce hydrogen atoms and hydroxyl groups. Non-dissociated water molecules and hydroxyl groups combine to form a hexagonal network on the top of Cu(110) where water donates one hydrogen to the hydroxyl, while uncoordinated hydroxyls bind to the second layer intact water molecules. Following excitation by tunneling electron or by heat, the water molecules in the hexagonal network gradually dissociate. The oxygen atoms involved in the reaction of water dissociation return to its original position, leaving ordered Cu-O and hydroxyl dimer chains on the Cu(110) surface which both align along <001> direction. Our results demonstrate that the oxygen atoms pre-adsorbed on the Cu(110) surface lower the energy barrier for water dissociation on the Cu(110) surface.

9:40am SP+AS+NS+SS-ThM6 Probing Local Electrochemical Activity within Yttria-Stabilized-Zirconia *via In Situ* High-Temperature Atomic Force Microscopy, *Jiaxin Zhu*, University of Massachusetts - Amherst, *C. Perez, T. Oh, R. Kungas, J. Vohs, D. Bonnell*, University of Pennsylvania, *S.S. Nonnenmann*, University of Massachusetts - Amherst
Considerable interest in understanding interfacial phenomena occurring across nanostructured solid oxide fuel cell (SOFC) membrane electrode assemblies has increased demand for *in situ* characterization techniques with higher resolution. We briefly outline recent advancements in atomic force microscopy (AFM) instrumentation and sub-systems in realizing real time imaging at high temperatures and ambient pressures, and the use of these *in situ*, multi-stimuli probes in collecting local information related to physical and fundamental processes. Here we demonstrate direct probing of local surface potential gradients related to the ionic conductivity of yttria-stabilized zirconia (YSZ) within symmetric SOFCs under intermediate operating temperatures (500 °C – 600 °C) via variable temperature scanning surface potential microscopy (VT-SSPM). The conductivity values obtained at different temperatures are then used to estimate the activation energy. These locally collected conductivity and activation energy values are subsequently compared to macroscopic electrochemical impedance results and bulk literature values, thus supporting the validity of the approach.

Surface Science
Room: 113 - Session SS+AS+EM+EN-ThM

Semiconductor Surfaces and Interfaces - I
Moderator: Yves J. Chabal, University of Texas at Dallas

8:00am SS+AS+EM+EN-ThM1 Reaction of 1,2,3-Benzenetriol with the Ge(100)-2x1 Surface, *Tania Sandoval, S.F. Bent*, Stanford University
Functionalization of semiconductor surfaces can provide tunable control of interfacial properties in organic-inorganic hybrid devices. In particular, multifunctional molecules have the potential to change the surface chemistry by leaving unreacted functional groups available after adsorption. Understanding the adsorption of these complex molecules could lead to various applications as sensors, selective film deposition, and molecular electronics.

In this work, the reaction of 1,2,3-benzenetriol on Ge(100)-2x1 surface was investigated. While the reaction of hydroxyl groups has been previously studied, differences in selectivity can be expected due to the position of the functional groups along the ring. The purpose of this study is to determine the extent of these differences and the effect on product distribution.

An analysis of the adsorption energetics was carried out by density functional theory. As expected, a proton transfer reaction was shown to be the most stable adsorbate configuration. However, after the adsorbate reacts

with the surface through its first OH group, the energetics of the second OH dissociation showed differences based on two factors: (i) surface configuration (cross or diagonal trench and end or cross bridge) and more interestingly (ii) which two of the OH groups (1 and 2 or 1 and 3) are reacting with Ge. The latter constraint affects the adsorption energy of the second dissociation, where adsorption regardless of the surface configuration is less stable when the OH groups are next to each other. Finally, transition states for dissociation of the third OH were found to be limited by the configuration of the second dissociation, and in some cases were not possible to find without unrealistic distortions of the molecule.

Chemisorbed and physisorbed O(1s) and C(1s) spectra were obtained by X-ray photoelectron spectra. Differences between these spectra can be used to identify the reaction products. No change in the C(1s) spectra was observed, suggesting that no carbon forms a bond directly with the Ge surface. On the other hand, clear differences between the chemisorbed and physisorbed O(1s) spectra are observed. The presence of a second peak with a lower binding energy only in the chemisorbed spectra, assigned to oxygen bonded to Ge, confirms that 1,2,3-benzenetriol reacts with the Ge surface through OH dissociation. Quantitative analysis of the chemisorbed O(1s) spectra provides information on the fraction of OH groups reacting with the surface. Interestingly, about 66% of the total hydroxyl groups in 1,2,3-benzenetriol are involved in reaction with Ge, indicating that there is a significant fraction of unreacted OH groups.

8:20am SS+AS+EM+EN-ThM2 Ethylenediamine Grafting on Oxide-free H-, F-, and Cl- terminated Si(111) Surfaces, *Tatiana P. Chopra*, R.C. Longo, K.J. Cho*, University of Texas at Dallas, *M.D. Halls*, Schrodinger, Inc., *P. Thissen*, Karlsruhe Institute of Technology, Germany, *Y.J. Chabal*, University of Texas at Dallas
Amine termination of surfaces constitutes a core platform for fields as diverse as microelectronics and bioengineering, and for nanotechnology in general. Diamines are particularly attractive for surface amination because, unlike ammonia or simple amine molecules, they have a metal chelating capability useful in fabricating heterostructures. They can act as a linker molecule between inorganic electronic materials and biomolecules or photoactive quantum dots for applications in microlectronic, photonics and biosensing. Most work in the field utilizes self-assembled monolayers (SAMs) on oxidized substrates to present an amine termination of the surface. However, grafting on oxides through silanes or phosphonates is not robust. Moreover, several applications require as short a distance between the substrate and the amine group, which is hindered by the thickness of the oxide. Therefore, diamine grafting directly on oxide-free substrates is important, yet remains unexplored.

In this work, the attachment of liquid and vapor-phase ethylenediamine on three types of oxide-free (H-, F- and Cl-terminated) Si(111) surfaces is examined by infrared absorption spectroscopy and X-ray photoelectron spectroscopy in conjunction with first-principles calculations. We find that chemisorption is only possible on F- and Cl-terminated Si surfaces, with H-terminated Si surfaces yielding only physisorbed diamine molecules. On Cl-terminated Si surfaces, diamines adsorb in a mixture of monodentate and bridging configurations (chemical reaction of both amine endgroups), while on partially F-terminated Si surfaces the adsorption occurs primarily at one end of the molecule. The reaction of ethylenediamine with Cl-terminated Si surfaces is also characterized by complete removal of Cl and partial Si-H (~25% ML) formation on the surface. This unexpected result suggests that a proton-chlorine exchange may take place, with the endothermic barrier possibly reduced via a silicon lattice assisted process after an initial attachment of ethylenediamine to the surface.

8:40am SS+AS+EM+EN-ThM3 Reaction of Phenylhydrazine with Cl-Si(111) Surface by Wet Chemistry and with Clean Silicon Surface in UHV, *A.V. Teplyakov, Fei Gao*, University of Delaware
The monolayer coatings with aromatic functional groups can be used to tune mechanical, electronic, and chemical properties of semiconductor surfaces. This work focuses on obtaining well-defined surface of silicon functionalized with phenylhydrazine to produce an oxygen-free platform for further functionalization. Single crystalline Si(111) surface has been prepared using modified RCA procedure to produce well-ordered H-Si(111) surface. Next, Cl-terminated Si(111) surface is prepared from H-terminated Si(111) surface using PCl_5 in chlorobenzene solvent with trace amount of benzoyl peroxide as a reaction initiator under nitrogen atmosphere following previously established procedures. Phenylhydrazine-functionalized Si(111) sample is obtained from Cl-Si (111) surface with phenylhydrazine at 38ºC under N_2 atmosphere. To confirm the presence of Si-N bonds following this procedure, establish the structures of surface species produced and to investigate the oxidation mechanism, we followed the reaction by Fourier-transform infrared spectroscopy, X-ray

---

* Morton S. Traum Award Finalist

photoelectron spectroscopy, and time-of-flight secondary ion mass spectrometry. To study the formation of Si-NH$_x$ groups, this result was compared with the results of phenylhydrazine reactions on clean silicon surface under ultra-high vacuum (UHV) conditions. Density functional theory (DFT) calculations were performed to infer the mechanisms of surface reactions and further oxidation steps, and to compare the predicted vibrational spectra and core-level energies with the results of experimental studies.

9:00am SS+AS+EM+EN-ThM4 Anomalously Low Surface Recombination Velocity for Fluorine Terminated Nanopatterned Si Surfaces, *W.N. Peng, **Jonghan Park**, L.-H. Liu, R.C. Longo,* University of Texas at Dallas, *D.J. Michalak,* Intel Corporation, *D.M. Pak, Y.J. Lee, J.X. Hsu, K.J. Cho, Y.J. Chabal,* University of Texas at Dallas

Recently, oxide-free and partially methoxy-terminated Si surfaces[1] have been developed as a novel platform for surface reactions because of their superior reactivity compared to hydrogen termination[2]. As a result, strong polar bonds such as Si-F could be stabilized on these surfaces. Since the electrical quality is critical for many applications (i.e. surface defects can degrade the device performance), we performed contactless surface recombination velocity measurements to examine the electronic quality of partially covered surfaces. Interestingly, we found that the carrier lifetime is significantly increased after fluorine termination, with the carrier lifetime 10 times higher than that of hydrogen terminated Si surfaces, approaching 1.5 ms. This anomalously long carrier lifetime can be explained either by a better surface passivation or by surface band bending effects. We therefore performed UPS and kelvin probe measurements to investigate the band structure of these surfaces after fluorine termination and found evidence for band bending. A potential model of a surface dipole layer induced band bending is supported by DFT calculations. Regardless of the mechanism controlling the recombination time, this method is well suited to explore the fluorination mechanism of H-terminated surfaces.

[1] D. Michalak, S. Amy, D. Aureau, M. Dai, A. Esteve, and Y. J. Chabal, *Nature Materials*, **9**, (2010)

[2] P. Thissen, T. Peixoto, R. Longo, W. Peng, W. Schmidt, K. Cho, and Y.J. Chabal, *JACS*, **134** (2012)

9:20am SS+AS+EM+EN-ThM5 Molecular Functionalization of Semiconductor Surfaces: From Single Crystals to Quantum Dots, *Stacey Bent*, Stanford University   **INVITED**

Because the surfaces of small structures can dominate their properties, implementing functional nanoscale materials depends to a large extent upon understanding and controlling the surface reactivity. This talk will focus on studies of the adsorption of organic molecules at semiconductor surfaces, toward the ultimate goal of controlling the chemical and electrical properties of the substrate. We will describe model studies of molecular functionalization on both flat and nanostructured surfaces. The presentation will begin by examining adsorption on the Ge(100)-2×1 surface. Using a combination of experimental (infrared spectroscopy, X-ray photoelectron spectroscopy) and theoretical (density functional theory calculation, Monte Carlo simulation) methods, we will show how the molecular structure as well as the identity of the reactive moieties of organic molecules can affect the product distribution upon adsorption. We will then present results of a study in which the organic ligands bonded to semiconductor quantum dots (QDs) are used to tune the electronic properties of the QDs. We will describe experimental and theoretical studies of the effects of such interface engineering on the band gap and relative band positions in lead sulfide (PbS) QDs. These ligand-exchanged quantum dots are tested in multilayer colloidal QD solar cells, and the results show that molecular functionalization can be used to achieve enhanced photogenerated carrier collection in the devices.

11:00am SS+AS+EM+EN-ThM10 Periodic Trends in the Hydrogen Elimination Thermal Decomposition Reaction on Si(100)-2×1: Linear and Branched Alkyl Halides, Alcohols, and Amines, *Andrew Pohlman, K.L. Romolino, N.J. Burgener, S.M. Casey,* University of Nevada

The hydrogen elimination thermal decomposition reaction was studied on the Si(100)-2×1 surface using temperature programmed desorption mass spectrometry (TPDMS) and electronic structure methods for a selection of linear and branched alkyl halides, alcohols, and primary amines. Desorption activation energies and pre-exponential factors were determined using several analysis techniques from TPDMS spectra and compared to calculations based on ab initio canonical transition state theory using density functional theory (DFT). Values for activation energies and pre-exponential factors for dissociative desorption are compared within an adsorbate class based on a varying ratio of available alpha:beta:gamma hydrogens for elimination. Kinetic parameters are also compared between classes of adsorbates for general structure-activity periodic trends. TPDMS experiments reveal desorbing masses consistent with hydrogen elimination

in all cases; however, the different elimination channels remain convoluted. Rate constants for each desorption channel were calculated using DFT and used to determine branching ratios for each dissociative desorption reaction. Reaction barrier trends are consistent with previous reports; however, numerical values were found to be much lower when considering inter-dimer reaction mechanisms.

11:20am SS+AS+EM+EN-ThM11 Diffusion of Arsenic Oxides During the Atomic Layer Deposition of Metal Oxide Films on GaAs(100) Surfaces, *Alex Henegar, T. Gougousi,* University of Maryland, Baltimore County

It is known that native oxides of III-V semiconductors are consumed during atomic layer deposition using certain subsets of precursors. It was believed these surface oxides were completely removed during the first few deposition cycles because once the surface was covered by a coalesced film the native oxides would be protected. It has been observed, however, that native oxide consumption in systems such as ALD TiO$_2$ on GaAs(100) and InAs(100) proceeds continuously well after the surface is completely covered. Therefore there must be a transport mechanism that continuously moves these oxides through the developing film in order to interact with the precursor at the surface and be removed.

The aim of this work was to find unequivocal evidence of the transport mechanism needed for continuous oxide removal during ALD at typical processing conditions. ALD processes using metal organics and H$_2$O were used to deposit TiO$_2$, Al$_2$O$_3$ and HfO$_2$ films on GaAs(100). The experiments were designed so as to decouple the native oxide consumption from the native oxide transport and provide convincing evidence for the existence of this unacknowledged thus far mechanism. We will provide results that solidify the hypothesis that native oxide diffusion is a critical component in the complete and continuous removal of the interfacial layer.

11:40am SS+AS+EM+EN-ThM12 Ultrafast Non-Equilibrium Effects in Ti Overlayers on P-Type GaAs(100) Investigated by Femtosecond XUV Photoemission Spectroscopy, *Mihai E. Vaida,* University of California, Berkeley, *S.R. Leone,* University of California, Berkeley and Lawrence Berkeley National Laboratory

Time resolution, surface sensitivity and element specificity are technical ingredients required to investigate ultrafast photoinduced processes and charge localization at semiconductor surfaces. All these requirements are fulfilled by a new experimental apparatus that consists of a tunable femtosecond high harmonics XUV source, a pump-probe setup, and an ultra-high vacuum surface science chamber for surface preparation and investigation.

The present contribution focuses on the charge carrier dynamics at the surface of a bare p-type GaAs(100) as well as Ti overlayers on p-type GaAs(100). The charge transfer between the bulk and the surface of the bare GaAs(100) is produced by the pump laser pulse at the central wavelength of 800 nm and is investigated by monitoring the surface photovoltage through the shift of the Ga 3d photoemission peak with the XUV probe laser pulse as a function of the pump-probe time delay. A transient shift of the Ga 3d photoemission peak to lower binding energy at early pump-probe time delay, with a magnitude of 0.3 eV, is observed and is attributed to transport of the electrons from the bulk to the surface. Upon increasing the pump-probe time delay, a restoration of the Ga 3d peak is observed, which corresponds to the recombination of the positive and negative carriers.

When a Ti overlayer is deposited on the p-type GaAs(100) surface, a Schottky diode is formed. If the 800 nm pump laser pulse has sufficient intensity to produce a photoemission process via multi-photon excitation, non-equilibrium effects occur at the Ti-GaAs interface independently from the presence of the surface photovoltage. In this case, positive charges accumulate at the surface and are not effectively screened by the electrons coming from the bulk, and the Schottky diode is transiently driven into a reversed bias mode. The formation of the reverse bias Schottky diode, which is studied in real time with the XUV probe laser pulse by monitoring the Ti Fermi level photoemission shift as a function of the pump-probe time delay will be presented and discussed.

12:00pm SS+AS+EM+EN-ThM13 Improving the Quality of p-type AlGaN Layers by Reactive-ion Etching, *Joy McNamara, K.L. Phumisithikul, A.A. Baski, M.A. Reshchikov,* Virginia Commonwealth University, *J. Marini, F. Shahedipour-Sandvik,* SUNY Polytechnic Institute

AlGaN layers prepared by metal-organic chemical vapor deposition, with varying composition of Al (6 – 17%), were studied using the surface photovoltage (SPV) technique. Previous SPV studies on both *n* and *p*-type GaN allowed us to calculate the value of the surface band bending, by applying a thermionic model to explain the transfer of charges over the near surface barrier in various conditions (air, vacuum, and for a wide range of temperatures, T = 80 – 600 K). [1,2] The band bending was estimated to be

1.0 eV and – 2.0 eV, for *n*-type GaN and *p*-type GaN, respectively. SPV measurements on *p*-type AlGaN layers were expected to have similar behaviors to their *p*-type GaN counterparts. However, numerous measurements showed that this was not the case. The SPV transients (upon turning on or off the excitation source) showed significantly slower transients and smaller values than expected from the thermionic model. Moreover, the restoration of the band bending, as indicated by the restoration of the SPV signal to its dark value, did not occur within a reasonable amount of time. The data could not be fit by the thermionic model, and thus we were unable to calculate the band bending. We attribute the slow transients and lack of restoration to a defective surface region which interferes with thermionic processes. To verify this assumption, the top 40 nm of the AlGaN layer was etched using a reactive-ion etch (RIE). After etching, the SPV behavior exhibited substantially different behavior. Fast transients and close-to-thermionic behavior was recovered. Additionally, the effect of annealing the samples after etching provided even closer values to what is predicted by the thermionic model. From this study, it can be concluded that a defective, near surface region is inhibiting the transfer of holes over the near surface barrier under illumination, and hole trapping may be occurring during restoration. In both cases, this behavior cannot be modeled by theory. Etching removes the defective layer, and reveals a region of presumably higher quality as evidenced by the subsequent thermionic behavior.

[1] M. A. Reshchikov, M. Foussekis, and A. A. Baski. *J. Appl. Phys*. **107**, 113535 (2010).

[2] M. Foussekis, J. D. McNamara, A. A. Baski, and M. A. Reshchikov, *Appl. Phys. Let.* **101**, 082104 (2012).

Thursday Afternoon, October 22, 2015

2D Materials Focus Topic
Room: 212C - Session 2D+EM+MG+NS+SS+TF-ThA

Heterostructures of 2D Materials

Moderator: Stefan Förster, Martin-Luther-Universität Halle-Wittenberg, Michael Naguib, Oak Ridge National Laboratory

2:20pm 2D+EM+MG+NS+SS+TF-ThA1 Dielectrics Layer Deposition on 2D Materials by Functionalization with Polar Titanyl Phthalocyanine, *JunHong Park*, UC San Diego, *S. Fathipour*, University of Notre Dame, *I.J. Kwak*, UC San Diego, *H.C.P. Movva*, UT-Austin, *S. Vishwanath, H. Xing*, Cornell University, *S.K. Banerjee*, UT-Austin, *A.C. Seabaugh*, University of Notre Dame, *A.C. Kummel*, University of California at San Diego

Several novel designs for beyond CMOS devices have emerged using two-dimensional semiconductors. These devices require deposition of thin insulators on 2D semiconductors or between two sheets of 2D semiconductors. However, 2D semiconductors are nearly inert surfaces thereby making uniform nucleation of oxide growth challenging preventing scaling of the insulator thickness. A new technique has been developed to employ a monolayer of ordered metal phthalocyanines (MPc) on 2D semiconductors directly as a nucleation layer for growth of ALD dielectric. TiOPc monolayers were deposited on HOPG surfaces and WSe_2 by organic molecular beam epitaxy. TiOPc forms a monolayer with only few defects, and the crystal structure of monolayer has four-fold symmetry in a 1.6 x 1.6 nm grid on both HOPG and WSe_2. Observation of bright protrusions on each O-TiPc indicates that each O-TiPc in the monolayer is directed outward to vacuum. After exposure O-TiPc monolayer to 5 cycles ALD pulse (tri-methyl-aluminum (TMA)+H_2O), insulating aluminum oxide was deposited uniformly on TiOPc/HOPG. After formation of AlO_x on TiOPc/HOPG, the band gap of surface increases from 1.7 eV to 3.4 eV, while the conductance decreased. A metal-oxide-TiOPc-graphene capacitor has the lower thickness and the higher capacitance value than any reported graphene MOSCAPs. In the dual gated graphene FET with 40 cycles of AlO_x, TiOPc assisted AlO_x shows very low leakage current. Employing the TiOPc seeding layer also can be expanded to other TMD materials. The bottom gated WSe_2 FET was fabricated. On the bottom gated WSe2 FET, the TiOPc monolayer was deposited, then 50 cycle of AlO_x was deposited via ALD. In this dual gated WSe_2 FET, the leakage current of the AlO_x is measured as ~0.05 $pA/\mu m^2$ at 0.5 VTG. As a control, 20 cycles of Al_2O_3, and 140 cycles of HfO_2 were deposited on bare WSe_2. The leakage current of the TiOPc assisted 50 cycle Al_2O_3 oxide is 3 orders of magnitude lower than $HfO_2/Al_2O_3/WSe_2$, consistent with a high nucleation.

2:40pm 2D+EM+MG+NS+SS+TF-ThA2 Direct Probing of the Electronic Structure of Bilayer Homo- and Hetero-Structures and Tracking their Evolution with Interlayer Twist-Angle, *Nader Zaki, P. Yeh, W. Jin, R.M. Osgood, Jr.*, Columbia University

2D atomic layer materials such as graphene and transition-metal dichalcogenides such as MoS_2 have garnered much interest over the last few years due to their surprising electronic properties. For example, graphene possesses an exceptionally high mobility while monolayer MoS_2 possesses a direct bandgap with an exceptionally high light-matter interaction. One of the directions the 2D materials community is now pursuing is one in which these materials are combined together by way of vertical stacking in order to fabricate custom layered structures with potentially rich physics and unique device properties. Naturally, determining the electronic structure of these custom assembled structures is a necessary task to understanding their electronic behavior. While the electronic structure of the constituent materials have already been studied for monolayer form, the electronic structure of the stacked structures has only recently started to be deciphered. This talk will report on the direct determination of the electronic structure of two bilayer systems: twisted bilayer MoS_2 and twisted graphene/MoS_2. Using LEEM, µLEED, and µARPES, the stack quality, stack orientation, and stack electronic structure are directly probed and resolved with few *µm* and higher spatial resolution. To be discussed will be the evolution of the electronic structure with twist angle and its implications on the electronic properties of the respective homo- and hetero-structures.

3:00pm 2D+EM+MG+NS+SS+TF-ThA3 *In Situ* Microscopy on 2D Materials: Heterostructures, Nanostructures, Novel Materials Systems, *Peter Sutter*, University of Nebraska - Lincoln **INVITED**

Two-dimensional (2D) materials, such as graphene, hexagonal boron nitride, and a family of metal dichalcogenides have fascinating properties and show promise for applications. The broad exploration and use of these materials depends on the development of scalable synthesis methods, and of a fundamental understanding of their properties. I will discuss recent advances in understanding the synthesis, processing, and properties of 2D materials derived primarily from in-situ surface imaging.

In-situ microscopy provides the basis for creating complex heterostructures of different 2D materials, such as graphene and hexagonal boron nitride, and for studying atomically precise graphene nanostructures. Real-time imaging yields quantitative information on the growth and processing of new classes of 2D materials, such as metal dichalcogenide semiconductors. Finally, the combination of in-situ microscopy with synchrotron-based spectroscopy represents a unique approach for exploring the electronic band structure of 2D materials.

Our results illustrate that in-situ microscopy can be a powerful tool for realizing and probing the unique characteristics of two-dimensional materials.

4:00pm 2D+EM+MG+NS+SS+TF-ThA6 Direct Growth of Graphene/h-BN(0001) Multilayer Heterostructures for Novel Device Applications, *S. Driver, D. Beatty, B. Olanipekun, S. Reid, Jeffry Kelber*, University of North Texas

We report the direct layer-by-layer growth of h-BN(0001) multilayers on Co(0001) by atomic layer epitaxy (ALE), and the direct growth of graphene multilayers on h-BN(0001) by molecular beam epitaxy (MBE). For the first time, this allows the growth of graphene/BN heterostructures with graphene and BN thicknesses controlled with atomic precision, and with all graphene and BN layers in azimuthal registry. Such control is a prerequisite for many proposed spintronic and electronic applications that emphasize charge or spin transport perpendicularly through the heterojunction. Further, the growth by direct, scalable methods without physical transfer, is essential for industrial development of such devices. h-BN(0001) multilayers have been deposited on Co(0001)/Al_2O_3(0001), using a BCl_3/NH_3 ALE process at 600 K. X-ray photoelectron spectroscopy (XPS) indicates B:N atomic ratios of 1:1 with negligible Cl contamination or reaction with the metallic substrate. Low energy electron diffraction (LEED) data indicate BN domain sizes of ~ 300 A or greater, with the lattice in registry with that of the Co(0001) substrate. LEED data also indicate BN domains larger than those of the Co substrate, suggesting BN overgrowth of Co domain boundaries. The XPS-derived average BN film thickness scales linearly with the number of BCl_3/NH_3 cycles, and the lack of Co oxidation after ambient exposure of a BN bilayer indicates that these films are macroscopically continuous over the 1 cm x 1 cm sample size. Graphene formation on h-BN(0001) was achieved using MBE with a graphite rod source, with deposition carried out at 800 K. LEED data show the expected 6-fold LEED pattern in exact registry with that of the h-BN(0001)/Co(0001) substrate. XPS C 1s spectra indicate a C 1s binding energy near 284.5 eV and with the expected pi-to-pi* transition. A heterojunction consisting of ~ 3 monolayers (ML) graphene/3 ML h-BN on Co(0001) proved stable in vacuum to at least 1000 K, indicating the adaptability of this growth process to a variety of industrial applications. Other recent results indicate the adaptability of this process to other substrates, such as Ru(0001) or $CoSi_2$(111). These developments make possible a variety of spin filters, spin valves, and tunneling transistors proposed on the basis of close BN/graphene lattice matching, but not readily achievable with physically transferred films.

4:20pm 2D+EM+MG+NS+SS+TF-ThA7 Al_2O_3 on Black Phosphorus by Atomic Layer Deposition: An *in situ* Interface S tudy, *Hui Zhu, S. McDonnell, X. Qin, A. Azcatl, L. Cheng, R. Addou, J. Kim*, UT-Dallas, *P.D. Ye*, Purdue University, *R.M. Wallace*, UT-Dallas

Black phosphorus ("black-P") is considered to be an appealing 2D material because of its novel properties and potential application in few-layer transistor structures.[1,2,3] However, a clear challenge in the implementation of black-P is the strong hydrophilic[4] and oxidation[5] reactions during device processing and thereafter. Thus, efficient isolation layers are necessary for black-P to preserve its electronic properties. Al_2O_3[2] or HfO_2[6] dielectric layers deposited by atomic layer deposition (ALD) have been used as isolation layers in recent black-P transistors. In this work, three different samples oxidized by ambient air were investigated to understand the interfacial chemistry, and nucleation of atomic layer deposited Al_2O_3 on black-P using *in situ* X-ray photoelectron spectroscopy (XPS). This work suggests that exposing a sample that is initially free of phosphorus oxide to the ALD precursors does not result in detectable oxidation. However, when

the phosphorus oxide is formed on the surface prior to deposition, the black-P can react with both the surface adventitious oxygen contamination and the H_2O precursor at the deposition temperature of 200 °C. As a result, the concentration of the phosphorus oxide increases after both annealing and the atomic layer deposition process. The nucleation rate of Al_2O_3 on black-P is correlated with the amount of oxygen on samples prior to the deposition. The growth of Al_2O_3 follows a "substrate inhibited growth" behavior where an incubation period is required. *Ex situ* atomic force microscopy is also used to investigate the deposited Al_2O_3 morphologies on black-P where the Al_2O_3 tends to form islands on the exfoliated black-P simples.

Reference:
1 L. Li, Y. Yu, G.J. Ye, Q. Ge, X. Ou, H. Wu, D. Feng, X.H. Chen, and Y. Zhang, Nat. Nanotech. 9, 372 (2014).

2 H. Liu, A.T. Neal, Z. Zhu, Z. Luo, X. Xu, D. Tománek, and P.D. Ye, ACS Nano 8, 4033 (2014).

3 F. Xia, H. Wang, and Y. Jia, Nat. Comm. 5, 4458 (2014).

4 J.D. Wood, S.A. Wells, D. Jariwala, K. Chen, E. Cho, V.K. Sangwan, X. Liu, L.J. Lauhon, T.J. Marks, and M.C. Hersam, Nano Lett. 14, 6964 (2014).

5 A. Favron, E. Gaufrès, F. Fossard, P.L. Lévesque, Anne-Laurence, Phaneuf-L' Heureux, N.Y.-W. Tang, A. Loiseau, R. Leonelli, S. Francoeur, and R. Martel, arXiv:1408.0345 (2014).

6 N. Haratipour, M.C. Robbins, and S.J. Koester, arXiv:1409.8395 2 (2014).

4:40pm **2D+EM+MG+NS+SS+TF-ThA8 Topological Winding Number Change and Broken Inversion Symmetry in a Hofstadter's Butterfly**, *Marc Bockrath*, UC Riverside
Recently several research groups have demonstrated accurate placement of graphene on hexagonal BN (hBN) with crystallographic alignment. Due to the resulting superlattice formed in the graphene/hBN heterostructures, an energy gap, secondary Dirac Points, and Hofstadter quantization in a magnetic field have been observed. Using aligned layer transfer we are able to produce graphene/hBN heterostructures with ~1 degree alignment accuracy, and measure the transport properties of the resulting systems. We observe an additional π Berry's phase shift in the magneto-oscillations when tuning the Fermi level past the secondary Dirac points, originating from a change in topological winding number from odd to even when the Fermi-surface electron orbit begins to enclose the secondary Dirac points. At large hole doping inversion symmetry breaking generates a distinct hexagonal pattern in the longitudinal resistivity versus magnetic field and charge density. This results from a systematic pattern of replica Dirac points and gaps, reflecting the fractal spectrum of the Hofstadter butterfly.

5:00pm **2D+EM+MG+NS+SS+TF-ThA9 Compliant Substrate Epitaxy: Au on MoS$_2$**, *Yuzhi Zhou*, C. Daryl, UC Berkeley
The heteroepitaxial growth of Au on MoS_2, a layered van der Waals bonded dichalcongenide, is analyzed. It is argued that the weak coupling between the layers in the dichalcogenides enables the first substrate layer to deform elastically almost independently from the substrate layers below, and hence enables epitaxial growth for a larger mismatch than might otherwise be expected. Linear, continuum elasticity theory and density functional theory are used to show that a {111} oriented Au film is the preferred over an {001} oriented Au film, despite the fact that the {111} orientation leads to a much higher elastic strain. During the initial stages of growth, the {111} orientation is favored over the {001} orientation due to its lower surface and interfacial energies. As the Au film grows thicker, the elastic relaxation of the first layer of the substrate leads to a reduction in the elastic energy of the growing film. This reduces the elastic energy difference between the {001} and {111} orientations enabling the {111} orientation to remain stable for all film thicknesses. This work is supported by the Director, Office of Science, Office of Basic Energy Sciences, Division of Materials Sciences and Engineering, of the U.S. Department of Energy under Contract No. DE-AC02-05CH11231.

5:20pm **2D+EM+MG+NS+SS+TF-ThA10 Direct Synthesis of 2D van der Waals Heterostructures**, *Judy Cha*, Yale University **INVITED**
Two-dimensional (2D) chalcogenides have gained renewed interest due to their interesting electrical properties such as topological insulator surface states in Bi_2Se_3 and hydrogen evolution catalytic activities in MoS_2. Our ability to thin them down to a single layer and their anisotropic bonding nature opens up possibilities for novel heterostructures where we can tailor their electronic properties. I will present one-step, scalable heterostructure synthesis method to synthesize these chalcogenide nanostructures and examine their electronic transport properties. Intercalation into 2D materials will be considered as a novel way to design 2D heterostructures, in which the optical and electrical properties of the host 2D materials can drastically change. I will also discuss ways to control the alignment of molecular layers in these 2D chalcogenides, which exploits stress and strain built in the film during the growth. Electron tomography will be used to reconstruct the 3D structure of vertically oriented molecular layers in MoS_2 thin films. In the second part of the talk, I will present synthesis and electronic properties of SnTe topological crystalline insulator nanoplates. Although SnTe is cubic and not a layered material, large SnTe nanoplates expanding hundreds of microns in lateral dimension with ~ 100 nm in thickness are possible. I will discuss effects of substrates and growth conditions to promote thin film growth of non-layered materials.

Applied Surface Science
Room: 212D - Session AS+SS-ThA

Advances in 2D Chemical Mapping and Data Analysis
Moderator: Kathryn Lloyd, DuPont Corporate Center for Analytical Sciences, Svitlana Pylypenko, Colorado School of Mines

2:20pm **AS+SS-ThA1 ASSD 30th Anniversary Lecture: Why Do (or Don't) People use Chemical State XPS Imaging?**, *Julia Fulghum*, K. *Artyushkova*, University of New Mexico, A. Barlow, P. Cumpson, Newcastle University, UK **INVITED**
XPS imaging can be used to acquire chemical-state specific information with a spatial resolution of several microns. In response to perceived user interest, instrument manufacturers have put significant resources into developing chemical state XPS imaging and image processing capabilities. Current instrumentation allows for parallel image acquisition over a range of photoelectron energies, resulting in quantitative, lateral surface chemistry determinations. Although publications citing XPS continue to increase, XPS imaging contributes to only a small percentage of published work.

In this talk, we'll present an overview of laboratory XPS imaging capabilities using a variety of examples to demonstrate the practical (and not-so-practical) experiments that are possible. Recent multivariate and multitechnique analysis applications, including Multivariate Auger Feature Imaging (MAFI) and XPS-Raman image correlation will be used to highlight current research utilizing XPS imaging. Results from a survey of instrument manufacturers, directors of XPS user facilities, and expert users will be presented, including speculation as to why the use of XPS imaging has not met expectations, recommendations for using XPS imaging and hopes for future developments.

3:00pm **AS+SS-ThA3 X-ray Photoelectron Spectromicroscopy: Combining Spectral and Spatial Information for Materials Characterization**, *Adam Roberts*, Kratos Analytical Limited, UK, N. *Fairley*, Casa Software Ltd, UK, J.R. Mora, University of Durham, UK
X-ray photoelectron spectroscopy is widely used in determining surface chemistry of materials. Improvements in instrument sensitivity mean that spectra are routinely acquired from areas with diameters in the tens of microns, although most routine analysis is performed at much larger areas. The assumption is that the material and spectra are homogeneous over the area probed is often made although it may not be true. Information of the lateral distribution of elemental and chemical states on a surface can be probed using XPS imaging either at a single binding (kinetic) energy or over a narrow energy range corresponding to a core-level photoemission peak.

Multispectral XPS imaging, also referred to as spectromicroscopy, where a series of images incremented in energy such that each pixel contains a spectrum, is relatively new and under exploited for surface characterisation. An advantage of spectromicroscopy is that spectral information can be reconstructed from defined areas which are smaller than those possible with focused x-ray or virtual probe selected area XPS. This means that the reconstructed spectra are no longer averaged over the total area from which the image is acquired such that both sample and instrument dependent differences can be studied.

The 256 x 256 pixel multi-spectral image contains >65,500 spectra which is ideally suited to multivariate analysis. Development of data processing to support spectromicroscopy data reduction has been necessary and a number of approaches have been successfully applied in the characterisation of model and real-world samples[1-3]. Multivariate analysis can be used to classify regions of interest across the field of view and data can be

partitioned such that chemical state, changes in peak position and background shape can be investigated. Here we detail the use of spectromicroscopy for the characterisation of complex materials including functionalised multiwall carbon nanotubes (MWCNT). This approach has allowed the considerable challenges of surface analysis of such materials to be addressed and has allowed the influence of signal from the substrate material to be removed from the MWCNT of interest.

References

[1] E.F. Smith, D. Briggs and N. Fairley Surf. Interface Anal. 2005, **38**, 69-75

[2] J. Walton, N. Fairley Surf. Interface Anal. 2008, **40**, 478 - 481

[3] A.J. Barlow, O. Scott, N. Sano and P.J. Cumpson Surf. Interface Anal. 2015, **47**, 173-175

3:20pm AS+SS-ThA4 Optimizing XPS Imaging Acquisition, *Jon Treacy*, C. Deeks, P. Mack, T.S. Nunney, Thermo Fisher Scientific, UK

Surface structure and chemistry are properties that are crucial to the successful production and operation of numerous devices, materials and coatings. X-ray photoelectron spectroscopy (XPS) is an ideal tool for investigating these properties due to its inherent surface sensitivity, and ability to quantify the chemical states detected.

Whilst XPS is most often used for point analysis and/or depth profiling, it is also able to produce compositional maps of multi-phase materials. This is of particular use in scenarios where other surface science techniques are unsuitable, for example especially rough surfaces that cannot be imaged using SPM or surfaces with multiple phases of similar elemental composition, which cannot be differentiated by SEM-EDS. However the widespread implementation of XPS as a mapping tool has been hindered by the long acquisition times required.

Here we shall present the effects of increased x-ray performance, increased spectrometer sensitivity and modifications in data processing, i.e. both instrumental and software improvements, on the required acquisition time for XPS mapping. This is demonstrated using data from several samples, where multi-phase maps were acquired up to an order of magnitude more quickly than previously possible through implementation of these improvements.

4:00pm AS+SS-ThA6 Enhancing Chemical Contrast: Latest Trends in Hyperspectral Image Analysis, *Barry Wise*, W. Windig, Eigenvector Research, Inc. **INVITED**

Many analytical techniques that were originally developed as single sample methods have been adapted to produce multivariate aka hyperspectral images where each pixel contains an entire spectrum. These imaging techniques are used to produce "chemical maps" which elucidate the arrangement and chemical makeup of areas on the surface. Imaging techniques produce an avalanche of data which is often underutilized. Multivariate statistical methods are increasingly being used to capture the information in these large data sets, condense it down to a manageable level, and improve the signal to noise ratio. This serves to enhance the chemical contrast in the images. This talk surveys methods for hyperspectral image analysis, discusses their pros and cons, and gives some examples demonstrating what can be accomplished. Methods considered include Principal Components Analysis (PCA), Multivariate Curve Resolution (MCR) with contrast constraints, Independent Components Analysis (ICA), Maximal Autocorrelation Factors (MAF) and sample clustering techniques.

4:40pm AS+SS-ThA8 Unambiguous Molecular Identification with TOF-SIMS Imaging MS/MS, *G.L. Fisher, J.S. Hammond,* Physical Electronics USA, *R.M.A. Heeren,* Maastricht University, The Netherlands, *Scott Bryan*, Physical Electronics USA

First results from a new tandem imaging mass spectrometer will be presented. The unique TOF-TOF design allows the simultaneous collection of standard TOF-SIMS spectra *and* collision induced dissociation (CID) spectra of specifically selected precursors [1]. This new analytical capability maximizes the information content from a single acquisition and provides all data from the same analytical volume. The ability to acquire MS/MS data at the same primary ion beam repetition rate as used in conventional TOF-SIMS allows high speed image acquisition. The ability to unambiguously identify and image peaks above m/z 200 was applied to polymer additives and to the study of lipid composition changes in mouse spleen specimens infected with *F. novicida*.

[1] P.E. Larson, J.S. Hammond, R.M.A. Heeren and G.L. Fisher, Method and Apparatus to Provide Parallel Acquisition of MS/MS Data, U.S. Patent 20150090874, 02 April 2015.

5:00pm AS+SS-ThA9 Utilizing Chemical State Mapping to Reveal Spatially Distributed Dynamics in Model Nanostructured Battery Electrodes, *Alexander Pearse**, *E. Gillette, S.B. Lee, G.W. Rubloff*, University of Maryland, College Park

The rate at which a battery can deliver energy is ultimately dominated by the ability or inability to effectively transport both ions and electrons throughout the electrodes. When charge transport is a limiting factor, material utilization within the battery becomes spatially inhomogeneous, reducing performance. Additionally, the material and architectural requirements for optimizing transport for both ions and electrons are not always synergistic, which can lead to design challenges. The effects of architecture on device performance are generally characterized by externally measured scalar quantities, such as cell potential or current, but these quantities do not reveal where within the electrode any problem may lie. There is a growing need to develop models which can accurately predict spatially resolved dynamics within battery electrodes, as well as experimental techniques to verify them, particularly as nanoscience produces more and more sophisticated electrode designs.

Here we show that chemical state mapping with X-ray photoelectron spectroscopy (XPS) is a powerful tool for revealing transport-limit-induced dynamics within battery electrodes, and connect surface science with electrochemical modeling. We examine the specific problem of facile ion transport but limited electronic transport, which often occurs in high aspect ratio electrodes made of low conductivity semiconductors or insulators. While characterizing complex structures using XPS is normally very challenging, it is possible to gain much more useful and accurate information when a model device is designed from the ground up to exploit the strengths of XPS. By fabricating battery chips in which the anticipated gradients of material utilization (i.e. the spatially varying amount of lithium intercalated) are laid out laterally on a flat substrate, we can clearly map chemical changes in the electrode as a function of distance from a current collector. By using transition metal oxide (M_xO_y) cathode materials, we are able to track the state of charge through local quantification of the reaction $M^{n+} + e^- \to M^{(n-1)+}$. Our data clearly reveal that as the applied current density increases, ion insertion activity is dramatically contracted towards the current collector, which leads to performance limitations at high rates. Importantly, we also use our spatially resolved data to validate the predictions of a sophisticated finite element multiphysics battery model. The visualization and understanding of design induced performance limits, as well as the validation of a predictive model, allow us to optimize the design of future high performance nanostructured battery electrodes.

5:20pm AS+SS-ThA10 Microstructural and Chemical Mapping of Discharged Hybrid CF$_x$–SVO Cathodes from Primary Li Batteries, *D. Reifsnyder Hickey,* University of Minnesota, *Jeffrey Fenton*, K. Chen, P. Yurek, J. Lesser, G. Jain, Medtronic plc

Primary lithium batteries with hybrid carbon monofluoride–silver vanadium oxide (CFx–SVO) cathodes have become widely commercialized as power sources in implantable medical devices. Although CFx and SVO have been used separately as cathode materials, CFx–SVO hybrid cathodes have been developed to meet the increased energy-density, power, and longevity requirements specific to multiyear operation at physiological temperature. However, the microstructural basis for the performance characteristics has not been well understood, including chemical changes in the cathode materials as they discharge. This work presents a microstructural study of discharged cathode materials, aimed at identifying chemical and structural characteristics that can be related to the observed battery-performance characteristics. As a result, the relationships established can be used to improve the performance of future medical device technologies. Scanning electron microscopy with energy dispersive spectroscopy, X-ray photoelectron spectroscopy, and X-ray diffraction were used to probe the cathodes chemistry and structure. Although a single analytical method cannot give a full picture of the cathode chemistry and microstructure, the combination of these complementary techniques makes it possible to develop a clearer picture of the structural and chemical changes that occur within the cathode as the battery discharges. The discharged cathodes of SVO, CFx, and SVO-CFx hybrid are compared, which demonstrates that the relatively gradual transformation of SVO that occurs in SVO-only cathodes is accelerated in the hybrid cathodes. Several trends will be shown including: (1) SVO loses its crystalline structure and silver content (replaced by lithium) with discharge; (2) CFx converts into carbon and LiF with discharge; (3) and the hybrid cathodes show steady conversion of CFx, accelerated conversion of SVO (as soon as 5% depth of dischage), and the beginning of LiF formation (as early as 10% depth of discharge).

---

* ASSD Student Award Finalist

5:40pm AS+SS-ThA11 A Novel Test Sample for the Spatially Resolved Quantification of Illicit Drugs on Fingerprints using Imaging Mass Spectrometry, *Shin Muramoto*, *T.P. Forbes*, NIST, *A.C. van Asten*, Netherlands Forensic Institute, *G. Gillen*, NIST

A novel test sample for the spatially resolved quantification of illicit drugs on the surface of a fingerprint using time-of-flight secondary ion mass spectrometry (ToF-SIMS) and desorption electrospray ionization mass spectrometry (DESI-MS) was demonstrated. Calibration curves relating the signal intensity to the amount of drug deposited on the surface was generated from inkjet-printed arrays of cocaine, methamphetamine, and heroin with a deposited-mass ranging nominally from 10 pg to 50 ng per spot. These curves were used to construct concentration maps that visualized the spatial distribution of the drugs on top of a fingerprint, as well as being able to quantify the amount of drugs in a given area within the map. For the drugs on the fingerprint on silicon, ToF-SIMS showed great success as it was able to generate concentration maps of all three drugs. On the fingerprint on paper, only the concentration map of cocaine could be constructed using ToF-SIMS and DESI-MS as the signals of methamphetamine and heroin were completely suppressed by matrix and substrate effects. Spatially resolved quantification of illicit drugs using imaging mass spectrometry is possible, but the choice of substrates could significantly affect the results.

Scanning Probe Microscopy Focus Topic
Room: 212A - Session SP+BI+NS+SS+TF-ThA

Probing Material Growth on the Surface
Moderator: Chuanxu Ma, Oak Ridge National Laboratory

2:20pm SP+BI+NS+SS+TF-ThA1 Tailoring the Growth of Organic Thin Films via Chemical Reactions at the Molecular Scale, *Pengpeng Zhang*, Michigan State University **INVITED**

Control of highly ordered organic molecular thin films with extended π systems is currently of intense interest for integrating molecules into modern electronics due to their tunable nature. Selection of molecules and substrates can lead to desired transport properties such as charge transfer, charge injection, exciton diffusion, etc., at the heterointerface, which is crucial to the development of organic and molecular electronics. However, achieving large-scale molecular ordering remains a significant challenge that requires a thorough understanding of the growth mechanism. I will discuss our recent discovery of the anisotropic crystalline step-flow growth of the prototypical metal phthalocyanine molecules on the deactivated Si(111)-B surface. I will then address the growth mechanism and show that the molecular ordering and molecular orientation can be effectively controlled through selective orbital coupling between the molecule and substrate. Finally, I will illustrate an abnormal temperature dependent growth evolution and discuss the associated mechanism.

This research is funded by the U.S. Department of Energy (DOE) Office of Science Early Career Research Program (DE-SC0006400) through the Office of Basic Energy Sciences.

3:00pm SP+BI+NS+SS+TF-ThA3 Investigation of Initial Stages of Oxidation of Ni-Cr and Ni-Cr-Mo alloys by Scanning Tunneling Microscopy and Spectroscopy, *Gopalakrishnan Ramalingam**, *P. Reinke*, University of Virginia

Ni-Cr alloys are excellent candidates for use in highly corrosive environments due to the formation of a protective Cr_2O_3 layer. Molybdenum is a common alloying addition as it improves the resistance to localized corrosion and prevents the breakdown of the oxide layer. While the effect of Mo addition on corrosion resistance is well known, the underlying mechanisms at the atomic scale and the role of electronic structure changes due to Mo addition are poorly understood. In the current work, we have used STM/STS to investigate the initial stages of oxidation of Ni, Cr and Ni-Cr (10-25wt.% Cr) alloy thin films and subsequently, the effect of Mo addition (2-10 wt.%) on the oxidation behavior. The alloy thin films are grown on MgO(001) substrates using two recipes that yielded smooth films: (a) deposition at 100 °C and subsequent anneal at 300 °C for 2 hours, and (b) deposition at 400 °C with no post-growth annealing. While recipe (a) yielded smooth Ni films, co-deposition of Ni and Cr resulted in the formation of secondary Ni_2Cr phases. Alloy films grown using recipe (b) did not result in secondary phases and are optimal for oxidation studies of alloy films. STM/STS data of the oxidation (30 L of O_2) of a pure Ni thin film at 200 °C reveal preferential oxidation of some terraces compared to others and indicates a dependence of oxidation rate on the crystallographic

orientation of the terrace. dI/dV maps of a Cr surface after 10 L oxidation at 200 °C shows the presence of a bandgap (1.32 eV) throughout the surface and indicates the growth of a uniform oxide layer. In the case of Ni-13wt.%Cr binary alloy, a 25 L exposure (at 1×10^{-8} mbar) at 300 °C results in a complete loss of step structure with a fully formed oxide layer as shown by STS spectra. A bandgap of 1.42 eV is observed throughout the surface and this value is less than the bulk bandgap of all possible oxide species (NiO, Cr_2O_3 or mixed). We will present the results of the initial stages of oxidation (<3 L) of the pure Ni thin films and discuss the differences in the oxidation processes due to the addition of 8-25 wt.% Cr. The progression from chemisorption regime (at low temperatures) to the oxide nucleation regime will be shown for different alloys by performing room temperature O_2 exposures and post-exposure annealing cycles and the effect of alloying additions on this transition will be discussed. Preliminary data on the changes in the atomic and electronic structure of the thin film and oxidation behavior due to the addition of Mo will be presented.

4:00pm SP+BI+NS+SS+TF-ThA6 Growth and Properties of Skyrmionic Nanowires and Thin Film, *Zheng Gai*, Oak Ridge National Laboratory, *J. Yi, S. Tang,* University of Tennessee, Oak Ridge National Laboratory, *D. Mandrus*, University of Tennessee **INVITED**

Magnetic skyrmion lattice, a vortex-like spin texture recently observed in chiral magnets, is of great interest to future spin-electronic data storage and other information technology applications. The combined effect of a large ferromagnetic exchange and a weak DM interaction is to twist the magnetization into a long-period spiral that can be tens to hundreds of nanometers in length. As these spirals are only weakly bound to the underlying lattice in cubic systems, they can be readily manipulated with modest applied fields. The skyrmion lattice in MnSi appears in a small region (known as the A phase) of the H-T phase diagram in bulk samples, but in 2D samples like thin films the skyrmion phase is much more robust. If skyrmion ordering can persist in one-dimensional MnSi nanowires and 2D films, then these systems are very promising for spintronics applications as the magnetic domains and individual skymions could be manipulated with small currents. We have systematically explored the synthesis of single crystal MnSi nanowires via controlled oxide-assisted chemical vapor deposition and observed a characteristic signature of skyrmion magnetic ordering in MnSi nanowires. The SiO_2 layer plays a key role for the high yield, correct stoichiometric and crystalline growth of the B20 MnSi nanowires. A growth phase diagram was constructed. For the thin films, an unique growth receipt was developed for the growth of high quality of thin films. The structure and magnetic properties of the films at different thickness were studied.

4:40pm SP+BI+NS+SS+TF-ThA8 Sulfur-induced Structural Motifs on Cu(111) and Au(111) Surfaces, *Holly Walen‡‡‡*, Iowa State University, *D.-J. Liu*, Ames Laboratory, *J. Oh, H. Lim*, RIKEN, Japan, *J.W. Evans*, Iowa State University, *C.M. Aikens*, Kansas State University, *Y. Kim*, RIKEN, Japan, *P.A. Thiel*, Iowa State University

The interaction of sulfur with copper and gold surfaces plays a fundamental role in important phenomena that include coarsening of surface nanostructures, and self-assembly of alkanethiols. Here, we identify and analyze unique sulfur-induced structural motifs observed on the (111) surfaces of these two metals. We choose very specific conditions: very low temperature (5 K), and very low sulfur coverage ($\leq$ 0.05 monolayers, ML). In this region of temperature-coverage space, which has not been examined previously for these adsorbate-metal systems, the effects of individual interactions between metals and sulfur are most apparent and can be assessed extensively with the aid of theory and modeling. Furthermore, at this temperature diffusion is minimal and relatively-mobile species can be isolated. The primary technique is scanning tunneling microscopy (STM).

On Cu(111), at 0.004 ML S, we find unexpected heart-shaped Cu_2S_3 complexes on the terraces, made up of intersecting linear S-Cu-S units. With supporting density functional theory (DFT) and reaction-diffusion equation analysis, we propose that these hearts are a viable candidate for S-enhanced mass transport of Cu on Cu(111) at higher temperature. As S coverage increases (up to 0.05 ML), a diverse group of Cu-S structures develops which includes concatenated hearts, and eventually the known ($\sqrt{43}$ x $\sqrt{43}$)R±7.5° reconstruction[1-2]. Analysis of the step edges of Cu(111) indicates that S decorates the step edges preferentially (relative to the terraces) and that the complexes observed on terraces originate at the step edges.

In contrast, no metal-sulfur complexes are observed on Au(111) under similar conditions (0.03 ML). Instead, we observe striking $\sqrt{3}$R30° rows made up of S adatoms. Using DFT and *ab-initio* Monte Carlo analysis, we construct and test a lattice gas model. This analysis shows that these short rows of S adatoms form because of a complex set of through-metal interactions: a linear three-body attraction, as well as long-range pairwise interactions (up to 5a) between S atoms.

---

* **Morton S. Traum Award Finalist**

These experimental observations for Cu(111) and Au(111) surfaces—made under essentially-identical conditions—together with extensive DFT analyses, allow comparisons and insights into factors that favor the existence of metal-sulfur complexes, vs. chemisorbed atomic sulfur, on metal terraces.

[1] E. Wahlström, I. Ekvall, H. Olin, S. A. Lindgren, and L. Wallden, Phys. Rev. B **60** 10699 (1999).

[2] E. Wahlström, I. Ekvall, T. Kihlgren, H. Olin, S. A. Lindgren, and L. Wallden, Phys. Rev. B **64** 155406 (2001).

5:00pm SP+BI+NS+SS+TF-ThA9 Surface Strain-Modulated Binding of Adsorbates on TiO$_2$(110), *D.V. Potapenko, Richard Osgood, Jr.*, Columbia University

Mechanical elastic strain is commonly present in nanostructured materials and it has been found to change chemical and electronic properties in a broad range of solids. Systematic study of reactivity-strain relationship on surfaces is difficult because of the fact that only very low values of strain (~0.1%) are achievable through mechanical deformation of macroscopic samples. We have developed a method of preparation of nano-scale strain fields on TiO$_2$ rutile(110) surface by low energy (1keV) Ar ion bombardments combined with specific thermal treatment. Titanium oxide is a brittle material regarded as a prototypical photocatalyst with numerous applications in the areas of solar energy utilization. Subsurface Ar clusters, which are formed through our preparation procedure, cause 5 – 25 nm wide surface deformations with the tensile strain values as high as 4 %. Surface distributions of various molecular and atomic adsorbates on TiO$_2$(110) have been studied with atomically resolved STM imaging. Our results indicate significant strain-related variations in the surface binding properties. In this presentation we will concentrate on surface hydroxyl groups (OH) as a mobile adsorbate. We derive the O-H binding energy from the statistical analysis of the adsorbate distribution. Then we demonstrate a roughly linear relationship between the values of surface strain and the O-H binding energy.

5:20pm SP+BI+NS+SS+TF-ThA10 STM/STS Investigation of Organic Charge Transfer Complex TTF-TCNQ on Noble Metal Surfaces at 4.3K, *Seokmin Jeon, P. Doak, P. Ganesh, B. Sumpter*, Oak Ridge National Laboratory, *J.I. Cerda*, Instituto de Ciencia de Materiales de Madrid, Spain, *P. Maksymovych*, Oak Ridge National Laboratory

TTF-TCNQ (TTF = tetrathiafulvalene; TCNQ = 7,7,8,8-tetracyanoquinodimethane) is a prototypical organic charge-transfer complex providing with a metallic conductivity (up to 900 ohm-1cm-1 at 300K). It also represents a broad class of organic electronic compounds that exhibit strong electron correlations and a rich gamut of phase transitions involving charge ordering, Mott and Peierls metal-insulator transitions and superconductivity, etc. Despite decades of research in this area, quantitative understanding of this compound is still elusive and their low-dimensional form is barely explored. We investigated ultrathin films of TTF-TCNQ on silver surfaces using scanning tunneling microscopy/spectroscopy (STM/STS) at 4.3 K. TTF-TCNQ forms self-assembled molecular lattices on noble metal surfaces with a few different TTF-to-TCNQ ratios depending on evaporation condition. Among them the islands with 1 to 1 stoichiometric ratio are found ubiquitously in less dependent on the evaporation condition. Structures of the monolayer islands are elucidated from sub-molecular resolution STM topography images. Single-point conductivity spectroscopy and conductivity mapping elucidate new electronic states which do not stem from their molecular orbital states are spatially located in the void areas of the TTF-TCNQ molecular lattices. We propose the *sp*-derived metal surface states are confined in the molecular lattices. Due to small periodicity of the lattice, the band minimum of the *sp*-derived metal surface states is shifted by as much as 1eV. This shift is much more significant than the ones normally observed in organic self-assemblies. As a result, we can also infer the height of the potential barrier within a 1D potential well model, which in turn is directly related to strong molecular dipole associated with large charge transfer and bent molecular geometry due to metal-molecule interactions.

Surface Science
Room: 113 - Session SS+AS+EM+EN-ThA

Atomistic Modeling of Surface Phenomena & Semiconductor Surfaces and Interfaces - II
Moderator: Talat Rahman, University of Central Florida

2:20pm SS+AS+EM+EN-ThA1 Ideas Old and New Applied to Non-Ideal Surface Adsorption and Reaction, *William Schneider*, University of Notre Dame **INVITED**

Free energies of adsorption are arguably the most elementary quantities in heterogeneous catalysis. These free energies depend on the surface and adsorbate (reactant, intermediate, or product) of interest, system temperature and adsorbate coverage. The free energy represents a balance between the energetic driving force for creating bonds between an adsorbate and a surface and the entropic cost of moving an adsorbate from a fluid phase to a surface. Standard density functional theory (DFT) approaches generally begin by optimizing the location of an adsorbate on a surface, computing a binding energy, and approximating the internal, translational, and configurational contributions to the free energy. In this work we examine the reliability of standard approximations and describe easily applied improvements that give reliable free energy estimates. We describe applications to adsorption at metal surfaces and in the pores of zeolites.

3:00pm SS+AS+EM+EN-ThA3 Insights into the Oxidation of Stepped Cu Surfaces using Multiscale Investigations, *Q. Zhu, W.A. Saidi, Judith Yang*, University of Pittsburgh

Surface defects can induce non-canonical oxidation channels on metal surfaces that may lead to the formation of novel nanostructures. Recently, in situ environmental transmission electron microscopy (ETEM) experiments showed that the oxidation of stepped Cu surfaces promotes the formation of a flat metal-oxide interface through Cu adatoms detachment from steps and diffusion across the terraces. To bridge the gap between experiments and theory, we are investigating Cu oxidation using a multiscale computational approach. Our previous MD simulations based on a reactive force field (ReaxFF) demonstrated that the oxidation of stepped Cu(100) takes place on the upper terrace at a faster rate than the lower terrace due to a preferable oxygen diffusion from the lower to upper terraces. We have extended this study using first-principles density functional theory (DFT) and kinetic Monte Carlo (KMC), and performed a systematic study of all stepped Cu surfaces with a low Miller index. The DFT results show that the oxygen diffusion trend varies with the surface type, where in most cases the oxygen ascending diffusion is more favored. This result is confirmed also with ReaxFF MD and KMC simulations. The MD simulations, with a fine-tuned ReaxFF force field parametrization, have also indicated that oxygen adatoms on the upper terrace can enhance the interlayer Cu atom mass transport. These theoretical simulations provide essential fundamental understanding of the experimentally observed smoothing of the Cu surface during in situ oxidation.

3:20pm SS+AS+EM+EN-ThA4 Reconciling Complimentary Analyses of Epitaxial Growth: Role of Transient Mobility for para-Hexaphenyl on Mica, *Josue Morales-Cifuentes, T.L. Einstein,* University of Maryland, College Park, *A. Pimpinelli*, Rice University

In studies of epitaxial growth, a major goal is to assess the size of the smallest stable cluster (with *i + 1* monomers, where *i* is the critical nucleus size). This is accomplished by analyzing either the capture zone distribution (CZD), the scaling of incident flux *F* to the density of stable islands *N* or the island-size distribution (ISD). For CZD, generalized Wigner distributions (GWD) have proven useful, [1,2] with successful applications to, non-comprehensively: polar-conjugated molecule Alq$_3$ on passivated Si(100), self-assembled Ge/Si(001) nanoislands and para-Hexaphenyl (6P) films on amorphous mica. [3] We concentrate on the last, for which the Winkler group found that $i \approx 3$.

Scaling of *N* usually follows $N \propto F^\alpha$, where α is the growth exponent. For 6P films, a difference in scaling behaviors at small and large *F* is attributed to DLA and ALA dynamics (i.e. $i = 5 \pm 2$, and $i = 7 \pm 2$, respectively). [4] This discrepancy motivates our current work, where transient mobility effects modify scaling non-trivially. [5]

Consider that monomers begin in a (ballistic) hot precursor state before thermalizing (random walk). The competing times of ballistic monomers becoming thermalized vs. being captured by an island naturally define a "thermalization" scale for the system. We obtain an analytic solution and elaborate on the physical meaning behind the energies and dimensionless parameters used. Novel scaling regimes are retrieved for which power-law scaling applies, with non-monotonic crossovers between them and the growth exponent exclusively dependent on *i*. Applying the model to the 6P

films results in good agreement for the scaling and the activation energies: experimental values of the activation energies of 0.26eV (high-T) and 0.04eV (low-T) match model predictions of 0.3eV (high-T) and 0.04eV (low-T). Furthermore, the high-flux regime is interpreted not as ALA (attachment-limited aggregation) or HMA (hot monomer aggregation) but rather as an intermediate scaling regime related to DLA (diffusion-limited aggregation). Lastly, we discuss a simplifying approximation for the model and connections to some capture zone distribution considerations of α. [6]

[1] T.L. Einstein, A. Pimpinelli, D. González, J. Cryst. Growth 401, 67 (2014)

[2] T.L. Einstein, A. Pimpinelli, D. González, and J. R. Morales-Cifuentes, Proc. CCP2014, J. Phys.: Conf. Series (2015), in press.

[3] T. Potocar, G. Lorbek, D. Nabok et al. 2011 Phys. Rev. B 83 075423

[4] L. Tumbek & A. Winkler, Surf. Sci. 606, L55 (2012)

[5] J. R. Morales-Cifuentes, T. L. Einstein, and A. Pimpinelli. Phys. Rev. Lett. 113, 246101(2014)

[6] J. R. Morales-Cifuentes, T. L. Einstein, and A. Pimpinelli (in preparation)

4:00pm SS+AS+EM+EN-ThA6 Probing 2-DEG at InN Surface by Electrolyte-Gated Raman Spectroscopy, *E. Alarcon Llado,* Ecole Polytechnique Fédérale de Lausanne (EPFL), Switzerland, *Tommaso Brazzini,* Lawrence Berkeley Lab, University of California, Berkeley, *J.W. Ager*, Lawrence Berkeley National Laboratory (LBNL)

Indium nitride has attracted much attention as its narrow bandgap (~0.67eV) expands the range of the direct gaps of the group III-N alloys into the visible and near-IR and thus offers an outstanding potential for solar energy conversion and optoelectronic applications. However, experimental demonstration of high efficiency In-rich III-V pn rectification junctions has been hampered by the existence of an intrinsic interface electron accumulation layer, which seems to persist regardless of surface treatment. The large capacitance of the Helmholtz double layer that forms on a surface of an object in contact with an electrolyte allows the 2-DEG at the surface of InN to be tuned and even depleted. Using this effect, we demonstrated the first pn rectification behavior in InN.[1]

In addition, the 2-DEG accumulation layer affects not only the electrical properties, but also has brought many controversies in the interpretation of optical experiments. Raman spectroscopy probes not only the lattice dynamics in a crystal, but also the electronic structure and free carriers. In particular, the interaction between the free electrons at the surface and the longitudinal optical (LO) phonon in InN has been addressed by several studies. However some questions still remain.

In this work, we present an in-situ micro-Raman study that confirms the presence of a surface related Raman mode in InN and shows its interaction with accumulated electrons at the surface. Electrolyte gated Raman spectroscopy (EGRS) on InN layers was performed in order to modulate and in-situ probe the surface electron accumulation region in InN. A reversible shift of the LO phonon with the applied gate potential is found (see figure 1). The peak position and shift depends on the probing light energy, however it is independent of bulk doping. We explain these findings by Martin's double scattering mechanism and bandgap narrowing at the surface tuned by the gate voltage. InN nanocolumns were also investigated by EGRS. The LO mode lies at higher frequencies in all nanocolumn samples. This fact corroborates the nature of the scattering mechanism, which is strongly dependent on the surface orientation. In summary, our results clearly demonstrate the surface origin of this feature and allow the fundamental study and understanding of the electronic structure of InN.

1.Alarcón-Lladó, E. et al. PN junction rectification in electrolyte gated Mg-doped InN. Appl. Phys. Lett. 99, 102106 (2011).

4:20pm SS+AS+EM+EN-ThA7 Surface Termination of Single Crystal Bi₂Se₃ Investigated by Low Energy Ion Scattering, *Weimin Zhou, J.A. Yarmoff*, UC Riverside

Bismuth Selenide (Bi$_2$Se$_3$) is a prototypical topological insulator (TI) with a two-dimensional layered structure that enables clean and well-ordered surfaces to be prepared by cleaving. Although some surface structure studies have concluded that the cleaved surface is terminated with Se, as is expected from the bulk crystal structure, there are other reports that show either a Bi- or mixed-termination [1]. Low Energy Ion Scattering (LEIS) and low energy electron diffraction (LEED) are used here to compare surfaces prepared by *ex-situ* cleaving, *in-situ* cleaving and Ar$^+$ ion bombardment and annealing (IBA) in ultra-high vacuum. Surfaces prepared by *in-situ* cleaving always have a sharp 1x1 LEED patterns and are Se-terminated. Surfaces prepared by IBA show a transition from Bi- to Se-termination with increasing annealing temperature. Samples inserted into the vacuum chamber following *ex-situ* cleaving have much dimmer LEED patterns, show surface contamination with Auger electron spectroscopy, and

could be terminated either with Se or Bi. The angular dependence of LEIS spectra, which is sensitive to the surface atomic structure, doesn't indicate any substantial differences between surfaces prepared by IBA or *in-situ* cleaving. Ion scattering simulations using Kalypso are compared to experimental angular data to obtain more details about the structure. Exposure of clean surfaces to gaseous species will also be discussed in an effort to determine the surface chemical reactions responsible for the termination change.

[1] X. He, W. Zhou, Z. Y. Wang, Y.N. Zhang, J. Shi, R.Q. Wu and J.A. Yarmoff, Phys. Rev. Lett. **110**, 156101 (2013).

4:40pm SS+AS+EM+EN-ThA8 Real-Time Imaging with Atomic-level Spatial Resolution of Silicon Oxidation, *Bryan Wiggins, L.G. Avila-Bront, R. Edel, S.J. Sibener*, University of Chicago

The investigation of the initial stages of molecular oxygen adsorption on Si(111)-7x7 with real-time and real-space visualization will be discussed in this presentation. We will present the first results from a newly built supersonic molecular beam paired with a scanning probe microscope instrument. The system is designed with an oil free differentially pumped supersonic beam and has a custom scanning probe microscope with the surface plane normal to the beam. This geometric arrangement allows us to perform real-time and real-space *in-situ* experiments. This study consists of exploring the potential energy surface for molecular oxygen adsorption on Si(111)-7x7. The questions that are being addressed are fundamental for issues relating to semiconductor oxidation as well as being of direct relevance to semiconductor processing. The site-specific locations of molecular oxygen reactivity on Si(111)-7x7 surfaces are not clear and remains a topic of current discussion. Recent spectroscopic studies show that by controlling the molecular beam energy (E_k) one can activate different adsorption pathways for molecules on surfaces. However, the effect of collimated and energy-selected beams impacting the surface at different incident angles has not been observed *in-situ* at the local molecular level until now. We will show high-resolution spatial images of the initial stages of oxygen adsorption on Si(111)-7x7 at different beam energies. The comparison of Si(111)-7x7 oxidation *via* thermal oxygen versus the specific adsorption sites that arise at different beam energies will also be discussed. The results indicate that using supersonic beams in this matter may provide enhanced control of semiconductor oxidation chemistry.

5:00pm SS+AS+EM+EN-ThA9 Surface Band-Bending Upon Oxidation of Wurtzite and Zincblende InAs Depending on Surface Orientation and atomic Structure, *Rainer Timm, M. Hjort, J. Knutsson, O. Persson, A. Troian, S. Lehmann, K.A. Dick, A. Mikkelsen*, Lund University, Sweden

InAs is known to typically show n-type behavior with an electron accumulation layer at the surface. Many studies have been performed for evaluating to which extend this behavior is due to adsorbates such as a native oxide layer, or to specific surface orientations and reconstructions of clean InAs. InAs nanowires (NWs) add an extra degree of complexity, since they can exist both in zincblende and wurtzite crystal structure, typically exhibiting unintended switching between both stacking orders during epitaxial growth. During recent years, a strong debate has been going on about how far such crystal phase mixing influences the conductivity of InAs NWs and therewith their suitability for high-mobility device application [1]. A staggered band alignment with band offsets in the range of up to 0.1 eV between zincblende and wurtzite conduction band edges has been reported, based on transport measurements in ambient atmosphere [2]. In contrast, our recent study of clean and unreconstructed InAs NW surfaces based on scanning tunneling microscopy and spectroscopy (STM/S) in ultrahigh vacuum showed aligned conduction band edges for zincblende [110[and wurtzite [11-20[surfaces [3].

Here, we present a systematic study of surface band-bending upon cleaning and oxidation of various InAs surfaces, including purely zincblende or purely wurtzite NWs, obtained by synchrotron-based X-ray photoemission spectroscopy (XPS). We were able to clean all investigated InAs surfaces from their native oxide by annealing them in the presence of atomic hydrogen [3]. Different rates of cleaning and re-oxidation were observed for the different surfaces. Even more importantly, from the energy shifts of the investigated core-levels upon oxidation, varying between 0.1 and 0.3 eV for various surfaces, we obtained significant differences in oxide-induced surface band-bending for different surface orientations. We will compare our XPS results with the atomic and local electronic structure of the specific surfaces as obtained by STM/S [4]. Our results indicate that the band alignment along InAs heterostructures, and therewith the transport properties of InAs NWs, depend on the surface orientation, composition, and atomic structure rather than the crystal phase of the specific InAs segments.

[1] Thelander *et al.*, Nano Lett. **11**, 2424 (2011)

[2] Dayeh *et al.*, Adv. Funct. Mater. **19**, 2102 (2009)

[3] Hjort *et al.,* ACS Nano **12**, 12346 (2014)

[4] Knutsson *et al.*, ACS Appl. Mater. Interfaces **7**, 5748 (2015)

5:20pm SS+AS+EM+EN-ThA10 Control of Oxygen Defect Surface Injection in ZnO via Sub-Monolayer Sulfur Adsorption, *Ming Li*, *E. Seebauer*, University of Illinois at Urbana-Champaign

Native oxygen defects within metal oxide semiconductors such as ZnO affect the material's performance in applications for photovoltaics, nanoelectronics, gas sensing, and photocatalysis. Previous work in this laboratory has shown that the semiconducting metal oxides surfaces can be used to manipulate the concentrations and spatial distributions of bulk oxygen defects, particularly oxygen vacancies. The interaction chemistry between bulk point defects and reactive sites on semiconductor surfaces is comparable in richness to the reactions of surfaces with gases. The present work discusses a novel mechanism of controlling oxygen defect injection in c-plane ZnO(0001) through surface active sites blocking with sub-monolayer sulfur adsorption. Oxygen diffusion rates were measured by exposing single-crystal ZnO to isotopically labeled oxygen ($^{18}O_2$) gas. Sulfur was deposited controllably via an electrochemical cell and characterized *in situ* by Auger Electron Spectroscopy (AES). The resulting diffusion profiles were measured by secondary ion mass spectrometry (SIMS). Kinetic parameters were extracted by fitting the diffusion profiles with a previously derived mass transport model. The preliminary data shows that sulfur adsorption decreases the oxygen defect injection rate by roughly three times through affecting the injection flux, which points to a site blocking model. Subsequent temperature and pressure dependence study will help us gain insights into detailed injection kinetic pathways.

5:40pm SS+AS+EM+EN-ThA11 Investigation of the Role of Electronic Defects and Grain Boundaries in Sputter Deposited CdS/CdTe Junctions and Solar Cells, *Mohit Tuteja*, University of Illinois at Urbana Champaign, *P. Koirala*, University of Toledo, *J. Soares*, University of Illinois at Urbana Champaign, *R. Collins*, University of Toledo, *A. Rockett*, University of Illinois at Urbana Champaign

Device quality CdS/CdTe heterostructures and completed solar cells (~12% efficient) have been studied using low-temperature photoluminescence (PL) as a function of temperature (82-295 K) and laser excitation power (0.02-2 mW). The CdS/CdTe junctions were grown on transparent conducting oxide covered soda lime glass using rf-sputter deposition. It was found that the luminescence shifts from being dominated by sub-gap defect-mediated emission at lower excitation powers to near band edge excitonic emission at higher excitation powers. The effect of copper (Cu) used in making back contacts was studied in connection with the CdS/CdTe junction PL. It was found that the presence of Cu suppresses the sub-band gap PL emissions. This effect was concluded to be due either to Cu occupying cadmium vacancies (V_{Cd}) or forming acceptor complexes with them. This points to a potential role of Cu in plugging sub-band gap recombination routes and hence increasing charge separation ability of the device. An energy band diagram is presented indicating various observed transitions and their possible origins.

Tribology Focus Topic
Room: 230B - Session TR+AS+NS+SS-ThA

Molecular Origins of Friction
Moderator: Nicolas Argibay, Sandia National Laboratories

2:20pm TR+AS+NS+SS-ThA1 Atomic-Scale Mechanisms of Single Asperity Sliding, *Ashlie Martini*, *X. Hu*, University of California Merced, *M.V.P. Altoe*, Lawrence Berkeley National Laboratory **INVITED**

Isolating a single asperity to characterize its response to sliding is a heuristic approach to understanding the fundamental mechanisms that underlie friction and wear. A single asperity can be realized experimentally as the tip of an atomic force microscope cantilever. When the tip slides across a surface, friction is measured with atomic lattice-scale resolution and wear can be quantified in terms of nano- or even atom-scale volumes of material removed. However, challenges remain in interpreting these measurements because the observed friction and wear are due to processes that take place in the interface buried between the tip and the substrate on which it slides. Further, the nanometer scale of the contact implies that discrete atomic events in the interface may determine sliding behavior. Together, these observations suggest that the experiments could be complemented by atomistic models of the apex of the tip, near-contact substrate material and, of course, the interface itself. Although the simulations are limited to relatively small size and time scales, they have the potential to provide detailed information about mechanisms underlying phenomena that occur over short periods of time and small sliding

distances. Specifically, in this research, we focus on the initial stages of friction and wear, and the processes that occur during the first tens of nanometers of sliding. The simulations are carefully designed such that they faithfully capture the corresponding experiments, including matching the materials, crystallography and geometry of the contacting bodies as observed through transmission electron microscope images of the tip and atomic force microscope images of the substrate taken at 10 nm intervals during the sliding process. The experiments offer an unprecedented view of wear occurring single atomic layers at a time, and the simulations provide detailed complementary information about the atomic-scale mechanisms underlying this process.

3:00pm TR+AS+NS+SS-ThA3 Investigation of Epitaxy and Friction in Model Boundary Films, *Hongyu Gao*, University of California Merced, *W.T. Tysoe*, University of Wisconsin-Milwaukee, *A. Martini*, University of California Merced

Sliding friction of boundary films is investigated using ultrahigh vacuum (UHV) tribometer measurements of model alkali halide films on metals with complementary molecular dynamics (MD) simulations. We focus on a model system consisting of thin potassium chloride (KCl) films on an iron (Fe) substrate. The interaction potential between KCl and Fe is tuned using activation energy obtained from temperature programmed desorption (TPD) data and structures inferred from low-energy electron diffraction (LEED) measurements. The simulation is then used to explore the effect of film thickness and pressure on the formation of an epitaxial KCl film. The nature of this film and its near surface structure is then correlated with sliding friction behavior.

3:20pm TR+AS+NS+SS-ThA4 Temperature Dependence of Atomic-scale Friction on Two-dimensional Materials, *Zhijiang Ye*, University of California Merced, *X.Z. Liu*, *K. Hasz*, *R.W. Carpick*, University of Pennsylvania, *A. Martini*, University of California Merced

Temperature plays an essential, yet complex role in determining atomic-scale friction. Recent studies of the temperature dependence of atomic-scale friction have reported different trends that suggest distinct and possibly contradictory underlying mechanisms. Specifically, friction is usually found to decrease with increasing temperature (due to thermolubricity), but this behavior is not always observed (attributed to adsorbates or meniscus effects). To understand the origins of these trends, we use molecular dynamics (MD) simulations and parallel replica dynamics (PRD) to study the temperature dependence of atomic friction on two-dimensional (2-D) materials, such as molybdenum disulfide. The MD simulations are designed to be closely-matched with corresponding atomic force microscope (AFM) measurements [1, 2]. Using the simulations and experiments, we explore how friction varies with temperature and how that variation is affected by other parameters, including sliding velocity, material, and environment. These studies provide new insights into how temperature affects friction on 2-D materials, and into the origins of atomic-scale friction generally.

References:

1. Xin-Z. Liu, Zhijiang Ye, Yalin Dong, Philip Egberts, Robert W. Carpick, and Ashlie Martini. Dynamics of Atomic Stick-Slip Friction Examined with Atomic Force Microscopy and Atomistic Simulations at Overlapping Speeds, *Phys. Rev. Lett.***114**, 146102 (2015).

2. Qunyang Li, Yalin Dong, Danny Perez, Ashlie Martini, and Robert W. Carpick. Speed dependence of atomic stick-slip friction in optimally matched experiments and molecular dynamics simulations. *Physical Rev. Lett.* **106**, 126101 (2011).

4:20pm TR+AS+NS+SS-ThA7 Single Molecule Experiments to Explore Friction and Adhesion, *Rémy Pawlak*, *S. Kawai*, *A. Baratoff*, *T. Meier*, University of Basel, Switzerland, *W. Ouyang*, Tsinghua University, China, *T. Glatzel*, University of Basel, Switzerland, *E. Gnecco*, IMDEA-Nanociencia - Universidad Autónoma de Madrid, Spain, *A. Filippov*, Donetsk Institute of Physics and Engineering, Ukraine, *M. Urbakh*, Tel Aviv University, Israel, *E. Meyer*, University of Basel, Switzerland **INVITED**

Controlled manipulation processes of single-molecules with an atomic force microscope (AFM) provide valuable information about their interactions with surfaces, leading to fundamental insights into adhesion and friction properties. To understand such phenomena at such scale, tuning-fork based AFM operated at low temperature is an appropriate tool since complex manipulations of single-molecules can be readily performed and detected via advanced force spectroscopic techniques **[1]** . With such approach however, the measured frequency shifts are related to normal force gradients, and thus the interpretation of friction phenomena is not fully straightforward. To overcome this issue, we developed analytical models to simulate the experimental AFM data which allow us to determine adhesive energy and nanoscale friction. In this presentation, a first example will be given by the vertical pulling of long polymeric chains on Au(111), where

their detachment leads to oscillations of the normal and lateral forces [2] . As in Frenkel-Kontorova (FK) models of friction, the polymer is represented by a chain of units connected by springs of stiffness k , each one interacting with a 2D periodic substrate potential. Force and gradient variations are dominated by the sequential detachment of each molecular units if k i s large enough to cause superlubric sliding. A second example will show vertical and lateral manipulations over a Cu(111) surface of a single porphyrin molecule attached to the AFM tip apex. In the frequency shift traces, atomic sawtooth modulations are systematically observed while sliding over the surface and are related to the internal degree of freedom of the molecular structure [3] .

References:

[1] R. Pawlak, S. Kawai, T. Glatzel, E. Meyer. *Single Molecule Force Spectroscopy* (ncAFM, *vol.3*, Springer, Japan 2015).

[2] S. Kawai et al., Quantifying the atomic-level mechanics of single long physisorbed molecular chains, *Proc. Nat. Acad. Sci.*, **111**, 3968–3972 (2014)

[3] R. Pawlak *et al* . *Intramolecular response of a single porphyrin molecule during AFM manipulations.* Submitted.

5:00pm TR+AS+NS+SS-ThA9 Effects of Humidity on the Adhesion and Friction of Carbon-Based Materials, *Judith Harrison*, *M. Fallet, K.E. Ryan,* United States Naval Academy, *T. Knippenberg,* High Point University, *S.H. Kim, A. Al-Azizi*, Pennsylvania State University

Atomic-scale wear in nanoscale contacts is of particular importance for tip-based nanomanufacturing applications. As a result, wear resistant materials, such as diamond-like carbon (DLC), have been used to coat AFM tips to improve the lifespan and reliability of AFM probes and surfaces. Unfortunately, the tribological performance of these materials is known to depend on environmental conditions, such as humidity levels. We have performed macroscopic and atomic force microscopy friction experiments and molecular dynamics (MD) simulations aimed at examining adhesion and wear of DLC in humid environments.

Macro-scale friction tests showed friction and transfer film dependence on humid conditions. Low humidity suppresses transfer film formation while keeping the friction low. Intermediate humidity, however, does not reduce transfer film formation and increases the friction. The effect of humidity on friction was found to agree with the adhesion dependence on relative humidity as measured with atomic force microscopy.

Because it is difficult to elucidate atomic-scale mechanisms via experimental methods, molecular dynamics simulations have been employed to examine this behavior. Adhesion and sliding simulations of non-hydrogenated, ultrananocrystalline diamond (UNCD) and DLC surfaces with various levels of hydrogen in the presence of water using the qAIREBO and the ReaxFF potentials have been performed. Because both of these potentials are able to model chemical reactions, the atomic-scale mechanisms responsible for adhesion and wear can be identified. Results obtained with both potentials will be compared to the experimental results.

5:20pm TR+AS+NS+SS-ThA10 Single Asperity Tribochemical Wear of Silicon AFM Tips Sliding on Aluminum Oxide, *Erin Flater*, *S. Sorenson,* Luther College, *N. Ansari, A. Poda, W.R. Ashurst,* Auburn University, *B.P. Borovsky*, St. Olaf College

Understanding of tribological mechanisms at the submillimeter scale continues to be relevant since friction and wear limit the commercial viability of small-scale mechanical devices such as microelectromechanical systems (MEMS). For example, tribochemical processes play a significant role in many materials systems, including silicon oxide and aluminum oxide, which are relevant materials for MEMS devices. Our work focuses on understanding tribological processes at the interface of silicon AFM tips and amorphous aluminum oxide surfaces. We observe wear of silicon tips after repetitive sliding on the aluminum oxide surface, which occurs even at low contact pressures, implying that the wear process is chemical in nature. We quantify tip wear by intermittently interrupting the wear experiment to perform indirect *in-situ* tip imaging on a sharp-spiked sample. We use these tip images to quantify volume of material lost during scanning. Wear as a function of sliding distance is modeled using reaction rate theory and is compared to the Archard wear model. While some of our results appear to agree with an Archard model, these results may be more appropriately interpreted in light of the more fundamental reaction rate theory.

5:40pm TR+AS+NS+SS-ThA11 Molecular Simulation of Indentation as a Probe of Scanning Probe Tip Mechanical Properties, *J. David Schall*, *K. Vummaneni,* Oakland University, *J.A. Harrison*, United States Naval Academy

Scanning probe tips should be robust, have low adhesion, and low wear to ensure repeatability and long tip life. As new tip materials are developed these properties must be quantified and compared to existing tip materials.

In this study, molecular simulation is used to measure the elastic modulus and work of adhesion of a variety of tips against a common substrate material, in this case H-terminated diamond (111). The tip materials investigated include Si, SiC, amorphous SiC, diamond, diamond like carbon and ultra-nanocrystalline diamond (UNCD). SiC was recently proposed as a new high hardness, low wear tip material. In simulation the tip geometry can be controlled to enable direct comparisons between each tip material. Both dynamic simulations at 300K and quasi-static indentions using stepwise energy minimization with and with out adhesion between tip and substrate were used. Simulations of sliding friction and wear have also been conducted to investigate the correlation between tip materials properties and friction and wear.

2D Materials Focus Topic
Room: 212C - Session 2D+EM+IS+NS+PS+SP+SS-FrM

Surface Chemistry of 2D Materials: Functionalization, Membranes, Sensors

Moderator: Peter Sutter, University of Nebraska - Lincoln, Judy Cha, Yale University

8:20am 2D+EM+IS+NS+PS+SP+SS-FrM1 Chemically Modifying Graphene for Surface Functionality, *Paul Sheehan*, *S. Tsoi, S.C. Hernández, S.G. Walton, T.L. Reinecke, K.E. Whitener, J.T. Robinson,* Naval Research Laboratory, *R. Stine*, Nova Research
Graphene has many superlative properties that may be tailored for specific applications, or even enhanced, through chemical functionalization. Chemical functionalization dramatically changes almost every critical property of graphene, changing it from opaque to transparent, from diamagnetic to ferromagnetic, from electron rich or electron poor, from electrically conducting to insulating (and back again!). This extensive control suggests that chemically modified graphene may aid applications from flexible sensors to surface engineering. I will discuss how stacks of 2D materials can control the dominant surface forces—van der Waals,[1] acid-base interactions, electrostatic interactions, etc.—and so surpass conventional methods of preparing surfaces with, for example, self-assembled monolayers. I will also briefly address goals as diverse as biosensing[2] or sloughing off chemical warfare agents.[3]

[1] ACS Nano, **2014**, *8* (12), pp 12410–12417

[2] BioTechniques, Vol. 57, No. 1, July 2014, pp. 21–30

[3] ACS Nano. 2013 Jun 25;7(6):4746-55.

8:40am 2D+EM+IS+NS+PS+SP+SS-FrM2 Structural Phase Stability Control of Monolayer $MoTe_2$ with Adsorbed Atoms and Molecules, *Yao Zhou, E.J. Reed*, Stanford University
Of the Mo- and W- dichalcogenide monolayers, $MoTe_2$ is particularly interesting because it exhibits a small energy difference (approximately 31 meV per $MoTe_2$) between its semiconducting 2H phase and metallic 1T' crystal structures. This feature makes it particularly interesting for potential phase change applications.

We study the adsorption of some common atoms and molecules onto monolayer $MoTe_2$ and the potential for adsorption to induce a phase change between the semiconducting 2H and metallic 1T' crystal structures of the monolayer. Using density functional theory with spin orbit and van der Waals energy contributions, we determined the most energetically favorable adsorption positions and orientations on the two phases of monolayer $MoTe_2$. We then obtained the formation energies for these adsorption reactions and found that atomic adsorption generally favors 1T' metallic phases while molecular adsorption favors semiconducting 2H phases. A possible application of this work may be the chemical stabilization of a preferred phase during the growth process.

Further, we consider the $Mo_xW_{1-x}Te_2$ alloy monolayers that exhibit even smaller energy difference between phases. Our calculations indicate that it may be possible to engineer an alloy ($0<x<0.5$) such that specific molecules will induce a phase change to 1T' while other molecules studied stabilize the 2H phase, which suggests that alloying may provide some molecular selectivity. This potentially provides the basis for molecular sensing applications due to the large electronic contrast between 2H and 1T' phases.

9:00am 2D+EM+IS+NS+PS+SP+SS-FrM3 Selective Nanochemistry on Graphene/Silicon Carbide: Substrate Functionalization and Polycyclic Aromatic Hydrocarbons Formation, *Patrick Soukiassian*, CEA, France
INVITED
Graphene & silicon carbide (SiC) are advanced semiconductors having figures of merit scaling well above those of well-established ones [1,2]. Understanding/mediating SiC and graphene surfaces & interfaces properties are of central importance toward functionalization and applications. As a 2D material, graphene is a single atomic layer of carbon atoms in a *sp2* bonding configuration. Therefore, functionalization remains challenging since interacting too strongly with the graphene atomic layer may change its bonding configuration and properties. Instead, interacting with the SiC substrate offers an alternative approach. The 1st case of hydrogen-induced metallization of a semiconductor surface has been shown for a 3C-SiC(001) surface [3]. Here, combining investigations using advanced experimental techniques such as STM/STS, vibrational & 3rd generation synchrotron radiation-based photoelectron spectroscopies together with state-of-art

calculations will be presented and discussed. It includes: i) the 1st evidence of H/D-induced nanotunnel opening at a semiconductor sub-surface shown here for SiC [4]. Depending on H coverage, these nanotunnels could either be metallic or semiconducting. Dangling bonds generated inside the nanotunnels offer a promising template to capture atoms or molecules. These features open nano-tailoring capabilities towards advanced applications in electronics, chemistry, storage, sensors or biotechnology. Understanding & controlling such a mechanism open routes towards selective surface/interface functionalization of epitaxial graphene [4]. ii) The role of H interaction with graphene on SiC dust grains in polycyclic aromatic hydrocarbons (PAH) formation in the interstellar space with a possible route toward prebiotic roots of life in the universe [5].

1–W. Lu, P. Soukiassian, J. Boeckl *"Graphene: fundamentals and functionalities"* **MRS Bull. 37**, 1119 (2012)

2–P. Soukiassian *"Will graphene be the material of the 21th century?"* **MRS Bull. 37**, 1321 (2012)

3-V. Derycke, P. Soukiassian, F. Amy, Y.J Chabal, M. D'angelo, H. Enriquez, M. Silly, *"Nanochemistry at the atomic scale revealed in hydrogen-induced semiconductor surface metallization"*, **Nature Mat.2**, 253 (2003)

4–P. Soukiassian, E. Wimmer, E. Celasco, Cl. Giallombardo, S. Bonanni, L. Vattuone, L. Savio, A. Tejeda, M. Silly, M. D'angelo, F. Sirotti, M. Rocca *"Hydrogen-induced nanotunnel opening within semiconductor subsurface"* **Nature Com. 4**, 2800 (2013)

5–P. Merino, M. Švec, J.I. Martinez,P. Jelinek, P. Lacovig, M. Dalmiglio, S. Lizzit, P. Soukiassian, J. Cernichara, J.A. Martin-Gago *"Graphene etching on SiC grains as a path to interstellar PAHs' formation"* **Nature Com. 5**, 3054 (2014)

9:40am 2D+EM+IS+NS+PS+SP+SS-FrM5 Intrinsic Wettability of Graphene, *Haitao Liu*, Department of Chemistry, University of Pittsburgh
Graphene and graphite are long believed to be hydrophobic. Here we show that a clean graphitic surface is in fact mildly hydrophilic [1]. We find that an as-prepared graphene sample is hydrophilic with a water contact angle of ca. 40°. Upon exposure to ambient air, the water contact angle gradually increased to ca. 60° within 20 min and plateaued at ca. 80° after 1 day. Infrared (IR) spectroscopy and X-ray photoelectron spectroscopy (XPS) showed that airborne hydrocarbon adsorbed onto the graphene surface during this process. Both thermal annealing and controlled UV/O_3 treatment removed the hydrocarbon contaminants, which was accompanied by a concurrent decrease in the water contact angle. Our findings show that graphene is more hydrophilic than previously believed and suggest that the reported hydrophobic nature of graphene is due to unintentional hydrocarbon contamination from ambient air.

Reference

[1] Zhiting Li; et al.; Nature Materials, 12, 925-931, (2013)

10:00am 2D+EM+IS+NS+PS+SP+SS-FrM6 Au-doped Graphene As a Promising Electrocatalyst for the Oxygen Reduction Reaction in Hydrogen Fuel Cells: Prediction from First Principles, *Sergey Stolbov*, University of Central Florida, *M. Alcantara Ortigoza*, Tuskegee University
One of the main obstacles hindering large scale practical application of hydrogen fuel cells is a prohibited cost of the Pt (or Pt-based) catalysts for the oxygen reduction reaction (ORR) on the fuel cell cathode. In this work, we consider Au-doped graphene as an alternative to Pt for facilitating ORR. Our first-principles calculations show that Au atoms incorporated into graphene di-vacancies form a thermodynamically and electrochemically stable structure. Furthermore, calculation of the binding energies of the ORR intermediates reveals that Au-C bonding makes the C atoms neighboring to Au optimally reactive for ORR. The calculated ORR free energy diagrams suggest that the Au-graphene structures have an ORR onset potential as high as that of Pt. We also demonstrate that the linear relation among the binding energy of the reaction intermediates assumed in a number of works on computational high-throughput material screening does not hold, at least for this none purely transition-metal material.

10:20am 2D+EM+IS+NS+PS+SP+SS-FrM7 Spontaneous Deposition of Palladium Nanoparticles on Graphene through Redox Reaction, *Xiaorui Zhang*, *W. Ooki, Y.R. Kosaka, T. Kondo, J. Nakamura*, University of Tsukuba, Japan
Due to its unique properties such as huge surface area and excellent conductivity, graphene becomes great interesting for supporting noble metal catalysts. Some noble metals such as palladium, platinum, gold nanoparticles was reported to be able to spontaneous deposition on as-synthesized reduced graphene oxide with external reducing agent-free

recently. Yet the mechanism of spontaneous deposition of metals on graphene has not been clarified until now. In the present research, we spontaneously deposited palladium nanoparticles on as-synthesized reduced graphene oxide in H_2O medium without external reducing agent. It was found that the deposited amount of palladium varied with pH, meanwhile, the bivalent Pd^{2+} precursor was reduced to metallic palladium, and graphene was oxidized simultaneously with an increasing of its oxygen functional groups. The atomic ratio of the deposited Pd and the increased O in rGO located in a range from 1 to 2. As reducing agent-free, the mechanism on spontaneous redox deposition of metal nanoparticles on graphene was proposed, firstly, an efficient adsorption of metal precursor on graphene is a prerequisite which is determined by their electrical charges and adjusted by pH. Secondly, a positive galvanic potential between metal precursor and graphene is necessary for metal spontaneous deposition.

10:40am **2D+EM+IS+NS+PS+SP+SS-FrM8 Gradient Electrochemical Response of Template Synthesized Thickness Sorted MoS$_2$ Nanosheets for Cellular Level Free Radical Detection**, *Ankur Gupta*, T. Selvan, S. Das, S. Seal, University of Central Florida

The human body is a complex system capable of defending in adverse conditions. A classic example of such complex process is balanced equilibrium production between pro-oxidant and antioxidant in cells. However, when this equilibrium is disturbed, production of free radicals such as superoxide and nitric oxide strengthen, and causes serious cellular damages. Furthermore, myeloperoxidase (MPO) is released during the oxidative burst. This MPO combines with hydrogen peroxide (H_2O_2) and Cl^- and generate hypochlorous acid (HOCl). This is a short-lived and powerful diffusible oxidant strong oxidizer and could react with O^{2-} to produce OH^-. Therefore, in physiological condition HOCl has a major role as a potent microbicidal agent in the immune defense; however, during the oxidative burst HOCl not only damage healthy tissue and generate radicals that are extremely reactive. Therefore, monitoring of the production of free radicals at the cellular level is important for diagnostic purpose. Over past years, several material have been used to develop sensors for free radical detection such as cerium oxide nanoparticles, MoS$_2$ nanosheets and nanoparticles. However, detection of free radicals at cellular level is still a challenge.

In this attempt, layered molybdenum disulfide (MoS$_2$) were synthesized via hydrothermal method. SBA-15 polymer template were utilized during hydrothermal process to grow MoS$_2$ around it to develop porosity. After the hydrothermal synthesis and washing, polymer template was removed by dissolving it in isopropanol which leaves high surface area layered MoS$_2$ crystal. Wet chemical exfoliation of MoS$_2$ were carried out in aqueous solution of Pluronic$^{\mathrm{O}}$ F-127 having hydrophobic and hydrophilic chains. Pluronic$^{\mathrm{O}}$ F-127 was used to bring down the buoyant density of MoS$_2$. Non-templated nanosheets were synthesized as control. The exfoliated solution were centrifuged at 3000 rpm to remove large particle and supernatant was collected for density gradient ultracentrifugation (DGU). Separation of different thickness layers is carried out by DGU. Thickness sort MoS2 nanosheets were characterized using AFM, XPS, HRTEM, Raman and UV-Vis spectroscopy for structural and chemical analysis. XPS, HETEM and EFTEM analysis of nanosheets have illustrate the sulfur deficiency at the edges of the nanosheets. MoS2 nanosheets were deposited on glassy carbon electrode for cyclic-voltammetry and chronoamperometry measurements. Higher sensitivity and repeatability were demonstrated by nanosheets prepared via template method as compared to control for reactive oxygen and nitrogen species, and HOCl.

11:00am **2D+EM+IS+NS+PS+SP+SS-FrM9   Methanol Synthesis on Defect-Laden Single-Layer MoS$_2$ Supported on Cu(111): Results of a First Principles Study**, D. Le, *Takat B. Rawal*, T.S. Rahman, University of Central Florida

Despite being found to be the preferred structure in single layer MoS$_2$, the sulfur vacancy row does not facilitate alcohol synthesis from syngas [1] because its narrow size limits adsorption, diffusion, and formation of possible intermediates. On the Cu(111) surface, strong interactions between MoS$_2$ and Cu are expected to reduce the corrugations caused by sulfur vacancy rows, resulting in a larger exposure of vacancies to adsorbates which could enhance the catalytic activity of the row towards alcohol synthesis from syngas. Based on the results of our density functional theory (DFT) simulations utilizing the DFT-D3 correction for accounting the van der Waals interactions, we show that: (1) there is a significant charge transfer from the Cu(111) surface to MoS$_2$, enhancing its catalytic properties, (2) the binding energies of CO and dissociated H_2 increase by 0.3 eV in comparison to that on unsupported MoS$_2$, indicating stronger interactions, and (3) the barriers for forming intermediate species in alcohol synthesis process reduce significantly in comparison to that on unsupported MoS$_2$. On the basis of these energetics, we conclude the Cu(111) substrate promotes methanol synthesis from syn gas on single-layer MoS$_2$ with a vacancy row. We will also present the energetic pathways for the

formations of other reaction products such as methane, formaldehyde, and water, as well as that of (the reverse) water gas-shift reaction.

[1] D. Le, T. B. Rawal, and T. S. Rahman, *J. Phys. Chem. C* **118**, 5346 (2014).

11:20am **2D+EM+IS+NS+PS+SP+SS-FrM10 The Happy Marriage of Graphene and Germanium: Graphene Achieves Exceptional Conductivity and Protects Germanium from Oxidizing**, *Richard Rojas Delgado*, University of Wisconsin-Madison, F. Cavallo, University of New Mexico, R.M. Jacobberger, J.R. Sanchez Perez, D. Schroeder, M.A. Eriksson, M.S. Arnold, M.G. Lagally, University of Wisconsin-Madison

The properties of graphene (G) make it an outstanding candidate for electronic-device applications, especially those that require no band gap but a high conductance. The conductance, involving both carrier mobility and carrier concentration, will depend critically on the substrate to which G is transferred. We demonstrate an exceptionally high conductance for G transferred to Ge(001) and provide an understanding of the mechanism.[1] Essential in this understanding is an interfacial chemistry consisting of Ge oxide and suboxide layers that provide the necessary charges to dope the graphene sheet, and whose chemical behavior is such that one can obtain long-term stability in the conductance. In contrast, when high-quality G is grown directly on Ge (100), (111), or (110), the conductance is unexceptional, but oxidation of the surface is significantly delayed and slowed, relative to both clean Ge and Ge with G transferred to its surface . [2,3] We fabricate Hall bars in G transferred to Ge and G grown using atmospheric-pressure CVD with methane precursors . X-ray photoelectron spectroscopy (XPS) is used to investigate the oxide in all stages of the measurements. The sheet resistance and Hall effect are measured from 300K to 10K for transferred and grown samples. Values of mobility and carrier concentration are extracted. It appears we have reached the highest combination of mobility and carrier concentration in graphene (suspended or supported) for temperatures from 10 to 300K. The implication is that the primary mechanisms for scattering charge in the G, roughness and a non-uniform electrostatic potential due to fixed charges, have limited effect when the substrate is oxidized Ge. Finally the subsequent oxidation kinetics of Ge (001) are compared for graphene directly grown on Ge and for graphene transferred to Ge. XPS shows that for graphene grown on Ge(001) the interface is oxide-free and remains so over long periods of time. For graphene transferred to Ge(001) the interface contains stoichiometric and substoichiometric oxides. The thickness of these oxides increases with time, but quite slowly. Using spatially resolved XPS, we propose a model of diffusion limited oxidation initiated at edges of the graphene.

Research supported by DOE.

[1]Cavallo, Francesca, et al. "Exceptional Charge Transport Properties of Graphene on Germanium." *ACS nano* 8.10 (2014): 10237-10245.

[2] R. M. Jacobberger, et al. "*Oriented Bottom-Up Growth of Armchair Graphene Nanoribbons on Germanium.*" *Nature Comm.*, under review.

[3] R. Rojas, et. al "Passivation of Ge by Graphene.", in process.

Plasma Science and Technology
Room: 210B - Session PS+SS+TF-FrM

Atomic Layer Etching (ALE) and Low-Damage Processes II
Moderator: Toshihisa Nozawa, Tokyo Electron Ltd.

8:20am **PS+SS+TF-FrM1 Atomic Layer Etching of Silicon Dioxide to Enable Self-aligned Contact Integration**, B. Finch, H. Singh, *Eric Hudson*, Lam Research Corporation   **INVITED**

CMOS devices have continued to scale dimensionally following the implementation of FinFET transistors. Self-alignment of the source and drain contact to the gate has been presented as an integration solution starting at the 22nm technology node[1]. This self-aligned contact (SAC) integration creates additional challenges and constraints on the etch process for the 10 nm node and beyond. Due to smaller feature dimensions, lithography overlay, and full contact wrap-around of the transistor fins, unprecedented etch precision is now required.

A novel approach for SAC oxide etching has been developed which addresses the many tradeoffs of this application using a directional atomic layer etch process (ALE) as reported by Hudson et al[2]. Key trade-offs to enable contact etching capability of CDs as small as 10 nm include SAC spacer loss, lack of profile control, and contact not-opens. This cyclic SiO$_2$ ALE process repeats discrete unit process steps of fluorocarbon deposition

and ion bombardment to achieve high selectivity of SiO_2 to Si_3N_4 while simultaneously addressing these tradeoffs. Oxide removal rates can be precisely controlled with minimal removal of Si_3N_4 films, enabling a highly selective etch process. Anisotropic, directional etch behavior superior to traditional SiO2 etch is enabled, creating vertical oxide profiles. This capability is highly desirable for SAC etch applications as it maintains the integrity of the gate electrode spacer during etch. Experimental results showing the ability of this oxide ALE process to eliminate tradeoffs is presented

[1] C. Auth, et al, "A 22 nm high performance and low-power CMOS technology featuring fully-depleted tri-gate transistors, self-aligned contacts and high density MIM capacitors," accepted in VLSI Symp. Tech. Dig., Jun. 2012.

[2] E. Hudson, et al, "Highly Selective Atomic Layer Etching of Silicon Dioxide Using Fluorocarbons," accepted in AVS 61st International Symp. & Exhibition, Nov. 2014.

9:00am PS+SS+TF-FrM3 High Performance Self Align Contact Etching with Newly developed Quasi-ALE, *Akihiro Tsuji*, Tokyo Electron Miyagi Limited, Japan, *M. Tabata, H. Watanabe, T. Katsunuma*, Tokyo Electron Miyagi Limited, *M. Honda*, Tokyo Electron Miyagi Limited, Japan

The Self-Aligned Contact (SAC) process has been widely adopted to achieve aligned narrow contacts between electrodes as the pitch shrinkage has progressed with the miniaturization of devices in high-scale integration. In SAC fabrication, it is important to achieve high selectivity of the interlayer insulator (SiO_2) over an etch stop film (SiN) to improve insulation tolerance between the contact plug and the wiring. Such high-selective etch processes have been realized by depositing fluorocarbon (FC) film selectively on the SiN film by using the composition difference between SiO_2 and SiN with fluorocarbon plasma, which protects SiN surface during SiO_2 etch. In order to minimize SiN loss, a balance of FC film thickness and the penetration depth of the ion energy on SiN become significant [1,2]. When trying to achieve improved SiN loss reduction, reducing ion energy is one effective solution, but a balance of ion energy flux and FC radical flux ($E_i \Gamma_i / \Gamma_{CF}$) breaks down, resulting in an excess amount of deposition, causing etch stop to occur. This is caused by the limited control margin of the ion energy flux over the FC radical flux ratio using conventional processes.

Atomic Layer Etching (ALE) concept has attracted great attention in recent years for its precise fabrication potential at the atomic level and its ability to solve this issue [3,4]. ALE method enables clear separation of ion energy flux and FC radical flux supply by controlling $E_i \Gamma_i / \Gamma_{CF}$ dynamically using a new parameter of flux ratio respective to step time. Furthermore, specific control of the surface condition at each cycle is expected to be effective for precise fabrication. This report discusses the application of the ALE concept in the SAC process as a Quasi-ALE scheme with consideration for implementation to volume production. This scheme realized a dramatic improvement of SiO_2 etch performance with substantial reduction of SiN loss. Further analysis of the surface condition by XPS, SIMS, HR-RBS helped determine the mechanism of selectivity enhancement. Quasi-ALE technology is a promising weapon, corresponding to leading-edge processes of various fabrication requirements along with the miniaturization of devices, towards 10nm and beyond.

Reference

[1] T.Tatsumi, M.Sekine et al. JVST B 18(4), 2000

[2] M.Matsui, M.Sekine et al. JVST A 19(4), 2001

[3] D.Metzler, G.S.Oehrlein et al. JVST A 32(2), 2014

[4] M. Honda, AVS 61th Int. Symp. & Exhibit. (2014)

9:20am PS+SS+TF-FrM4 Fluorocarbon Based Atomic Layer Etching of Si_3N_4 and Selectivity of SiO_2 over Si_3N_4, *Chen Li*, D. Metzler, G.S. Oehrlein, University of Maryland, College Park, *C.S. Lai, M. Danek, E.A. Hudson, A. Dulkin*, Lam Research Corporation

Angstrom-level plasma etching precision is required by semiconductor manufacturing for the sub-14 nm technology node. Atomic layer etching (ALE), achieved by a series of self-limiting cycles, can precisely control the amount of reactant available and resulting etching depths. Recently, controlled etching of SiO_2 at the Angstrom-level based on steady-state Ar plasma, periodic injection of a defined number of fluorocarbon (FC) molecules, and synchronized plasma-based Ar^+ ion bombardment has been demonstrated [1,2]. This novel ALE approach is achieved by deposition of a thin (several Angstroms) reactive FC layer on the material surface using pulsed FC flow. Subsequent low energy Ar^+ ion bombardment removes the FC layer along with SiO_2 from the surface. The ion energies were selected to allow only chemical enhanced etching to take place without any physical sputtering, which enables a self-limited SiO_2 removal. We report on controlled etching of Si_3N_4 and SiO_2 layers of the order of one to several

Angstroms using this cyclic ALE approach. The work was performed in an inductively coupled plasma reactor. Using SiO_2-Si_3N_4-SiO_2 multi-layer stacks on a Si substrate enabled precise evaluation of selectivity, self-limitation, and modification by *in situ* real time ellipsometry. Si_3N_4 etching and etch selectivity of SiO_2 over Si_3N_4 were studied and evaluated with regard to the dependence on FC surface coverage, precursor selection, ion energy, and etch step length. Surface chemistries of SiO_2 and Si_3N_4 were investigated by vacuum transferred x-ray photoemission spectroscopy (XPS) at each stage of the ALE process. The choice of precursor can have a significant impact on the surface chemistry and therefore the chemically enhanced etching characteristics.

References:

[1] D. Metzler, R. Bruce, S. Engelmann, E. A. Joseph, and G. S. Oehrlein, "Fluorocarbon assisted atomic layer etching of SiO_2 using cyclic Ar/C_4F_8 plasma", J Vac Sci Technol A 32, 020603 (2014)

[2] E. Hudson, V. Vidyarthi, R. Bhowmick, R. Bise, H.J. Shin, G. Delgadino, B. Jariwala, D. Lambert, S. Deshmukh, "Highly selective etching of Silicon Dioxide Using Fluorocarbons"; AVS 61st International Symposium & Exhibition (2014);

9:40am PS+SS+TF-FrM5 Chamber Wall Effect for Fluorocarbon Assisted Atomic Layer Etching of SiO_2 Using Cyclic Ar/C_4F_8 Plasma, *Masatoshi Kawakami*, Hitachi High-Technologies, Japan, *D. Metzler, C. Li, G.S. Oehrlein*, University of Maryland, College Park

The requirement for atomic scale etching is becoming more important with increasing miniaturization of semiconductor devices. A novel approach for oxide etching has been developed by Metzler et al [1]. Controlled etching of SiO_2 at the angstrom-level is based on steady-state Ar plasma and deposition of a thin reactive fluorocarbon layer enabled by precise, periodic C_4F_8 injection. High process stability is necessary for the success of this method and its use in mass production. Chamber wall interactions are crucial to the stability of this process. In this research, we studied the influence of chamber wall temperature and chamber wall chemical state on ALE process performance. The experiments were conducted in an inductively coupled plasma system excited at 13.56 MHz. The temperature of the quartz coupling window was measured with an infrared temperature sensor. *In situ* real time ellipsometry allows for film thickness measurements during the process. Plasma gas-phase chemistry was characterized by optical emission spectroscopy. We conducted the cyclic Ar/C_4F_8 SiO_2 ALE process using different initial chamber temperature, and chamber wall polymer coverage condition. It was found that although the polymer film thickness deposited in each cycle is constant, the etching behavior changed, likely related to a change in depositing species. Chamber wall temperature shows a clear effect on the CO and SiF emission and their relative ratio. When the surface of the quartz coupling window started to be covered by a fluorocarbon film, the overall CO and SiF intensity decreased while the CO/SiF emission peak ratio did not change. The relationship to observed etching behavior will be discussed.

References:

[1]D. Metzler, R. Bruce, S. Engelmann, E.A. Joseph, and G.S. Oehrlein, J Vac Sci Technol A **32**, 020603 (2014)

10:00am PS+SS+TF-FrM6 Potential Solutions for Atomic Precision Etching, *Olivier Joubert*, LTM-CNRS, France, *E. Despiau-Pujo*, LTM, France, *G. Cunge*, LTM - CEA/LETI, France, *L. Vallier, J. Dubois, A. Tavernier*, Univ. Grenoble Alpes-CNRS-CEA/Minatec-LTM, France, *O. Luere, S. Banna, Y. Zhang*, Applied Materials **INVITED**

The continuous downscaling of device dimensions and introduction of new transistor architectures such as FDSOI or FINFEts transistors is bringing up new challenges for plasma etching technologies. For the gate transistor for example, future technological nodes require patterning capabilities in a range of dimension going below 10 nm. Extremely thin layers (less than 1nm) of materials are now involved in the stacks of materials to pattern requiring in some cases an etch precision better than 1 nm. In other words, the etch selectivity and physical/ chemical damage induced by the plasma must be controlled in a way such as the plasma can stop in a layer of materials as thin as 1nm without damaging the underlayers or the substrate material. Such a precision in processes becomes difficult to reach with the state of the art plasma technologies.

In this presentation, we will describe two plasma technologies that could potentially reach that goal.

A new Technology is the so-called "Thin Layer Etching" technology. In the first step of the TLE technology, H2 or He Ions produced by a capacitive plasma induce modification of silicon based materials while in a second step the modified material is removed in an all dry NF3/NH3 remote plasma that form volatile products with the modified silicon based materials. Performance achieved by TLE for nitride spacer etching will be shown and compared to conventional ICP results.

Fast gas pulsing technology could also be a promising way to form ultra-thin reactive layer during plasma processing, allowing atomic precision etching to be achieved. This concept will be explained and discussed based on preliminary result of silicon etching in chlorine plasmas using atomistic simulation.

10:40am PS+SS+TF-FrM8 Molecular Dynamics Simulations of Atomic Layer Etching by Low Energy Ions, *Jun-Chieh Wang*, *S. Rauf, J.A. Kenney, L. Dorf, K.S. Collins*, Applied Materials Inc.

In the semiconductor industry, the use of atomic layer etching (ALE) makes it feasible to accurately control the critical dimensions to nanometer level or smaller. In ALE, the target substrate is first exposed to a reactive gas that passivates the surface, which is then followed by ion bombardment with energy below the sputtering threshold. It is critical to precisely control the ion energy and flux during the etching process to remove the topmost layer of the passivated surface without damaging the underlying substrate. Once the passivation layer is removed, the etch process stops. The passivation and etching steps are repeated until one has etched to the desired thickness. In contrast to conventional plasma etch processes, microfabrication using ALE promises high selectivity and low damage to the substrate.

In this presentation, we discuss the properties of ALE using results from molecular dynamics (MD) simulations. The simulation procedure is conceptually similar to those described in previous publications [1,2]. In this study, a crystalline Si(100)-(2x1) or amorphous surface (made by low energy Ar^+ ion bombardment) was generated and equilibrated at room temperature. The bottom layers were fixed in space, and the periodic boundary conditions were applied laterally to remove the boundary effect. The ions are modeled as energetic neutrals. The surface was passivated by repeated bombardment with low energy Cl atoms at normal incident, which was followed by Ar^+ or Cl^+ ion bombardment to remove the passivation topmost layers. The Berendsen scheme is used between ion/neutral impacts to remove the energy from the surface region and cool the surface layer to room temperature. The Stillinger Weber (SW) type potentials are used for Si-Si, Si-Cl and Cl-Cl interactions. The Ar-Si and Ar-Cl interactions were modeled using Moliere potentials. The leap-frog form of Verlet algorithm was used to numerically integrate the Newton's equation of motion. The MD is applied to study several variants of the ALE process. The fundamental properties of Si etching are also investigated for both bare and Cl-passivated Si surfaces with several ions including Ar^+, Cl^+ and Cl_2^+. These fundamental studies are used to interpret our layer-by-layer ALE experiments in our laboratory.

Reference

[1] N. A. Kubota, D. J. Economou and S. J. Plimpton, J. Appl. Phys. 83, 4055 (1998).

[2] B. A. Helmer and D. B. Graves, J. Vac. Sci. Technol. A. 16, 3502 (1998).

11:00am PS+SS+TF-FrM9 Atomic Layer Etching of InGaAs using Cl2/Ar Ion Beam, *Jinwoo Park*, *D.H. Yun, H.S. Kim, G.Y. Yeom*, Sungkyunkwan University, Republic of Korea

Atomic layer etching can be one of next-generation etching techniques that can be applied to various materials including III-V compounds semiconducting materials such as indium-gallium arsenide (InGaAs) which is a great potential material due to the high carrier mobility for nano-scale devices. In this study, the atomic layer etching characteristics of InGaAs has been investigated using chlorine as adsorption gas and low energy Ar ion for desorption during the etch cycle to control the etch depth precisely and to minimize the surface damage of the material. For the chlorine adsorption, chlorine radical was adsorbed on the InGaAs surface and, during the desorption, the chlorine adsorbed InGaAs was removed by the Ar ion with the energy of about 20eV. By using the atomic layer etching technique, the controlled InGaAs etch depth per cycle and very high etch selectivity of InGaAs over dielectric materials such as silicon dioxide and hafnium dioxide could be obtained. The surface roughness of etched InGaAs characterized by atomic force microscopy was similar to that of un-etched InGaAs at the atomic layer etching condition.

11:20am PS+SS+TF-FrM10 InGaN Quantum Nanodisks Fabrication by Bio-Template and Neutral Beam Etching, *Yi-Chun Lai*, National Chiao Tung University, Taiwan, Republic of China, *A. Higo, C. Thomas, C.Y. Lee, T. Tanikawa, K. Shojiki, S. Kuboya, R. Katayama*, Tohoku University, Japan, *T. Kiba*, Hokkaido University, Japan, *I. Yamashita*, Nara Institute of Science and Technology, Japan, *A. Murayama*, Hokkaido University, Japan, *P.Yu. Yu*, National Chiao Tung University, Taiwan, Republic of China, *S. Samukawa*, Tohoku University

III-N quantum dots (QDs) gain media have generated great interest because of their desirable properties such as low threshold and temperature independence due to the discrete nature of the density of states. A uniform and high-density two-dimensional (2D) array of an isolated QD structure is required when considering applications in visible wavelength such as white LED. In general, size distribution, uniformity, and high-density are trade-offs when using a conventional self-assembly method; therefore, we have developed a technique that integrates a bio-template with neutral beam etching (NBE) process.

In this work, quantum nanodisks (QNDs) were fabricated from InGaN/GaN single quantum well (SQW) by using a bio-template and NBE. We developed a damage-less, top-down fabrication process for achieving high density of QNDs such as 2 x 10^{11} cm^{-2} embedded in 10 nm in diameter and 20 nm high nanopillars. The fabricated QNDs have great potential for fabricating quantum optoelectronic devices because of controllable diameter and thickness.

The InGaN/GaN SQW wafer was grown on a 2-inch c-plane sapphire substrate by metal-organic vapor phase epitaxy (MOVPE). The structure consisted of a 1μm-thick GaN buffer layer, 3nm-thick $In_{0.1}GaN$ and a 10nm-thick GaN capping layer. We used ferritins modified with polyethylene glycol (PEG ferritins) that include a metal oxide core for the etching mask. Oxygen annealing in vacuum was used to remove the ferritin protein shell at 350˚C, at chamber pressure of 32 Pa. Therefore the 7 nm diameter iron core was remained on the surface. Then hydrogen radial treatment, hydrogen passivation and NBE etching process were performed. At first, hydrogen radical treatment was realized to remove the surface oxide at chamber pressure of 32 Pa at 350˚C. Subsequently, hydrogen passivation was done to avoid any re-oxidation during the process. Finally, SQW was etched completely to form nanopillars using 40 sccm Cl$_2$ at a chamber pressure of 0.1 Pa, with a substrate temperature of 100˚C, ICP power of 800 W and bottom electrode bias power of 10W. As a result, InGaN/GaN 10 nm in diameter and 20 nm high nanopillars could be fabricated. The etching profile was confirmed by Transmission electron microscopy (TEM).

After etching, we measured the photoluminescence (PL) and time-resolved PL (TRPL) to observe the quantum confinement energy levels. According to the PL measurements, we found an energy shift of 1.25 eV, from 2.9eV for SQWs to 2.75eV for QNDs. Although these measurements are still on-going now, we will clearly analyze and discuss the phenomena related to this shift in energy in the near future.

11:40am PS+SS+TF-FrM11 Towards a Nanoscale Plasma Etching Precision: Molecular Dynamics Simulations of Si-Cl Interactions, *Paulin Brichon*, Univ. Grenoble Alpes-CNRS-CEA/Minatec-LTM,38000 Grenoble-France, *E. Despiau-Pujo*, LTM, France, *O. Mourey*, Univ. Grenoble Alpes-CNRS-CEA/Minatec-LTM,38000 Grenoble-France, *G. Cunge*, LTM - CEA/LETI, France, *O. Joubert*, Univ. Grenoble Alpes-CNRS-CEA, France

Due to high ion bombardment energies and significant fragmentation rates, conventional CW plasma processes are not able to selectively etch ultrathin films without damaging the active layers of advanced nanoelectronic devices (FDSOI, FinFET). In order to achieve uniform and damage-free etching of sub-nm-thick materials, one alternative is to lower the electron temperature (T_e) of the plasma. This can be achieved temporally by pulsing the plasma (i.e. switching on and off the RF source power), which introduces two additional parameters to tune an etching process, the pulsation frequency and the duty cycle (DC). Pulsed-plasma discharges exhibit lower average ion energies (E_i~5-10eV); their chemical reactivity (or dissociation rate) can also be controlled by varying the DC. Another alternative is to lower T_e spatially, by segregating the electron heating region far from the wafer. These low-T_e plasmas are characterized by very low E_i (E_i<5eV) and high radical densities.

With lower E_i and controllable reactivity, these plasmas are promising to etch sub-nm-thick stacked materials. However, the interactions between reactive plasmas and surfaces are so complex that the efficient development of new processes can require numerical simulations. Therefore, we develop Molecular Dynamics (MD) simulations to understand the impact of various plasma technologies on the interactions between ultrathin Si films and Cl$_2$ plasmas under a wide range of plasma conditions. They help to understand the precise role of E_i in plasma-surface interactions, the relationship between the flux/energy of reactive species bombarding the surface and its structural/chemical modifications.

In this study, MD simulations - coupled with experiments - are performed to quantify modifications (plasma-induced damage, etch rate) of Si films after exposition to various Cl_2 plasma conditions, simulated by bombarding the substrate with both ion and neutral species. All simulations show the formation of a stable $SiCl_x$ reactive layer and a constant etch yield (EY) at steady state. The key plasma parameter to control the etching of ultrathin Si layers is E_i, which lowers both the damaged layer thickness and EY when it is decreased. The neutral-to-ion flux ratio (Γ) is the 2nd key parameter: its increase reduces the damaged layer thickness while the etch rate grows. While maintaining Γ constant, the neutral dissociation rate and the ion composition do not influence significantly the etching process. Etching simulations of a simple Si pattern are then compared to the etching of blanket silicon, focusing on phenomena such as ion channeling, passivation/damage of pattern sidewalls and top pattern erosion.

Scanning Probe Microscopy Focus Topic
Room: 212A - Session SP+AS+MI+NS+SS-FrM

Probe-Sample Interactions
Moderator: Carl Ventrice, Jr., SUNY Polytechnic Institute

8:20am **SP+AS+MI+NS+SS-FrM1** **Direct Visualization of Magnetoelectric Domains in Hexagonal Manganites**, *Weida Wu*, Rutgers University **INVITED**
Multiferroics are materials with coexisting magnetic and ferroelectric orders, where the cross-coupling between two ferroic orders can result in strong magnetoelectriceffects [1-4]. Therefore, it is of both fundamental and technological interest to visualize cross-coupled magnetoelectric domains and domain walls in multiferroics. Recently, intriguing topological defects with six interlocked structural antiphase and ferroelectric domains merging into a vortex core were revealed in multiferroic hexagonal REMnO$_3$ (R=rare earths) [5, 6]. Many emergent phenomena, such as enhanced conduction and unusual piezoelectric response, were observed in charged ferroelectric domain walls protected by these topological defects [7-9]. More interestingly, alternating uncompensated magnetic moments were discovered at coupled structural antiphase and ferroelectric domain walls in hexagonal manganites using cryogenic magnetic force microscopy (MFM) [10], which demonstrates the cross-coupling between ferroelectric and magnetic orders. Here we present the application of a magnetoelectric force microscopy (MeFM) technique that combines MFM with *in situ* modulating high electric fields. This new microscopy technique allows us to image the magnetoelectric response of the domain patterns in hexagonal manganites directly [11, 12]. We find that this response changes sign at each structural domain wall, a result that is corroborated by symmetry analysis and phenomenological modelling , and provides compelling evidence for a lattice-mediated magnetoelectric coupling. The direct visualization of magnetoelectric domains at mesoscopic scales opens up explorations of emergent phenomena in multifunctional materials with multiple coupled orders.

References

[1] N. A. Spaldin, and M. Fiebig, Science 309, 391 (2005).

[2] W. Eerenstein, N. D. Mathur, and J. F. Scott, Nature 442, 759 (2006).

[3] S-W. Cheong, and M. Mostovoy, Nat. Mater. 6, 13 (2007).

[4] N. A. Spaldin, S.-W. Cheong, and R. Ramesh, in Physics Today2010), pp. 38.

[5] T. Choi et al., Nature Materials 9, 253 (2010).

[6] T. Jungk et al., Appl. Phys. Lett. 97, 012904 (2010).

[7] E.B. Lochocki et al., Appl. Phys. Lett. 99, 232901 (2011).

[8] D. Meier et al., Nat. Mater. 11, 284 (2012).

[9] W. Wu et al., Phys. Rev. Lett. 108, 077203 (2012).

[10] Y. Geng et al., Nano Letters 12, 6055?6059 (2012).

[11] Y. Geng, and W. Wu, Rev. Sci. Instrum. 85, 053901 (2014).

[12] Y. Geng et al., Nat. Mater. 13, 163 (2014).

9:00am **SP+AS+MI+NS+SS-FrM3** **Kelvin Probe Force Microscopy Studies of Magnetic Atoms on Ultrathin Insulating MgO Film**, *Taeyoung Choi*, W. Paul, S. Baumann, C.P. Lutz, A. Heinrich, IBM Almaden Research Center
The interplay of single atoms and their local environment on surfaces influences the atoms' spin excitations and dynamics, which can be utilized in progress toward atomic-scale memory and quantum information processing. We find that spin-excitation energy of Fe atoms on an insulating MgO film shifts depending on the tip-to-atom separation. This may be attributed to the electric field across the tunneling junction, as well as to local charge and structural changes around the atom. The Kelvin Probe Force Microscopy (KPFM) has been very useful tool to measure changes of local contact potential differences between a tip and a sample at the atomic level [1]. In this talk, we employ tuning fork KPFM/STM and show preliminary results on the charge character and spin excitations of Fe atoms.

This work is supported by grants from IBM.

[1] Leo Gross et al., Phys. Rev. B **90**, 155455 (2014).

9:20am **SP+AS+MI+NS+SS-FrM4** **Nanoscale Schottky Barrier Height Mapping Utilizing Ballistic Electron Emission Microscopy**, *C. Durcan, W. Nolting,* College of Nanoscale Science and Engineering, *Vincent LaBella*, SUNY Polytechnic Institute
The Schottky barrier is the electrostatic barrier between a metal and a semiconductor that results in rectification and is found in many types of devices such as source drain contacts to sub 20-nm-node transistors. Naturally, the Schottky barrier height can fluctuate across the interface due to variations in bonding, compositional fluctuations in the materials, and the presence of defects. However measuring and mapping these electrostatic fluctuations is impossible with bulk IV or CV techniques. This presentation will demonstrate how the Schottky barrier height can be mapped to nanoscale dimensions using an STM based technique called ballistic electron emission microscopy (BEEM). The STM tip is positioned on a regularly spaced grid and BEEM spectra are acquired from which the barrier height can be extracted. A map and histogram is then generated by measuring and fitting thousands of these spectra. These maps provide detailed insight into the electrostatic fluctuations occurring at the buried interface with nanoscale resolution that cannot be accomplished with other bulk measurements.

9:40am **SP+AS+MI+NS+SS-FrM5** **Electron Transport Studies of Metal Films Utilizing Ballistic Electron Emission Microscopy**, *Christopher Durcan*, SUNY College of Nanoscale Science and Engineering, *V. LaBella*, SUNY Polytechnic Institute
Understanding scattering of electrons in nanometer thick metal films is of fundamental and technological importance. One method to study electron scattering is with ballistic electron emission microscopy (BEEM), which is a three terminal STM based technique that measures both scattering through a metal film and the Schottky barrier height for metal-semiconductor junctions with both nanometer spatial resolution and meV energy resolution. This presentation will describe our work at understanding the relationship between the metal resistivity and the electron scattering lengths measured with BEEM by exploring metals with a range of resistivities from Ag (1.7 $\mu\Omega$-cm) to Cr (12.6 $\mu\Omega$-cm). In addition, nanoscale mapping of the Schottky barrier height of these metals to silicon will also be presented to understand the spatial uniformity of the transport.

10:00am **SP+AS+MI+NS+SS-FrM6** **Utilizing Ballistic Electron Emission Microscopy to Study Sidewall Scattering of Electrons**, *Westly Nolting, C. Durcan, R. Balsano,* College of Nanoscale Science and Engineering, University of Albany, *V. LaBella*, College of Nanoscale Science and Engineering, SUNY Polytechnic Institute
Sidewall scattering of electrons within aggressively scaled metallic interconnects increases the resistance since the mean free path (~40 nm) is larger than the dimensions of the material. One method to study hot-electron scattering in nm-thick metallic films is Ballistic Electron Emission Microscopy (BEEM), which is an STM based technique. In this work, we perform BEEM scattering measurements on lithographically patterned fin structures with a Schottky diode interface to determine its ability to measure sidewall scattering. This is accomplished by acquiring BEEM spectra on a regularly spaced grid and fitting the results to determine both the Schottky barrier height and the slope of the spectra. The slope of the spectra is related to the scattering in the film and interface. The position of fin structures are then determined by mapping both the Schottky height and slope over a square micron to observe scattering at the interface caused by the patterned structures. The poster will discuss the fabrication of the patterned 50-nm-pitched sidewall structures that are used for mapping the sidewall scattering. In addition, it will present the preliminary BEEM measurements on these structures.

10:20am **SP+AS+MI+NS+SS-FrM7** **Progress in Nanoscale Magnetic Resonance Imaging**, *Daniel Rugar*, IBM Research Division **INVITED**
Nuclear magnetic resonance (NMR) is the basis of powerful spectroscopic and imaging techniques, but extension to nanoscale samples has been a longstanding challenge due to the insensitivity of conventional detection methods. We are exploring the use of individual, near-surface nitrogen-vacancy (NV) centers in diamond as atomic-size magnetometers to detect proton NMR in organic material located external to the diamond. Using a combination of electron spin echoes and proton spin manipulation, the NV

center senses the nanotesla field fluctuations from the protons, enabling both time-domain and spectroscopic NMR measurements on the nanometer scale. By scanning a small polymer test object past a near-surface NV center, we have recently demonstrated proton magnetic resonance imaging (MRI) with spatial resolution on the order of 10 nm.

One key issue in NV-NMR experiments is the loss of spin coherence when the NV center is located near the diamond surface. Although this loss of coherence is frequently attributed to the effect of magnetic noise emanating from unpaired spins on the diamond surface, we will show evidence that electric field noise from fluctuating surface charge may be the dominant factor.

Work performed in collaboration with M. Kim, H. J. Mamin, M. H. Sherwood, C. T. Rettner, K. Ohno, and D. D. Awschalom

11:00am SP+AS+MI+NS+SS-FrM9 Reactive Intermediates Created and Analyzed by Scanning Probe Microscopy, *Bruno Schuler*, IBM Research - Zurich, Switzerland, *N. Pavliček*, IBM Research - Zurich, *S. Collazos*, CIQUS, Universidade de Santiago de Compostela, *N. Moll, S. Fatayer*, IBM Research - Zurich, *D. Pérez, E. Guitán*, CIQUS, Universidade de Santiago de Compostela, *G. Meyer*, IBM Research - Zurich, *D. Peña*, CIQUS, Universidade de Santiago de Compostela, *L. Gross*, IBM Research - Zurich

Reactive intermediates are involved in most chemical transformations. However, their characterization is a great challenge because of their short lifetime and high reactivity.

Here we report on the creation of single radicals and diradicals on a thin insulating surface by means of atomic manipulation. Importantly, the thin insulating film facilitates the stabilization of these reactive intermediates at cryogenic temperatures. The molecules were characterized by atomic-resolution atomic force microscopy (AFM) imaging with a CO functionalized tip [1] and scanning tunneling microscopy (STM) orbital imaging [2]. We show that the molecules' reactivity is preserved even at low temperatures by performing different on-surface reactions by atomic manipulation. As an example, the generation of aryne is discussed, a very reactive intermediate caught for the first time [3].

References:

[1] L. Gross et al. Science **325**, 1110 (2009)

[2] J. Repp et al. Phys. Rev. Lett. **94**, 026803 (2005)

[3] N. Pavliček et al. On-surface generation and imaging of arynes by atomic force microscopy. (submitted)

11:20am SP+AS+MI+NS+SS-FrM10 The Negative Stiffness and Positive Damping of Squeezed Air in Dynamic Atomic Force Microscopy, *x. Yu, M. Tao*, *Nancy Burnham*, Worcester Polytechnic Institute

By oscillating a micro-sized cantilever beam at a certain frequency and observing its interaction with the sample surface, dynamic mode atomic force microscopy (AFM) has gained attention for characterizing mechanical properties of a variety of materials at the micro and nano scales. The thin air film, confined between the oscillating cantilever beam and the stationary sample surface, causes the so-called "squeeze-film effect" when the gap between the two boundaries is less than a hundred microns. Although studies have shown that the squeeze film can act as a spring and a damper in accelerometers and microelectromechanical systems [1], the influence of the squeeze-film effect on the dynamics of an AFM cantilever has not been previously explored, to the authors' knowledge. In this project, the stiffness and damping properties of the squeeze film between an oscillating AFM cantilever and a glass slide were calculated from the cantilevers' amplitude and phase responses as recorded by the AFM digital system. The smaller the cantilever-sample gap, the larger the absolute values of the stiffness and the damping of the squeeze film. Results from different cantilevers (consequently having different spring constants and resonant frequencies) indicated that the air film exhibited **negative stiffness and positive damping**, with normalized changes from free values of up to 40%. Theoretical analysis was conducted using an equivalent-circuit model [2] along with the phasor diagram, and the derived stiffness and damping values were in excellent agreement with the experimental ones. Interestingly, a rotation angle between 20° and 30° in the fit of the data to the model reveals a phase *lead* of the squeeze-film damping before the usual air damping when the cantilever is far from a surface: the maximum squeeze-film damping occurs before the maximum velocity of the cantilever because air becomes less dense as it rushes out of the tip-sample gap. The surprising sign of the stiffness is thus explained by the phase lead. Future work includes incorporating the squeeze-film effect into more accurate measurements of a material's stiffness and damping properties using dynamic AFM.

References:

1. Starr, James B. "Squeeze-film damping in solid-state accelerometers." *Solid-State Sensor and Actuator Workshop, 1990. 4th Technical Digest., IEEE*. IEEE, 1990.

2. Veijola, Timo. "Compact models for squeezed-film dampers with inertial and rarefied gas effects." *Journal of Micromechanics and Microengineering* 14.7 (2004): 1109.

Authors Index
Bold page numbers indicate the presenter